Title
Physical drivers of spatiotemporal genetic patterns and evolutionary processes among and within species of the North American southwest

Permalink
https://escholarship.org/uc/item/90g010gt

Author
Dolby, Greer Andersen

Publication Date
2015

Peer reviewed|Thesis/dissertation

UNIVERSITY OF CALIFORNIA

Los Angeles

Physical drivers of spatiotemporal genetic patterns

and evolutionary processes among and within species of the

North American southwest

A dissertation submitted in partial satisfaction

of the requirements for the degree Doctor of Philosophy

in Biology

by

Greer Andersen Dolby

2015

ABSTRACT OF THE DISSERTATION

Physical drivers of spatiotemporal genetic patterns

and evolutionary processes among and within species of the

North American southwest

by

Greer Andersen Dolby

Doctor of Philosophy in Biology

University of California, Los Angeles, 2015

Professor David K. Jacobs, Chair

Over 150 years of investigation has yielded knowledge of the patterns and mechanisms of

biological evolution. Yet rarely do such studies integrate the physical mechanisms that

drive this evolution on a timescale that is biologically meaningful. Without integrating

physical and biological processes, we risk overlooking the co-evolutionary nature of

Earth and life. This thesis presents first a broad synthesis of how geologic, climatic, and

environmental mechanisms drive patterns of evolution on long (> 5 Myr), medium (1–2

Myr), and short (10s–100s kyr) timescales. It secondly presents a detailed assessment of

how estuaries and their inhabitants co-evolve through time and space in response to

changing sea levels and the physical landscape. Chapter 1 is a meta-analysis and review

of the biological and geological histories of the Sonoran Desert and Gulf of California

(Gulf) from 15 Ma to present. We suggest a middle-Miocene marine embayment could explain the deposition of reworked marine microfossils and speciation ages and distributions of Gulf endemics. Assessment of the Pleistocene-age mid-peninsular seaway hypothesis reveals that the uplift age of the Baja peninsula and strong genetic discordance of highly dispersive taxa render this hypothesis unlikely. Finally, we document the distribution patterns of 527 plants disjunct between the mainland and Baja California peninsula and suggest postglacial responses that underlie these patterns. In Chapters 2 and 3 I develop a paleohabitat modeling technique that estimates the size and distribution of estuarine habitat from 20 kya to present on a near-millennial timescale using physical parameters. I apply this model to ~4,600 km of coastal distance from San Francisco, USA to Sinaloa, MX. Independent of this is an assessment of the genetic history of 524 individuals of three co-distributed fishes using mtDNA and large microsatellite datasets. Together, there is statistically significant agreement from these findings; lowstand greatly reduced estuarine habitat and individuals evolved independently in these isolated refugia. Tectonic and oceanographic processes have shaped the regional geomorphology of coastlines and thus the degree to which these refugia and refugial populations are isolated. This isolation-recolonization pattern is likely global, and is not restricted to glacier-adjacent coastlines at high latitudes.

The dissertation of Greer Andersen Dolby is approved.

Michael Alfaro

Paul Barber

Kyle Cavanaugh

David K. Jacobs, Committee Chair

University of California, Los Angeles

2015

TABLE OF CONTENTS

LIST OF TABLES

LIST OF FIGURES

ACKNOWLEDGEMENTS

that became my first chapter. I would like to thank them and thank the Journal of the Southwest for allowing me to include it here. I must also thank Ryan Hechinger, Ryan Ellingson, Lloyd Findley, and Julio Lorda for contributing collections, analyses, expertise, and text to my second chapter.

Towards the home front—I have called my parents almost every Sunday for 11 years. They have heard the good, the bad, and the mundane over this time and have been persistently supportive, and loving, and proud. Thank you mom; thank you dad. My brother, Sam, who manages to always be right on matters of life, has grounded me through this journey. John and Faye offered me respite, fun, and family whenever I needed it on the West coast; I cherished this time and thoroughly miss him. Friends new and old made these years more fun and rewarding than I ever imagined: S. Cimino, A. Cummings, K. Henning, J. Antico, V. Chegar, L. White, S. McCree, M. Dolby-Shriver, L. Taylor, A. Garraffa, L Stuivenvolt-Allen, B. DeSalvo, J.C.E. Therrien, L. Wang, the 'game-nighters,' and my cohort members. Finally, I am immensely grateful to Nathaniel, whose presence in my life I am still convinced is too good to be true. Thanks to him, I have learned what it is to be part of a team and he has kept me laughing throughout.

VITA

2008	B.A., Earth Sciences; Biology w/ spec. in Cons. & Ecol.
	Boston University
	Boston, Massachusetts

2013	M.S., Biology
	University of California, Los Angeles
	Los Angeles, CA

AWARDS

2006	Research Experience for Undergraduates, NSF
	Columbia University
	New York, NY

2009-2010; 2011-2013	GAANN Fellowship, US Dept of Education
	University of California
	Los Angeles, CA

2011-2013	Doctoral Dissertation Improvement Grant, NSF
	University of California
	Los Angeles, CA

2014-2015	Dissertation Year Fellowship, Graduate Division
	University of California
	Los Angeles, CA

2014	Lerner Gray Memorial Grant, AMNH
	University of California
	Los Angeles, CA

PUBLICATIONS

Dolby GA, Bennett SE, Lira-Noriega A, Wilder BT, Munguía-Vega A (2015) Assessing the Geological and Climatic Forcing of Biodiversity and Evolution Surrounding the Gulf of California. *Journal of the Southwest*, 57, 391–455.

Assessing the Geological and Climatic Forcing of Biodiversity and Evolution Surrounding the Gulf of California

Greer A. Dolby, Scott E. K. Bennett, Andrés Lira-Noriega, Benjamin T. Wilder, and Adrian Munguía-Vega

> The biota of the lands has had a restless place and has endured displacements, inundations, extinctions, and has been forced into migrations with the coming and going of the sea, with the submergence or emergence of mountains, and with the concomitant changes of local climate. Close study of the plant and animal life, when directed by a correlating intelligence, should reveal a course of evolution, expressed jointly by plant and rock, hardly equaled in plant geography.
>
> —Howard Scott Gentry (1949:82)

Introduction

For almost a century the Baja California peninsula (Peninsula), Gulf of California (Gulf), and broader Sonoran Desert region (figure 1) have drawn geologists and biologists alike to study its unique physical and evolutionary processes (e.g., Wittich 1920; Darton 1921; Nelson 1921; Johnston 1924; Beal 1948; Durham and Allison 1960). The challenge remains to untangle the long, intricate, and at times enigmatic geological and climatological histories that have shaped the high levels of endemism and biodiversity observed in the region today (Van Devender 1990; Grismer 2000; Riddle et al. 2000).

Evolutionary theory argues that areas of endemism are generated through increased speciation rates or an unusual capacity to sustain species whose populations go extinct elsewhere. Areas with such high levels of unique biodiversity also demand conservation effort to preserve the underlying evolutionary processes and mitigate the extinction risk posed to species with limited ranges (Myers et al. 2000). Endemism rates

1
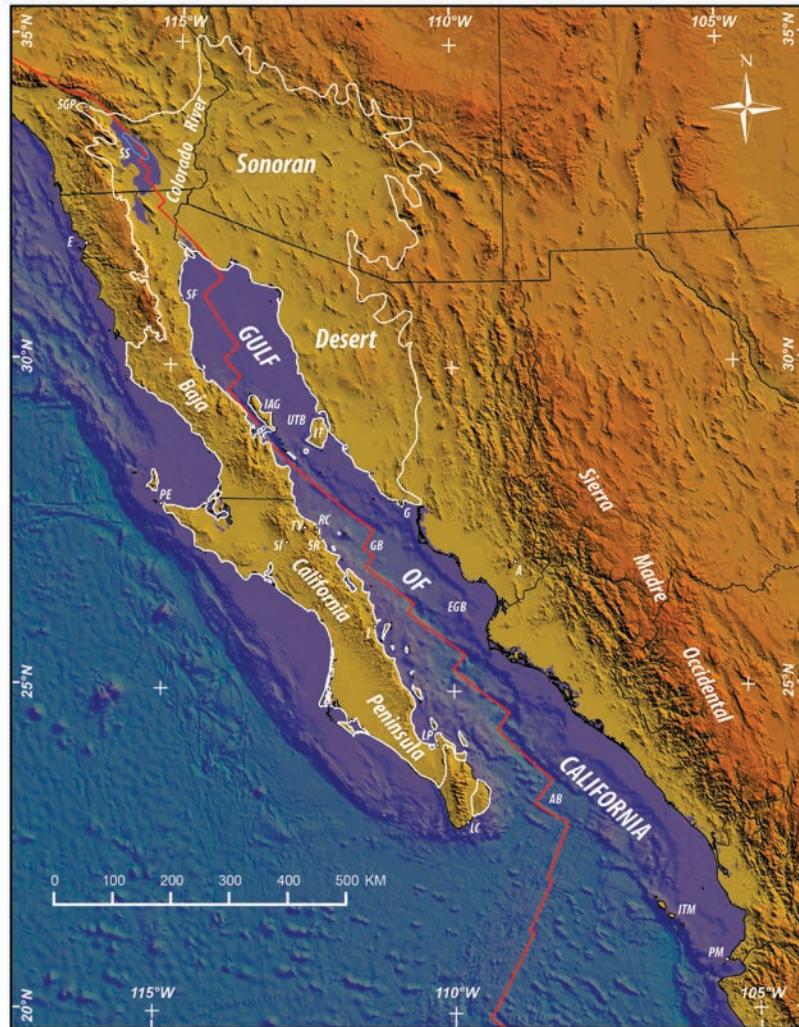
Figure 1: Physiographic map of the Gulf of California–Salton Trough–Sonoran Desert regions of western North America. Outline of Sonora Desert in white. Towns: E-Ensenada, SF-San Felipe, G-Guaymas, SR-Santa Rosalía, SI-San Ignacio, A-Alamos, L-Loreto, LP-La Paz, LC-Los Cabos. Places: SGP-San Gorgonio Pass, SS-Salton Sea, BC-Ballenas Channel, PE-Punta Eugenia, TV-Las Tres Virgenes volcanoes, RC-La Reforma Caldera, PM-Punta Mita. Islands: IAG-Isla Ángel de la Guarda, IT-Isla Tiburón, ITM-Islas Tres Marías. Marine Basins: UTB-Upper Tiburón basin, GB-Guaymas basin, EGB-East Guaymas basin, AB-Alarcon basin. All geographic analyses and maps use base map elevation data from the Shuttle Radar Topography Mission (SRTM) [http://srtm.usgs.gov/].

for reptiles and plants reach 54% and 30%, respectively, along the Peninsula (Grismer 2002; Brusca et al. 2005; Riemann and Ezcurra 2005; Munguía-Vega 2011; Rebman and Roberts 2012), and the Gulf is one of the world's marine diversity hotspots (Roberts et al. 2002). Yet, after almost a century of investigation into the geology, climate, and biology of this region, questions of timing and causality between these perspectives remain. In this article we attempt to unite the wealth of knowledge that remains divided along disciplinary lines, bridge their perspectives, and guide future study. To do so we include examples from the emerging field of geogenomics, in which large-scale genetic data inform geological hypotheses (Baker et al. 2014). The interdisciplinary nature of this effort is founded on the belief that through a synthetic approach incorporating plate tectonics, fossils, climate, ecology, and genetics we can better answer the long-standing questions about the physical history and origins and patterns of biodiversity surrounding the Gulf of California.

Reviews with varying scopes and emphases have summarized previous geological and biological work (Case and Cody 1983; Atwater and Stock 1998; Helenes and Carreño 1999; Case et al. 2002; Oskin and Stock 2003a; Riddle et al. 2000; Hafner and Riddle 2005; Lindell et al. 2006; Riddle and Hafner 2006). This contribution presents geological and climatological processes with the biological patterns they are hypothesized to create, under an explicit discussion of the timescales on which these phenomena occur. Geological processes are organized into three tiers (figure 2, table 1) based on the typical duration of the process. First-order processes fundamentally shape the landscape and take the longest to occur (>5 million years [Myr]). These processes involve plate tectonics, such as continental rifting of the Peninsula away from Mainland Mexico (Mainland). Second-order processes are physical land-sea interactions with local effects that occur on the timescale of 3–1 Myr, such as seaways that may have flooded low passes across the Peninsula. Third-order processes are predominantly climatic phenomena that occur on the shortest timescales of tens to hundreds of thousands of years (kyr). In theory, impacts of third-order events are only observable during or relatively soon after the event ends as the resulting biological signal may be temporary. By contrast, first-order events such as tectonic rifting may isolate a population, which becomes a separate species observable long after the process ends, yet may be difficult to observe over a short period during the event. These three categories are not absolute nor should be interpreted as such, but will prove useful in organizing the variables at play when correlating the histories of this region (table 1).
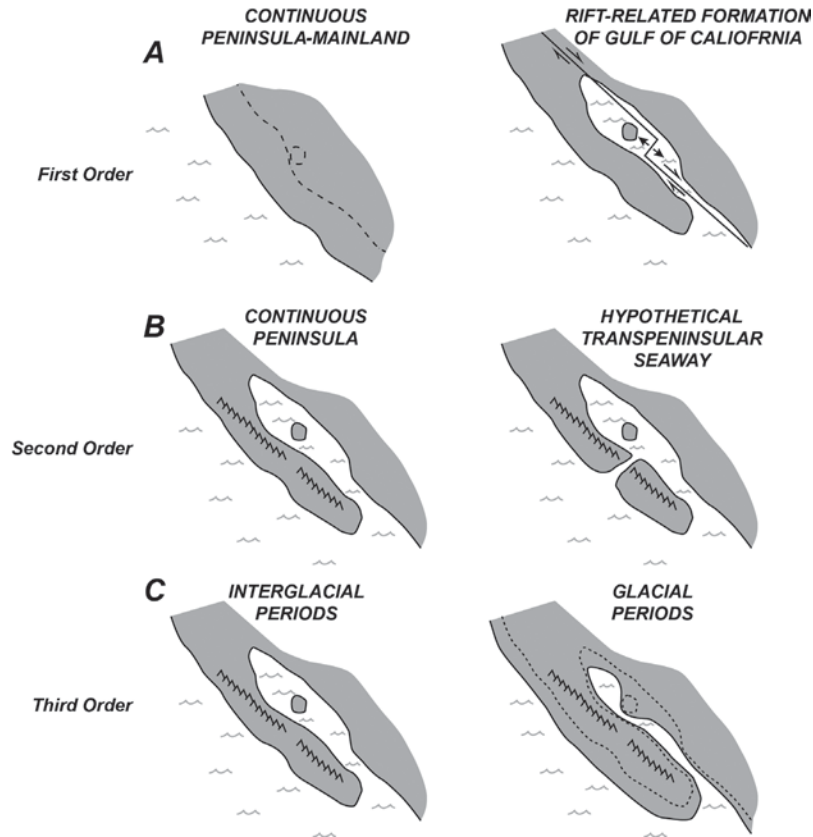
Figure 2: Schematic depictions of geologic/climatic processes evaluated in this study. (A) Rifting of the Baja Peninsula and formation of the Gulf. (B) Formation of transpeninsular seaways. (C) Sea-level lowstand associated with glaciations.

New contributions presented here address well-documented hypotheses. First, a topographical analysis evaluates the feasibility of proposed midpeninsular seaways, both middle Miocene and Plio-Pleistocene in age, by estimating the vertical tectonic uplift rates required for topographic passes to host seaways at these times, and comparing these rates to those documented along the Baja California peninsula. Second, a novel mapping technique visually summarizes previous terrestrial genetic patterns for peninsular taxa to assess regions of high and low biodiversity. Third, the first full listing of plant species shared

between the Mainland and Peninsula is presented with preliminary analysis of geographic patterns. Fourth, distribution and speciation of marine species are presented as new, independent lines of evidence to assess the proto-Gulf embayment and midpeninsular seaway hypotheses. Finally, we offer a discussion of sampling schemes, biological study systems, datasets, and analyses most informative for future work.

Table 1. *Geological processes organized by tier (first order, second order, third order) with duration of each and corresponding biological hypotheses for the events given. Biological patterns for Evolutionary Significant Units (ESUs) are specific to marine (M), terrestrial (T), terrestrial non-volant (T-nv), or terrestrial volant (T-v) species. Hypothesis numbers (e.g., 2a) are used throughout the text.*

Order	Process	Duration (Myr)	Hypothesized biological pattern
First	Peninsula rifting from mainland Mexico: - Formation of Gulf - Isolation of islands and peninsula - Proto-Gulf	>5	**1a.** Interspecific disjunct mainland-peninsular sister-species distributions (T) **1b.** Island endemism (T) **1c**. Presence of distinct mainland-peninsular ESUs (T) **1d.** Gulf of California endemism (M) **1e.** Ecological speciation (M)
Second	Land-sea interactions -Seaways	3 - 1	**2a.** Intraspecific north-south genetic discontinuity and multiple ESUs (T-nv) **2b.** No Intraspecific discordance; 1 ESU (T-v) **2c.** Little morphological discordance (T) **2d.** Intraspecific north-south genetic discordance (M) **2e.** Transpeninsular dispersal (M)
Third	100 kyr glacial-interglacial cycles -Precipitation changes -Temperature changes	0.8 - 0.02	**3a.** Postglacial range expansion (T) **3b.** Similar discontinuity/diversity patterns between taxa that are ecologically similar (T) **3c.** No pattern of discontinuity/diversity (T) between taxa based on dispersal ability (T) **3d.** Recent gene flow between islands (T) connected to Peninsula at lowstand (T) **3e.** High genetic diversity at predicted glacial refugia (T) **3f.** Current plant distributions reflect varying species responses to climatic change but show consistent biogeographic patterns (T)

Methods

Geology

To analyze the feasibility of a midpeninsular seaway in the geologic past, we constructed topographic profiles for the two lowest topographic passes in the midpeninsular region (section 1.1.3). The pass elevation (maximum elevation of each transect) reflects the minimum amount of uplift (positive vertical movement) required for the region to have flooded in the past. We calculated the rate of tectonic uplift necessary to achieve this change and compared it to uplift rates documented around the Gulf of California rift.

Phylogenetic Diversity

Using 85 studies of terrestrial taxa along the Peninsula (table S1), we created a GIS database with the geographic coordinates of sampling locations corresponding to each Evolutionary Significant Unit (ESU), which describes deep or significant genetic divergence for haploid (i.e., mitochondrial DNA in animals, chloroplast DNA in plants) and/or diploid markers (i.e., nuclear DNA). An ESU is a group of individuals that has been isolated from other individuals (conspecifics) for long enough to exhibit meaningful genetic divergence (Ryder et al. 1988), and contribute substantially to the ecological or genetic diversity of a taxon as a whole. Following Moritz (1994), ESUs must be reciprocally monophyletic for mtDNA (mitochondrial DNA) supported by bootstrap/ posterior probability values (e.g., a phylogroup with ≥ 0.80 statistical support) and/or exhibit significant divergence of allele frequencies at nuclear loci (e.g., Fst ≥ 0.2), or be statistically supported by Bayesian assignment tests.

We generated a convex polygon for each ESU with more than one sampling locality to represent the spatial extent of each group. The density, or overlap, of ESUs was measured over a 10-km x 10-km grid. We generated maps by taxonomic group, marker ploidy, and dispersal ability. Species that barely enter the northern part of the Peninsula and show phylogeographic structure north of the 33o00'N associated with the Transverse Range discontinuity in California (e.g., Chatzimanolis and Caterino 2007) were excluded unless their southern distribution reached the 30o00'N latitude on the Peninsula.

We constructed a frequency distribution from the geographical location of the genetic discontinuities in the Peninsula for a subset of 52 taxa, as described in detail in Munguía-Vega (2011). Genetic discontinuities are areas along the Peninsula separating two distinct ESUs. Given the shape and orientation of the Peninsula, we divided the analysis by latitude. A first analysis included discontinuities covering $\leq 1°20'00"$ latitude (narrow discontinuities) that could be confidently assigned to a single degree of latitude. With a chi-square goodness-of-fit test, the resulting distribution was compared against a null hypothesis of uniformly distributed genetic discontinuities (X^2 = 20.22, df = 10, P = 0.027). Since only a fraction of discontinuities adhered to the definition of narrow discontinuities (N = 19 taxa), the geographic location of all observed genetic discontinuities $\leq 3°00'00"$ latitude (broad discontinuities) was also estimated for the 52 taxa and superimposed to further explore the regions that showed a higher density of genetic discontinuities.

Plant Distribution Patterns

We assembled several lists to identify plant species co-occurring between the Peninsula and state of Sonora, Mexico. The list of Sonoran plants was assembled from the following regional floras: the Midriff Islands (Wilder 2014), Isla Ángel de la Guarda (Moran 1983a; Wilder 2014), the Guaymas region (unpublished checklist last edited in February 2014 from Dr. Richard Felger), and Río Chuchujaqui for the Alamos region (Van Devender et al. 2000). We cross-referenced this list against peninsular species documented in Sierra Libertad (Wehncke et al. 2012), the central Gulf coast of the Peninsula (Cody et al. 1983; Turner et al. 1995), and the Cape region of Baja California Sur (Lenz 1992).

The cross listing yielded 526 plant taxa present on the Mainland and Peninsula (table S2). All available herbarium records for these taxa were downloaded from the SEINet herbarium database (Southwest Environmental Information Network [SEINet] 2014), resulting in ca. 165,000 georeferenced herbarium records that matched the taxonomic name in addition to all known synonyms of the input list (table S2). These distribution records were merged with the input table in the R programming environment and multiple shape files were created. We used GIS to determine distributions throughout the Sonoran Desert and mapped species exhibiting one of four patterns from the high number of records (>165,000) and shared species (526). Baja California plant

distributions are underrepresented due to incomplete digitization pojects and restricted data sets during the period of the development of this paper.

1. First-Order Processes—Peninsular Rifting from Mainland Mexico

1.1. Geological Processes

1.1.1. Formation of the Modern Gulf of California

Rifting apart a previously contiguous continent fundamentally alters the landscape. Stretching and thinning Earth's crust, lowering its surface, and forming alternating valleys and ridgelines (e.g., Basin and Range) can cause climate heterogeneity and fragment existing populations. Prolonged rifting can lower Earth's surface below sea level, enabling flooding of marine waters that may serve as barriers to gene flow in terrestrial organisms, and as dispersal corridors for marine species. A notable example of this process is the rifting of the African and South American continents to form the proto-Atlantic Ocean (Wegener 1912). This rifting event isolated species on both rift margins of the Atlantic Ocean (Africa and South America) in the Mesozoic era (ca. 130 Ma), forming separate species. Similar geological processes have recently initiated in the Gulf (figure 3) and may be controlling intra- or interspecific genetic patterns, widespread speciation events, and changing species distributions between the Mainland and Peninsula.

Rifting began in northwestern Mexico as early as ca. 30 Ma (Ferrari et al. 2013), stretching Earth's crust and forming small Basin and Range-style valleys in eastern Sonora, Sinaloa, and Nayarit. The location of active rifting gradually migrated westward and concentrated in the Gulf sometime after ca. 12.3 Ma (Atwater and Stock 1998). At this time, the Pacific plate began sliding northwest along the San Andreas Fault system away from the Mainland. Unlike in California where Pacific–North America relative plate motion is parallel to the plate boundary (the San Andreas Fault), relative plate motion in the Gulf is oblique to the plate boundary. As a result, the Gulf consists of a stepped pattern of short

spreading centers connected by transform (strike-slip) faults (figure 2A).

The modern Gulf gradually flooded northward, as recorded in sedimentary rocks containing marine fossils from near the southern mouth of the Gulf up to near San Gorgonio Pass in southern California. In the southern Gulf, evidence for marine conditions exists as early as 10 Ma at Punta Mita near Puerto Vallarta (Gastil and Krummenacher 1978), ca. 8–7 Ma on Islas Tres Marías (Carreño 1985; McCloy et al. 1988), and ~7.5–7 Ma near Los Cabos (Carreño 1992; Molina-Cruz 1994), which may represent a local embayment of the Pacific Ocean
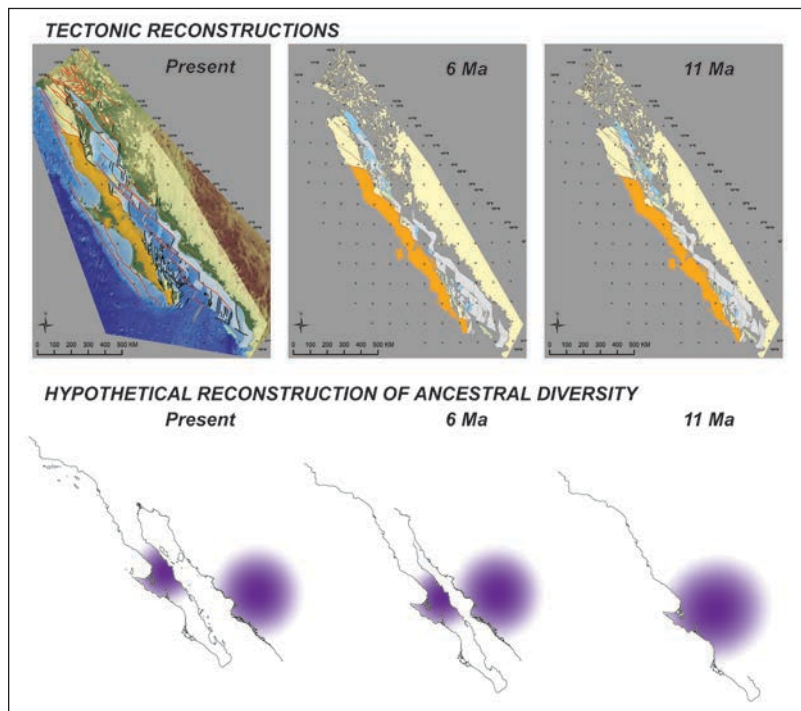
Figure 3: Plate tectonic reconstruction maps back to Miocene time (upper row) reconstruct motion on faults to restore the past positions of fault blocks around the Gulf of California. Polygons are areas of continental crust, colored by relative amounts of extension and thinning due to continental rifting (yellow, unextended; gray, moderately extended; blue, highly extended). Baja California microplate is colored orange for clarity. See Bennett et al. (2013b) for more details and animations of this plate tectonic reconstruction. Lower row schematically shows where an 11-Ma hypothetical ancestral biodiversity center (purple) would be today due to plate tectonics.

9

instead of a full-fledged Gulf at that time. Farther north, correlative marine salt deposits near Santa Rosalía (Holt et al. 2000) and in the offshore East Guaymas basin (Miller and Lizarralde 2013) provide evidence for inundation at a slightly later time, ca. 7 Ma.

During the same period that the southern Gulf flooded (ca. 10–7 Ma), the northern Gulf and Salton Trough regions show no evidence for marine conditions, as rift valleys were filling with nonmarine sediments in coastal Sonora (Darin 2011; Bennett et al. 2013a), northeastern Baja California (Lewis 1996; Seiler et al. 2010), and in the Salton Trough area (Dorsey et al. 2011) at that time. A stack of unique volcanic ash deposits, now located in coastal Sonora, on Isla Tiburón, and in northeastern Baja California, correlate across the northern Gulf (Oskin et al. 2001) and are not associated with marine conditions. Correlation of these ash deposits is based on several similarities, including their ages, lithology, geochemistry, thickness, and unique paleomagnetic direction (see Bennett 2013 for detailed summary). Restoring outcrops of these ash deposits to their locations ca. 6 Ma requires moving Baja California back to the southeast ~250 km (figure 3), a similar distance to what extrapolation of modern-day plate tectonic rates would predict (Oskin and Stock 2003b).

At ca. 6.3 Ma, fossil-rich marine sediments first record flooding at several locations in the northern Gulf and Salton Trough (summaries in Oskin and Stock 2003a; Bennett 2013). This flooding event is exceptional, with the northernmost 400–500 km of the Gulf flooding synchronously, 6.3 ± 0.1 Ma, from southwestern Isla Tiburón to San Gorgonio Pass in southern California. With this event the modern Gulf took form and was quite distinctive in shape, only ~50 km wide and up to ~1,400 km long (figures 1 and 3). Flooding of the northern Gulf coincides with, and is attributed to, the full development of the Pacific–North America plate boundary in both time and space. These tectonic events provided a mechanism for the subsidence (lowering of Earth's surface) required for marine flooding (figure 2A; Oskin and Stock 2003b). Rifting and subsidence continued and the Colorado River began draining into the Gulf by 4.1 Ma (Dorsey et al. 2007; House et al. 2008; McDougall and Miranda-Martinez 2014). A detailed plate tectonic reconstruction (figure 3) is the most up-to-date paleotectonic view of how the Peninsula, Gulf islands, and shoreline evolved through time (Bennett et al. 2013b), which provides visual-spatial context for discussions of how geological and climatic processes may impact biodiversity in the region (Bennett et al. 2013b).

1.1.2. Proto-Gulf Hypothesis

Although the inundation of the modern Gulf is well documented, the presence, extent, timing, and cause of an older proto-Gulf embayment are debated. If an earlier incarnation of the Gulf existed (i.e., the proto-Gulf embayment), it could have initiated biological processes, such as speciation, much earlier than effects imparted by the modern Gulf (section 1.2.3). The geological and biological interpretations of the proto-Gulf hypothesis differ, and will be treated separately (for biological evidence see section 1.2.2). In the geological literature, Moore and Buffington (1968) first hypothesized a late Miocene proto-Gulf of California marine basin to explain an area of anomalously old oceanic crust offshore Puerto Vallarta at the entrance (mouth) of the Gulf. The proto-Gulf concept was later expanded to include faulting related to continental rifting and evidence of marine sedimentary rocks from the northern and central parts of the Gulf ca. 15–5 Ma (e.g., Karig and Jensky 1972; Gastil et al. 1979) and was envisioned as a Gulf of varying sizes, as large as the distance from Puerta Vallarta to the Lower Colorado River (e.g., Moore 1973). With increased knowledge of plate tectonic (e.g., Atwater 1970) and subduction zone history (e.g., Hausback 1984) in northwestern Mexico, the proto-Gulf term was used differently (e.g., Stock and Hodges 1989; Gans 1997; Fletcher et al. 2007). The proto-Gulf began to specifically refer to the tectonic period beginning ca. 12.5 Ma with the transition from subduction to oblique rifting, and ending at ca. 6 Ma, when the Pacific–North America plate boundary became localized in the Gulf. Thus, conceptions of a proto-Gulf have evolved in the geological literature.

Evidence for a middle Miocene embayment in the northern Gulf has been reported, which calls upon an older (pre-11-Ma) incarnation of the Gulf of California. One group of studies documented marine conditions ca. 13–11 Ma on southwest Isla Tiburón (Smith et al. 1985; Gastil et al. 1999), which marks the only terrestrial exposure of marine strata of supposed proto-Gulf age. However, recent reexamination of these marine strata indicates that the oldest marine deposits on Isla Tiburón are actually 6.4 to 6.1 Ma (Bennett 2013), consistent with the regional flooding event ca. 6.3 Ma (Oskin and Stock 2003a). Another group of studies documented middle Miocene marine microfossils in cuttings from deep oil exploration wells throughout the Salton Trough and northern Gulf (Helenes et al. 2009) and interpreted the specimens to be *in situ* (in the original place of deposition). Helenes et al. (2009)

suggest these specimens are evidence for a pre-11-Ma proto-Gulf embayment and that marine waters might have fed this proto-Gulf from the Pacific Ocean across what is now the Baja California peninsula near the towns of Santa Rosalía and San Ignacio (Helenes and Carreno 1999) through a midpeninsular seaway (see section 1.1.3). However, the sediments hosting these microfossils are chemically and mineralogically similar to the diagnostic, quartz-rich rocks of the Colorado Plateau (Jiménez 2013) that are eroded and transported by the Colorado River, which first reached the Gulf of California between 5.7 and 4.1 Ma (Dorsey et al. 2007; House et al. 2008). This suggests that these middle Miocene (pre-11-Ma) microfossils were eroded from older middle Miocene marine sediments elsewhere and included in these younger, late Miocene sediments.

Though uncontested *in situ* middle Miocene marine strata within the Gulf region have not been found, the mere presence of reworked middle Miocene marine microfossils (e.g., McDougall 2008; Helenes et al. 2009) requires that marine conditions existed somewhere nearby during middle Miocene time and deposits from this unidentified source contributed the reworked fossils into late Miocene marine basins. Three hypothesized origins of middle Miocene strata exist (for a detailed review, see Bennett 2013). The first is from deposits related to a middle Miocene proto-Gulf embayment, similar to what Helenes and Carreño (1999) proposed, where marine waters were fed eastward from the Pacific Ocean, because southern (Gulf entrance) and northern (Los Angeles basin) connections to the Pacific are doubtful (Helenes and Carreño 1999). The second hypothesized source is a shallow embayment northeast of and parallel to the modern-day Gulf, within Sonora and Sinaloa, behind a NW-SE oriented chain of middle Miocene volcanic centers (Fenby and Gastil 1991; Smith 1991; Helenes and Carreño 1999; Bennett 2013). However, no outcrops of middle Miocene marine strata have been observed here; only nonmarine strata of this age have been documented in this region (Herman and Gans 2006; Darin 2011; Bennett et al. 2013a). Also, the regionally extensive ash deposit outcrops of the 12.5-Ma tuff of San Felipe and the 6.4-Ma tuffs of Mesa Cuadrada (Bennett and Oskin 2014) never overlie marine sediments, which suggests nonmarine conditions throughout northwestern Mexico when these volcanoes erupted. A third hypothetical source is from the continental shelf on the Pacific side of the southernmost Peninsula, where middle Miocene marine strata were exposed to wave-base erosion during late Miocene time (Brothers et al. 2012) and could have contributed middle

Miocene specimens into the northern Gulf of California. Each of these scenarios requires further exploration (see section 1.3).

1.1.3. Geological Assessment of Middle Miocene Midpeninsular Seaways

The existence of a middle Miocene proto-Gulf embayment in the general region of the modern-day northern Gulf requires a sea-level connection to the Pacific Ocean. Because a southern (via Gulf mouth) or northern (via L.A. basin) connection to the Pacific Ocean is unlikely, some other low-lying region is required to feed marine water from the Pacific into a hypothesized proto-Gulf embayment. Helenes and Carreño (1999) proposed a middle Miocene midpeninsular seaway (referred here as San Ignacio) located through the San Ignacio area. We identify an additional low topographic pass (Agua Armada) as another candidate that may have hosted a middle Miocene midpeninsular seaway. Due to the absence of a middle Miocene marine sedimentary rock record in the two proposed midpeninsular seaway paths, we evaluate the feasibility of these two hypothetical midpeninsular seaways through analysis of topographic data (figure 4) and comparison to published tectonic uplift histories.

Vertical topographic changes to the midpeninsular region since middle Miocene time include faulting, local inflation from magma chambers, deposition of volcanic rocks, and differential erosion. The rates of these processes vary over short distances and render determination of high-resolution paleo-topography difficult. The process of regional-scale rift flank uplift (uplift of the margins surrounding a rift) can affect larger regions (e.g., Mueller et al. 2009) and is likely to be the main driving cause of the 400 ± 200 m of vertical tectonic uplift observed along the crest of the central Peninsula (Mark et al. 2014). This rift flank uplift is attributed to intense crustal extension and localized oceanic spreading in the rift axis to the east (Mueller et al. 2009) and constrained to have occurred between ~6 and 3 Ma (Mark et al. 2014).

The more frequently cited potential pass (San Ignacio) is located through the town of San Ignacio and branches in the east around Las Tres Virgenes volcanoes and La Reforma caldera, connecting to the Gulf near Punta Santa Ana in the north and/or Santa Rosalía in the south (figure 4C). These branches may have been a single path as the intervening area may have been much lower prior to the 1.2-Ma and younger

13
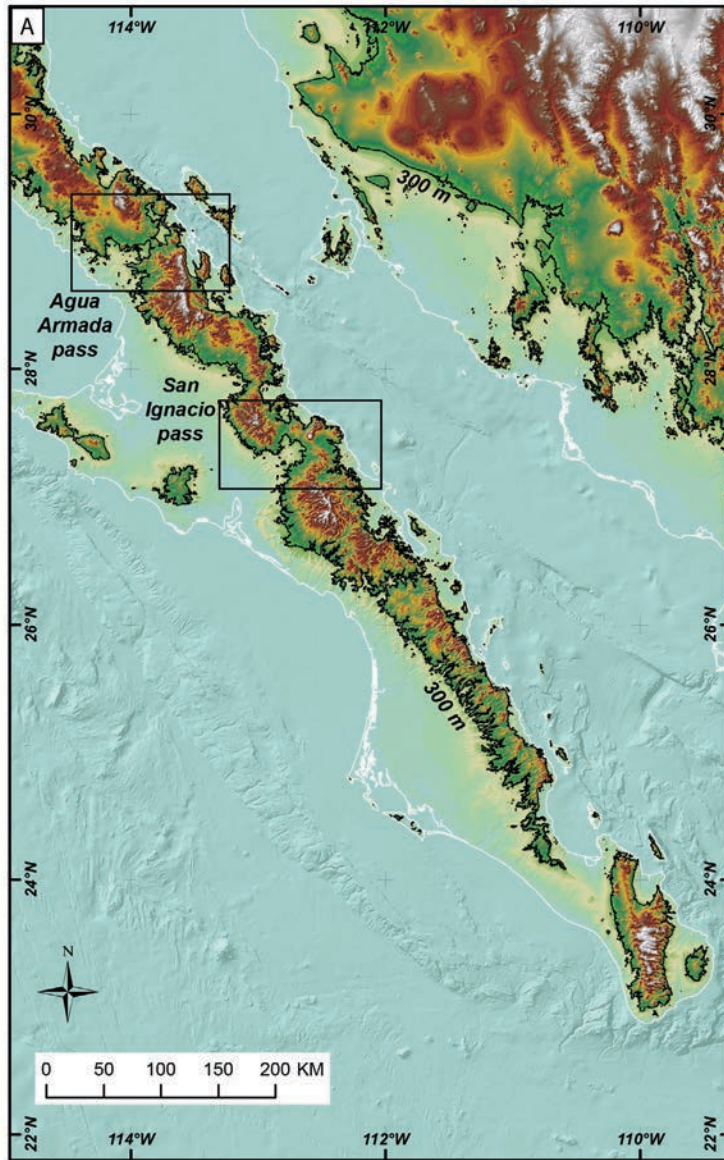
Figure 4: Topographic analysis of seaways across the Baja California peninsula. Modern shoreline in white. (A) Regional topography of the Peninsula with 300-m elevation contour (black line). (B) A broad topographic pass with a pass (maximum) elevation just over 300 m exists in the Agua Armada region. The northern branch (red) is lower than the southern branch (blue), which has a secondary, eastern pass over 350
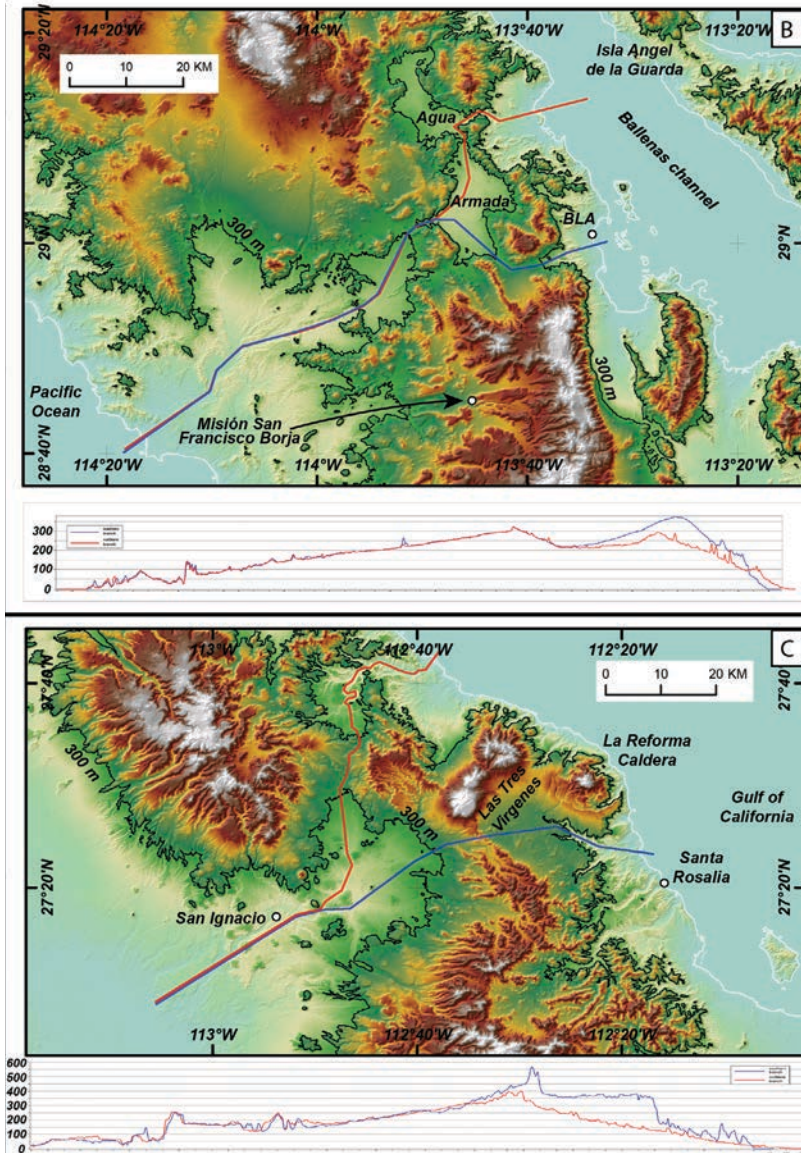
m. BLA, Bahía de Los Angeles. (C) A broad topographic pass also exists in the San Ignacio region. The northern branch (red) has a pass elevation near 400 m. The southern branch (blue) has a pass elevation just over 550 m. The northern branch appears to be more feasible than the southern branch, as it is ~150 m lower than the southern branch.

15

eruptions that built the volcanic hills of Las Tres Virgenes and La Reforma (Garduño-Monroy et al. 1993; Schmitt et al. 2006). The northern branch of this San Ignacio path has a pass elevation near ~400 meters above sea level (masl) and the southern is ~550 masl (figure 4C). The southern path appears to cross a NW-SE oriented normal fault with possibly ~100 m of down-to-the-northeast fault motion during Quaternary time, which may contribute to its relatively higher modern elevation. If these branches of the San Ignacio pass were at sea level during latest middle Miocene time (~12 Ma) and were uplifted ~6–3 Ma (e.g., Mark et al. 2014) uplift rates of ~0.1–0.2 mm/yr are required over that ~3-Myr period to uplift this pass to its modern-day elevation.

We identify a second SW-NE oriented potential pass (Agua Armada) through the Agua Armada region, with a pass elevation just over 300 masl (figure 4B). This pass may be more feasible for flooding than the more frequently cited San Ignacio pass because of its relatively lower elevation. About 25 km south of the Agua Armada pass (figure 4B), Wittich (1920) observed fossil-rich dune deposits at ~400-m elevation near Misión San Francisco Borja (San Borja). If these dunes were deposited as part of a middle Miocene shoreline and are now at ~400 m, then the nearby 300-m-high Agua Armada pass could have been flooded in middle Miocene time. If this pass (~300 m) was at sea level during latest middle Miocene time and was also uplifted ~6–3 Ma, uplift rates of ~0.1 mm/yr during that time are required to uplift this pass to its modern-day elevation. If uplift occurred over a longer period of time (e.g., ~12–3 Ma), slower rates of uplift would be required to bring both the San Ignacio and Agua Armada passes to their modern-day elevations.

The uplift rates required for the San Ignacio and Agua Armada passes to have hosted a middle Miocene seaway are within the uplift rates (0 to 0.3 mm/yr) observed along the northwestern Baja coastline (Mueller et al. 2009). Thus, these uplift rate estimates suggest that a middle Miocene seaway through Agua Armada is plausible. This is further supported by 400 ± 200 m of modeled uplift at the peninsular drainage divide (Mark et al. 2014). However, importantly, Mueller et al. (2009) observed that uplift rates along the western Peninsula coastline decrease from ~0.1 mm/yr to near 0 mm/yr just north of Isla Ángel de la Guarda, signifying that the magnitude of rift flank uplift may have been smaller at the latitudes of San Ignacio and Agua Armada. From these geological observations, topographic analysis, and comparison to the timing and rates of vertical tectonic uplift, it is feasible that these passes could have

hosted transpeninsular seaways that connected a middle Miocene proto-Gulf embayment to the Pacific Ocean. However, direct geological evidence, such as marine sedimentary rocks of middle Miocene age, is required to confirm any transpeninsular hypothesis. Additionally, this evidence does not speak to the location and size of a middle Miocene embayment, only that transpeninsular seaways in this region were possible at this time.

1.1.4. Midriff Islands

The Midriff Islands are an archipelago stretching across the central Gulf, comprising islands with heterogeneous and distinct geologies. Some are fragments of continental crust similar to the Peninsula and Mainland that originated from the rifting of the Peninsula and flooding of the Gulf (Ángel de la Guarda, San Lorenzo, Tiburón, San Pedro Nolasco). Other islands are volcanic (e.g., San Esteban, San Pedro Mártir, Tortuga) and formed from accumulation of volcanic deposits that breached sea level after the modern Gulf formed. Their physical size ranges across four orders of magnitude from the largest island (Isla Tiburón, ~1,200 km²) to small rocky outcrops.

In the northern Gulf, evidence from volcanic rocks (Oskin et al. 2001; Oskin and Stock 2003b) and submerged continental shelves on both rift margins (offshore Sonora/Tiburón and northeastern Baja California) suggest the modern shorelines were separated by ~30 km until 6.4–6.1 Ma (Bennett 2013). Such narrow gaps were likely devoid of marine water until the 6.3-Ma flooding event, which would have then isolated island species (section 1.2.2). From plate tectonic restorations of the Baja California peninsula back to the southeast (Bennett et al. 2013b), the lateral extent of marine deposits interpreted to be middle Miocene by Helenes et al. (2009) appears too extensive in offshore geophysical data (e.g., Mar-Hernández et al. 2012) for the space available (~30 km) during middle Miocene time. Geological and geophysical observations from offshore basins (e.g., Aragón-Arreola and Martín-Barajas 2007; Mar-Hernández et al. 2012) indicate marine conditions have continuously existed in the Lower Tiburón and Upper Tiburón basins between Isla Tiburón and the Puertecitos area of Baja California since at least ca. 6 Ma. Similar observations from the Lower Delfín basin suggest that the short, northwestern shoreline of Isla Ángel de la Guarda disconnected from Baja California slightly later, ca. 3.3–2 Ma (Aragón-Arreola and

17

Martín-Barajas 2007). The timing of formation for the narrow Ballenas Channel, which separates Ángel de la Guarda from Baja California, is less well known, but the development of a major strike-slip fault in the Channel likely occurred ca. 3.3–2 Ma (Nagy and Stock 2000; Stock 2000). Finally, isolation of Isla Tiburón from coastal Sonora has likely been transient, with the island connected to the Mainland by land bridges during periods of low sea level (Lambeck and Chappell 2001; Davis 2006; Felger and Wilder 2012; section 3).

1.2. Biological Patterns

1.2.1. Speciation between the Mainland and Peninsula and Endemism (Hypotheses 1a–1d)

Given enough time, a vicariant event that physically divides and isolates a population so the daughter populations no longer interbreed will produce two distinct species as those new populations drift independently and adapt to different environments (Wiley 1988). Given the age of Gulf flooding (8–7 Ma in the south, ca. 6.3 Ma in the north), species with low dispersal potential that cannot interbreed across the Gulf are expected to have started speciating in late Miocene time (hypothesis 1a; see table 1 for hypotheses). Species-level designations of disjunct or widely separated sister lineages have been proposed for several taxa, including gopher, bull, and pine snakes (Rodriguez-Robles and De Jesus-Escobar 2000), crotaphytid lizards (McGuire et al. 2007), desert rodents (Riddle et al. 2000), and spiders (Crews and Hedin 2006), to name a few. The iconic Baja Californian succulent plant, cirio (boojum, *Fouquieria columnaris*), is sister to all other members of Fouquieriaceae, likely due to its isolated evolution on the Peninsula (Schultheis and Baldwin 1999). These studies hint at a widespread pattern of vicariant speciation between the Mainland and Peninsula, which contributes to higher biodiversity. Additional genetic and morphological studies are needed to reveal whether Mainland-Peninsula rifting instigated speciation in species with higher dispersal potential such as plants and birds (hypothesis 1c).

Following rift-related speciation (or at least vicariance), new species are narrowly distributed on an isolated peninsula, which is ideal for generating high levels of endemism, as documented to a stronger effect on islands (Kier et al. 2009). By conservative estimates, over 6,000 species of plants and animals exist on the Peninsula, 30% of which are endemic

(Riemann and Ezcurra 2005; Rebman and Roberts 2012). Of 856 invertebrate species, only tenebrionid beetles, bees, ants, scorpions, and butterflies have been well studied and 30.7% of those studied are endemic. Mammals have 42 species (19% endemic) and reptiles have 96 species (33.3% endemic; see Munguía-Vega 2011 for summary).

The Pacific and Gulf islands host 115 species of reptiles, of which almost half (42.6%) are endemic. Forty-five species of mammals are present on Gulf islands (excluding bats) with a 48.8% endemism rate. Endemism levels are far lower in volant (able to fly or glide) species such as birds and plants, which can likely disperse between islands (Case and Cody 1987; Wilder 2014, and see Rebman 2002 for review of island plants) (the most isolated island, San Pedro Mártir, is only ~50 km from either coast). In Gulf waters, there are 766 documented invertebrate taxa endemic to the Gulf (Brusca et al., 2005). The Gulf is also host to the world's smallest cetacean, the vaquita (*Phocoena sinus*), which is near extinction, and the region provides important spawning and nursery habitat for many fishes and marine mammals.

Ancestral levels of biodiversity that existed before rifting and northward translation of the Peninsula should be considered (for a reconstructed example, see figure 3). For instance, if the region already hosted high levels of biodiversity, then rifting of that region and isolation of the Peninsula and islands would have led to much higher levels than if the region had been species poor prior to rifting. Additionally, movement of the Peninsula northwest over the past few million years could have shifted temperature and rainfall gradients, and should be considered when evaluating modern species distributions and historical barriers. Moreover, while vicariance models of speciation are most commonly applied in this region due to its tectonic and topographic complexity, we must also note the potential for sympatric speciation. For example, adaptation of individuals toward different traits (e.g., food type) may divide a population over time as individuals segregate by those traits and hybrids formed between them are selected against (Maynard Smith 1966). Therefore, even in scenarios where vicariance is likely, similar ecological or sympatric speciation processes may also be occurring.

1.2.2. Biological Evaluation of a Proto-Gulf (Hypothesis 1d)

For geologists, the precise details of how, when, and where a proto-Gulf embayment might have formed are contentious and still under

investigation. For biologists, however, these details are less important than the biological patterns they would affect regarding speciation and geographic distributions. The concept of a middle Miocene proto-Gulf embayment is relatively new to biological work (e.g., Hurtado et al. 2010; Dolby et al. 2012); it could have isolated individuals of marine species from their ancestral ranges, potentially leading to vicariant speciation in many taxa. Recent work indicates that speciation ages between Gulf-endemic and non-endemic sister species within the east Pacific bay gobies (estuarine-nearshore marine fishes) cluster between 16 and 10 Ma (Ellingson 2012; Ellingson et al. 2014). This timing coincides with the proto-Gulf embayment hypothesized by Helenes et al. (2009); however, this genetic analysis cannot provide geographic information for where the potential embayment would have existed. Such a biological scenario requires an embayment that continuously persisted from the middle Miocene until the modern northern Gulf flooded ~6.3 Ma, and requires it then physically connected with the modern Gulf to account for modern geographic distributions of these fishes. No evidence presently exists for marine deposits between 11 Ma and ~6.3 Ma, but this theoretical embayment could have produced the middle Miocene marine sediments discussed in section 1.1.2. A middle Miocene—or proto-Gulf—embayment is the most parsimonious explanation for these speciation data. Alternatively, the onset of middle Miocene upwelling in the east Pacific could have played a role, but how this would cause synchronous speciation among Gulf endemics is unclear (Jacobs et al. 2004). Replication of these phylogenetic results with other Gulf endemics and integration with the existing geological framework are needed.

1.2.3. Modern Gulf Influence on Marine Biodiversity (Hypothesis 1e)

Flooding of the modern Gulf 8–6 Ma expanded available marine habitat in the eastern Pacific. Although paleo-oceanographic details of this region since late Miocene time are not well constrained, many have argued that the modern Gulf exerts unique selection pressures on its inhabitants relative to the Pacific for several reasons. First, the Gulf is sheltered from the strong waves driven by the fetch of the Pacific Ocean. Second, tides in the Gulf are notoriously high, reaching 7 m in the north (Roden 1964). Third, sea surface temperatures fluctuate annually up to 16°C in the Gulf compared with <2°C in the Pacific (Ellingson 2012).

Fourth, islands in the Gulf mark localized regions of seasonal upwelling (Zeitzshel 1969). Finally, since the Colorado River first drained into the Gulf ca. 4.1 Ma until twentieth-century damming, it discharged significant volumes of freshwater and sediment into the northern Gulf. When the large Colorado Delta ecosystem formed it offered unique habitat to which delta endemics adapted (Swift et al. 2011). Many species also thrived in the new, extensive riparian habitat (Leopold 1949). Therefore, the abiotic conditions in the Gulf are more seasonally and annually variable than those in the Pacific, and combine to form a unique habitat likely to impart divergent selection pressures. Over time these factors may cause differentiation, and perhaps ecological speciation between Gulf and Pacific marine populations (e.g., Littler and Littler 1981).

1.3. Tectonic Rifting-Associated Hypotheses: Future Work

To test whether rifting of the Peninsula caused speciation in more highly dispersive lineages, such as plants (hypotheses 1a, 1c), additional plant phylogenies are needed at the inter-specific level. The null expectation is that speciation events are distributed evenly throughout a phylogenetic tree between the base and tips. If speciation events within the phylogeny cluster in age and significantly deviate from the null evenly distributed model, then one may infer an external mechanism (i.e., rifting) contributed to that pattern. Phylogenies for plant families Anacardiaceae, Cactaceae, and Fabaceae, with Mainland-Peninsula sister species, would be appropriate for such an analysis. Additionally, trans-Gulf species pairs would provide an opportunity to calibrate the rate of evolution for genes used in other work where time calibration is elusive and reveal interspecific differences in diversification times.

If a proto-Gulf embayment existed and caused the observed diversification of east Pacific bay gobies between 16 and 10 Ma, then one would expect to observe similar synchronous speciation in other taxonomic groups between Gulf-endemic and non-endemic sister species (assuming similar levels of dispersal and population differentiation). Constructing age-calibrated phylogenies of groups with Gulf-endemic and non-endemic taxa is the most direct way to address this question (Magallón 2004; Rutschmann 2006). If similar patterns of parallel speciation and timing are observed in other groups (fish, mollusks, arthropods) with different ecological affinities it would support vicariant speciation via a marine embayment because ecological or environmental

mechanisms would be expected to affect such taxa differently. Also, applying different rate-based reconstruction methods is needed (e.g., Drummond et al. 2006; Drummond and Suchard 2010) to determine how robust the east Pacific bay gobies diversification ages are to the assumptions of different evolutionary models. Also, because the existence of a middle Miocene proto-Gulf embayment relies upon a connection to the Pacific Ocean, geologists should locate direct geological evidence of middle Miocene deposits in the San Ignacio or Agua Armada passes to evaluate whether conditions at this time in these regions were marine or nonmarine.

One could evaluate whether ecological speciation is occurring in marine taxa between the modern Gulf and Pacific by focusing on specific traits thought to be under divergent selection pressures between the two habitats, such as body size, and larval or metabolic characteristics that might associate with different salinity or temperature regimes. Differences in gene expression levels across environments can be assessed using RNAseq (transcriptomics), which sequences the messenger RNA produced from the genome to infer how highly expressed a set of genes is with the assumption that genes will be expressed at different levels in different environments (Wang et al. 2009). This method has been used to study hypoxia tolerance in the goby *Gillichthys mirabilis* (Gracey et al. 2001). Additional "common garden" experiments using RNAseq could be used to determine whether any observed physiological differences in expression levels are fixed differences between the populations or plastic, meaning the expression patterns of a population can change in response to the environment.

2. Second-Order Processes— Land-Sea Interactions

2.1. Geological Processes

2.1.1. Geological Assessment of Plio-Pleistocene Midpeninsular Seaways

Over a decade of phylogeographic study has revealed repeated patterns of genetic discordance in topographically low regions along the Peninsula (Riddle et al. 2000; Murphy and Aguirre-León 2002; Hafner and Riddle 2011), but any geological evidence to explain such isolation remains

elusive (Lindell et al. 2006; Brusca 2015). Biologists have attributed this vicariance to transient Plio-Pleistocene age transpeninsular seaways that connected the Gulf to the Pacific Ocean through these narrow passes (figure 2B), temporarily isolating northern and southern terrestrial populations. For seaways to have existed through passes now hundreds of meters above sea level requires that the pass was at sea level when the isolation occurred and has since uplifted, possibly due to its proximity to the rift zone (e.g., Mueller et al. 2009; Mark et al., 2014). Two commonly cited locations for these seaways are (1) the Isthmus of La Paz and (2) the midpeninsular region near the towns of San Ignacio and Santa Rosalía. The proposed midpeninsular seaway locations are similar to that suggested by Helenes et al. (2009) for a ca. 12-Ma seaway that would have connected to a proto-Gulf embayment (see sections 1.1.2 and 1.1.3).

No obvious modern barriers to gene flow exist at these locales, and due to a paucity of alternative explanations (but see Gottscho 2014), seaways remain the favored explanation for the genetic discontinuities observed (Hafner and Riddle 2011). The La Paz seaway is thought to have ended ca. 3 Ma, and would not have significantly affected dispersal of marine species because of its proximity to the entrance of the Gulf, but would have isolated terrestrial taxa. For a review of the La Paz seaway see Gentry (1949) and Murphy and Aguirre-Léon (2002).

The midpeninsular seaway is thought to have flooded ca. 2–1 Ma based on the amount of genetic divergence between northern and southern populations and assumed strict molecular clock mutation rates. A Plio-Pleistocene midpeninsular seaway explanation has gained favor in the biological literature because it accounts for dozens of genetic discordance patterns between northern and southern peninsular populations in one explanation. In the Santa Rosalía area the marine Plio-Pleistocene Santa Rosalía formation and rocks of similar age extend inland, reported at elevations as high as 340 masl (Ortlieb 1978). If this observation is accurate, it could support a midpeninsular seaway hypothesis, suggesting that this region was ~340 m lower during Pleistocene time. Alternatively, marine rocks at these coastal sites could be explained by a local inundation of the Gulf during a sea-level highstand, and therefore do not necessitate, though are consistent with, a midpeninsular seaway.

The principal challenge to the Plio-Pleistocene hypothesis arises from the lack of physical or geological evidence (Lindell et al. 2006); no 2- to

1-Ma sedimentary deposits have been discovered in the purported regions despite reconnaissance missions (e.g., Darton 1921; Beal 1948; Wilson 1948). Lack of sedimentary evidence indicates either that the seaway did not exist, or the sediments were deposited and subsequently eroded. Another major challenge to the Plio-Pleistocene midpeninsular seaway hypothesis comes from geologic data that constrain the timing of uplift that formed the high, east-facing topographic escarpment along the spine
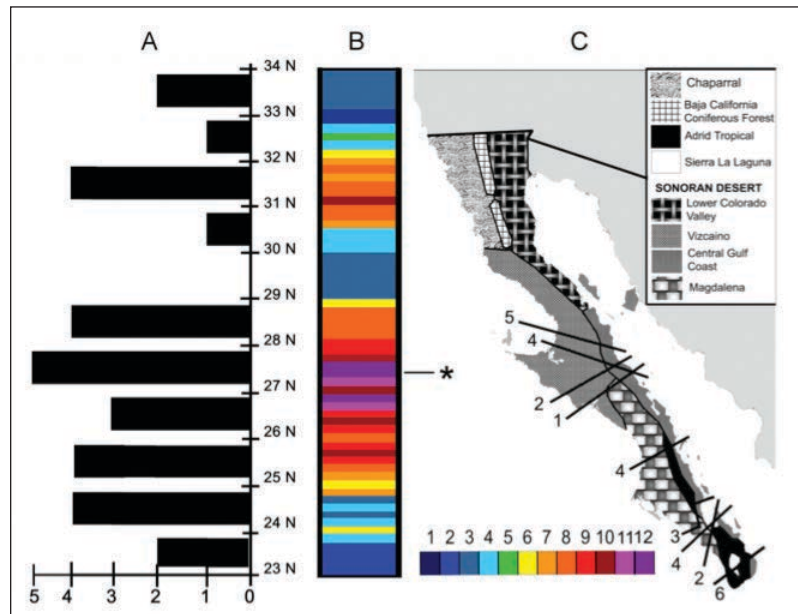
Figure 5: Latitudinal distribution of genetic discontinuities (regions separating two distinct ESUs) along the Baja California peninsula for a subset of 52 taxa analyzed by Munguía-Vega (2011). (A) Frequency of narrow discontinuities (spanning less than 1°20' latitude) in 19 taxa; (B) frequency of narrow and broad (spanning less than 3°0' latitude) discontinuities in 52 taxa, plotted with a resolution of 0°10' latitude; (C) phytogeographic regions on the Peninsula (following Shreve and Wiggins 1964; Wiggins 1980) and approximate location of the discontinuities suggesting the seaways as depicted by different authors. References for the location of proposed seaways: (1) Upton and Murphy 1997, (2) Nason et al. 2002, (3) Alvarez-Castañeda and Patton 2004, (4) Lindell et al. 2005, (5) Crews and Hedin 2006, (6) Lindell et al. 2008. Asterisk indicates area between 27°20' and 27°30'N with 14 genetic discontinuities, the largest value observed in the Peninsula.
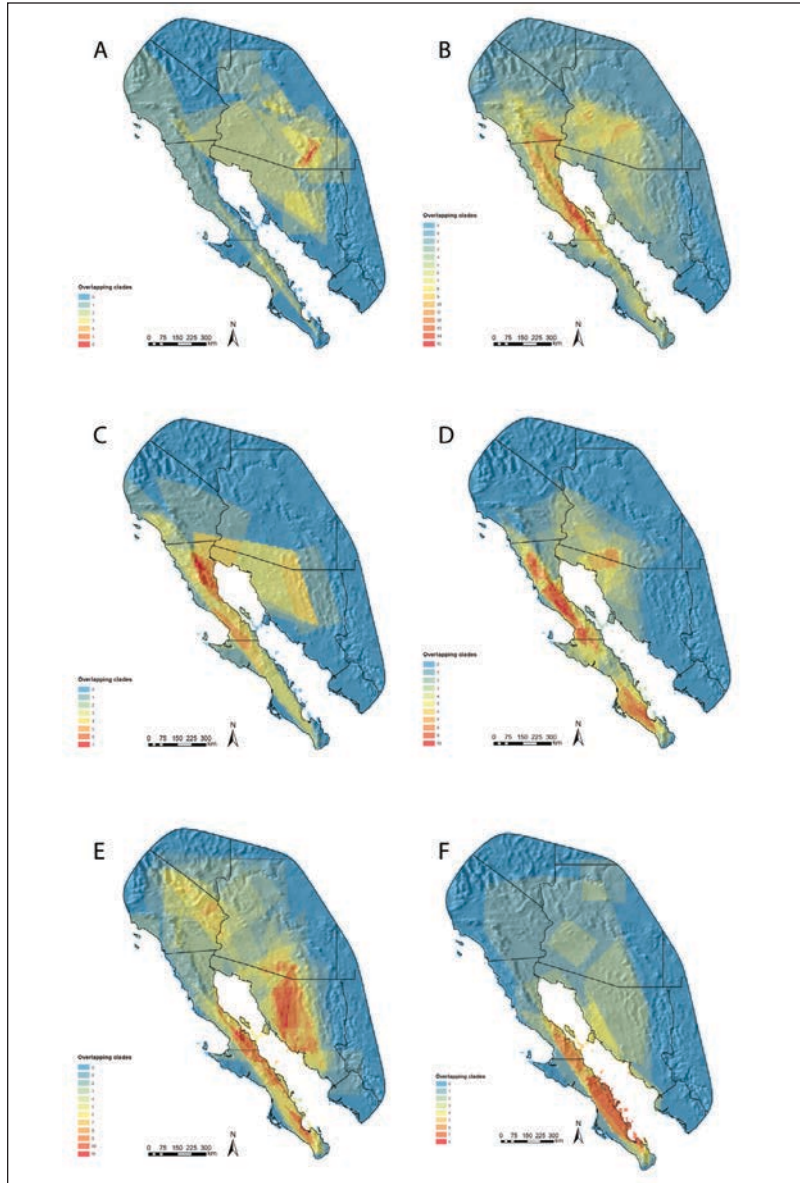
Figure 6: Phylogenetic diversity data illustrating spatial overlap of ESUs from genetic markers (both haploid and diploid) for different taxa: (A) amphibians, N = 4 taxa; (B) reptiles, N = 32 taxa; (C) birds, N = 8 taxa; (D) mammals, N = 14 taxa; (E) invertebrates, N = 21 taxa; (F) plants, N = 6 taxa.
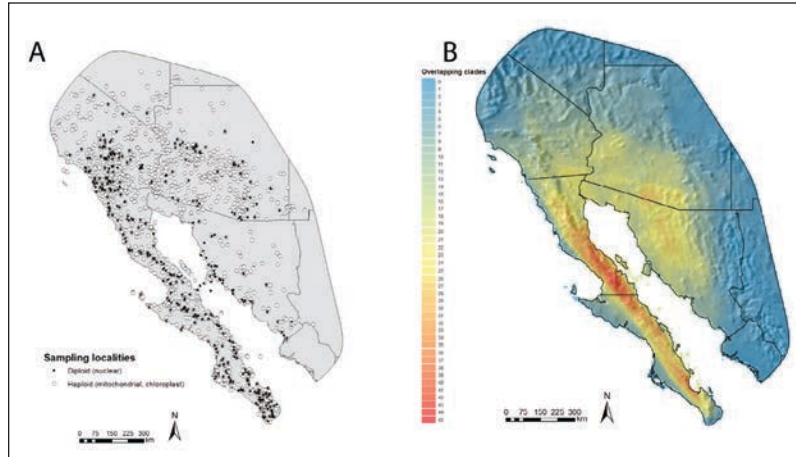
Figure 7: (A) Sampled localities for genetic markers across all taxa with haploid (open circles) and diploid (closed circles) data (N = 85 taxa). (B) Phylogenetic diversity data illustrating spatial overlap of ESUs from genetic markers (both haploid and diploid) for all taxa (N = 85 taxa). See tables S1 and S2 for details on taxa.
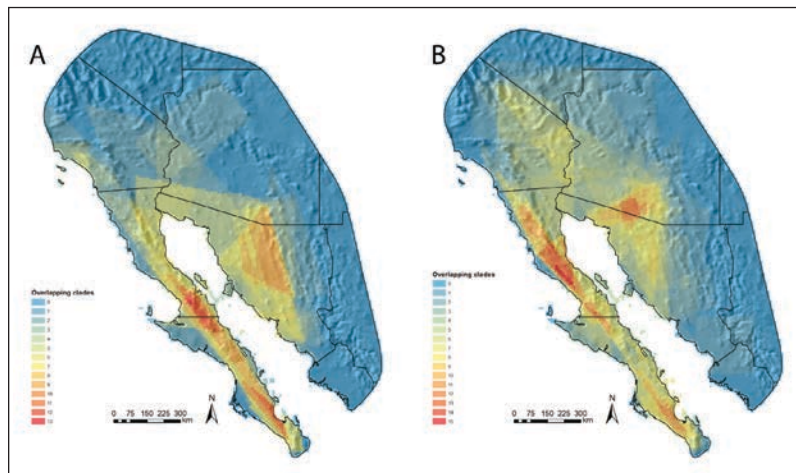
Figure 8: Phylogenetic diversity data illustrating spatial overlap of ESUs from genetic markers (both haploid and diploid) for (A) volant animals, N = 22 taxa, and (B) non-volant animals, N = 57 taxa.

of the Peninsula. Near Loreto, ~15- to 6-Ma lava flows west of the Peninsula's topographic spine have been uplifted and incised, recording a history of vertical tectonic uplift (Mark et al., 2014). Younger lava flows (~3 Ma to recent) have subsequently flowed into these uplift-related canyons. These findings indicate that the majority of vertical tectonic uplift occurred ~6–3 Ma and preclude the possibility that a younger (~2- to 1-Ma) seaway flowed across the central Baja California peninsula since the region had already reached significant elevation. Thus, it is challenging to explain the observed Plio-Pleistocene genetic discordance with a midpeninsular seaway hypothesis.

2.2. Biological Patterns

2.2.1. Genetic Evidence for Midpeninsular Vicariance (Hypotheses 2a, 2b, 2c)

While the geological uplift history makes a 2- to 1-Ma transpeninsular seaway unlikely, this seaway hypothesis motivated much of the terrestrial phylogeographic research in the region. We will review the results of this work generally and formalize the seaway-associated hypotheses.

The meta-analysis presented here of phylogeographic studies along the Peninsula confirms previous work that species exhibit a high degree of geographical structure concentrated in this area (Riddle et al. 2000; Hafner and Riddle 2005; Lindell et al. 2006; Riddle and Hafner 2006; Leache et al. 2007, Munguía-Vega 2011). The frequency of narrow genetic discontinuities departs significantly from a null expectation of uniform geographic distribution over the Peninsula (figure 5A; Munguía-Vega 2011), but the spatial overlap of ESUs is not consistent across organismal groups (figure 6).

Analyses incorporating all previous genetic studies (both haploid and diploid markers) reveal the area of largest phylogenetic diversity in the entire Sonoran Desert is the high-elevation peninsular region between 28°N and 30°N latitude (figure 7B). The northern boundary of this diverse area (30°N) has been previously identified as a region with a high density of genetic discontinuities spanning less than 3º latitude (observed in 52 taxa here; Munguía-Vega 2011; figure 5B). At 30°N, the desert transitions to Mediterranean climate and marks a dramatic change in modern vegetation (Vanderplank et al. 2014). Conservation principles and the Coriolis effect

limit the southward migration of the jet stream to ~30°N regardless of the climate state (Minnich et al. 2014), and might explain the northern extent of the diversity center seen in these analyses. The area of highest phylogenetic overlap (and thus likely highest genetic diversity) for non-volant animals is located around 30°N latitude (figure 8B). The area of highest overlap for volant animals is between 28°N and 29°N (figure 8A). Whether this difference is random or indicates that different mechanisms limit the northern limit of diversity for these two groups is unclear.

The number of ESUs observed within taxonomic groups negatively correlates with the ability of individual species to disperse, as expected (Dawson 2001; Soltis et al. 2006; but see Patarnello et al. 2007). Among taxa, reptiles show the largest average number of ESUs per group for haploid markers (3.32; table S1, figure S1C), whereas the lowest was observed within birds (1.57). For diploid markers, largest values were observed for invertebrates (2.75) and lowest for birds (1) (table S2, figure S2G). Within animals, volant animals showed lower levels of genetic structure (average 2 ESUs per taxa for haploid markers) compared to non-volant animals (2.98) (figure S3), but this pattern was not observed for diploid markers (table 2).

Genetic discontinuities in this midpeninsular region in our meta-analysis are broader than authors previously suggested, and vary latitudinally by taxonomic group (figure 6). Both San Ignacio and Agua Armada passes, which were suggested sites of Plio-Pleistocene transpeninsular seaways, are narrow (35–40 km between the northern and southern 400-m contours). The expectation from flooding of these passes is that low-dispersal species (e.g., rodents, reptiles) would be genetically discordant (different) on either side of the barrier (hypothesis 2a), and that high-dispersal species (birds, wind-dispersed plants) would disperse over the barrier and exhibit no genetic discordance (hypothesis 2b). In contrast to this expectation, plants exhibit the greatest genetic discordance in this region (figure 6F). Additionally, both volant (figure 8A) and non-volant animals (figure 8B) exhibit discordance in the middle of the Peninsula.

Importantly, these spatial analyses are only as robust as the sampling density on which they are based, and it is likely many of these studies have sampling schemes that preclude fine-scale geographic interpretation. The average number of sampled localities included in each study is 20, but ranges from 8 (birds) to 40 (reptiles) (table 2). Because the length of the Peninsula is ~1,200 km, 10 sampling locations distributed evenly along a longitudinal transect yield only 1 sample per 120 km. For

comparison, the distance between the Agua Armada and San Ignacio seaway passes is only ~65 km. This lack of spatial resolution should be considered when drawing inferences from such data and should guide sampling efforts for future studies.

2.2.2. Marine Patterns and the Midpeninsular Seaway (Hypotheses 2d, 2e)

Riginos (2005) uncovered a north-south genetic discontinuity to varying degrees in five nearshore fishes in the western Gulf, and other studies revealed similar patterns (Stepien et al. 2001; Hurtado et al. 2013). North-south genetic discordance was interpreted as consistent with a midpeninsular seaway, which would have produced a break in otherwise contiguous habitat for nearshore inhabitants. However, fishes with pelagic larval phases can often disperse well. For instance, given a 30-day larval duration, strong Gulf currents can transport larvae up to hundreds of kilometers from the source (Munguía-Vega et al. 2014; Soria et al. 2014), suggesting that even in the presence of a seaway, larvae should likely have maintained genetic connectivity. Also, the precise geographic site of discordance differs between species, which might be expected given species-specific factors governing post-barrier gene flow. Alternatively, the midpeninsular region marks a zone of ecological transition that may better explain these results. The midpeninsular seaway passes (Agua Armada and San Ignacio) are located between present-day northern and southern seasonally driven gyres in the Gulf (Lavin et al. 1997; Marinone 2003) and are currently characterized by cooler temperatures at least half the year (Lluch-Cota et al. 2007). The site of discordance is also near the Midriff Islands where seasonal upwelling occurs (Zeitzshel 1969), and roughly coincides with the northern extent of mangrove habitat in the western Gulf (Whitmore et al. 2005; Aburto-Oropeza et al. 2008). Therefore, any of these ecological factors could produce or contribute to a north-south genetic discordance in the absence of a seaway.

2.3. Land-Sea Interactions: Future Work

More detailed reconstructions of past topography in the midpeninsular region would improve our understanding of land-sea interactions and enable biological interpretations to progress in a geologically feasible framework. Additionally, geologists can use available volcanic dates in
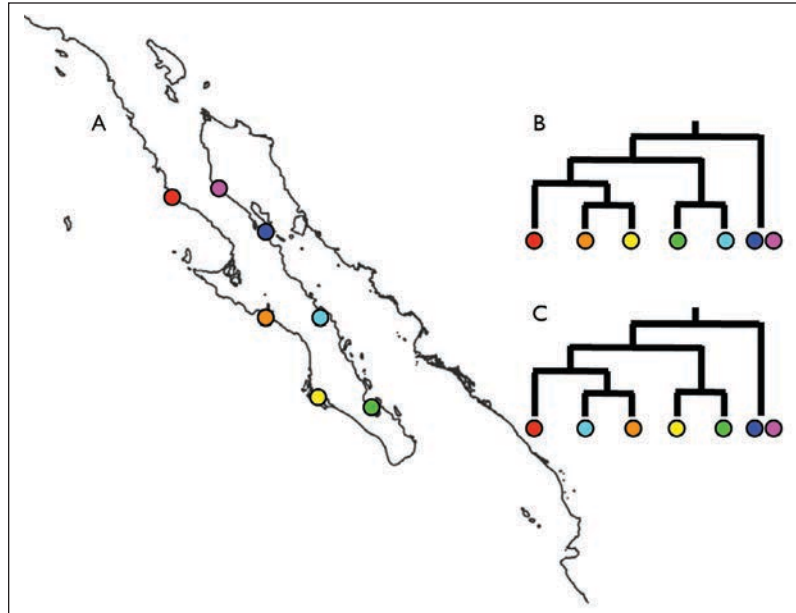
Figure 9. (A) Map of the Baja California coastal marine populations with each population's genetic identity denoted by color (red to violet Hypothesized topologies are presented under two different dispersal scenarios: (B) a null isolation by distance model and (C) topology expected with addition of gene flow through a midpeninsular seaway.

the region to evaluate candidate regions where Plio-Pleistocene strata may be exposed in these passes, which would provide more direct evidence regarding any seaway or regional flooding at this time.

For biological interpretations, it is necessary to learn whether the differences observed between patterns of haploid and diploid markers (figures S1, S2; see section 4.2) are due to mutation rate or marker characteristics (e.g., effective population size). If differences were due to mutation rate it would mean the isolating event was biologically relevant and nuclear (diploid) markers generally evolve too slowly to record the event. If, however, discordance in the mtDNA (mitochondrial DNA) lineages results from the fact that mtDNA records events more readily due to its haploidy and single-parent inheritance, it might indicate that the event, though widespread taxonomically, may not have been as significant as previously thought. Developing robust nuclear datasets with resolution similar to mtDNA could clarify whether this signal is observable in diploid markers. Single Nucleotide Polymorphisms (SNPs)

or sequence data through targeted approaches, such as the quickly evolving flanking regions of ultraconserved elements (Faircloth et al. 2013), restriction associated DNA (Miller et al. 2007), or introns, may give comparable nuclear data. Using taxa for these studies that previously exhibited mtDNA discordance provides a natural comparison. Additionally, genetically underrepresented groups (e.g., amphibians, birds) should be prioritized in future studies.

It is possible to use marine taxa to further test the midpeninsular seaway hypothesis. Rather than preventing gene flow along the western coastline of the Gulf as previously studied, for some marine species a transpeninsular seaway would have facilitated gene flow and/or dispersal between the Pacific and Gulf, which today is limited or entirely inhibited for many species by prohibitively warmer southern waters (Bernardi et al. 2003). Under a null hypothesis with no seaway, isolation by distance around the Peninsula is expected, where genetic relatedness between populations is primarily a function of coastal distance between them (figure 9B). The alternative hypothesis includes dispersal facilitated between the Gulf and Pacific Ocean through a midpeninsular seaway. Under this experimental hypothesis, individuals adjacent to the seaway region along the Gulf and Pacific coasts are more closely related than under the null hypothesis (figure 9B compared to 9C). The relatedness of seaway-adjacent populations can be assessed topologically in tree reconstructions, through assignment tests, or via metrics such as Fst (fixation index). If the alternative hypothesis is supported, it would provide independent support for the midpeninsular seaway hypothesis that is less confounded by terrestrial ecological factors (see section 3.2).

3. Third-Order Processes— 100-kyr Glacial-Interglacial Cycles

3.1. Climatic Phenomena

3.1.1. Climate History

The middle Miocene climate transition (14.2–13.8 Ma) is observed in isotope records from deep-sea sediments, which record a dramatic cooling episode of 6–7°C (Shevenell et al. 2004), marking the onset of

long-term cooling during which Antarctica's ice volume dramatically grew (Zachos et al. 2001). During the middle Miocene, coastal upwelling intensified along California (White et al. 1992), which imparted a tempering effect on regional climate, delivering cool, nutrient-rich waters that promote primary production and summer fog (for review of biological responses, see Jacobs et al. 2004). Upwelling intensification also led to a general aridification of the western coast, permitting more arid-adapted species over time and the precursor community to the Sonoran Desert (Axelrod 1979), which existed by 8–5 Ma. In late Miocene (11.6–5.3 Ma), offshore sea surface temperatures increased substantially from a winter minimum of 10°C to 17°C by the earliest Pliocene (Barron 1973). Sea surface temperatures off the California coast were still several degrees warmer than today during the early Pliocene warm period (Dekens et al. 2007), beginning 4.6 Ma and ending ~3 Ma with the onset of northern hemisphere glaciations, driven primarily by cyclical changes in Earth's axis and orbit around the sun. Between ca. 3 and 0.8 Ma northern hemisphere glaciations occurred with a 41-kyr periodicity, after which the periodicity increased to 100 kyr, yielding larger temperature and sea-level fluctuations (Mudelsee and Schulz 1997). During these later glaciations, sea levels lowered 100–150 meters below sea level (mbsl), dramatically changing island footprints and forming some land bridges (figure 2C). Since the last glacial maximum (LGM) ca. 20 ka (thousand years ago), temperatures have increased, with slightly higher than present temperatures at the start of the Holocene (ca. 10 ka). Temperatures decreased during the middle Holocene Climate Optimum, which also brought drier conditions in some places (Steig 1999), but the Mexican monsoon climate continued.

3.1.2. Future Climate Change Predictions

Climate change research predicts globally increased temperatures, regional aridification, and increased frequency and/or magnitude of extreme weather events (e.g., droughts, floods, storms) and a rise in mean sea level by 2100 (IPCC 2012). Although the details of how these effects will manifest on the Peninsula and the Sonoran Desert are uncertain, trends are suggested. Some (though not all) Complex General Circulation Models predict El Niño Southern Oscillation (ENSO) activity will increase in strength or become more frequent (Collins et al. 2010). Bakun (1990) proposed that if climate change increased the strength of

alongshore winds, then coastal upwelling would intensify along the California coast, increasing both nutrient availability for primary producers and coastal summer fog, which is an additional water source for coastal vegetation in rain-limited climates. The Gulf of California, however, might limit the offshore-onshore temperature disparity by moderating the land-sea temperature disparity and thereby limit or prevent such an increase in summer fog. Lower annual precipitation, primarily through decreased winter rainfall, is predicted, along with lower snowpack volume in high-altitude regions that will melt earlier in the year (Seager and Vecchi 2010). Under increased temperature and decreased precipitation expectations, Ecological Niche Modeling predicted extensive turnover (>30% of species modeled) for those species living on the Peninsula (Peterson et al. 2002). If accurate, the ecosystem constituents observed today might be different in the future, which is of particular concern for endemic species that would have to migrate or face extinction. High-altitude chaparral communities, by contrast, are suggested to be relatively impervious to future climate change (Minnich et al. 2014). Finally, damming and diversion of river waters has already had a marked impact, particularly in the Colorado River delta, which has lost most if not all of the freshwater and sediment discharge it previously had (Brusca 2015), with significant impacts on biology (Kowalewski et al. 2000). Any future regional aridification will further perturb this highly modified hydrographic state, the consequences of which are difficult to predict, but will be challenging for the artisanal fishermen and coastal towns that depend on the Gulf's productivity.

3.2. Biological Patterns

3.2.1. Glacial-Interglacial Vegetation Changes

Significant differences exist between the vegetation during glaciations and what we observe today. Desert scrub, the dominant Sonoran Desert vegetation type today, probably existed for only 10% to 20% of the Pleistocene, unlike open woodland vegetation, which was widespread for ca. 80% to 90% of glacial periods (Van Devender 2002). Fossil packrat middens (*Neotoma* sp.) document expansion of temperate and mesic or moderate moisture-adapted trees and shrubs into desert elevations since the last glacial maximum (LGM) ca. 20 ka (Betancourt et al. 1990),

though midden data may be biased toward mesic-adapted species in rocky areas, thus overestimating climate-associated change (Minnich et al. 2014). In the Arizona Upland subdivision of the Sonoran Desert (300–1,550 masl), single-leaf pinyon-juniper woodlands with shrub live oak and Joshua tree dominated during the LGM. Desert trees and scrub plants fully established by 9 ka, when the summer rainfall climate regime was established. More subtropical associated desert plants (e.g., paloverde, saguaro) didn't arrive until 4.5 ka (Van Devender 1990; Metcalfe 2006), and the Sonoran Desert established its present-day boundaries ca. 6 ka (Thompson and Anderson 2000).

On the Peninsula, pinyon-juniper and chaparral species probably extended about 400 km south of their current distributions ca. 10 ka, while the mid-Peninsula may have experienced the Mediterranean climate of southern California and northern Baja California today (Metcalfe 2006) with almost no areas of pure desert vegetation north of 27°N (Holmgren et al. 2011). Lake sediment cores from Laguna Chapala and Laguna Seca in the northern Peninsula support a change from wetter to drier conditions during the early to middle Holocene (Davis 2003; Metcalfe 2006; Roy et al. 2010). Packrat middens from Sierra San Pedro Mártir 650–900 masl record the expansion downslope of chaparral species during the latest Pleistocene followed by their rapid replacement by Sonoran Desert species during the early Holocene (Holmgren et al. 2011). Cataviña (640–680 masl) and San Fernando middens suggest a pinyon-juniper woodland/chaparral in the LGM was replaced by mesquite, and then cactus by middle Holocene ca 5 ka (Van Devender 2002; Metcalfe 2006). In the mid-Peninsula (Sierra San Francisco) a 10.2-ka midden preserves *Juniperus californica* and other chaparral species (laurel sumac, *Malosma laurina*; Baja manzanita, *Arctostaphylos peninsularis*; American wild carrot, *Daucus pusillus*) at 780 masl, suggesting a mild Mediterranean climate 5°C to 6°C cooler with at least twice the winter precipitation of today (Rhode 2002). These cooler conditions in the southern Peninsula are further supported by chaparral communities isolated on high mountain peaks south of 28°N (Moran 1983b).

While desert scrub expanded and the chaparral/woodland vegetation contracted to higher elevations and latitudes toward their current distributions ca. 11 ka, small, isolated areas of mesic environments remained in sheltered canyon oases (Arriaga and Rodriguez-Estrella 1997) and montane habitat above 800 masl throughout the Peninsula (Moran 1983b; Minnich et al. 2014).

3.2.2. Climate, Refugia, and Genetic Discontinuities (Hypotheses 3a–3e)

Glacial refugia are populations that survive glaciations and harbor the majority of the modern genetic diversity within a species (Hewitt 2000, but see Petit et al. 2003). The location, nature, and expansion from refugia on the Peninsula remain unclear.

Northern (Nason et al. 2002) and southern (Garrick et al. 2009) expansion from refugia has been observed along the Peninsula in arid-adapted succulent plant taxa, though the southern expansion results may instead result from differential pollination rates. Instead of unidirectional postglacial migration, topographic relief along the Peninsula may have provided an array of microclimates that hosted refugia during the LGM (Garrick 2010; hypothesis 3c). This view is supported by our analyses showing that areas of highest genetic (phylogroup) overlap correspond to high-elevation ranges in the Peninsula, Sonora, and southern Arizona (hypothesis 3e; figures 7B, S1B, S2B). If the concentration of phylogroups corresponds with historical refugia, then volant animals were located farther south than non-volant animals, both on the Mainland and on the Peninsula. The locations, however, are different for each animal taxonomic group (figure 6); reptile diversity centers between 28°N and 30°N in high elevations of the Peninsula. In contrast, maximum diversity overlap for birds is north of 30°N at higher elevations, and in the lowlands of the lower Colorado Valley east of the mountains. For mammals, the highest diversity centers between 28°N and 30°N at lower elevations west of the mountains, and in the Magdalena plains north of La Paz. Invertebrates and plant patterns were more similar than any other groups and included higher elevations around 28°N latitude and in Baja California Sur (hypothesis 3b). This observation supports ecological co-associations, which are constraints imposed by biotic interactions between insects, herbivores, parasites, and their host plants where one group cannot thrive without the other and vice versa (Garrick et al. 2013). It is therefore expected that distributions (and thus diversity patterns) of such groups are similar. In summary, if individuals retreated to mountainous regions during glaciations, it could create areas of low ESU overlap in the topographically low regions between mountains that could resemble a historical barrier, like a seaway.

Discontinuities for some peninsular species have been explained by regions of poor habitat quality and low density of individuals (e.g., Leache

and Mulcahy 2007; Garrick et al. 2009). When species encounter ecological gradients or abrupt changes in climate individuals may adapt to local environments (Grismer 2002), as suggested elsewhere (Lapointe and Rissler 2005; Davis et al. 2008). The strong 30°N non-volant genetic discontinuity (northern diversity limit) corresponds with the transition between the cool, mesic California coastal scrub and chaparral vegetation, and the arid, temperate Vizcaíno region at the start of the Sonoran Desert (figure 5C). This climatic transition is the southern extent of the jet stream, which was likely stable throughout Pleistocene glacial-interglacial cycles (section 2.2.1; Minnich et al. 2014). Climatic stability may have contributed to the high levels of endemism in the California Floristic Province–Sonoran Desert transition zone (Vanderplank et al. 2014) as seen in other Mediterranean regions (Cowling et al. 2014). In other areas, such as California, transition zones between animals and plants known or suspected to hybridize are also located across such climatic gradients (Remington 1968). Another example of regional climate anomalies is the Vizcaíno peninsula (Punta Eugenia), which diverts cold upwelling Pacific waters offshore and marks the transition to increased summer rainfall in the south (Minnich et al. 2014). This transition zone coincides geographically with the midpeninsular discontinuity. Depending on when this phenomenon began, it may have contributed to the midpeninsular genetic discontinuity, or to differential selection pressures across this transition zone that could produce a discontinuity over time. Another alternative, more recently posited hypothesis attributes such biological transition zones to Pacific fracture zones (Gottscho 2014).

Climate-driven ecological gradients may have limited the migration of individuals at intermediate elevations such as mountain passes. Distributions of well-adapted animal subspecies contracted and expanded with different vegetation types during glacial fluctuations (Van Devender 2002). Some desert scrub inhabitants from the Sonoran Desert, such as reptiles (*Sauromalus obesus*, *Uta stansburiana*, *Aspidoscelis* [*Cnemidophorus*] *tigris*, *Trimorphodon biscutatus*, *Hypsiglena torquata*, *Lichanura trivirgata*), an amphibian (*Bufo punctatus*), and mammals (*Dipodomys merriami*, *Neotoma lepida*, *Chaetodipus baileyi*, *Thomomys bottae*, *Peromyscus* sp., *Ammospermophilus* sp.), were found in LGM–early Holocene woodland packrat middens from California and Arizona (Mead et al. 1983; Van Devender 1990). Such occurrences indicate many desert animals were not restricted to southern refuges during glacial periods but remained *in situ*. These observations suggest the phylogeographic patterns observed for some desert reptiles and mammals may not have arisen from

extinction and recolonization from southern refugia, but by adaptation to different areas with divergent selection pressures (Davis et al. 2008). A packrat midden from the Lower Colorado River basin (>55 ka) showed a mixture of woodland and desert species that might have survived in small, separate populations within dry patches of woodlands, opposing the traditional concept of desert refugia (Holmgren et al. 2014).

The absence of a desert refugium in the rain shadow of the Sierra San Pedro Mártir (one of the most arid regions of the Sonoran Desert) and the individualistic nature of species' responses to climatic change (Whittaker 1953; Van Devender 1977; Huntley 1991) suggest the concept of a desert refugium should be reconsidered. It seems unlikely that a community of arid-adapted taxa resembling modern Sonoran Desert communities existed during glacial periods. Instead, arid-adapted taxa may have segregated by niche and assembled at the onset of modern climatic conditions ca. 6 ka to form the communities we now term the Sonoran Desert.

3.2.3. Plant Distribution Patterns (Hypothesis 3f)

To define the biogeographic patterns and links between the Peninsula and Mainland we identified plant species co-distributed between them. Through assembly of trans-Gulf floristic listings, georeferenced herbarium patterns for 526 disjunct taxa (table S2) were mapped and four biogeographic patterns were identified.

Widespread taxa (N = 346; table S2): The majority of species shared between the Peninsula and Mainland are widely distributed throughout the Sonoran Desert, and generally extend far beyond the boundaries of the desert. Most have long-range dispersal syndromes and produce a widespread biogeographic pattern.

Northern taxa (N = 20; figure 10A; table S2): A group of predominantly temperate species wraps around the northern head of the Gulf. They are lowland desert species (e.g., *Ephedra aspera* and *Peucephyllum shottii*) or occur primarily at higher elevations (e.g., *Crossosoma bigelovii*, *Rhus kearnyi*, and *Sideroxylon leucophyllum*).

These species may have been distributed above 32°N and dispersed southward to the Peninsula and Sonora. Many of these species are on the Peninsula and Midriff Islands across the Gulf, but remain confined to the northwest corner of Sonora. The horseshoe distribution pattern resembles that of ring species complexes, which is a unique form of speciation in which the terminal populations (those most distant) are
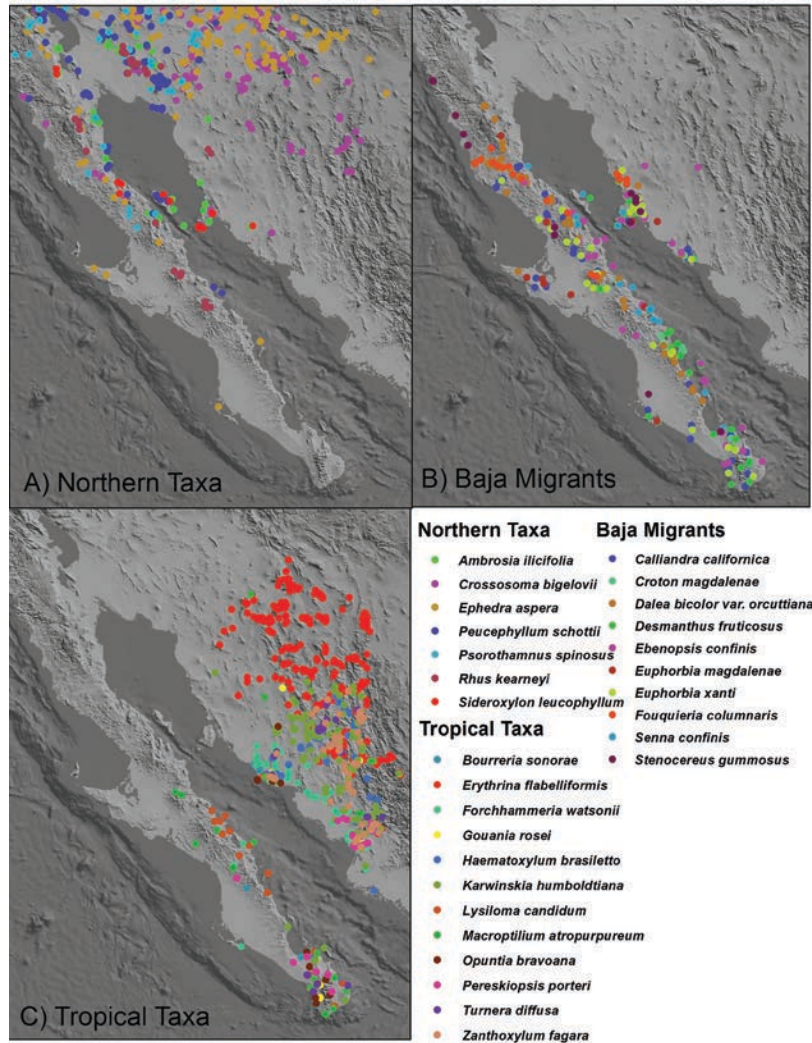
Figure 10: Three distribution patterns are shown, including (A) northern taxa, distributed in a horseshoe pattern around the head of the Gulf, (B) Baja migrants, widely distributed throughout the Peninsula, Midriff Islands, and very limited in Sonora, and (C) tropical taxa, which have southerly distributions with varying northern limits. Sample dots are color-coded according to species (bottom right panel).

reproductively isolated, but remain genetically connected through the intervening populations (Irwin et al. 2001, 2005). For example, Baja California and Arizona/Sonora populations of the *Agave deserti* complex (Navarro-Quezada et al. 2003) are reciprocally monophyletic and the Gulf is a reproductive barrier (Gentry 1978). If such trans-Gulf gene flow at the southern range of such a species is absent, studies into whether ring speciation is occurring and its prevalence among species with this distribution pattern might be of interest.

Baja migrants ($N = 48$; figure 10B; table S2): First identified by Cody et al. (1983), a sizable group of plants is broadly distributed over the Peninsula, across the Midriff Islands, and narrowly on the Sonoran coast. Unlike the northern taxa group, these species are not distributed north, or around the head, of the Gulf.

A hypothesis for the origin of this pattern is that species migrated from the Peninsula to the Mainland via the Midriff Islands. Previous work shows that the Mainland clades, when present, often nest within peninsular ones (Clark-Tapia and Molina-Freaner 2003; Garrick et al. 2009, but see Fehlberg and Ranker 2009). Sea-level lowstands associated with glaciations would have increased island footprints and could have facilitated this gene flow.

Tropical taxa ($N = 112$; figure 10C; table S2): Species with tropical affinities are clustered to the south on either side of the Gulf in Sonora near Guaymas/Alamos and the Cape region of Baja California Sur. These taxa have varying northern limits as they follow the foothills of the Sierra Madre Occidental on the Mainland or the peninsular range in Baja California.

The southern boundaries of the Sonoran Desert are near Guaymas, Sonora (27°55'N), and farther south at the Cape region in Baja California Sur (23°32'N). These areas have mean annual precipitation of 200–400 mm, of which more than half arrives as summer rain (Cody et al. 1983), and might account for the large number of tropically affiliated plants shared across the Gulf.

3.3. Climatic Patterns: Future Work

Future work should test whether the absence of genetic overlap of species in the topographically low midpeninsular region is due to montane glacial refugia or abiotic clines with north-south differential local adaptation, among other hypotheses. If the northern and southern

mountains hosted glacial refugia, then within-species genetic diversity should be highest in those regions and decrease toward low-lying regions, and display a strong spatial pattern. Analyses using haplotype networks, or new spatially explicit genetic software programs such as BioGeoBEARS (Matzke 2013), may offer insight given enough data and proper spatial sampling. Such programs can model or test different historical biogeographic scenarios and, given the genetic data, indicate a most probable history. Performing such analyses comparatively on previously studied species would reveal whether this history is shared. The role of local adaptation to abiotic clines could be tested through gene expression or genome methylation studies, which would reveal genes that are differentially expressed between northern and southern populations across numerous taxa. This information would provide specific genes and physiological pathways that are facilitating local adaptation to abiotic factors such as temperature and precipitation.

Our analysis shows strong geographic, taxonomic, and genetic marker biases in previous phylogeographic work that should be improved in future studies (table S1). Sonora is the least sampled area in the Sonoran Desert, particularly for diploid markers (figure S2A). More studies of birds, plants, and amphibians should be included as they compose 9%, 7%, and 5% of the total studies, respectively. Studies using nuclear markers are lacking (only 25.8%), and genetic overlap of distinct ESUs is most commonly observed in studies using haploid markers (compare figures S1 and S2). Even microsatellite data are largely absent, and it is a widely used approach to assess postglacial expansion patterns (e.g., Heuertz et al. 2004). Studies in the Sonoran Desert region have yet to incorporate next-generation sequencing technologies and genomic analyses (e.g., O'Neill et al. 2013). Such methodologies (McCormack et al. 2013) should be applied to desert-woodland/chaparral transition zones such as the La Rumerosa or Magdalena-Cucurpe to infer the histories of modern desert edge communities. Exemplar taxa in the sky island relictual habitats could also be investigated to see if these regions are, in fact, stable over Pleistocene time. Finally, ancient DNA from packrat middens would provide an ancient analogue to modern conditions, perhaps with the ability to assess historical biogeographical patterns as a comparison to today.

4. Conclusions

4.1. Summary of Findings

Rifting of the Baja California peninsula from Mainland Mexico and formation of the Gulf of California produced speciation of terrestrial taxa (e.g., reptiles, amphibians, arachnids) that do not disperse around or across the Gulf. More species-level genetic work is needed to address whether similar divergence occurred frequently in highly dispersive groups (e.g., plants and birds). The high degrees of insular, peninsular, and Gulf endemism stem from this rifting combined with subsequent isolation. Flooding of the modern Gulf (ca. 6 Ma) created new marine habitat that likely exerts different selection pressures on its marine inhabitants compared to the Pacific Ocean, and may be a source of ecological speciation, though explicit testing is required. The proto-Gulf hypothesis of an old (ca. 15- to 12-Ma) marine embayment differs in detail between biology and geology. Geological evidence for its location and cause is lacking, but reworked middle Miocene marine microfossils and synchronous speciation of Gulf endemic and non-endemic sister species of east Pacific bay gobies may suggest the presence of a middle Miocene marine embayment somewhere in northwestern Mexico. The precise location, size, and shape of such an embayment remain unknown.

Physical evidence for midpeninsular seaways is absent and recent uplift estimates indicate these passes may have been floodable during middle Miocene time, but are unlikely to have flooded during the Plio-Pleistocene. Additional support against Plio-Pleistocene seaways comes from our analyses showing that north-south midpeninsular genetic breaks are also observed in highly dispersive taxa, which would probably have been able to disperse over such a barrier. We offer alternative explanations for the ubiquitous north-south discordance pattern observed: (1) Stability and range of microhabitats afforded in montane regions to the north and south may have afforded glacial refuges so populations were repeatedly isolated, or (2) there was differential north-south adaptation to temperature and precipitation gradients; each of these explanations would explain why midpeninsular valleys exhibit low ESU overlap.

Four plant species distribution patterns are uncovered that may originate from rifting and/or postglacial migration. Future genetic studies should focus on these species to understand connections between the Mainland and peninsular portions of the Sonoran Desert. Packrat midden

data indicate that glacial refuges probably did not resemble modern Sonoran Desert communities. Instead, response to climatic events may be much more individualistic and less community oriented (except for obligate or co-associated species). We suggest the opportunities to advance this knowledge are in application of large nuclear and ancient DNA data.

Finally, the analyses performed herein reveal a major bias toward taxonomic group (reptiles and mammals) and mtDNA (table 2). We suggest that, to differentiate between competing hypotheses and eliminate confounding variables, these patterns be reevaluated with nuclear data, for which several methods are suggested (section 2.3). Additionally, alternative approaches using topographical analysis and marine species would provide novel, independent perspectives on long-debated hypotheses.

4.2. Caveats and Concerns of Mitochondrial Genetics

Genetic discontinuities decrease quickly, independent of a population's size, after gene flow is restored between temporarily isolated populations (Irwin 2002). However, the non-recombining (i.e., it acts as a single gene) nature and single-parent inheritance pattern of the mitochondrion can make this discontinuity observable much longer in mitochondrial than nuclear DNA (Rubinoff et al. 2006). Therefore, the lasting discordance observed among many taxa along the Peninsula may be biased by a heavy reliance on mtDNA.

Another caveat is that since the mitochondrion does not recombine, mtDNA-based interpretations may reflect a gene lineage and not necessarily the true history of the populations. In the absence of several independent markers, stochastic coalescence processes may drive patterns and interpretations in the absence of a "real" biological signal. Munguía-Vega (2011) demonstrated that mtDNA discontinuities can arise spontaneously if the migration rate is only one successful migrant per generation between populations. As an example, reciprocal mitochondrial monophyly could arise (assuming one generation per year) in just 20,000 years (e.g., since the LGM, Andrews and Barry 1978), with a census size of 400,000 individuals (e.g., $Ne = 20,000$, 5% of census size), without any physical barrier. These findings signify that continuously distributed species with restricted dispersal can form genetic discontinuities in regions

where migration has never been completely impeded, and therefore an impassable physical barrier is not always required.

Another process that may be occurring in some species is reinforcement, in which permanent biological barriers such as low hybrid fitness, incompatibility of alleles, and postzygotic isolation mechanisms limit interbreeding between previously isolated populations (Crews and Hedin 2006). The hybrids form in the zone of secondary contact (i.e., purported seaway region), the width of which is proportional to fitness of the hybrids. In this case, strong selection pressure against hybrids would be required to explain the narrow north-south genetic discontinuity, but this could be aided by ecological gradients imparting divergent selection regimes during isolation (Barton and Hewitt 1985; Phillips et al. 2004; Macholan et al. 2007). Whether selection against hybrids in the secondary contact zone would affect so many taxa similarly is uncertain, and the general absence of morphological diversification has termed this "cryptic" divergence.

4.3. The Assumption of Parsimony

Parsimony, the assumption that the simplest explanation is most likely, is among the most widely used assumptions in biology, yet its veracity and appropriateness are rarely testable. To date, researchers have favored parsimonious explanations where a single event (i.e., a seaway) is used to explain dozens of intra-specific patterns of diversity and discordance among co-distributed species (as theory advises). However, this review suggests that a single discrete explanation is sometimes insufficient to account for the patterns observed, many species with complex histories may not be shaped by a single barrier, and that barrier or event may not affect all species similarly. The actual biodiversity patterns can result from different underlying factors operating at different times and locations that result in similar phylogenetic patterns (i.e., pseudocongruence) (Lapointe and Rissler 2005; Feldman and Spicer 2006; Riddle and Hafner 2006; Soltis et al. 2006; Chatzimanolis and Caterino 2007). This vicariance explanation also highlights what may have been a reluctance to call on ecological factors as primary agents in isolation and diversity patterns along the Peninsula.

As a region with complicated tectonic and climatic histories, the Gulf of California and broader Sonoran Desert constitute a setting where the assumption of parsimony in interpreting evolutionary patterns should be reconsidered.

4.4. An Interdisciplinary Future

Significant debates have persisted in geology regarding existence and nature of a proto-Gulf of California, timing and details of modern Gulf formation, and translation and structure of the Peninsula through time. Similar debates within biology regarding presence of a midpeninsular seaway, the role of abiotic gradients, and Pleistocene refugia have continued as well. Widespread biological patterns, however, are usually the genuine result of physical or climatic processes (e.g., seaways, rifting, glacial-interglacial oscillations), and can thus be used to inform the nature of such underlying events even in the absence of physical evidence or reason to search. Biological patterns, however, can also arise from random

Table 2. *Average number of ESUs, sample size (number of taxa, N) and standard deviation (SD) for taxonomic groups, haploid and diploid markers, and average number of sampled localities per taxon.*

Taxa		Haploid	Diploid	Sampled localities per taxa
Amphibians	N	4	2	
	Average	2.8	2.5	20.5
	SD	0.5	0.7	
Birds	N	7	2	
	Average	1.6	1	7.9
	SD	0.5	0	
Invertebrates	N	17	4	
	Average	2.5	2.8	20.3
	SD	1.6	1.5	
Mammals	N	14	3	
	Average	2.4	2	20.2
	SD	1.3	1	
Plants	N	2	5	
	Average	3	1.6	22.5
	SD	1.4	0.9	
Reptiles	N	28	4	
	Average	3.3	1.5	40.4
	SD	2.0	0.6	
Volant animals	N	16	5	
	Average	2	2.2	
	SD	1.0	1.6	
Non-volant animals	N	54	10	
	Average	3.0	1.9	
	SD	1.8	0.7	

or biotic factors, in which case geological evidence can rule out competing external mechanisms, and remains the only source for absolute dating. Each discipline provides an opportunity for independent knowledge and evaluation that should be used to advance the understanding within each field, particularly when faced with conflicting evidence within a discipline. In light of the emerging field of geogenomics and a broad emphasis on interdisciplinary research, our review suggests that to move such debates forward and construct a holistic understanding, synthetic, cross-disciplinary research is not just innovative, but necessary. ❖

References

Aburto-Oropeza, O., Ezcurra, E., Danemann, G., Valdez, V., Murray, J., and Sala, E. (2008) Mangroves in the Gulf of California increase fishery yields *Proceedings of the National Academy of Sciences* 105:10456–10459.

Alvarez-Castañeda, S. T., and Patton, J. L. (2004) Geographic genetic architecture of pocket gopher (*Thomomys bottae*) populations in Baja California, Mexico. *Molecular Ecology* 13:2287–2301.

Andrews, J. T., and Barry, R. G. (1978) Glacial inception and disintegration during the last glaciation. *Annual Review of Earth and Planetary Sciences* 6:205–228.

Aragón-Arreola, M., and Martín-Barajas, A. (2007) Westward migration of extension in the northern Gulf of California, Mexico. *Geology* 35:571–574.

Arriaga, L., and Rodriguez-Estrella, R. (1997) *Los Oasis de la Peninsula de Baja California*. Centro de Investigaciones Biologicas del Noroeste, S.C., La Paz.

Atwater, T. (1970) Implications of plate tectonics for the Cenozoic evolution of western North America. *Geological Society of America Bulletin* 81:3513–3536.

Atwater, T., and Stock, J. (1998) Pacific–North America plate tectonics of the Neogene southwestern United States: An update. *International Geology Review* 40:375–402.

Axelrod, D. I. (1979) Age and origin of the Sonoran Desert. *California Academy of Sciences Occasional Paper* 13:1–74.

Baker, P. A., Fritz, S. C., Dick, C. W., Eckert, A. J., Horton, B. K., Manzoni, S., Ribas, C. C., Garzione, N., and Battisti, D. S. (2014) Earth-science reviews. *Earth-Science Reviews* 135:1–10.

Bakun, A. (1990) Global climate change and intensification of coastal ocean upwelling. *Science* 247:198–201.

Barron, J. (1973) Late Miocene-early Pliocene paleotemperatures for California from marine diatom evidence. *Palaeogeography, Palaeoclimatolog,y Palaeoecology* 14:277–291.

Barton, N. H., and Hewitt, G. M. (1985) Analysis of hybrid zones. *Annual Review of Ecology and Systematics* 16:113–148.

Beal, C. H. (1948) Reconnaissance of the geology and oil possibilities of Baja California, Mexico. *Geological Society of America Memoirs* 31:1–150.

Bennett, S. E. K. (2013) "The Role of Rift Obliquity in Formation of the Gulf of California." Ph.D. dissertation, Department of Geology, University of California, Davis.

Bennett, S. E., and Oskin, M. E. (2014). Oblique rifting ruptures continents: Example from the Gulf of California shear zone. *Geology* G34904-1.

Bennett, S. E. K., Oskin, M. E., and Iriondo, A. (2013a) Transtensional rifting in the proto-Gulf of California, near Bahía Kino, Sonora, México. *Geological Society of America Bulletin* 125:1752–1782.

Bennett, S. E., Skinner, L. A., Darin, M. H., Umhoefer, P. J., Oskin, M. E., and Dorsey, R. J. (2013b) New Constraints on Baja California-North America Relative Plate Motion Since 11 Ma. American Geophysical Union Fall Meeting, #T14C-02.

Bernardi, G., Findley L., and Rocha-Olivares, A. (2003) Vicariance and dispersal across Baja California in disjunct marine fish populations. *Evolution* 57:1599–1609.

Betancourt, J. L., Van Devender, T. R., and Martin, P. S. (1990) *Packrat Middens: The Last 40,000 Years of Biotic Change.* University of Arizona Press, Tucson.

Brothers, D., Harding, A., González-Fernández, A., Holbrook, W. S., Kent, G., Driscoll, N., Fletcher, J., Lizarralde, D., Umhoefer, P., and Axen, G. (2012) Farallon slab detachment and deformation of the Magdalena Shelf, southern Baja California. *Geophysical Research Letters* 39:L09307.

Brusca, R. C. (2015) "A Brief Geological History of Northwestern Mexico." Unpublished manuscript, 10 July 2015. Available at www.rickbrusca.com.

Brusca, R. C., Findley, L. T., Hastings, P. A., Hendrickx, M. E., Cosio, J. T., and van der Heiden, A. M. (2005) Macrofaunal Diversity in the Gulf of California. In Cartron, J. E., Ceballos, G., and Felger, R. S. (eds.), *Biodiversity, Ecosystems and Conservation in Northern Mexico.* Oxford University Press, Oxford. Pp. 179–103.

Carreño, A. L. (1985) Biostratigraphy of the late Miocene to Pliocene on the Pacific island Maria Madre, Mexico. *Micropaleontology* 31:139–166.

Carreño, A. L. (1992) Neogene microfossils from the Santiago Diatomite, Baja California Sur, Mexico. *Paleontología Mexicana* 59:1–38.

Case, T. J., and Cody, M. L. (1983) *Island Biogeography of the Sea of Cortés.* University of California Press, Berkeley.

Case T. J., and Cody, M. L. (1987) Testing theories of island biogeography. *American Scientist* 75:402–411.

Case, T. J., Cody, M. L., and Ezcurra, E. (2002) *A New Island Biogeography of the Sea of Cortés.* Oxford University Press, New York.

Chatzimanolis, S., and Caterino, M. S. (2007) Toward a better understanding of the "Transverse range discontinuity": Lineage diversification in southern California. *Evolution* 61:2127–2141.

Clark-Tapia, R., and Molina-Freaner, F. (2003) The genetic structure of a columnar cactus with a disjunct distribution: *Stenocereus gummosus* in the Sonoran Desert. *Heredity* 90:443–450.

Cody, M., Moran, R., and Thompson, H. (1983) The Plants. In Case, T. J, and Cody, M. L. (eds.), *Island Biogeography in the Sea of Cortés.* University of California Press, Berkeley. Pp. 49–97.

Collins, M., An, S. I., Cai, W., Ganachaud, A., Guilyardi, E., Jin, F. F., Jochum, M., Lengaigne, M., Power, S., Timmermann, A., Vecchi, G., and Wittenberg, A. (2010) The impact of global warming on the tropical Pacific Ocean and El Niño. *Nature Geosciences* 3:391–397.

Cowling, R. M., Potts, A. J., Bradshaw, P. L., Colville, J., Arianoutsou, M., Ferrier, S., Forest, F., Fyllas, N. M., Hopper, S. D., Ojeda, F., Proches, S., Smith, R. J., Rundel, P. W., Vassilakis, E., and Zutta, B. R. (2014) Variation in plant diversity in Mediterranean-climate ecosystems: The role of climatic and topographic stability. *Journal of Biogeography* doi:10.1111/jbi.12429.

Crews, S. C., and Hedin, M. (2006) Studies of morphological and molecular phylogenetic divergence in spiders (Araneae: Homalonychus) from the American Southwest, including divergence along the Baja California peninsula. *Molecular Phylogenetics and Evolution* 38:470–487.

Darin, M. H. (2011) "Late Miocene Extensional Deformation in the Sierra Bacha, Coastal Sonora, México: Implications for the Kinematic Evolution of the Proto–Gulf of California." Master of science dissertation, University of Oregon, Eugene.

Darton, N. (1921) Geologic reconnaissance in Baja California. *Journal of Geology* 29:720–748.

Davis, L. G. (2003) Geoarchaeology and geochronology of pluvial Lake Chapala, Baja California, Mexico. *Geoarchaeology* 18:205–223.

Davis, M. (2006) Bridging the gap or crossing a bridge? Bridging scales and knowledge systems. *Concepts and Applications in Ecosystem Assessment* 2006:145–164.

Davis, E. B., Koo, M. S., Conroy, C., Patton, J. L., and Mortiz, C. (2008) The California Hotspots Project: Identifying regions of rapid diversification of mammals. *Molecular Ecology* 17:120–138.

Dawson, M. N. (2001) Phylogeography in coastal marine animals: A solution for California? *Journal of Biogeography* 28:723–736.

Dekens, P. S., Ravelo, A. C., and McCarthy, M. D. (2007) Warm upwelling regions in the Pliocene warm period. *Paleoceanography* 22:PA3211, doi:10.1029/2006PA001394.

Dolby, G. A., Ellingson, R. E., Day, P. P., and Jacobs, D. K. (2012) How origination of modern fish lineages may reflect timing of when the Gulf of California opened: A new biological approach. *Geological Society of America Abstracts with Programs* 44:18.

Dorsey, R. J., Fluette, A., McDougall, K. A., Housen, B. A., Janecke, S. U., Axen, G. J., and Shirvell, C. R. (2007) Chronology of Miocene-Pliocene deposits at Split Mountain Gorge, southern California: A record of regional tectonics and Colorado River evolution. *Geology* 35:57–60.

Dorsey, R. J., Housen, B. A., Janecke, S. U., Fanning, C. M., and Spears, A. L. F. (2011) Stratigraphic record of basin development within the San Andreas Fault system: Late Cenozoic Fish Creek–Vallecito basin, southern California. *Geological Society of America Bulletin* 123:771–793.

Drummond, A. J., and Suchard, M. A. (2010) Bayesian random local clocks, or one rate to rule them all. *BMC Biology* 114:1–112.

Drummond, A. J., Ho, S. Y. W., Phillips, M. J., and Rambaut, A. (2006) Relaxed phylogenetics and dating with confidence. *PloS Biology* 4:e88.

Durham, J. W., and Allison, E. C. (1960) The geologic history of Baja California and its marine faunas. *Systematic Zoology* 9:47–91.

Ellingson, R. (2012) "Phylogenetics and Phylogeography of North Pacific Bay Gobies: Adaptive Convergence, Relictual Endemism, and Climate-Driven Population Structure." Ph.D. dissertation, Department of Ecology and Evolutionary Biology, UCLA.

Ellingson, R. A., Swift, C. C., Findley, L. T., and Jacobs, D. K. (2014) Convergent evolution of ecomorphological adaptations in geographically isolated Bay gobies (Teleostei: Gobionellidae) of the temperate North Pacific. *Molecular Phylogenetics and Evolution* 70:464–477.

Faircloth, B. C., Sorenson, L., Santini, F., and Alfaro, M. E. (2013) A phylogenomic perspective on the radiation of ray-finned fishes

based upon targeted sequencing of ultraconserved elements (UCEs). *PLoS ONE* 8:e65923.

Fehlberg, S. D., and Ranker, T. A. (2009) Evolutionary history and phylogeography of *Encelia farinosa* (Asteraceae) from the Sonoran, Mojave, and peninsular deserts. *Molecular Phylogenetics and Evolution* 50:326–235.

Feldman, C. R., and Spicer, G. S. (2006) Comparative phylogeography of woodland reptiles in California: Repeated patterns of cladogenesis and population expansion. *Molecular Ecology* 15:2201–2222.

Felger, R. S., and Wilder, B. T., in collaboration with Romero-Morales, H. (2012) *Plant Life of a Desert Archipelago: Flora of the Sonoran Islands in the Gulf of California*. University of Arizona Press, Tucson.

Fenby, S. S., and Gastil, R. G. (1991) Geologic-tectonic map of the Gulf of California and surrounding areas. *The Gulf and Peninsular Province of the Californias: American Association of Petroleum Geologists, Memoir* 47:79–83.

Ferrari, L., López-Martínez, M., Orozco-Esquivel, T., Bryan, S. E., Duque-Trujillo, J., Lonsdale, P., and Solari, L. (2013) Late Oligocene to Middle Miocene rifting and synextensional magmatism in the southwestern Sierra Madre Occidental, Mexico: The beginning of the Gulf of California rift. *Geosphere* 9:1161–1200.

Fletcher, J. M., Grove, M., Kimbrough, D., Lovera, O., and Gehrels, G. E. (2007) Ridge-trench interactions and the Neogene tectonic evolution of the Magdalena shelf and southern Gulf of California: Insights from detrital zircon U-Pb ages from the Magdalena fan and adjacent areas. *Geological Society of America Bulletin* 119:1313–1336.

Gans, P. B. (1997) Large-magnitude Oligo-Miocene extension in southern Sonora: Implications for the tectonic evolution of northwest Mexico. *Tectonics* 16:388–408.

Garduño-Monroy, V., Vargas-Ledezma, H., and Campos-Enriquez, J. (1993) Preliminary geologic studies of Sierra-el-Aguajito (Baja-California, Mexico): A resurgent-type caldera. *Journal of Volcanology and Geothermal Research* 59:47–58.

Garrick, R. C. (2010) Montane refuges and topographic complexity generate and maintain invertebrate biodiversity: Recurring themes across space and time. *Journal of Insect Conservation* 15:469–478.

Garrick, R. C., Nason, J. D., Meadows, C. A., and Dyer, R. J. (2009) Not just vicariance: Phylogeography of a Sonoran Desert euphorb indicates a major role of range expansion along the Baja peninsula. *Molecular Ecology* 18:1916–1931.

Garrick, R. C., Nason, J. D, Fernandez-Manjarres, J. F., and Dyer, R. J. (2013) Ecological coassociations influence species' responses to past climatic change: An example from a Sonoran Desert bark beetle. *Molecular Ecology* 22:3345–3361.

Gastil, R. G., and Krummenacher, D. (1978) A reconnaissance geologic map of the west-central part of the state of Nayarit, Mexico. *Geological Society of America Map and Chart Series* MC-24, scale 1:200,000.

Gastil, R. G., Krummenacher, D., and Minch, J. A. (1979) The record of Cenozoic volcanism around the Gulf of California. *Geological Society of America Bulletin* 90:839–857.

Gastil, R. G., Neuhaus, J., Cassidy, M., Smith, J. T., Ingle, J. C., and Krummenacher, D. (1999) Geology and paleontology of southwestern Isla Tiburón, Sonora, Mexico. *Revista Mexicana de Ciencias Geológicas* 16:1–34.

Gentry, A. H. (1949) *Land Plants Collected by the* Vallero III, *Allan Hancock Pacific Expeditions 1937–1951.* Allan Hancock Pacific Expeditions 13. University of Southern California Press, Los Angeles.

Gentry, A. H. (1978) The agaves of Baja California. *Occasional Papers of the California Academy of Sciences* 130:1–119.

Gottscho, A. D. (2014) Zoogeography of the San Andreas Fault system: Great Pacific Fracture Zones correspond with spatially concordant phylogeographic boundaries in western North America. *Biological Reviews* 2014:1–21.

Gracey, A. Y., Troll, J. V., and Somero, G. N. (2001) Hypoxia-induced gene expression profiling in the euryoxic fish *Gillichthys mirabilis. Proceedings of the National Academy of Sciences* 98:1993–1998.

Grismer, L. L. (2000) Evolutionary biogeography on Mexico's Baja California peninsula: A synthesis of molecules and historical geology. *Proceedings of the National Academy of Sciences* 97:14017–14018.

Grismer, L. L. (2002) *Amphibians and Reptiles of Baja California, Its Associated Pacific Islands and Islands in the Sea of Cortez.* University of California Press, Berkeley.

Hafner, D. J., and Riddle, B. R. (2005) Mammalian Phylogeography and Evolutionary History of Northern Mexico's Deserts. In Cartron, J. L., Ceballos, G., and Felger, R. S. (eds.), *Biodiversity, Ecosystems and Conservation in Northern Mexico*. Oxford University Press, Oxford. Pp. 225–245.

Hafner, D. J., and Riddle, B. R. (2011) Boundaries and Barriers of North American Warm Deserts: An Evolutionary Perspective. In Upchurch, P., McGowan, A., and Slater, C. (eds.), *Palaeogeography and Palaeobiogeography: Biodiversity in Space and Time*. CRC Press, Boca Raton. Pp. 73–112.

Hausback, B. P. (1984) Cenozoic Volcanic and Tectonic Evolution of Baja California Sur, Mexico. In Frizzell, V. A. (ed.), *Geology of the Baja California Peninsula*. SEPM Society for Sedimentary Geology. Vol. 39, pp. 219–236.

Helenes, J., and Carreño, A. L. (1999) Neogene sedimentary evolution of Baja California in relation to regional tectonics. *Journal of South American Earth Sciences* 12:589–605.

Helenes, J., Carreño, A. L., and Carrillo, R. M. (2009) Middle to late Miocene chronostratigraphy and development of the northern Gulf of California. *Marine Micropaleontology* 72:1å0–25.

Herman, S. W., and Gans, P. B. (2006) A paleomagnetic investigation of large scale vertical axis rotations in coastal Sonora: Evidence for transtensional proto-Gulf deformation. *Geological Society of America Abstracts with Programs* 38:311.

Heuertz, M., Hausman, J. F., Hardy, O. J., Vendramin, G. G., Frascaria Lacoste, N., and Vekemans, X. (2004) Nuclear microsatellites reveal contrasting patterns of genetic structure between western and southeastern European populations of the common ash (*Fraxinus excelsior* L.). *Evolution* 58:976–988.

Hewitt, G. (2000) The genetic legacy of the Quaternary ice ages. *Nature* 405:907–913.

Holmgren, C. A., Betancourt, J. L., and Rylander, K. A. (2011) Vegetation history along the eastern, desert escarpment of the sierra San Pedro Mártir, Baja California, Mexico. *Quaternary Research* 75:647–657.

Holmgren, C. A., Betancourt, J. L., Cristina, P. M., Delgadillo, J., Zuravnsky, K., Hunter, K. L., Rylander, K. A., and Weiss, J. L. (2014) Evidence against a Pleistocene desert refugium in the Lower Colorado River Basin. *Journal of Biogeography* 41:1769–1780.

Holt, J. W., Stock, J. M., and Holt, E. W. (2000) An age constraint on Gulf of California rifting from the Santa Rosalía basin, Baja California Sur, Mexico: *Geological Society of America Bulletin* 112:540–549.

House, P. K., Pearthree, P. A., and Perkins, M. E. (2008) Stratigraphic evidence for the role of lake spillover in the inception of the lower Colorado River in southern Nevada and western Arizona. *Geological Society of America Special Papers* 439:335–353.

Huntley, B. (1991) How plants respond to climate change: Migration rates, individualism and the consequences for plant communities. *Annals of Botany* 67:15–22.

Hurtado, L. A., Mateos, M., and Santamaria, C. A. (2010) Phylogeography of supralittoral rocky intertidal *Ligia* isopods in the Pacific region from central California to central Mexico. *PLoS ONE* 5:e11633.

Hurtado L. A., Lee E. J., and Mateos, M. (2013) Contrasting phylogeography of sandy vs. rocky supralittoral isopods in the megadiverse and geologically dynamic Gulf of California and adjacent areas. *PLoS ONE* 8:e67827.

IPCC (2012) Managing the Risks of Extreme Events and Disasters to Advance Climate Change Adaptation. In Field, C. B., Barros, V., Stocker, T. F., Qin, D., Dokken, D. J., Ebi, K. L., Mastrandrea, M. D., Mach, K. J., Plattner, G.-K., Allen, S. K., Tignor, M., and Midgley, P. M. (eds.), *A Special Report of Working Groups I and II of the Intergovernmental Panel on Climate Change.* Cambridge University Press, Cambridge/New York. Pp. 178–182.

Irwin, D. (2002) Phylogeographic breaks without geographic barriers to gene flow. *Evolution* 56:2383–2394.

Irwin, D. E., Bensch, S., and Price, T. (2001) Speciation in a ring. *Nature* 409:333–337.

Irwin, D. E., Bensch, S., Irwin, J. H., and Price, T. D. (2005) Speciation by distance in a ring species. *Science* 307:414–416.

Jacobs, D. K., Haney, T., and Louie, K. (2004) Genes, diversity, and geologic process on the Pacific coast. *Annual Review of Earth and Planetary Science* 32:601–652.

Jiménez, E. L. (2013) "Proveniencia y Caracterizacion Geoqumica e Isotopica (Sm-Nd) de Sedimentos en las Cuencas del Norte del Golfo de California." [Master of science thesis]: Ensenada, Baja California, Mexico, Centro de Investigacion Científica y de Educacion Superior de Ensenada.

Johnston, I. M. (1924) Expedition of the California Academy of Sciences to the Gulf of California in 1921: The botany (vascular plants). *Proceedings of the California Academy of Sciences* 12:951–1218.

Karig, D. E., and Jensky, W. (1972) The proto-Gulf of California. *Earth and Planetary Science Letters* 17:169–174.

Kier, G., Kreft, H., Lee, T. M., Jetz, W., Ibisch, P. L., Nowicki, C., Mutke, J., and Barthlott, W. (2009) A global assessment of endemism and species richness across island and mainland regions. *Proceedings of the National Academy of Sciences* 106:9322–9327.

Kowalewski, M., Serrano, G. E. A., Flessa, K. W., and Goodfriend, G. A. (2000) Dead delta's former productivity: Two trillion shells at the mouth of the Colorado River. *Geology* 28:1059–1062.

Lambeck, K., and Chappell, J. (2001). Sea level change through the last glacial cycle. *Science* 292:679–686.

Lapointe, F. J., and Rissler L. J. (2005) Congruence, consensus and the comparative phylogeography of codistributed species in California. *American Naturalist* 166:290–299.

Lavin, M. F., Durazo, R., Palacios, E., Argote, M. L., and Carrillo, L. (1997) Lagrangian observations of the circulation in the northern Gulf of California. *Journal of Physical Oceanography* 27:2298–2305.

Leache, A. D., and Mulcahy, D. G. (2007) Phylogeny, divergence times and species limits of spiny lizards (*Sceloporus magister* species group) in western North American deserts and Baja California. *Molecular Ecology* 16:5216–5233.

Leache, A. D., Crews, S. C., and Hickerson, M. J. (2007) Two waves of diversification in mammals and reptiles of Baja California revealed by hierarchial Bayesian analysis. *Biology Letters* 3:646–650.

Lenz, L. W. (1992) *An Annotated Catalogue of the Plants of the Cape Region, Baja California Sur, Mexico.* Cape Press, Claremont, California. Pp. 1–114.

Leopold, A. (1949) *A Sand County Almanac.* Oxford University Press, New York.

Lewis, C. J. (1996) Stratigraphy and geochronology of Miocene and Pliocene volcanic rocks in the Sierra San Fermín and southern Sierra San Felipe, Baja California, Mexico. *Geofísica Internacional* 35:1–31.

Lindell, J., Mendez-de la Cruz, F. R., and Murphy, R. W. (2005) Deep genealogical history without population differentiation: Discordance between mtDNA and allozyme divergence in the zebra-tailed lizard (*Callisaurus draconoides*). *Molecular Phylogenetics and Evolution* 36:682–694.

Lindell, J., Ngo, A., and Murphy, R. (2006) Deep genealogies and the mid peninsular seaway of Baja California. *Journal of Biogeography* 33:1327–1331.

Lindell, J., Mendez-de la Cruz, F., and Murphy, R. W. (2008) Deep biogeographical history and cytonuclear discordance in the black-tailed brush lizard (*Urosaurus nigricaudus*) of Baja California. *Biological Journal of the Linnean Society* 94:89–104.

Littler, M. M., and Littler, D. S. (1981) Intertidal macrophyte communities from Pacific Baja California and the upper Gulf of California: Relatively constant vs. environmentally fluctuating systems. *Marine Ecology-Progress Series* 4:145–158.

Lluch-Cota, S. E., Aragon-Noriega, E. A., Arreguin-Sanchez, F., Aurioles-Gamboa, D., Bautista-Romero, J. J., Brusca, R. C., Cervantes-Duarte R., Cortes-Altamirano R., Del-Monte-Luna, P.,

Esquivel-Herrera, A., Fernandez, G., Hendrickx, M. E., Hernandez-Vazquez, S., Herrera-Cervantes, H., Kahru, M., Lavin, M., Lluch-Belda, D., Lluch-Cota, D. B., Lopez-Martinez, J., Marinone, S. G., Nevarez-Martinez, M. O., Ortega-Garca, S., Palacios-Castro, E., Pares-Sierra, A., Ponce-Diaz, G., Ramirez-Rodriguez, M., Salinas-Zavala, C. A., Schwartzlose, R. A., and Sierra-Beltran, A. P. (2007) The Gulf of California: Review of ecosystem status and sustainability challenges. *Progress in Oceanography* 73:1–26.

Macholan, M., Munclinger, P., Sugerkov, M., Dufkov, P., Bimova, B., Bozikova, E., Zima, J., and Pialek, J. (2007) Genetic analysis of autosomal and X-linked markers across a mouse hybrid zone. *Evolution* 61:746–771.

Magallón, S. A. (2004) Dating lineages: Molecular and paleontological approaches to the temporal framework of clades. *International Journal of Plant Sciences* 165:S7–S21.

Mar-Hernández, E., González-Escobar, M., and Martin-Barajas, A. (2012) Tectonic framework of Tiburón Basin, Gulf of California, from seismic reflection evidence. *International Geology Review* 54:1271–1283.

Marinone, S. G. (2003) A three-dimensional model of the mean and seasonal circulation of the Gulf of California. *Journal of Geophysical Research* 108:3325–3351.

Mark, C., Gupta, S., Carter, A., Mark, D. F., Gautheron, C., and Martín, A. (2014) Rift flank uplift at the Gulf of California: No requirement for asthenospheric upwelling. *Geology* 42:259–262.

Matzke, N. J. (2013) Probabilistic historical biogeography: New models for founder-event speciation, imperfect detection, and fossils allow improved accuracy and model-testing. *Frontiers of Biogeography* 5:242–248.

Maynard Smith, J. (1966) Sympatric speciation. *American Naturalist* 100:637–650.

McCloy, C., Ingle, J. C., and Barron, J. A. (1988) Neogene stratigraphy, foraminifera, diatoms, and depositional history of Maria Madre Island, Mexico: Evidence of early Neogene marine conditions in the southern Gulf of California. *Marine Micropaleontology* 13:193–212.

McCormack, J. E., Hird, S. M., Zellmer, A. J., Carstens, B. C., and Brumfield, R. T. (2013) Applications of next-generation sequencing to phylogeography and phylogenetics. *Molecular Phylogenetics and Evolution* 66:526–538.

McDougall, K. (2008). Late Neogene marine incursions and the ancestral Gulf of California. *Special Papers—Geological Society of America* 439:355.

McDougall, K., and Miranda-Martinez, A. Y. (2014) Evidence for a marine incursion along the lower Colorado River corridor. *Geosphere* 10:842–869.

McGuire, J. A., Linkem, C. W., Koo, M. S., Hutchison, D. W., Lappin, A. K., Orange, D. I., Lemos-Espinal, J., Riddle, B. R., and Jaeger, J. R. (2007) Mitochondrial introgression and incomplete lineage sorting through space and time: Phylogenetics of crotaphytid lizards. *Evolution* 61:2879–2897.

Mead, J. I., Van Devender, T. R., and Cole, K. L. (1983) Late Quaternary small mammals from Sonoran Desert packrat middens, Arizona and California. *Journal of Mammalogy* 64:173–180.

Metcalfe, S. E. (2006) Late Quaternary environments of the northern deserts and central transvolcanic belt of Mexico. *Annals of the Missouri Botanical Garden* 93:258–273.

Miller, M. R., Atwood, T. S., Eames, B. F., Eberhart, J. K., Yan, Y. L., Postlethwait, J. H., and Johnson, E. A. (2007) RAD marker microarrays enable rapid mapping of zebrafish mutations. *Genome Biology* 8:R105.

Miller, N. C., and Lizarralde, D. (2013) Thick evaporites and early rifting in the Guaymas Basin, Gulf of California. *Geology* 41:283–286.

Minnich, R. A., Franco-Vizcaíno, E., and Goforth, B. R. (2014) Distribution of Chaparral and Pine-Oak "Sky Islands" in Central and Southern Baja California and Implications of Packrat Midden Records on Climate Change since the Last Glacial Maximum. In Wehncke, E. V., Lara-Lara, J. R., Álvarez-Borrego, S., and Ezcurra, E. (eds.), *Conservation Science in Mexico's Northwest: Ecosystem Status and Trends in the Gulf of California*. University of California Institute for Mexico and the United States (UC MEXUS) and Instituto Nacional de Ecología y Cambio Climático (INECC), Mexico, D.F. doi: 10.13022/M3QG60.

Molina-Cruz, A. (1994) Biostratigraphy and paleoceanographic significance of the radiolarians from the protomouth of the Gulf of California. *Ciencias Marinas* 20:441–465.

Moore, D. G. (1973) Plate-edge deformation and crustal growth, Gulf of California structural province. *Geological Society of America Bulletin* 84:1883–1906.

Moore, D. G., and Buffington, E. C. (1968) Transform faulting and growth of the Gulf of California since the late Pliocene. *Science* 161:1238–1241.

Moran, R. (1983a) The Vascular Flora of Isla Angel de la Guarda. In Case, T. J, and Cody, M. L. (eds.), *Island Biogeography in the Sea of Cortés.* University of California Press, Berkeley. Pp. 382–402.

Moran, R. (1983b) Relictual Northern Plants on Peninsular Mountain Tops. In Case, T. J, and Cody, M. L. (eds.), *Island Biogeography in the Sea of Cortés.* University of California Press, Berkeley. Pp. 408–410.

Moritz, C. (1994) Defining evolutionary significant units for conservation. *Trends in Ecology & Evolution* 9:373–375.

Mudelsee, M., and Schulz, M. (1997) The Mid-Pleistocene climate transition: Onset of 100 ka cycle lags ice volume build-up by 280 ka. *Earth and Planetary Science Letters* 151:117–123.

Mueller, K., Kier, G., Rockwell, T., and Jones, C. H. (2009) Quaternary rift flank uplift of the peninsular ranges in Baja and southern California by removal of mantle lithosphere. *Tectonics* 28: TC5003 [doi:10.1029/2007TC002227].

Munguía-Vega, A. (2011) "Habitat Fragmentation in Small Vertebrates from the Sonoran Desert in Baja California." Ph.D. dissertation, University of Arizona, Tucson.

Munguía-Vega, A., Jackson, A. , Marinone, S. G., Erisman, B., Moreno-Báez, M., Giron, A., Pfister, T., Aburto-Oropeza, O., and Torre, J. (2014) Asymmetric connectivity of spawning aggregations of a commercially important marine fish using a multidisciplinary approach. *PeerJ* 2:e511.

Murphy, R. W., and Aguirre-León, G. (2002) The Nonavian Reptiles. In Case, T. J, Cody, M. L., and Ezcurra, E. (eds.), *A New Island*

Biogeography in the Sea of Cortés. Oxford University Press, New York. Pp. 181–220.

Myers, N., Mittermeier, R. A., Mittermeier, C. G., Da Fonseca, G. A. B., and Kent, J. (2000) Biodiversity hotspots for conservation priorities. *Nature* 403:853–858.

Nagy, E. A., and Stock, J. M. (2000) Structural controls on the continent-ocean transition in the northern Gulf of California. *Journal of Geophysical Research* 105:16251–16269.

Nason, J. D., Hamrick, J. L., and Fleming, T. H. (2002) Historical vicariance and postglacial colonization effects on the evolution of genetic structure in lophocereus, a Sonoran Desert columnar cactus. *Evolution* 56:2214–2226.

Navarro-Quezada, A., Gonzalez-Chauvet, R., Molina-Freaner, F., and Eguiarte, L. E. (2003) Genetic differentiation in the *Agave deserti* (Agavaceae) complex of the Sonoran Desert. *Heredity* 90:220–227.

Nelson, E. W. (1921) *Lower California and Its Natural Resources.* Memoirs of the United States National Academy of Sciences, No. 16, Government Printing Office, Washington, D.C.

O'Neill, E. M., Schwartz, R., Bullock, C. T., Williams, J. S., Shaffer, H. B., Aguilar-Miguel, X., Parra-Olea, G., and Weisrock, D. W. (2013) Parallel tagged amplicon sequencing reveals major lineages and phylogenetic structure in the North American tiger salamander (*Ambystoma tigrinum*) species complex. *Molecular Ecology* 22:111–129.

Ortlieb, L. (1978) Reconocimiento de las Terrazas Marinas Cuaternarias en la Parte Central de Baja California. *Universidad Nacional Autónoma de México Instituto Geología Revista* 2:1–12.

Oskin, M., and Stock, J. M. (2003a) Marine incursion synchronous with plate-boundary localization in the Gulf of California. *Geology* 31:23–26.

Oskin, M., and Stock, J. M. (2003b) Pacific–North America plate motion and opening of the Upper Delfín basin, northern Gulf of California. *Geological Society of America Bulletin* 115:1173–1190.

Oskin, M., Stock, J., and Martín-Barajas, A. (2001) Rapid localization of Pacific–North America plate motion in the Gulf of California. *Geology* 29:459–462.

Patarnello, T., Volckaert, F. A. M. J., and Castilho, R. (2007) Pillars of Hercules: Is the Atlantic–Mediterranean transition a phylogeographical discontinuity? *Molecular Ecology* 16:4426–4444.

Peterson, A. T., Ortega-Huerta, M. A., Bartley, J., Sánchez-Cordero, V., Soberón, J., Buddemeier, R. H., and Stockwell, D. R. (2002) Future projections for Mexican faunas under global climate change scenarios. *Nature* 416:626–629.

Petit, R. J., Aguinagalde, I., de Beaulieu, J. L., Bittkau, C., Brewer, S., Cheddadi, R., Ennos, R., Fineschi, S., Grivet, D., Lascoux, M., Mohanty, A., Müller-Starck, G., Demesure-Musch, B., Palmé, A., Pedro Martín, J., Rendell, S., and Vendramin, G. G. (2003) Glacial refugia: Hotspots but not melting pots of genetic diversity. *Science* 300:1563–1565.

Phillips, B. L., Baird, S .J. E., and Moritz, C. (2004) When vicariants meet: A narrow contact zone between morphologically cryptic phylogeographic lineages of the rainforest skink *Carlia rubrigularis. Evolution* 58:1536–1548.

Rebman, J. P. (2002) Plants Endemic to the Gulf Islands. In Case, T. J., Cody, M. L., and Ezcurra, E. (eds.), *A New Island Biogeography in the Sea of Cortés.* Oxford University Press, New York. Pp. 540–544.

Rebman, J. P., and Roberts, N. C. (2012) *Baja California Plant Field Guide.* 3rd edition. San Diego Natural History Museum and Sunbelt Publications, San Diego.

Remington, C. L. (1968) Suture-Zones of Hybrid Interaction between Recently Joined Biotas. In Dobzhansky, T., Hecht, M. K., and Steere, W. C. (eds.), *Evolutionary Biology.* Appleton-Century-Crofts, New York. Pp. 321–428.

Rhode, D. (2002) Early Holocene juniper woodland and chaparral taxa in the central Baja California peninsula, Mexico. *Quaternary Research* 57:102–108.

Riddle, B. R., and Hafner D. J. (2006) A step-wise approach to integrating phylogeographic and phylogenetic biogeographic perspectives

on the history of a core North American warm deserts biota. *Journal of Arid Environments* 66:435–461.

Riddle, B. R., Hafner, D. J., Alexander, L. F., and Jaeger, J. R. (2000) Cryptic vicariance in the historical assembly of a Baja California peninsular desert biota. *Proceedings of the National Academy of Sciences* 97:14438–14443.

Riemann, H., and Ezcurra, E. (2005) Plant endemism and natural protected areas in the Peninsula of Baja California, Mexico. *Biological Conservation* 122:141–150.

Riginos, C. (2005) Cryptic vicariance in Gulf of California fishes parallels vicariant patterns found in Baja California mammals and reptiles. *Evolution* 59:2678–2690.

Roberts, C., McClean, C., Veron, J., Hawkins, J., Allen, G., McAllister, D., Mittermeier, C. G., Schueler, F. W., Spalding, M., Wells, F., Vynne, C., and Werner, T. B. (2002) Marine biodiversity hotspots and conservation priorities for tropical reefs. *Science* 295:1280–1284.

Roden, G. I. (1964) Oceanographic Aspects of Gulf of California. In Van Andel, T. H., and Shor, G. G., Jr. (eds.), *Marine Geology of the Gulf of California*. American Association of Petroleum Geologists, Tulsa, Oklahoma. Pp. 30–58.

Rodriguez-Robles, J. A., and De Jesus-Escobar, J. M. (2000) Molecular systematics of New World gopher, bull, and pinesnakes (Pituophis: Colubridae), a transcontinental species complex. *Molecular Phylogenetics and Evolution* 14:35–50.

Roy, P. D., Caballero, M., Lozano, R., Pi, T., Israde, I., and Morton, O. (2010) Geochemical record of late Quaternary paleoclimate from lacustrine sediments of paleo-lake San Felipe, western Sonoran Desert, Mexico. *Journal of South American Earth Sciences* 29:586–596.

Rubinoff, D., Cameron, S., and Kipling, W. (2006) A genomic perspective on the shortcomings of mitochondrial DNA for "barcoding" identification. *Journal of Heredity* 97:581–594.

Rutschmann, F. (2006) Molecular dating of phylogenetic trees: A brief review of current methods that estimate divergence times. *Diversity and Distributions* 12:35–48.

Ryder, O. A., Shaw, J. H., and Wemmer, C. M. (1988) Species, subspecies and ex situ conservation. *International Zoo Yearbook* 27:134–140.

Schmitt, A. K., Stockli, D. F., and Hausback, B. P. (2006) Eruption and magma crystallization ages of Las Tres Virgenes (Baja California) constrained by combined Th-230/U-238 and (U-Th)/He dating of zircon. *Journal of Volcanology and Geothermal Research* 158:281–295.

Schultheis, L. M., and Baldwin, B. G. (1999) Molecular phylogenetics of Fouquieriaceae: Evidence from nuclear rDNA ITS studies. *American Journal of Botany* 86:578–589.

Seager, R., and Vecchi, G. A. (2010) Greenhouse warming and the 21st century hydroclimate of southwestern North America. *Proceedings of the National Academy of Sciences* 107:21277–21282.

Seiler, C., Fletcher, J. M., Quigley, M. C., Gleadow, A. J. W., and Kohn, B. P. (2010) Neogene structural evolution of the Sierra San Felipe, Baja California: Evidence for proto-Gulf transtension in the Gulf Extensional Province? *Tectonophysics* 488:87–109.

Shevenell, A. E., Kennett, J. P., and Lea, D. W. (2004) Middle Miocene southern ocean cooling and Antarctic cryosphere expansion. *Science* 305:1766–1770.

Shreve, F., and Wiggins, I. R. (1964) *Vegetation and Flora of the Sonoran Desert*. Vols. I & II. Stanford University Press, Stanford, California.

Smith, J. T. (1991) Cenozoic Marine Mollusks and Paleogeography of the Gulf of California. In Dauphin, J. P., and Simoneit, B. R. T. (eds.), *The Gulf and Peninsular Province of the Californias*. American Association of Petroleum Geologists Memoir, Tulsa, Oklahoma. Pp. 637–666.

Smith, J. T., Smith, J. G., Ingle, J. C., Gastil, R. G., Boehm, M. C. J., Roldan, Q., and Casey, R. E. (1985) Fossil and K-Ar age constraints on upper middle Miocene conglomerate, SW Isla Tiburón, Gulf of California. *Geological Society of America, Abstracts with Programs* 17:409.

Soltis, D. E., Morris, A. B., McLachlan, J. S., Manos, P. S., and Soltis, P. S. (2006) Comparative phylogeography of unglaciated eastern North America. *Molecular Ecology* 15:4261–4293.

Soria, G., Torre-Cosio, J., Munguía-Vega, A., Marinone, S. G., Lavín, M. F., Cinti, A., and Moreno-Báez, M. (2014) Dynamic connectivity patterns from an insular marine protected area in the Gulf of California. *Journal of Marine Systems* 129:248–258.

Southwest Environmental Information Network, SEINet. (2014) http//:swbiodiversity.org/seinet/index.php. Accessed on May 22, 2014.

Steig, E. J. (1999) Mid-Holocene climate change. *Science* 286:1485.

Stepien, C., Rosenblatt, R., and Bargmeyer, B. (2001) Phylogeography of the spotted sand bass, *Paralabrax maculatofasciatus*: Divergence of Gulf of California and Pacific Coast populations. *Evolution* 55:1852–1862.

Stock, J. M. (2000). Relation of the Puertecitos Volcanic Province, Baja California, Mexico, to development of the plate boundary in the Gulf of California. *Geological Society of America Special Papers* 334:143–156.

Stock, J. M., and Hodges, K. V. (1989) Pre-Pliocene extension around the Gulf of California and the transfer of Baja California to the Pacific Plate. *Tectonics* 8:99–115.

Swift, C. C., Findley, L. T., Ellingson, R. A., Flessa, K. W., and Jacobs, D. K. (2011) The Delta Mudsucker, *Gillichthys detrusus*, a valid species (Teleostei: Gobiidae) endemic to the Colorado River Delta, northernmost Gulf of California, Mexico. *Copeia* 2011(1):93–102.

Thompson, R. S., and Anderson, K. H. (2000) Biomes of western North America at 18,000, 6000 and 0 14c yr bp reconstructed from pollen and packrat midden data. *Journal of Biogeography* 27:555–584.

Turner, R. M., Bowers, J. E., and Burgess, T. L. (1995) *Sonoran Desert Plants: An Ecological Atlas*. University of Arizona Press, Tucson.

Upton, D. E., and Murphy, R. W. (1997) Phylogeny of the side-blotched lizards (Phrynosomatidae: Uta) based on mtDNA sequences: Support for a midpeninsular seaway in Baja California. *Molecular Phylogenetics and Evolution* 8:104–113.

Vanderplank, S. E., Moreira-Muñoz, A., Hobohm, C., Pils, G., Noroozi, J., Clark, R., Barker, N. P., Yang, W., Huang, J., Ma, K., Tang, C. Q., Werger, M. J. A., Ohsawa, M., and Yang, Y. (2014)

Endemism in Mainland Regions—Case Studies. In Hobohm, C. (ed.), *Endemism in Vascular Plants.* Springer, New York.

Van Devender, T. R. (1977) Holocene woodlands in the southwestern deserts. *Science* 198:189–192.

Van Devender, T. R. (1990) Late Quaternary Vegetation and Climate of the Sonoran Desert, United States and Mexico. In Betancourt, J. L., Van Devender, T. R., and Martin, P. S. (eds.), *Packrat Middens: The Last 40,000 Years of Biotic Change.* University of Arizona Press, Tucson. Pp. 134–163.

Van Devender, T. R. (2002) Deep History of Immigration in the Sonoran Desert Region. In Tellman, B. (ed), *Invasive Exotic Species in the Sonoran Region.* University of Arizona Press, Tucson. Pp. 5–24.

Van Devender, T. R., Sanders, A. C., Wilson, R. K., and Meyer, S. A. (2000) Vegetation, Flora, and Seasons of the Río Cuchujaqui, a Tropical Deciduous Forest near Alamos, Sonora. In Robichaux, R. H., and Yetman, D. A. (eds.), *The Tropical Deciduous Forest of Alamos: Biodiversity of a Threatened Ecosystem in Mexico.* University of Arizona Press, Tucson. Pp. 36–101.

Wang, Z., Gerstein, M., and Snyder, M. (2009) RNA-Seq: A revolutionary tool for transcriptomics. *Nature Reviews Genetics* 10:57–63.

Wegener, A. (1912) "Die Herausbildung der Grossformen der Erdrinde (Kontinente und Ozeane), auf geophysikalischer Grundlage." Petermanns Geographische Mitteilungen (in German) 63:185–195, 253–256, 305–309. Presented at the annual meeting of the German Geological Society, Frankfurt am Main (January 6, 1912).

Wehncke, E. V., Rebman, J., López-Meddellín, X., and Ezcurra, E. (2012) Sierra de la Libertad: A major transition between two desert regions in Baja California, Mexico. *Botanical Sciences* 90:239–261.

White, L. D., Garrison, R. E., and Barron, J. A. (1992) Miocene intensification of upwelling along the California margin as recorded in siliceous facies of the Monterey Formation and offshore DSDP sites. *Geological Society, London, Special Publications* 64:429–442.

Whitmore, R. C., Brusca, R. C., León de la Luz, J. L., Gonzalez-Zamorano, P., Mendoza-Salgado, R., and Amador-Silva, E. S. (2005) The Ecological Importance of Mangroves in Baja California Sur: Conservation Implications for an Endangered Ecosystem. In Cartron, J. E., Ceballos, G., and Felger, R. S. (eds), *Biodiversity, Ecosystems, and Conservation in Northern Mexico*. Oxford University Press, Oxford. Pp. 298–362.

Whittaker, R. H. (1953) A consideration of climax theory: The climax as a population and pattern. *Ecological Monographs* 23:41–78

Wiggins, I. L. (1980) *Flora of Baja California*. Stanford University Press, Stanford, California. Pp. 1–1025.

Wilder, B. T. (2014) "Historical Biogeography of the Midriff Islands in the Gulf of California, Mexico." Ph.D. dissertation, Plant Biology, University of California, Riverside.

Wiley, E. O. (1988) Vicariance biogeography. *Annual Review of Ecological Systems* 19:513–542.

Wilson, I. F. (1948) Buried topography, initial structures, and sedimentation in Santa Rosalia area, Baja California, Mexico. *AAPG Bulletin* 32:1762–1807.

Wittich, E. (1920) La emersion moderna de la costa occidental de la Baja California. *Memorias y Revista de la Sociedad Científica "Antonio Alzate"* 35:121–144.

Zachos, J., Pagani, M., Sloan, L., Thomas, E., and Billups, K. (2001) Trends, rhythms, and aberrations in global climate 65 Ma to Present. *Science* 292:686–693.

Zeitzshel, B. (1969) Primary productivity in Gulf of California. *Marine Biology* 3:201–207.
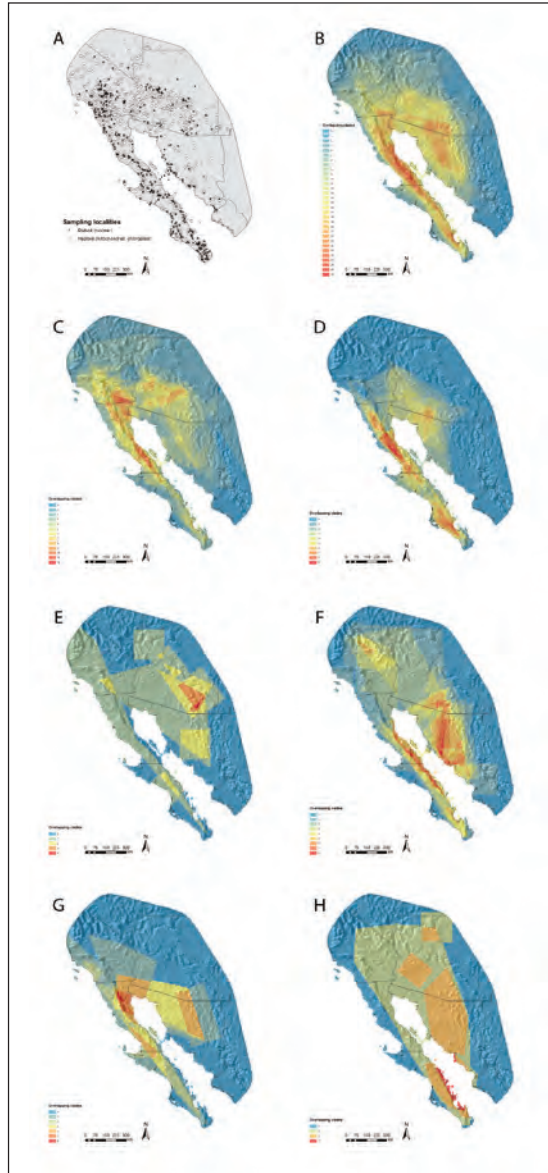
Figure S1: Maps showing sampled localities for genetic markers in all taxa (A: N = 85 taxa), and spatial overlap of Evolutionary Significant Units (ESUs) from haploid (i.e., mitochondrial and chloroplast DNA) genetic markers in all taxa (B: N = 72 taxa), reptiles (C: N = 28 taxa), mammals (D: N = 14 taxa), amphibians (E: N = 4 taxa), invertebrates (F: N = 17 taxa), birds (G: N = 7 taxa), and plants (H: N = 2 taxa).
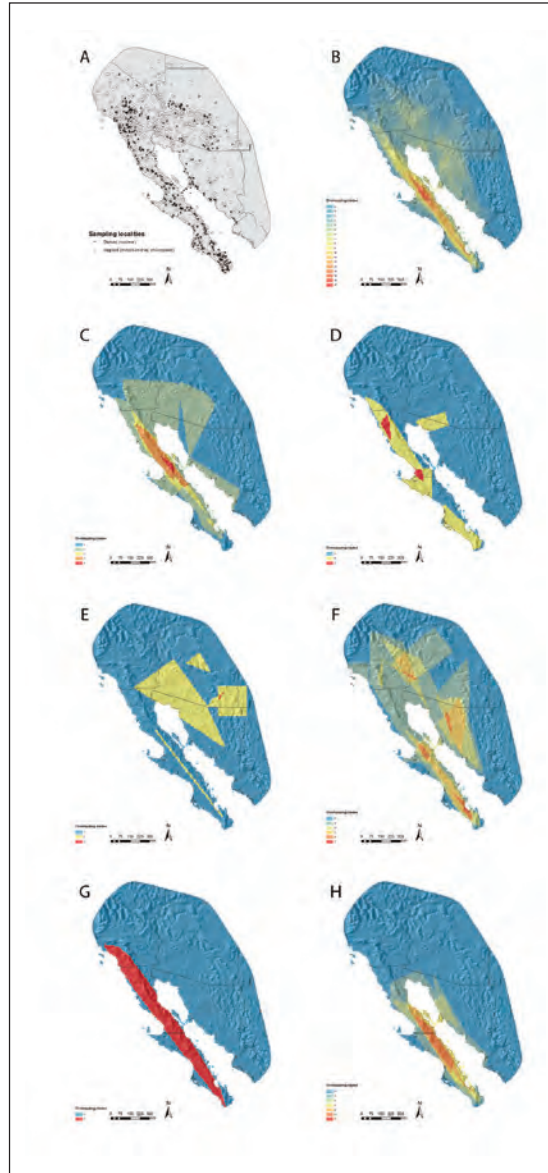
Figure S2: Maps showing sampled localities for genetic markers in all taxa (A: N = 85 taxa), and spatial overlap of Evolutionary Significant Units (ESUs) for diploid (i.e., nuclear) genetic markers in all taxa (B: N =20 taxa), reptiles (C: N = 4 taxa), mammals (D: N = 3 taxa), amphibians (E: N = 2 taxa), invertebrates (F: N = 4 taxa), birds (G: N = 2 taxa), and plants (H: N = 5 taxa).
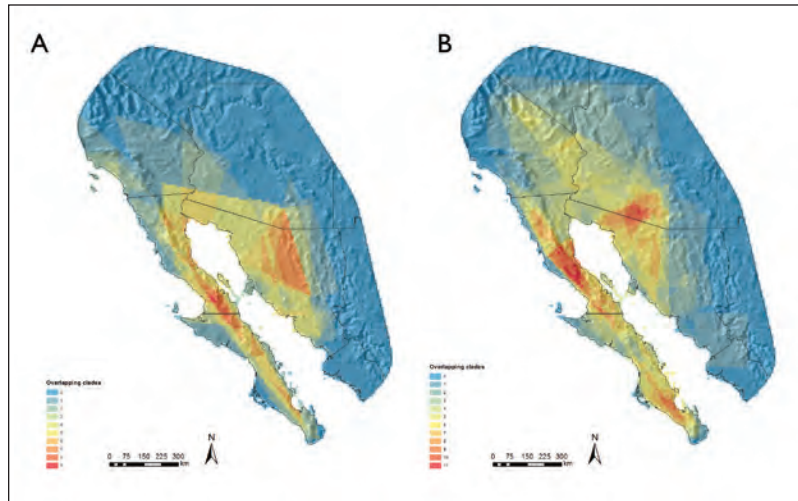
Figure S3: Map showing spatial overlap of Evolutionary Significant Units (ESUs) from haploid genetic markers in volant animals (A: N = 16 taxa) and non-volant animals (B: N = 54 taxa).

REPTILES

ID	Taxa	Haploid Marker (N) (bp)	Diploid Marker (N) loci	No. ESU's haploid/diploid	Vagility	References
1	*Sauromalus* spl	CB (23) 902			non-volant	(Petren and Case 1997; Petren & Case 2002)
2	*Aspidoscelis tigris*	CB (47) 887			non-volant	(Radtkey 1997)
3	*Aspidoscelis hyperythrus**	CB (29) 887			non-volant	(Radtkey 1997)
4	*Callisaurus draconoides*	CB (42) 1087 ATPase (42) 866	A (77) 20 No D 0.05	5/1	non-volant	(Lindell, Mendez-de-la Cruz, and Murphy 2005) (Adest 1987)
5	*Pituophis melanoleucus complex*	ND4 , tRNAs(46) 893		3/-	non-volant	(Rodriguez-Robles and De Jesus-Escobar 2000)
6	*Uta stansburiana*	CB , ATP6 (21) 890 CB+COIII (?) 1132	A	3/-	non-volant	(Upton and Murphy 1997) (Hollingsworth 1999)
7	*Xantusia sp.*	CB (122) 307 CB (508) 1143 ND4 (96) 615 ND2 (36) 1035	α-Enolase (100) 162 GAPD (231) 244	8/-	non-volant	(Sinclair et al. 2004) (Leavitt et al. 2007)
8	*Urosaurus nigricaudus**	CB+ATP8+6 (29) 1966	A (247) 25 No	6/-	non-volant	(Lindell, Mendez-de la Cruz, and Murphy 2005; Aguirre, Morafka, and Murphy 1999) (Murphy 1983)
9	*Petrosaurus repens**		A (100) 34	-/1	non-volant	(Aguilar-S, Sites, and Murphy 1988) (Grismer 1999)
10	*Crotalus mitchellii*	ATP8+6 (104) 676		3/-	non-volant	(Douglas et al. 2006)
11	*Crotalus ruber**	ATP8+6 (11) 676		1/-	non-volant	(Douglas et al. 2006)
12	*Crotalus tigris*	ATP8+6 (38) 676		3/-	non-volant	(Douglas et al. 2006)
13	*Crotalus cerastes*	ATP8+6 (21) 676		4/-	non-volant	(Douglas et al. 2006)
14	*Sceloporus zosteromus**	12S (11) 781 ND4 (12) 825 BDNF (8) 670 No RAG-1 (8)1043 No		2/-	non-volant	(Leache and Mulcahy 2007)
15	*Trimorphodon biscutatus*	ND4, tRNAs (91) 817		3/-	non-volant	(Devitt 2006)
16	*Sceloporus orcutti**	12S (6) 781 ND4 (4) 825 BDNF (2) 670 No RAG-1 (1)1043 No		2/-	non-volant	(Leache and Mulcahy 2007)
17	*Sceloporus magister*			3/-	non-volant	
18	*Crotaphytus vestigium**	ND2,CB (11) 1704		2/-	non-volant	(McGuire et al. 2007)
19	*Crotaphytus bicinctores*	ND2,CB (51) 1704		1/-	non-volant	(McGuire et al. 2007)
20	*Crotaphytus dickersonae*	ND2,CB (6) 1704		1/-	non-volant	(McGuire et al. 2007)
21	*Crataphytus grismeri*	ND2,CB (1) 1704		1/-	non-volant	(McGuire et al. 2007)
22	*Crotaphytus insularis*	ND2,CB (1) 1704		1/-	non-volant	(McGuire et al. 2007)
23	*Crotaphytus nebrius*	ND2,CB (20) 1704		3/-	non-volant	(McGuire et al. 2007)

24	*Phrynosoma coronatum*	ND1 (88) 969 ND2 (93) 1033 12S rRNA (92) 800	RAG-1 (68) 1100 BDNF (67) 700	4/2	non-volant	(Leache et al. 2009)
25	*Hypsiglena torquata / H. ochrorhyncha*	ND4, tRNAs (9) 800 Complete mtDNA(2) 15549 5 nuclear loci (2) 3315		6/-	non-volant	(Mulcahy 2008; Mulcahy and Macey 2009)
26	*Lichanura trivirgata*	ND1, 16S (131) 1105		8/-	non-volant	(Wood, Fisher, and Reeder 2008)
27	*Lampropeltis getula*	CB (261) 1117		2/-	non-volant	(Pyron and Burbrink 2009)
28	*Phyllodactylus nocticolus*/ P. xant*/ P. unctus**	COI (19) 420 NADH (19) 690 16S rRNA (19) 1600 12S rRNA (19) 900 BDNF (19) 670 C-mos (19) 380		4/-	non-volant	(Blair et al. 2009)
29	*Uma notata/inornata/scoparia*	ATPase6, CB (45) 1630		4/-	non-volant	(Trepanier and Murphy 2001)
30	*Phrynosoma mcallii*	NAD4 (82) 781		2/-	non-volant	(Mulcahy et al. 2006)
31	*Phrynosoma platyrhinos/goodei*	NAD4 (43) 812		2/-	non-volant	(Mulcahy et al. 2006)
32	*Chionactis occipitalis*	ND1 (81) 933 16S (81) 165		6/-	non-volant	(Wood et al. 2007)
AMPHIBIANS						
33	*Anaxyrus punctatus*	CB (214) 666 16S (17) 852	cryba (17) 341 POMC (17) 593 Rho1 (17) 315	2/2	non-volant	(Bryson et al. 2012; Jaeger, Riddle, and Bradford 2005; Riddle et al. 2000)
34	*Pseudacris regilla*	CB (110) 609		3/-	non-volant	(Recuero et al. 2006)
35	*Hyla arenicolor*	12S, tRNA16S (40) 2488	AFLP's (75)	3/3	non-volant	(Klymus and Gerhardt 2012)
36	*Rana yavapaiensis / R. magnaocularis*	ND2 (276) 1035 CB (23) 916		3/-	non-volant	(Olah-Hemmings et al. 2010)
MAMMALS						
37	*Ammospermophilus leucurus*	CB (73) 555 CR (73) 510 COIII (30) 699		2/-	non-volant	(Whorley, Alvarez-Castaneda, and Kenagy 2004; Riddle et al. 2000)
38	*Thomomys bottae*	CB (191) 499	IRPB (20) 396	4/3	non-volant	(Alvarez-Castaneda and Patton 2004; Trujano-Alvarez and Alvarez-Castaneda 2007, 2013; Alvarez-Castaneda 2010)
39	*Peromyscus fraterculus / P. eva**	COIII (73) 699		3/-	non-volant	(Riddle, Hafner, and Alexander 2000b; Riddle et al. 2000)
40	*Chaetodipus baileyi / C. rudinoris**	COIII (51) 699 CB (51) 450		3/-	non-volant	(Riddle, Hafner, and Alexander 2000a; Riddle et al. 2000)
41	*Chaetodipus arenarius*/ C. dalquesti**	COIII (36+21) 699 CB (21) 1140		5/-	non-volant	(Riddle et al. 2000; Alvarez-Castaneda and Rios 2011)
42	*Dipodomys merriami*	COIII (60+126) 699 CB (126) 1140		4/-	non-volant	(Riddle et al. 2000; Alvarez-Castaneda, Lidicker, and Rios 2009)

43	*Sorex ornatus*	CB (251) 392	A (122) 20 loci	1/1	non-volant	(Maldonado, Vila, and Wayne 2001)
44	*Peromyscus maniculatus*	CB (12) 1143 NADH (96) 1439		1/-	non-volant	(Dragoo et al. 2006; Walker et al. 2006)
45	*Otospermophilus atricapillus*	CB (118) 1140		2/-	non-volant	(Alvarez-Castaneda and Cortes-Calva 2011)
46	*Chaetodipus fallax*	CB (60) 650		3/-	non-volant	(Rios and Alvarez-Castaneda 2010)
47	*Odocoileus hemionus*	CR (1766) 585 CB (1766) 1028		1/-	non-volant	(Latch et al. 2009)
48	*Antilocapra americana*	CR (269) 483 CR (109) 906	MS (269) 5 MS (55) 18	2/2	non-volant	(Klimova et al. 2014; Stephen et al. 2005)
49	*Chaetodipus penicillatus*	CR (220) 955 COI (22) 690		2/-	non-volant	(Jezkova et al. 2009)
50	*Antrozous pallidus*	CR (194) 480 CB (80) 402		1/-	volant	(Weyandt and Van Den Bussche 2007)
INVERTEBRATES						
51	*Triatoma rubida*	CB (23) 682 COI (21) 636 CP Fst 0.863		4/-	non-volant	(Pfeiler et al. 2006)
52	*Triatoma recurva*	CB (23) 682 COI (21) 636		1/-	non-volant	(Pfeiler et al. 2006)
53	*Drosophila mettleri*	A (240+) 8 CP Fst 0.194, COI (117) 710 CP Fst 0.0			volant	(Markow, Castrezana, and Pfeiler 2002; Hurtado et al. 2004) (Markow & Castrezana 2000)
54	*Drosophila nigrospiracula*	A (180+) 8 CP Fst 0.059 COI (94) 710 CP Fst 0.008			volant	(Markow, Castrezana, and Pfeiler 2002; Hurtado et al. 2004) (Markow & Castrezana 2000)
55	*D. pachea*	COI (203) 710 CP ϕ_{st} 0.348			volant	(Hurtado et al. 2004)
56	*Homalonychus theologus/selenopoides*	16S (205) 600 NADH1 (198) 372	28S (20) 800	3/2	non-volant	(Crews and Hedin 2006)
57	*D. mojavensis*	A (?) 16 Significant differentiation at 4 loci Nei 0.124 MS (1657) 4		4/-	volant	(Zouros 1973; Ross and Markow 2006; Markow, Castrezana, and Pfeiler 2002) (Hocutt 2000)
58	*Tegeticula maculata*	COI (53) 755		2/-	volant	(Segraves and Pellmyr 2001)
59	*Odontoloxozus longicornis / O. pachycericola*	COI (76) 639		3/-	volant	(Pfeiler, Richmond, et al. 2013; Pfeiler et al. 2009)
60	*Iliotona beyeri*	COI (35) 658 16S (35) 453		1/-	volant	(Pfeiler, Johnson, et al. 2013)
61	*Carcinops gilensis*	COI (35) 658 16S (35) 453		1/-	volant	(Pfeiler, Johnson, et al. 2013)

63	*Carcinops consors/ Carcinops sp.*	COI (20) 658		3/-	volant	(Pfeiler, Johnson, et al. 2013)
64	*Culex quinquefasciatus*	COI (28) 624	MS (101-133) 4	1/1	volant	(Pfeiler, Flores-Lopez, et al. 2013)
65	*Culex tarsalis*	COI (48) 624		3/-	volant	(Pfeiler, Flores-Lopez, et al. 2013)
66	*Hadrurus arizonensis*	COI (256) 1029		7/-	non-volant	(Graham et al. 2013)
67	*Araptus attenuatus*	COI (292) 403	8 introns (365) enolase, elongation factor 1α, wingless, muscle protein 20, kuzbanian, ATP synthetase subunit α, lysidy aminoacyl transfer RNA synthetase	3/4	volant	(Garrick et al. 2013)
68	*Pardosa sierra*	COI (3) 710		1/-	non-volant	(Correa-Ramirez, Jimenez, and Garcia-De Leon 2010)
69	*Sphaerophthalma arota*		rDNA ITS1 (60) 518 rDNA ITS2 (60) 967	-/4	volant	(Wilson et al. 2012)
70	*Dinocheirus arizonensis*	COI (85) 551 PhiST = 0.860		2/-	non-volant	(Pfeiler et al. 2009)
71	*Moneilema gigas*	COI (98) 802		4/-	non-volant	(Smith and Farrell 2005)
BIRDS						
72	*Toxostoma arenicola / T. lecontei* *	CB (14) 433 ND6 (14) 186		2/-	volant	(Zink, Blackwell, and Rojas-Soto 1997)
73	*Polioptila californica*	ND2, CB, ND6, tGlu, CR (10) 2169 CR+ND6 (64) 1399	Introns: ACON1-I15 (82) 529 CEPUS-I1 (82) 249 CRYAB-I1 (82) 408 bFIB-17 (76) 278 RHO-I1 (92) 749 TGFB2 (74) 376 TROP-I5 (84) 271 exon MC1R (86) 506	1/1	volant	(Zink and Blackwell 1998; Zink et al. 2000; Zink et al. 2013)
74	*Polioptila melanura*	ND2, CB, ND6, tGlu, CR (10) 2169 CR+ND2 (34) 980		1/-	volant	(Zink and Blackwell 1998; Zink et al. 2001)
75	*Campylorhynchus brunneicapillus*	ND2 (60) 298		2/-	volant	(Zink et al. 2001)
76	*Auriparus flaviceps*	CR (45) 369		2/-	volant	(Zink et al. 2001)
77	*Pipilo fuscus*	CR (28) 333		1/-	volant	(Zink et al. 2001)
78	*Callipepla californica*		A (101) 37	-/1	volant	(Zink, Lott, and Anderson 1987)
79	*Passerculus sandwichensis*	NADH (112) 1041		2/-	volant	(Zink et al. 2005)
PLANTS						
80	*Lophocereus schottii*	A (1008) 15		-/3	non-volant	(Nason, Hamrick, and Fleming 2002)

82	Agave deserti complex	RAPD (420+) 41		-/1	non-volant	(Navarro-Quezada et al. 2003)
83	Pachycereus pringlei	A (336) 24		-/1	non-volant	(Fleming, Maurice, and Hamrick 1998)
84	Euphorbia lomelii	Maturase K (215) 465 NADH (215) 471	(215) 1 Indel (215) 1 SNP (327) Fst = 0.181 RFLPs 6 nDNA loci granule-bound starch synthase, floral meristem identity protein, alcohol dehydrogenase, pistillata, RNA polymerase II, malate synthase	2/2	non-volant	(Garrick et al. 2009)
85	Encelia farinosa	psbA–trnH (72) 456		4/-	non-volant	(Fehlberg and Ranker 2009)

Table S1. *Studies describing the geographic distribution of Evolutionary Significant Units (ESUs) based on genetic criteria for haploid and diploid markers on the terrestrial biota from the Baja California peninsula. For each taxa (N = 85), we include ID, name, markers employed, total number of samples analyzed (N), and where applicable the size (in base pairs, bp) of the DNA fragment analyzed. For non-sequence data, the total sample size (N) and the number of loci analyzed are indicated. CB = cytochrome, CR = control region, A= allozymes, MS = microsatellites.*

73

Family	Species	Infra rank	Infra Name	Non Native (*)	Widespread	Northern Taxa	Baja Migrant	Tropical Taxa
Acanthaceae	*Avicennia germinans*				WS			
Acanthaceae	*Carlowrightia arizonica*				WS			
Acanthaceae	*Carlowrightia pectinata*							TT
Acanthaceae	*Dicliptera resupinata*				WS			
Acanthaceae	*Elytraria imbricata*				WS			
Acanthaceae	*Henrya insularis*							TT
Acanthaceae	*Holographis virgata*	ssp.	*virgata*		WS			
Acanthaceae	*Justicia californica*				WS			
Acanthaceae	*Ruellia californica*				WS			
Acanthaceae	*Ruellia leucantha*	ssp.	*postinsularis*					TT
Acanthaceae	*Tetramerium fruticosum*						BM	
Acanthaceae	*Tetramerium nervosum*				WS			
Achatocarpaceae	*Phaulothamnus spinescens*							TT
Aizoaceae	*Sesuvium portulacastrum*				WS			
Aizoaceae	*Trianthema portulacastrum*				WS			
Alismataceae	*Echinodorus berteroi*				WS			
Amaranthaceae	*Allenrolfea occidentalis*				WS			
Amaranthaceae	*Amaranthus fimbriatus*				WS			
Amaranthaceae	*Amaranthus palmeri*				WS			
Amaranthaceae	*Amaranthus watsonii*				WS			
Amaranthaceae	*Arthrocnemum subterminalis*				WS			
Amaranthaceae	*Atriplex barclayana*				WS			
Amaranthaceae	*Atriplex canescens*				WS			
Amaranthaceae	*Atriplex linearis*				WS			
Amaranthaceae	*Atriplex polycarpa*				WS			
Amaranthaceae	*Chenopodium ambrosioides*	var.	*anthelminticum*	*	WS			
Amaranthaceae	*Chenopodium murale*			*	WS			
Amaranthaceae	*Froelichia interrupta*							TT
Amaranthaceae	*Gomphrena sonorae*							TT

Family	Species							
Amaranthaceae	*Iresine calea*							TT
Anacardiaceae	*Rhus kearneyi*				WS	NT		
Apiaceae	*Ciclospermum leptophyllum*	var.	*leptophyllum*	*	WS			
Apiaceae	*Daucus pusillus*				WS			
Apiaceae	*Eryngium nasturtiifolium*				WS	NT		
Apocynaceae	*Asclepias albicans*					NT		
Apocynaceae	*Asclepias currasavica*							TT
Apocynaceae	*Asclepias subulata*				WS			
Apocynaceae	*Cryptostegia grandiflora*			*				TT
Apocynaceae	*Funastrum cynanchoides*				WS			
Apocynaceae	*Matelea cordifolia*				WS			
Apocynaceae	*Matelea pringlei*							TT
Apocynaceae	*Metastelma californicum*	ssp.	*californicum*		WS			
Apocynaceae	*Plumeria rubra*							TT
Apocynaceae	*Vallesia glabra*				WS			
Apocynaceae	*Vallesia laciniata*							TT
Araceae	*Lemna aequinoctialis*				WS			
Arecaceae	*Brahea armata*						BM	
Arecaceae	*Brahea brandegeei*							TT
Arecaceae	*Washingtonia robusta*							TT
Asparagaceae	*Triteleiopsis palmeri*					NT		
Asteraceae	*Ambrosia ambrosioides*				WS			
Asteraceae	*Ambrosia camphorata*	var.	*leptophylla*				BM	
Asteraceae	*Ambrosia carduacea*						BM	
Asteraceae	*Ambrosia chenopodiifolia*						BM	
Asteraceae	*Ambrosia confertiflora*				WS			
Asteraceae	*Ambrosia deltoidea*				WS			
Asteraceae	*Ambrosia divaricata*						BM	
Asteraceae	*Ambrosia dumosa*				WS			
Asteraceae	*Ambrosia ilicifolia*					NT		
Asteraceae	*Ambrosia magdalenae*						BM	

Family	Taxon	var.	epithet		WS			
Asteraceae	*Ambrosia monogyra*				WS			
Asteraceae	*Ambrosia salsola*	var.	*pentalepis*		WS			
Asteraceae	*Baccharis salicifolia*				WS			
Asteraceae	*Baccharis sarothroides*				WS			
Asteraceae	*Bahiopsis chenopodina*						BM	
Asteraceae	*Bahiopsis triangularis*						BM	
Asteraceae	*Bajacalia crassifolia*						BM	
Asteraceae	*Bebbia juncea*	var.	*aspera*			NT		
Asteraceae	*Bidens aurea*							TT
Asteraceae	*Bidens bigelovii*				WS			
Asteraceae	*Bidens leptocephala*				WS			
Asteraceae	*Bidens pilosa*				WS			
Asteraceae	*Bidens riparia*							TT
Asteraceae	*Brickellia coulteri*	var.	*coulteri*		WS			
Asteraceae	*Carminatia tenuiflora*				WS			
Asteraceae	*Chloracantha spinosa*	var.	*spinosa*		WS			
Asteraceae	*Conyza canadensis*				WS			
Asteraceae	*Coreocarpus parthenioides*	var.	*parthenioides*				BM	
Asteraceae	*Coreocarpus sonoranus*	var.	*sonoranus*				BM	
Asteraceae	*Eclipta prostrata*			*	WS			
Asteraceae	*Encelia farinosa*	var.	*farinosa*		WS			
Asteraceae	*Encelia farinosa*	var.	*phenicodonta*		WS			
Asteraceae	*Galinsoga parviflora*				WS			
Asteraceae	*Gnaphalium palustre*				WS			
Asteraceae	*Gnaphalium purpureum*				WS			
Asteraceae	*Heliopsis anomala*						BM	
Asteraceae	*Hofmeisteria fasciculata*	var.	*fasciculata*		WS			
Asteraceae	*Logfia arizonica*					NT		
Asteraceae	*Palafoxia linearis*				WS			
Asteraceae	*Pectis cylindrica*				WS			
Asteraceae	*Pectis papposa*	var.	*papposa*		WS			

Family	Species				WS	NT	BM	TT
Asteraceae	Pectis prostrata				WS			
Asteraceae	Pectis uniaristata							TT
Asteraceae	Pelucha trifida						BM	
Asteraceae	Perityle aurea				WS			
Asteraceae	Perityle californica				WS			
Asteraceae	Perityle emoryi				WS			
Asteraceae	Perityle microglossa				WS			
Asteraceae	Peucephyllum schottii					NT		
Asteraceae	Pluchea salicifolia							TT
Asteraceae	Porophyllum gracile				WS			
Asteraceae	Senecio lemmonii					NT		
Asteraceae	Sonchus oleraceus			*	WS			
Asteraceae	Tagetes filifolia							TT
Asteraceae	Trixis californica	var.	californica		WS			
Asteraceae	Verbesina encelioides			*	WS			
Asteraceae	Verbesina palmeri						BM	
Asteraceae	Xanthisma spinulosum	var.	scaberella				BM	
Asteraceae	Xanthium strumarium			*	WS			
Asteraceae	Xylothamnia diffusa				WS			
Bataceae	Batis maritima				WS			
Begoniaceae	Begonia palmeri							TT
Bignoniaceae	Macfadyena unguis-cati				WS			
Bignoniaceae	Tecoma stans	var.	angustata		WS			
Boraginaceae	Bourreria sonorae							TT
Boraginaceae	Cordia curassavica							TT
Boraginaceae	Cordia parvifolia				WS			
Boraginaceae	Cryptantha angustifolia				WS			
Boraginaceae	Cryptantha fastigiata						BM	
Boraginaceae	Heliotropium angiospermum				WS			
Boraginaceae	Heliotropium curassavicum				WS			
Boraginaceae	Heliotropium fruticosum				WS			

Family	Species	var.	TT	BM	NT	WS
Boraginaceae	Heliotropium procumbens					WS
Boraginaceae	Johnstonella grayi	var. cryptochaeta				WS
Boraginaceae	Nama hispidum					WS
Boraginaceae	Nama stenocarpum					WS
Boraginaceae	Pectocarya recurvata					WS
Boraginaceae	Phacelia scariosa		TT			
Boraginaceae	Tiquilia cuspidata			BM		
Boraginaceae	Tournefortia hartwegiana		TT			
Boraginaceae	Tournefortia volubilis		TT			
Brassicaceae	Brassica tournefortii					WS
Brassicaceae	Descurainia pinnata					WS
Brassicaceae	Draba cuneifolia					WS
Brassicaceae	Lepidium lasiocarpum					WS
Brassicaceae	Lepidium virginicum					WS
Brassicaceae	Lyrocarpa coulteri	var. coulteri				WS
Brassicaceae	Sisymbrium irio					WS
Bromeliaceae	Hechtia montana		TT			
Bromeliaceae	Tillandsia recurvata					WS
Burseraceae	Bursera fagaroides	var. elongata	TT			
Burseraceae	Bursera hindsiana			BM		
Burseraceae	Bursera laxiflora		TT			
Burseraceae	Bursera microphylla					WS
Cactaceae	Cylindropuntia alcahes	var. alcahes		BM		
Cactaceae	Cylindropuntia bigelovii					WS
Cactaceae	Cylindropuntia cholla			BM		
Cactaceae	Cylindropuntia leptocaulis					WS
Cactaceae	Echinocereus engelmannii					WS
Cactaceae	Ferocactus cylindraceus				NT	
Cactaceae	Lophocereus schottii	var. schottii		BM		
Cactaceae	Opuntia bravoana		TT			
Cactaceae	Pachycereus pecten-aboriginum		TT			

Family	Species	Rank	Epithet	WS	BM	TT
Cactaceae	Pachycereus pringlei			WS		
Cactaceae	Peniocereus striatus			WS		
Cactaceae	Pereskiopsis porteri					TT
Cactaceae	Stenocereus gummosus				BM	
Cactaceae	Stenocereus thurberi			WS		
Campanulaceae	Triodanis biflora			WS		
Cannabaceae	Celtis pallida	ssp.	pallida	WS		
Cannabaceae	Celtis reticulata			WS		
Capparaceae	Atamisquea emarginata				BM	
Capparaceae	Forchhammeria watsonii					TT
Capparaceae	Wislizenia refracta	ssp.	palmeri	WS		
Caryophyllaceae	Drymaria arenarioides	ssp.	peninsularis			TT
Caryophyllaceae	Drymaria glandulosa			WS		
Caryophyllaceae	Drymaria gracilis	ssp.	carinata	WS		
Caryophyllaceae	Drymaria holosteoides	var.	holosteoides	WS		
Celastraceae	Maytenus phyllanthoides			WS		
Celastraceae	Schaefferia shrevei			WS		
Cleomaceae	Cleome tenuis					TT
Cochlospermaceae	Amoreuxia palmatifida					TT
Combretaceae	Laguncularia racemosa			WS		
Commelinaceae	Callisia monandra					TT
Commelinaceae	Commelina diffusa					TT
Commelinaceae	Commelina erecta			WS		
Commelinaceae	Tinantia longipedunculata					TT
Convolvulaceae	Cressa truxillensis			WS		
Convolvulaceae	Cuscuta corymbosa	var.	grandiflora	WS		
Convolvulaceae	Cuscuta leptantha			WS		
Convolvulaceae	Cuscuta tuberculata			WS		
Convolvulaceae	Evolvulus alsinoides			WS		
Convolvulaceae	Ipomoea bracteata					TT
Convolvulaceae	Ipomoea costellata			WS		

Family	Species							
Convolvulaceae	Ipomoea cristulata				WS			
Convolvulaceae	Ipomoea pes-caprae	ssp.	brasiliensis	*	WS			
Convolvulaceae	Jacquemontia abutiloides						BM	
Convolvulaceae	Jacquemontia agrestis							TT
Crossosomataceae	Crossosoma bigelovii					NT		
Cucurbitaceae	Brandegea bigelovii					NT		
Cucurbitaceae	Ibervillea sonorae							TT
Cucurbitaceae	Vaseyanthus insularis				WS			
Cyperaceae	Cyperus elegans				WS			
Cyperaceae	Cyperus flavicomus				WS			
Cyperaceae	Cyperus odoratus				WS			
Cyperaceae	Cyperus pallidicolor				WS			
Cyperaceae	Cyperus squarrosus				WS			
Cyperaceae	Cyperus surinamensis				WS			
Cyperaceae	Eleocharis montevidensis				WS			
Cyperaceae	Fuirena simplex	var.	simplex					TT
Cyperaceae	Lipocarpha micrantha				WS			
Cyperaceae	Schoenoplectus americanus				WS			
Ephedraceae	Ephedra aspera					NT		
Euphorbiaceae	Acalypha aliena							TT
Euphorbiaceae	Acalypha californica				WS			
Euphorbiaceae	Adelia virgata							TT
Euphorbiaceae	Cnidosculus palmeri						BM	
Euphorbiaceae	Croton californicus				WS			
Euphorbiaceae	Croton ciliatoglandulifer							TT
Euphorbiaceae	Croton magdalenae						BM	
Euphorbiaceae	Ditaxis lanceolata				WS			
Euphorbiaceae	Ditaxis serrata				WS			
Euphorbiaceae	Euphorbia albomarginata				WS			
Euphorbiaceae	Euphorbia californica	var.	californica					TT
Euphorbiaceae	Euphorbia capitellata				WS			

Family	Species	Rank	Infraspecies	*	WS	NT	BM	TT
Euphorbiaceae	Euphorbia ceroderma							TT
Euphorbiaceae	Euphorbia cyathophora				WS			
Euphorbiaceae	Euphorbia eriantha				WS			
Euphorbiaceae	Euphorbia heterophylla				WS			
Euphorbiaceae	Euphorbia hyssopifolia				WS			
Euphorbiaceae	Euphorbia incerta				WS			
Euphorbiaceae	Euphorbia lomelii						BM	
Euphorbiaceae	Euphorbia magdalenae						BM	
Euphorbiaceae	Euphorbia misera				WS			
Euphorbiaceae	Euphorbia pediculifera	var.	pediculifera		WS			
Euphorbiaceae	Euphorbia polycarpa				WS			
Euphorbiaceae	Euphorbia tomentulosa						BM	
Euphorbiaceae	Euphorbia xanti						BM	
Euphorbiaceae	Jatropha cinerea						BM	
Euphorbiaceae	Jatropha cordata							TT
Euphorbiaceae	Jatropha cuneata				WS			
Euphorbiaceae	Ricinus communis			*	WS			
Euphorbiaceae	Sebastiania bilocularis				WS			
Euphorbiaceae	Sebastiania pavoniana							TT
Fabaceae	Acmispon maritimus	var.	brevivexillus		WS			
Fabaceae	Acmispon strigosus					NT		
Fabaceae	Albizia sinaloensis							TT
Fabaceae	Caesalpinia pulcherrima			*				TT
Fabaceae	Calliandra californica						BM	
Fabaceae	Chamaecrista nictitans	ssp.	nictitans		WS			
Fabaceae	Coursetia caribaea	var.	caribaea		WS			
Fabaceae	Coursetia glandulosa				WS			
Fabaceae	Crotalaria incana							TT
Fabaceae	Crotalaria pumila				WS			
Fabaceae	Dalea bicolor	var.	orcuttiana				BM	
Fabaceae	Desmanthus covillei				WS			

Family	Species			*	WS		BM	TT
Fabaceae	Desmanthus fruticosus						BM	
Fabaceae	Desmodium procumbens				WS			
Fabaceae	Desmodium scorpiurus							TT
Fabaceae	Desmodium tortuosum							TT
Fabaceae	Diphysa occidentalis							TT
Fabaceae	Ebenopsis confinis						BM	
Fabaceae	Errazurizia megacarpa						BM	
Fabaceae	Erythrina flabelleformis							TT
Fabaceae	Haematoxylum brasiletto							TT
Fabaceae	Hoffmannseggia intricata						BM	
Fabaceae	Leucaena lanceolata							TT
Fabaceae	Lupinus arizonicus				WS			
Fabaceae	Lysiloma candidum							TT
Fabaceae	Lysiloma divaricatum							TT
Fabaceae	Macroptilium atropurpureum				WS			
Fabaceae	Marina evanescens				WS			TT
Fabaceae	Marina parryi				WS			
Fabaceae	Melilotus indica			*	WS			
Fabaceae	Mimosa aculeaticarpa	var.	biuncifera		WS			
Fabaceae	Mimosa distachya	var.	laxiflora		WS			
Fabaceae	Olneya tesota				WS			
Fabaceae	Parkinsonia aculeata			*	WS			
Fabaceae	Parkinsonia florida				WS			
Fabaceae	Parkinsonia microphylla				WS			
Fabaceae	Parkinsonia praecox							TT
Fabaceae	Phaseolus acutifolius	var.	acutifolius		WS			
Fabaceae	Phaseolus filiformis				WS			
Fabaceae	Phaseolus lunatus							TT
Fabaceae	Pithecellobium dulce			*	WS			
Fabaceae	Pithecellobium leucospermum							TT
Fabaceae	Prosopis articulata				WS			

82

Family	Species							
Fabaceae	Prosopis glandulosa	var.	torreyana		WS			
Fabaceae	Psorothamnus emoryi	var.	emoryi		WS			
Fabaceae	Psorothamnus spinosus					NT		
Fabaceae	Rhynchosia minima			*	WS			TT
Fabaceae	Rhynchosia precatoria							
Fabaceae	Senegalia greggii				WS			
Fabaceae	Senegalia occidentalis							TT
Fabaceae	Senna atomaria							TT
Fabaceae	Senna confinis						BM	
Fabaceae	Senna pallida	var.	shreveana					TT
Fabaceae	Senna polyantha				WS			
Fabaceae	Sphinctospermum constrictum							TT
Fabaceae	Tephrosia palmeri							TT
Fabaceae	Tephrosia vicioides				WS			
Fabaceae	Vachellia californica							TT
Fabaceae	Vachellia campechiana				WS			
Fabaceae	Vachellia constricta				WS			
Fabaceae	Vachellia farnesiana				WS			
Fagaceae	Quercus tuberculata							TT
Fouquieriaceae	Fouquieria columnaris						BM	
Fouquieriaceae	Fouquieria diguetii				WS			
Fouquieriaceae	Fouquieria splendens	ssp.	splendens		WS			
Frankeniaceae	Frankenia palmeri				WS			
Hydrocharitaceae	Najas guadalupensis				WS			
Juncaceae	Juncus acutus	ssp.	leopoldii		WS			
Juncaceae	Juncus bufonius				WS			
Koeberlineaceae	Koeberlinia spinosa					NT		
Krameriaceae	Krameria erecta				WS			
Lamiaceae	Hyptis albida				WS			
Lamiaceae	Salvia misella							TT
Lamiaceae	Salvia setosa							TT

Family	Species						
Lamiaceae	Salvia similis						TT
Lamiaceae	Stachys coccinea				WS		
Loasaceae	Eucnide cordata					BM	
Loasaceae	Mentzelia adhaerans				WS		
Loasaceae	Mentzelia aspera				WS		
Loasaceae	Petalonyx linearis				WS		
Loranthaceae	Psittacanthus calyculatus						TT
Malpighiaceae	Callaeum macropterum						TT
Malpighiaceae	Cottsia californica						TT
Malpighiaceae	Cottsia gracilis				WS		
Malvaceae	Abutilon californicum				WS		
Malvaceae	Abutilon incanum				WS		
Malvaceae	Abutilon palmeri				WS		
Malvaceae	Anoda crenatiflora						TT
Malvaceae	Anoda cristata				WS		
Malvaceae	Anoda lanceolata				WS		
Malvaceae	Ayenia jaliscana						TT
Malvaceae	Gossypium davidsonii						TT
Malvaceae	Herissantia crispa				WS		
Malvaceae	Hibiscus biseptus				WS		
Malvaceae	Hibiscus denudatus				WS		
Malvaceae	Horsfordia alata				WS		
Malvaceae	Horsfordia newberryi				WS		
Malvaceae	Kosteletzkya hispidula				WS		
Malvaceae	Malva parviflora			*	WS		
Malvaceae	Malvastrum bicuspidatum	ssp.	bicuspidatum		WS		
Malvaceae	Melochia tomentosa				WS		
Malvaceae	Sida abutifolia				WS		
Malvaceae	Sida ciliaris						TT
Malvaceae	Sphaeralcea ambigua	ssp.	ambigua		WS		
Malvaceae	Sphaeralcea coulteri				WS		

Family	Species	Rank	Epithet	*	WS	NT	BM	TT
Malvaceae	Waltheria indica				WS			
Martyniaceae	Proboscidea altheifolia				WS			
Molluginaceae	Glinus radiatus			*	WS			
Molluginaceae	Mollugo verticillata				WS			
Moraceae	Ficus palmeri				WS			
Myrtaceae	Psidium guajava			*				TT
Nyctaginaceae	Abronia maritima	ssp.	maritima		WS			
Nyctaginaceae	Allionia incarnata	var.	incarnata		WS			
Nyctaginaceae	Boerhavia coccinea				WS			
Nyctaginaceae	Boerhavia erecta				WS			
Nyctaginaceae	Boerhavia gracillima				WS			
Nyctaginaceae	Boerhavia xanti							TT
Nyctaginaceae	Commicarpus scandens				WS			
Nyctaginaceae	Mirabilis laevis	var.	crassifolia		WS			
Nyctaginaceae	Mirabilis tenuiloba				WS			
Oleaceae	Forestiera phillyreoides				WS			
Oleaceae	Menodora scabra					NT		
Onagraceae	Camissonia californica					NT		
Onagraceae	Gaura parviflora				WS			
Onagraceae	Ludwigia octovalvis							TT
Orchidaceae	Habenaria quinqueseta							TT
Orobanchaceae	Orobanche cooperi				WS			
Oxalidaceae	Oxalis corniculata				WS			
Papaveraceae	Argemone gracilenta				WS			
Papaveraceae	Argemone ochroleuca	ssp.	ochroleuca		WS			
Passifloraceae	Passiflora arida				WS			
Passifloraceae	Passiflora foetida	var.	gossypifolia		WS			
Passifloraceae	Passiflora palmeri						BM	
Passifloraceae	Turnera diffusa							TT
Phrymaceae	Erythranthe floribunda				WS			
Phyllanthaceae	Andrachne microphylla						BM	

Family	Species		Variety	*	WS	BM	TT
Phytolaccaceae	*Petiveria alliacea*						TT
Phytolaccaceae	*Rivinia humilis*				WS		
Plantaginaceae	*Conobea intermedia*				WS		
Plantaginaceae	*Conobea polystachya*						TT
Plantaginaceae	*Gambelia juncea*					BM	
Plantaginaceae	*Nuttallanthus texanus*				WS		
Plantaginaceae	*Pseudorontium cyathiferum*				WS		
Plantaginaceae	*Sairocarpus watsonii*					BM	
Plantaginaceae	*Stemodia durantifolia*				WS		
Plantaginaceae	*Veronica peregrina*	ssp.	*xalapensis*		WS		
Plumbaginaceae	*Plumbago zeylanica*				WS		
Poaceae	*Aegopogon cenchroides*				WS		
Poaceae	*Andropogon glomeratus*	var.	*scabriglumis*		WS		
Poaceae	*Aristida adscensionis*				WS		
Poaceae	*Aristida californica*	var.	*glabarata*		WS		
Poaceae	*Aristida ternipes*	var.	*ternipes*		WS		
Poaceae	*Arundo donax*			*	WS		
Poaceae	*Bothriochloa barbinodis*				WS		
Poaceae	*Bouteloua aristidoides*				WS		
Poaceae	*Bouteloua barbata*	var.	*barbata*		WS		
Poaceae	*Bouteloua repens*				WS		
Poaceae	*Brachiaria arizonica*				WS		
Poaceae	*Brachiaria fasciculata*				WS		
Poaceae	*Cenchrus brownii*			*	WS		
Poaceae	*Cenchrus ciliaris*			*	WS		
Poaceae	*Cenchrus echinatus*			*	WS		
Poaceae	*Cenchrus incertus*			*	WS		
Poaceae	*Cenchrus palmeri*				WS		
Poaceae	*Chloris chloridea*				WS		
Poaceae	*Chloris virgata*				WS		
Poaceae	*Cynodon dactylon*	var.	*dactylon*	*	WS		

Family	Species	Infraspecific	*	WS	TT
Poaceae	Dactyloctenium aegyptium		*	WS	
Poaceae	Digitaria bicornis		*	WS	
Poaceae	Digitaria californica			WS	
Poaceae	Digitaria ciliaris		*	WS	
Poaceae	Digitaria horizontalis			WS	
Poaceae	Distichlis littoralis			WS	
Poaceae	Distichlis palmeri			WS	
Poaceae	Distichlis spicata			WS	
Poaceae	Echinochloa colonum		*	WS	
Poaceae	Echinochloa cruspavonis		*	WS	
Poaceae	Enneapogon desvauxii			WS	
Poaceae	Eragrostis cilianensis			WS	
Poaceae	Eragrostis ciliaris			WS	
Poaceae	Eragrostis intermedia			WS	
Poaceae	Eragrostis mexicana			WS	
Poaceae	Eragrostis pectinacea	var. pectinacea		WS	
Poaceae	Eragrostis spicata			WS	
Poaceae	Eriochloa acuminata	var. acuminata	*	WS	
Poaceae	Hackelochloa granularis			WS	
Poaceae	Heteropogon contortus			WS	
Poaceae	Jouvea pilosa			WS	
Poaceae	Lasiacis ruscifolia	var. ruscifolia			TT
Poaceae	Leptochloa crinita			WS	
Poaceae	Leptochloa dubia			WS	
Poaceae	Leptochloa panicea			WS	
Poaceae	Leptochloa viscida			WS	
Poaceae	Muhlenbergia arizonica			WS	
Poaceae	Muhlenbergia microsperma			WS	
Poaceae	Muhlenbergia rigens			WS	
Poaceae	Oplismenus burmannii			WS	
Poaceae	Oplismenus hirtellus			WS	

Family	Species	rank	epithet	*	WS	TT
Poaceae	Panicum hirticaule	var.	hirticaule		WS	
Poaceae	Panicum virgatum				WS	
Poaceae	Paspalidium geminatum				WS	
Poaceae	Paspalum hartwegianum				WS	
Poaceae	Paspalum squamulatum				WS	
Poaceae	Paspalum vaginatum				WS	
Poaceae	Phragmites australis	ssp.	berlandieri		WS	
Poaceae	Polypogon monspeliensis			*	WS	
Poaceae	Setaria liebmannii				WS	
Poaceae	Setaria macrostachya				WS	
Poaceae	Setaria parviflora			*	WS	
Poaceae	Setariopsis auriculata				WS	
Poaceae	Sporobolus contractus				WS	
Poaceae	Sporobolus pyramidatus				WS	
Poaceae	Sporobolus virginicus				WS	
Poaceae	Tripsacum lanceolatum					TT
Poaceae	Vulpia octoflora	var.	hirtella		WS	
Podostemaceae	Oserya coulteriana				WS	
Polygalaceae	Antigonon leptopus					TT
Pontederiaceae	Heteranthera limosa				WS	
Portulacaceae	Portulaca oleracea				WS	
Portulacaceae	Portulaca suffrutescens				WS	
Potamogetonaceae	Potamogeton foliosus				WS	
Primulaceae	Anagallis arvensis			*	WS	
Pteridaceae	Adiantum capillus-veneris				WS	
Pteridaceae	Astrolepis sinuata	ssp.	sinuata		WS	
Pteridaceae	Cheilanthes wrightii				WS	
Pteridaceae	Notholaena californica	ssp.	californica		WS	
Pteridaceae	Notholaena lemmonii	var.	lemmonii			TT
Ranunculaceae	Clematis drummondii				WS	
Resedaceae	Oligomeris linifolia				WS	

Family	Species	var.		WS	NT	TT
Rhamnaceae	Colubrina californica				NT	
Rhamnaceae	Colubrina triflora					TT
Rhamnaceae	Colubrina viridis			WS		
Rhamnaceae	Condalia globosa	var.	globosa	WS		
Rhamnaceae	Condalia globosa	var.	pubescens	WS		
Rhamnaceae	Gouania rosei					TT
Rhamnaceae	Karwinskia humboldtiana					TT
Rhamnaceae	Sageretia wrightii			WS		
Rhamnaceae	Ziziphus obtusifolia	var.	canescens	WS		
Rhizophoraceae	Rhizophora mangle			WS		
Rubiaceae	Crusea setosa					TT
Rubiaceae	Diodia teres			WS		
Rubiaceae	Galium microphyllum			WS		
Rubiaceae	Galium stellatum	var.	eremicum		NT	
Rubiaceae	Hedyotis vergrandis					TT
Rubiaceae	Mitracarpus hirtus					TT
Rubiaceae	Randia capitata					TT
Rubiaceae	Randia obcordata					TT
Rubiaceae	Richardia scabra					TT
Ruppiaceae	Ruppia maritima			WS		
Rutaceae	Esenbeckia hartmanii					TT
Rutaceae	Zanthoxylum fagara					TT
Salicaceae	Salix bonplandiana			WS		
Santalaceae	Phoradendron brachystachyum			WS		
Santalaceae	Phoradendron californicum			WS		
Sapindaceae	Cardiospermum corindum			WS		
Sapindaceae	Dodonaea viscosa			WS		
Sapindaceae	Paullinia sonorensis					TT
Sapindaceae	Sapindus saponaria			WS		
Sapotaceae	Sideroxylon leucophyllum				NT	
Sapotaceae	Sideroxylon occidentale			WS		

Family	Species						
Saururaceae	Anemopsis californica				WS		
Scrophulariaceae	Mimulus guttatus				WS		
Simaroubaceae	Castela polyandra					BM	
Simmondsiaceae	Simmondsia chinensis				WS		
Solanaceae	Capsicum annuum	var.	glabriusculum				TT
Solanaceae	Datura discolor				WS		
Solanaceae	Lycium brevipes	var.	brevipes		WS		
Solanaceae	Lycium fremontii	var.	fremontii		WS		
Solanaceae	Nicotiana clevelandii				WS		
Solanaceae	Nicotiana glauca			*	WS		
Solanaceae	Nicotiana obtusifolia				WS		
Solanaceae	Petunia parviflora				WS		
Solanaceae	Physalis crassifolia	var.	versicolor		WS		
Solanaceae	Physalis pubescens			*	WS		
Solanaceae	Solanum hindsianum				WS		
Stegnospermataceae	Stegnosperma halimifolium				WS		
Talinaceae	Talinum paniculatum				WS		
Thelypteridaceae	Thelypteris puberula	var.	sonorensis		WS		
Typhaceae	Typha domingensis				WS		
Urticaceae	Parietaria hespera	var.	hespera		WS		
Verbenaceae	Citharexylum flabellifolium						TT
Verbenaceae	Lantana hispida				WS		
Verbenaceae	Lantana velutina						
Verbenaceae	Lippia palmeri						TT
Violaceae	Hybanthus attenuatus						TT
Violaceae	Hybanthus fruticulosus						TT
Vitaceae	Cissus trifoliata						TT
Zygophyllaceae	Fagonia barclayana					BM	
Zygophyllaceae	Kallstroemia californica				WS		
Zygophyllaceae	Larrea divaricata	ssp.	tridentata		WS		
Zygophyllaceae	Tribulus terrestris			*	WS		

Zygophyllaceae	Viscainoa geniculata	var.	geniculata				BM
Total	526			36	346	20	48	112

Table S2. *An appendix ordered by taxon family summarizing distribution patterns for 526 plant species co-distributed between Mainland Mexico and the Baja California peninsula (see methods section 4.2).*

Supplemental References

Adest, G. A. (1987) Genetic differentiation among populations of the zebratail lizard, *Callisaurus draconoides* (Sauria: Iguanidae). *Copeia* 1987:854–859.

Aguilars-S., M. A., Sites, J. W., Jr., and Murphy, R. W. (1988) Genetic variability and population structure in the lizard genus *Petrosaurus. Journal of Herpetology* 22:135–145.

Aguirre, G. L., Morafka, D. J., and Murphy, R. W. (1999) The Peninsular archipelago of Baja California: A thousand kilometers of tree lizard genetics. *Herpetologica* 55:369–381.

Alvarez-Castañeda, S. T. (2010) Phylogenetic structure of the *Thomomys bottae-umbrinus* complex in North America. *Molecular Phylogenetics and Evolution* 54:671–679.

Alvarez-Castañeda, S. T., and Cortes-Calva, P. (2011) Genetic evaluation of the Baja California rock squirrel *Otospermophilus atricapillus* (Rodentia: Sciuridae) *Zootaxa* 3138:35–51.

Alvarez-Castañeda, S. T., and Patton, J. L. (2004) Geographic genetic architecture of pocket gopher (*Thomomys bottae*) populations in Baja California, Mexico. *Molecular Ecology* 13:2287–2301.

Alvarez-Castañeda, S. T., and Rios, E. (2011) Revision of *Chaetodipus arenarius* (Rodentia: Heteromyidae). *Zoological Journal of the Linnean Society* 161:213–228.

Alvarez-Castañeda, S. T., Lidicker, W. Z., Jr., and Rios, E. (2009) Revision of the *Dipodomys merriami* complex in the Baja California peninsula, Mexico. *Journal of Mammalogy* 90:992–1008.

Blair, C., Mendez-de la Cruz, F. R., Ngo, A., Lindell, J., Lathrop, A., and Murphy, R. W. (2009) Molecular phylogenetics and taxonomy of leaf-toed geckos (Phyllodactylidae: Phyllodactylus) inhabiting the Peninsula of Baja California. *Zootaxa* 2027:28–42.

Bryson, R. W., Jr., Jaeger, J. R., Lemos-Espinal, J. A., and Lazcano, D. (2012) A multilocus perspective on the speciation history of a North American aridland toad (*Anaxyrus punctatus*). *Molecular Phylogenetics and Evolution* 64:393–400.

Clark-Tapia, R., and Molina-Freaner, F. (2003) The genetic structure of a columnar cactus with a disjunct distribution: *Stenocereus gummosus* in the Sonoran Desert. *Heredity* 90:443–450.

Correa-Ramirez, M. M., Jimenez, M .L., and Garcia-De Leon, F. J. (2010) Testing species boundaries in *Pardosa sierra* (Araneae: Lycosidae) using female morphology and COI mtDNA. *Journal of Arachnology* 38:538–554.

Crews, S. C., and Hedin, M. (2006) Studies of morphological and molecular phylogenetic divergence in spiders (Araneae: Homalonychus) from the American Southwest, including divergence along the Baja California Peninsula. *Molecular Phylogenetics and Evolution* 38:470–487.

Devitt, T. J. (2006) Phylogeography of the Western Lyresnake (*Trimorphodon biscutatus*): Testing aridland biogeographical hypotheses across the Nearctic-Neotropical transition. *Molecular Ecology* 15:4387–4407.

Douglas, M. E., Douglas, M. R., Schuett, G. W., and Porras, L. W. (2006) Evolution of rattlesnakes (Viperidae: Crotalus) in the warm deserts of western North America shaped by Neogene vicariance and Quaternary climate change. *Molecular Ecology* 15:3353–3374.

Dragoo, J. W., Lackey, J. A., Moore, K. E., Lessa, E. P., Cook, J. A., and Yates, T. L. (2006) Phylogeography of the deer mouse (*Peromyscus maniculatus*) provides a predictive framework for research on hantaviruses. *Journal of General Virology* 87:1997–2003.

Fehlberg, S. D., and Ranker, T. A. (2009) Evolutionary history and phylogeography of *Encelia farinosa* (Asteraceae) from the Sonoran, Mojave, and Peninsular Deserts. *Molecular Phylogenetics and Evolution* 50:326–335.

Fleming, T. H., Maurice, S., and Hamrick, J. L. (1998) Geographic variation in the breeding system and the evolutionary stability of trioecy in *Pachycereus pringlei* (Cactaceae). *Evolutionary Ecology* 12:279–289.

Garrick, R. C., Nason, J. D., Meadows, C. A., and Dyer, R. J. (2009) Not just vicariance: Phylogeography of a Sonoran Desert euphorb indicates a major role of range expansion along the Baja peninsula. *Molecular Ecology* 18:1916–1931.

Garrick, R. C., Nason, J. D, Fernandez-Manjarres, J. F., and Dyer, R. J. (2013) Ecological coassociations influence species' responses

93

to past climatic change: An example from a Sonoran Desert bark beetle. *Molecular Ecology* 22:3345–3361.

Graham, M. R., Jaeger, J. R., Prendini, L., and Riddle, B. R. (2013) Phylogeography of the Arizona hairy scorpion (*Hadrurus arizonensis*) supports a model of biotic assembly in the Mojave Desert and adds a new Pleistocene refugium. *Journal of Biogeography* 40:1298–1312.

Grismer, L. L. (1999) An evolutionary classification of reptiles on islands in the Gulf of California, Mexico. *Herpetologica* 55:446–469.

Hocutt, G.D. (2000) "Reinforcement of Premating Barriers to Reproduction between *Drosophila arizonae* and *Drosophila mojavensis.*" Ph.D. dissertation, Arizona State University, Tempe.

Hollingsworth, B. D. (1999) "The Molecular Systematics of the Side-Blotched Lizards (Iguania: Phrynosomatidae: *Uta*)." Ph.D. dissertation, Loma Linda University, Loma Linda, California.

Hurtado, L. A., Erez, T., Castrezana, S., and Markow, T. A. (2004) Contrasting population genetic patterns and evolutionary histories among sympatric Sonoran Desert cactophilic *Drosophila*. *Molecular Ecology* 13:1365–1375.

Jaeger, J. R., Riddle, B. R., and Bradford, D. F. (2005) Cryptic Neogene vicariance and Quaternary dispersal of the red-spotted toad (*Bufo punctatus*): Insights on the evolution of North American warm desert biotas. *Molecular Ecology* 14:3033–3048.

Jezkova, T., Jaeger, J. R., Marshall, Z. L., and Riddle, B. R. (2009) Pleistocene impacts on the phylogeography of the desert pocket mouse (*Chaetodipus penicillatus*). *Journal of Mammalogy* 90:306–320.

Klimova, A., Munguia-Vega, A., Hoffman, J. I., and Culver, M. (2014) Genetic diversity and demography of two endangered captive pronghorn subspecies from the Sonoran Desert. *Journal of Mammalogy* 95:1263–1277.

Klymus, K. E., and Gerhardt, H. C. (2012) AFLP markers resolve intra-specific relationships and infer genetic structure among lineages of the canyon treefrog, *Hyla arenicolor*. *Molecular Phylogenetics and Evolution* 65:654–667.

Latch, E. K., Heffelfinger, J. R., Fike, J. A., and Rhodes, O. E., Jr. (2009)

Species-wide phylogeography of North American mule deer (*Odocoileus hemionus*): Cryptic glacial refugia and postglacial recolonization. *Molecular Ecology* 18:1730–1745.

Leache, A. D., and Mulcahy, D. G. (2007) Phylogeny, divergence times and species limits of spiny lizards (*Sceloporus magister* species group) in western North American deserts and Baja California. *Molecular Ecology* 16:5216–5233.

Leache, A. D., Koo, M. S., Spencer, C. L., Papenfuss, T. J., Fisher, R. N., and McGuire, J. A. (2009) Quantifying ecological, morphological, and genetic variation to delimit species in the coast horned lizard species complex (*Phrynosoma*). *Proceedings of the National Academy of Sciences* 106:12418–12423.

Leavitt, D. H., Bezy, R. L., Crandall, K. A., and Sites, J. W., Jr. (2007) Multi-locus DNA sequence data reveal a history of deep cryptic vicariance and habitat-driven convergence in the desert night lizard *Xantusia vigilis* species complex (Squamata: Xantusiidae). *Molecular Ecology* 16:4455–4481.

Lindell, J., Mendez-de la Cruz, F. R., and Murphy, R. W. (2005) Deep genealogical history without population differentiation: Discordance between mtDNA and allozyme divergence in the zebra-tailed lizard (*Callisaurus draconoides*). *Molecular Phylogenetics and Evolution* 36:682–694.

Maldonado, J. E., Vila, C., and Wayne, R. K. (2001) Tripartite genetic subdivisions in the ornate shrew (*Sorex ornatus*). *Molecular Ecology* 10:127–147.

Markow, T. A., and Castrezana, S. (2000) Dispersal in cactophilic *Drosophila*. *Oikos* 89:378–386.

Markow, T. A., Castrezana, S., and Pfeiler, E. (2002) Flies across the water: Genetic differentiation and reproductive isolation in allopatric desert *Drosophila*. *Evolution* 56:546–552.

McGuire, J. A., Linkem, C. W., Koo, M. S., Hutchison, D. W., Lappin, A. K., Orange, D. I., Lemos-Espinal, J., Riddle, B. R., and Jaeger, J. R. (2007) Mitochondrial introgression and incomplete lineage sorting through space and time: Phylogenetics of crotaphytid lizards. *Evolution* 61:2879–2897.

Mulcahy, D. G. (2008) Phylogeography and species boundaries of the western North American nightsnake (*Hypsiglena torquata*):

Revisiting the subspecies concept. *Molecular Phylogenetics and Evolution* 46:1095–1115.

Mulcahy, D. G., and Macey, J. R. (2009) Vicariance and dispersal form a ring distribution in nightsnakes around the Gulf of California. *Molecular Phylogenetics and Evolution* 53:537–546.

Mulcahy, D. G., Spaulding, A. W., Mendelson, J. R., 3rd, and Brodie, E. D., Jr. (2006) Phylogeography of the flat-tailed horned lizard (*Phrynosoma mcallii*) and systematics of the *P. mcallii-platyrhinos* mtDNA complex. *Molecular Ecology* 15:1807–1826.

Murphy, R. W. (1983) Paleobiogeography and genetic differentiation of the Baja California herpetofauna. *Occasional Papers of the California Academy of Sciences* 137:1–48.

Nason, J. D., Hamrick, J. L., and Fleming, T. H. (2002) Historical vicariance and postglacial colonization effects on the evolution of genetic structure in lophocereus, a Sonoran Desert columnar cactus. *Evolution* 56:2214–2226.

Navarro-Quezada, A., Gonzalez-Chauvet, R., Molina-Freaner, F., and Eguiarte, L. E. (2003) Genetic differentiation in the *Agave deserti* (Agavaceae) complex of the Sonoran Desert. *Heredity* 90:220–227.

Olah-Hemmings, V., Jaeger, J. R., Sredl, M. J., Schlaepfer, M. A., Jennings, R. D., Drost, C. A., Bradford, D. F., and Riddle, B. R. (2010) Phylogeography of declining relict and lowland leopard frogs in the desert Southwest of North America. *Journal of Zoology* 280:343–354.

Petren, K., and Case, T. J. (1997) A phylogenetic analysis of body size evolution and biogeography in chuckwallas (*Sauromalus*) and other iguanines. *Evolution* 51:206–219.

Petren, K., and Case T. J. (2002) Updated mtDNA Phylogeny for *Sauromalus* and Implications for the Evolution of Gigantism. In Case, T. J., Cody, M. L., and Ezcurra, E. (eds.), *A New Island Biogeography of the Sea of Cortés*. Oxford University Press, New York. Pp. 574–579.

Pfeiler, E., Bitler, B. G., Ramsey, J. M., Palacios-Cardiel, C., and Markow, T. A. (2006) Genetic variation, population structure, and phylogenetic relationships of *Triatoma rubida* and *T. recurva* (Hemiptera: Reduviidae: Triatominae) from the Sonoran Desert

insect vectors of the Chagas' disease parasite *Trypanosoma cruzi*. *Molecular Phylogenetics and Evolution* 41:209–221.

Pfeiler, E., Bitler, B. G., Castrezana, S., Matzkin, L. M., and Markow, T. A. (2009) Genetic diversification and demographic history of the cactophilic pseudoscorpion *Dinocheirus arizonensis* from the Sonoran Desert. *Molecular Phylogenetics and Evolution* 52:133–141.

Pfeiler, E., Flores-Lopez, C. A., Mada-Velez, J. G., Escalante-Verdugo, J., and Markow, T. A. (2013) Genetic diversity and population genetics of mosquitoes (Diptera: Culicidae: Culex spp.) from the Sonoran Desert of North America. *Scientific World Journal* 2013:1–11.

Pfeiler, E., Johnson, S., Richmond, M. P., and Markow, T. A. (2013) Population genetics and phylogenetic relationships of beetles (Coleoptera: Histeridae and Staphylinidae) from the Sonoran Desert associated with rotting columnar cacti. *Molecular Phylogenetics and Evolution* 69:491–501.

Pfeiler, E., Richmond, M. P., Riesgo-Escovar, J. R., Tellez-Garcia, A. A., Johnson, S., and Markow, T. A. (2013) Genetic differentiation, speciation, and phylogeography of cactus flies (Diptera: Neriidae: Odontoloxozus) from Mexico and south-western USA. *Biological Journal of the Linnean Society* 110:245–256.

Pyron, R. A., and Burbrink, F. T. (2009) Lineage diversification in a widespread species: Roles for niche divergence and conservatism in the common kingsnake, *Lampropeltis getula*. *Molecular Ecology* 18:3443–3457.

Radtkey, R. R. (1997) Character displacement in some Cnemidophorus lizards revisited: A phylogenetic analysis. *Proceedings of the National Academy of Sciences* 94:9740–9745.

Recuero, E., Martinez-Solano, I., Parra-Olea, G., and Garcia-Paris, M. (2006) Phylogeography of *Pseudacris regilla* (Anura: Hylidae) in western North America, with a proposal for a new taxonomic rearrangement. *Molecular Phylogenetics and Evolution* 39:293–304.

Riddle, B. R., Hafner, D. J., and Alexander, L. F. (2000a) Comparative phylogeography of Baileys' pocket mouse (*Chaetodipus baileyi*) and the *Peromyscus eremicus* species group: Historical vicariance

of the Baja California Peninsular Desert. *Molecular Phylogenetics and Evolution* 17:161–172.

---------. (2000b) Phylogeography and systematics of the *Peromyscus eremicus* species group and the historical biogeography of North American warm regional deserts. *Molecular Phylogenetics and Evolution* 17:145–160.

Riddle, B. R., Hafner, D. J., Alexander, L. F., and Jaeger, J. R. (2000) Cryptic vicariance in the historical assembly of a Baja California peninsular desert biota. *Proceedings of the National Academy of Sciences* 97:14438–14443.

Rios, E., and Alvarez-Castañeda, S. T. (2010) Phylogeography and systematics of the San Diego pocket mouse (*Chaetodipus fallax*). *Journal of Mammalogy* 91:293–301.

Rodriguez-Robles, J. A., and De Jesus-Escobar, J. M. (2000) Molecular systematics of New World gopher, bull, and pinesnakes (Pituophis: Colubridae), a transcontinental species complex. *Molecular Phylogenetics and Evolution* 14:35–50.

Ross, C. L., and Markow, T. A. (2006) Microsatellite variation among diverging populations of *Drosophila mojavensis. Journal of Evolutionary Biology* 19:1691–1700.

Segraves, K. A., and Pellmyr, O. (2001) Phylogeography of the yucca moth *Tegeticula maculata*: The role of historical biogeography in reconciling high genetic structure with limited speciation. *Molecular Ecology* 10:1247–1253.

Sinclair, E. A., Bezy, R. L., Bolles, K., Camarillo, J. L., Crandall, K. A., Sites, J. W., Jr. (2004) Testing species boundaries in an ancient species complex with deep phylogeographic history: Genus *Xantusia* (Squamata: Xantusiidae). *American Naturalist* 164:396–414.

Smith, C. I., and Farrell, B. D. (2005) Range expansions in the flightless longhorn cactus beetles, *Moneilema gigas* and *Moneilema armatum*, in response to Pleistocene climate changes. *Molecular Ecology* 14:1025–1044.

Stephen, C. L., Devos, J. C., Lee, T. E., Jr., Bickham, J. W., Heffelfinger, J. R., Rhodes, O. E., Jr. (2005) Population genetic analysis of Sonoran pronghorn (*Antilocapra americana sonoriensis*). *Journal of Mammalogy* 86:782–792.

Trepanier, T. L., and Murphy, R. W. (2001) The Coachella valley fringe-toed lizard (*Uma inornata*): Genetic diversity and phylogenetic relationships of an endangered species. *Molecular Phylogenetics and Evolution* 18:327–334.

Trujano-Alvarez, A. L., and Alvarez-Castaneda, S. T. (2007) Taxonomic revision of *Thomomys bottae* in the Baja California Sur lowlands. *Journal of Mammalogy* 88:343–350.

---------. (2013) Phylogenetic structure among pocket gopher populations, genus *Thomomys* (Rodentia: Geomyidae), on the Baja California Peninsula. *Zoological Journal of the Linnean Society* 168:873–891.

Upton, D. E., and Murphy, R. W. (1997) Phylogeny of the side-blotched lizards (Phrynosomatidae: Uta) based on mtDNA sequences: Support for a midpeninsular seaway in Baja California. *Molecular Phylogenetics and Evolution* 8:104–113.

Walker, M. L., Chirhart, S. E., Moore, A. F., Honeycutt, R. L., and Greenbaum, I. F. (2006) Genealogical concordance and the specific status of *Peromyscus sejugis*. *Journal of Heredity* 97:340–345.

Weyandt, S. E., and Van Den Bussche, R. A. (2007) Phylogeographic structuring and volant mammals: The case of the pallid bat (*Antrozous pallidus*). *Journal of Biogeography* 34:1233–1245.

Whorley, J. R., Alvarez-Castaneda, S., and Kenagy, G. J. (2004) Genetic structure of desert ground squirrels over a 20-degree-latitude transect from Oregon through the Baja California peninsula. *Molecular Ecology* 13:2709–2720.

Wilson, J. S., Clark, S. L., Williams, K. A., and Pitts, J. P. (2012) Historical biogeography of the arid-adapted velvet ant *Sphaeropthalma arota* (Hymenoptera: Mutillidae) reveals cryptic species. *Journal of Biogeography* 39:336–352.

Wood, D. A., Meik, J. M., Holycross, A. T., Fisher, R. N., and Vandergast, A. G. (2007) Molecular and phenotypic diversity in *Chionactis occipitalis* (Western Shovel-nosed Snake), with emphasis on the status of *C. o. klauberi* (Tucson Shovel-nosed Snake). *Conservation Genetics* 9:1489–1507.

Wood, D. A., Fisher, R. N., and Reeder, T. W. (2008) Novel patterns of historical isolation, dispersal, and secondary contact across

Baja California in the Rosy Boa (*Lichanura trivirgata*). *Molecular Phylogenetics and Evolution* 46:484–502.

Zink, R. M., and Blackwell, R. C. (1998) Molecular systematics and biogeography of aridland gnatcatchers (genus *Polioptila*) and evidence supporting species status of the California gnatcatcher (*Polioptila californica*). *Molecular Phylogenetics and Evolution* 9:26–32.

Zink, R. M., Lott, D. F., and Anderson, D. W. (1987) Genetic variation, population structure and evolution of California quail. *Condor* 89:395–405.

Zink, R. M., Blackwell, R. C., and Rojas-Soto, O. (1997) Species limits in the Le Conte's Thrasher. *Condor* 99:132–138.

Zink, R. M., Barrowclough, G. F., Atwood, J. L., and Blackwell-Rago, R. C. (2000) Genetics, taxonomy, and conservation of the threatened California gnatcatcher. *Conservation Biology* 14:1394–1405.

Zink, R. M., Kessen, A. E., Line, T. V., and Blackwell-Rago, R. C. (2001) Comparative phylogeography of some aridland bird species. *Condor* 103:1–10.

Zink, R. M., Rising, J. D., Mockford, S., Horn, A. G., Wright, J. M., Leonard, M., and Westberg, M. C. (2005) Mitochondrial DNA variation, species limits, and rapid evolution of plumage coloration and size in the Savannah Sparrow. *Condor* 107:21–28.

Zink, R. M., Groth, J. G., Vazquez-Miranda, H., and Barrowclough, G. F. (2013) Phylogeography of the California gnatcatcher (*Polioptila californica*) using multilocus DNA sequences and ecological niche modeling: Implications for conservation. *Auk* 130:449–458.

Zouros, E. (1973) Genetic differentiation associated with the early stages of speciation in the mulleri subgroup of *Drosophila*. *Evolution* 27:601–621.

CHAPTER 2

Paleohabitat and genetic modeling reveal refugia and

postglacial mixing of estuarine fishes

Abstract

Using a novel combination of paleohabitat modeling and genetic mixture analyses, we identify and assess a sea-level driven recolonization process following the Last Glacial Maximum (LGM). Our paleohabitat modeling reveals dramatic changes in estuarine habitat distribution on the coast of California (USA) and Baja California (Mexico). When sea level was ~130 m lower during the LGM (~20 kya), tidal estuarine habitat was absent from regions where it is currently most abundant because the LGM paleo-shoreline was too steep for tidal estuarine habitat formation. Steepness reduced estuarine habitat to two refugia separated by 1,000 km. Through examining the distribution of refugium-associated alleles in three species of estuarine fishes, we assess recolonization of estuaries formed during post-LGM sea-level rise. Recolonized populations were sources from both refugia, consistent with our inference of rapid, extensive habitat formation during sea-level rise ~15–10 kya. Habitat area decreased once sea level stabilized ~7 kya, likely from sediment infill of large estuaries. Our habitat modeling and allele identification approaches reveal a previously undocumented dynamic and integrated relationship between sea-level change, coastal processes, and population genetics. These results extend glacial refugial dynamics to unglaciated subtropical coasts, and have significant implications for biotic response to predicted sea-level rise.

Introduction

Quaternary glacial cycles have helped shape genetic variation throughout the geographic ranges of many taxa by changing temperatures and size of glaciers. For instance, cooling and increased ice cover during the Last Glacial Maximum (LGM),

102

about 20 thousand years ago (kya), isolated European populations of boreal species in southern refugia. Population expansion from these refugia, following glacial retreat, resulted in genetic mixing from multiple sources in newly colonized areas (Taberlet *et al.* 1998; Hewitt 2000; 2004). Similarly, ice cover during the LGM also isolated high-latitude coastal marine taxa in ice-free refugia, from which they also mixed following glacial retreat (Fraser *et al.* 2009; Ilves *et al.* 2010). By changing global sea levels, glacial cycles can also connect and isolate populations far from the ice sheets. For example, lower LGM sea level connected the terrestrial taxa of Asia to the islands of the Sunda Shelf, yielding Wallace's Line (Mayr 1944). Here, we propose that glacially mediated sea-level changes can also strongly influence genetic mixing of marine species far from the poles. When sea-level change interacts with the variable topography of coastal margins, it can extirpate habitats over time. Altering the distribution of habitat through time affects the genetic structure of marine populations.

The estuaries of southern California and northern Baja California (Figure 2-1) serve as an excellent system to examine how sea-level change can isolate and reconnect populations living in discontinuous coastal habitat. Estuaries in this region are situated along a tectonically steepened and heterogeneous continental shelf (Ingersoll & Rumelhart 1999; Plattner *et al.* 2009). Because estuaries only form in certain geomorphic contexts (Jacobs *et al.* 2011), sea-level change would likely have changed the distribution of estuarine habitat and estuarine inhabitants over glacial cycles. We therefore chose to examine the population genetic structure of three species of co-distributed, low-dispersal estuarine fish in which inference of population history is likely. Two of these species were previously studied to ascertain phylogeographic patterns and exhibited separate

clades corresponding to southern California and central Baja California (Bernardi & Talley 2000; Huang & Bernardi 2001). Sequence divergences and the absence of modern dispersal barriers led to suggestions of historical isolation (Bernardi & Talley 2000; Jacobs *et al.* 2004). Interpreting these genetic patterns in the context of our prediction of estuarine habitat changes through time, we hypothesize that these clades were caused by isolation in estuarine refugia during the LGM when the shoreline was ~130 m lower.

To estimate estuarine paleohabitat distributions from the LGM to present, we developed and employed habitat modeling with parameters trained on the modern estuary habitat in which these fishes live. To then predict historical estuarine distribution, the model used information on historical sea level and modern bathymetry of the continental margin. For our expanded population genetic work, we generated highly polymorphic microsatellite and larger mitochondrial DNA (mtDNA; see Appendix 2-1) datasets for the two previously studied fishes (*Gillichthys mirabilis,* Longjaw Mudsucker and *Fundulus parvipinnis*, California Killifish) and did the same for a third co-distributed fish (*Quietula y-cauda,* Shadow Goby). These data permitted analyses of genetic mixing through a novel application of Discriminant Function Analysis (DFA) and a commonly used Bayesian clustering algorithm (STRUCTURE). Based on previous genetic patterns (Bernardi & Talley 2000; Huang & Bernardi 2001) we predicted that there would be two primary refugia, one in southern California and one in central Baja California (Figure 2-S1). We also predicted that microsatellite data would support two genetic groupings in accordance with the mitochondrial patterns previously observed, and that non-refugial populations would be genetically mixed from the two primary refugia.

Material and Methods

Habitat modeling   To predict historical estuarine habitat areas, we used three criteria that are essential to estuary formation: shoreline slope, bathymetry through time, and watershed area. Slope values were parameterized from the 18 modern estuaries in which fish were sampled (Table 2-S3). Slopes ranged between 0.0% and 1.3% (mean = 0.45%, median = 0.39%). In ArcGIS (ESRI, Redlands, CA), using a composite sea-level curve (Chaytor *et al.* 2008), we determined slope in a suite of 10-meter depth bins covering +5 to 140 meters below present sea level (mbpsl) that correlate to sea level from modern to LGM lowstand (20 kya). To locate areas that met the slope criteria (0.0–1.3%) we queried a SRTM30_PLUS (Shuttle Radar Topography Mission; Becker *et al.* 2009) 30 arc-second Digital Elevation Model (DEM) which yielded a sequence of depth-specific layers containing polygons of appropriate slope (Figures 2-2, 2-S7). The coastline was subdivided into crude regional areas corresponding to modern habitat regions (Figure 2-S7). Seven characteristics of habitat polygons were determined (e.g., summed polygon size, mean polygon size) within each coastal region and for each depth bin. We then excluded habitats that did not meet a minimum watershed area requirement, which corresponded to the minimum upland area adjacent to a modern estuary (Catalina Island, 190 km^2). This parameterization is for tidal estuaries, not smaller lagoons, which typically lack the species studied here (Earl *et al.* 2010; Jacobs *et al.* 2011).

We then refined and statistically assessed which, among these lowstand regions of appropriate slope, exhibited size attributes characteristic of modern habitat. To do so, we used the modern (0 kya, 0 ± 5 mbpsl) depth bin and species occurrences from this study to determine which polygon attribute(s) best predict modern species occurrences. We first

performed Discriminant Function Analysis (DFA) in JMP v11 (SAS, Cary, NC) on the seven polygon attributes grouped by: regions that meet slope requirements and support populations of these fishes (N = 6), and regions that meet slope requirements but do not support populations of these fishes (N = 2). Vizcaíno was excluded from this DFA after a Robust Fit Outliers analysis (using Huber and Quartile methods with the default K = 4) revealed bias due to anomalous coastal area size. A stepwise variable selection process (SVSP) in the DFA produced two predictive polygon attributes. We entered these into a Generalized Linear Model (GLM) with binomial distribution to determine which coastal region(s) were likely to have supported refugium populations within the 130–140 mbpsl (20 kya) LGM-associated depth bin. The GLMs were calculated with and without Firth's Biased Adjustment estimates to account for small sample sizes and highly correlated variables. Statistically significant models were re-run using a False Discovery Rate (see Appendix 2-2).

Genetic mixing Microsatellite markers were developed via Roche-454 sequencing (Appendix 2-1, Tables 2-S1, 2-S2). Screening, genotyping, and quality control yielded the following number of loci, total number of alleles, and sample sizes: *G. mirabilis* (16, 80, 100), *Q. y-cauda* (17, 148, 44), and *F. parvipinnis* (20, 199, 79). For general trends, full microsatellite datasets were analyzed in STRUCTURE (Pritchard *et al.* 2000) using an admixture model with correlated allele frequencies. Each run included 1 million burnin and 5 million post-burnin replications and was repeated three times each for *K*s 2–5 for each species. Results were analyzed with STRUCTURE HARVESTER (Earl &

vonHoldt 2011) and grouped in CLUMPP (Jakobsson & Rosenberg 2007). Tree

reconstruction details for mtDNA and microsatellite data are in Appendix 2-1.

To address more explicitly and in greater detail the patterns of genetic

recolonization between the inferred refugia at Vizcaíno and North Conception, we

performed DFA on allelic data and regressions against coastal distance. Microsatellite

genotypic data were converted to allele counts for all individuals. We performed DFA

(without SVSP) on the allele count data amongst individuals of the two groups: the North

Conception Refugium (N = 19, 12, 26) and the Vizcaíno Refugium (N = 14, 8, 18) for *G.*

mirabilis, Q. y-cauda and *F. parvipinnis,* respectively. Significant alleles ($\alpha = 0.05$) were

chosen for subsequent analysis. Each significant allele was designated as 'northern' or

'southern' based on its relative frequency within the two groups used in the DFA (Figure

2-4B). Individuals with missing data for loci containing significant alleles were excluded

from the analysis, as missing data would bias an individual towards lower allele counts.

We summed the frequency of northern and southern alleles separately for each individual

and graphed these sums against geographic coastal distance (Table 2-S1). Regressions

were performed (Table 2-S5) to assess how the number of refugium-associated alleles

changed with distance between the two purported refugia. All statistical analyses were

performed in JMP v11 (SAS Institute Inc.). For further methodological details see

Appendix 2-1.

Results

Habitat modeling   Estimated estuarine habitat area changed dramatically across time

and coastal location (Figures 2-2, 2-S7). Total estuarine habitat area (all sites) increased

almost six-fold, from 646 km^2 to 3019 km^2, between 20 kya and 13 kya, before

decreasing to the present 892 km^2; mean estuarine habitat area increased by 71 km^2 to

385 km^2 to 241 km^2, respectively (Figure 2-3B). Within southern California, most

habitats peaked in size between 12–9 kya (Figure 2-3C).

Estuarine habitat DFA produced two variables that significantly predicted the

presence/absence of our three co-distributed fish taxa given the 7 polygon attributes. The

significant variables were: maximum observed polygon size and summed habitat area.

These variables had a combined p-value of 0.026 with zero misclassifications when

predicting modern species distributions. We applied these predictive variables to

lowstand (130–140 mbpsl) paleohabitat models and tested 11 different refugium

scenarios. A series of Generalized Linear Models (GLMs) revealed 2 statistically

supported, and 4 near-significant refugium scenarios. Applying Firth's Bias-adjusted

corrections and False Discovery Rate to these 6 refugium scenarios eliminated 5, leaving

Vizcaíno + North Conception as the only statistically supported refugium scenario 20 kya

(p-value = 0.02, AICc = 12.9). A Vizcaíno-only refugium scenario is not statistically

supported (Table 2-S6).

Genetic analyses   STRUCTURE and STRUCTURE HARVESTER analyses of microsatellite

data for *G. mirabilis* and *Q. y-cauda* favored two groups ($K = 2$) using likelihood scores.

The two groups (north and south) are consistent with the two LGM refugia identified here

in that inter-refugium individuals are genetically mixed from the two inferred refugium

populations (Figure 2-4A). For *F. parvipinnis*, STRUCTURE favored three groups

(northern, central, southern), which could result from allele frequency changes associated with postglacial colonization or an additional factor.

Discriminant Function Analysis extracted 14, 15, and 39 alleles, respectively, for *G. mirabilis, Q. y-cauda,* and *F. parvipinnis,* that discriminated ($p < 0.05$) between the North Conception refugium and the Vizcaíno refugium. The results from STRUCTURE and regressions of discriminant alleles for the three species supports bidirectional mixing from two sources, consistent with scenario A in Figure 2-S1. The northern and southern source (refugium) localities are genetically distinct and intervening populations are genetic mixtures of those two sources in both analyses (Figure 2-4).

Bayesian phylogenetic tree reconstructions using mtDNA for *G. mirabilis* and *Q. y-cauda* reveal both southern and northern clades (Figures 2-S2A, 2-S3A). Intervening populations are mixed as expected under the bidirectional recolonization scenario. The mtDNA tree topology for *F. parvipinnis* reveals a northern clade and is otherwise unresolved (Figure 2-S4A). However, our microsatellite tree recovered northern and southern clades (Figure 2-S4B), consistent with the previous mtDNA work (Bernardi & Talley 2000). Our three microsatellite Neighbor-Joining tree topologies (Figures 2-S2B, 2-S3B, 2-S4B) exhibit higher resolution and are generally consistent with the mtDNA trees, which reflect two refugial sources through support for two generally 'northern' and 'southern' clades.

Discussion

Habitat through time   Our results reveal that coastal steepness reduced tidal estuarine habitat by more than half during the sea-level lowstand (130–140 mbpsl, ~20

kya) relative to present day. We find statistical support for two refugia (Vizcaíno

refugium and N. Conception refugium, Figure 2-3) separated by ~1,000 km of

uninhabited coast at lowstand (Figure 2-1). We find that, following lowstand, most

modern estuarine habitats rapidly formed during the first major meltwater pulse (~15

kya–12 kya, Figure 2-3A; Chaytor *et al.* 2008) and then decreased in area during the

present sea level stasis (~7 kya, Figure 2-3C). The inferred ~15–12 kya estuarine habitat

peak probably occurred as seawater rapidly flooded lower-gradient shelf and valley

topography, forming large, open tidal estuaries (Upson 1949). The subsequent inferred

Holocene estuarine habitat decline is consistent with coastal maturation where wave-

generated erosion causes coastal retreat, sediments infill estuaries (Sommerfield & Lee

2004), and bar formation at the estuary mouth reduces tidal influence (Jacobs *et al.*

2011). Such "bar-built" closed lagoons are intermittently non-tidal and support different

faunal assemblages than tidal systems studied here (Swift *et al.* 1993). Therefore, the

coastal maturation process reduces the abundance of larger systems where tidal estuarine

fishes live (Jacobs *et al.* 2011). Our detection of end-Pleistocene abundance and

Holocene decline of estuarine habitat is supported by previous archaeological and coastal

process research that used kitchen-midden deposits and found a similar decline of large

estuarine habitat over the Holocene (Masters 2006).

Southern California Bight geomorphic history   The coastal steepness of the

Southern California Bight (SCB; defined here as Point Conception to San Quintín),

which prevented estuary formation during sea-level lowstand, likely resulted from wave

protection afforded by the angle of the SCB (Sunamura 1976) and by offshore islands,

which emerged in greater number and area during lowstand (Figure 2-1; Graham *et al.* 2003; Kinlan & Graham 2005). These features absorb northwesterly wave energy, thus limiting the power of wave attack (Kirby & Dalrymple 1986). Without this buffer, wave action during successive lowstands would have eroded the paleo-coast (Benumof *et al.* 2000), forming a lower-slope, more estuary-permissive shelf topography. Supporting this inference, areas more open to wave attack such as N. Conception and Vizcaíno have lower sloped shelf topography and are the sites of lowstand refugia indicated by our models. Ongoing uplift of this region (Niemi *et al.* 2008) has further reduced the ability of waves to erode the lowstand paleo-coast by continually exposing lower, steep (uneroded) regions of the shelf. Thus, we propose that regional uplift, the angle of the shoreline, and protective offshore islands maintained a steep coastal shelf that limited the formation of tidal estuaries on this section of Pacific coast during glacial lowstand.

Phylogeography   In contrast with refugia invoked *a posteriori* in phylogeographic work, here our paleohabitat modeling enabled us to form and test explicit hypotheses of northern and southern estuarine refugia (Figure 2-S1), which was justified by previous work (Bernardi & Talley 2000; Huang & Bernardi 2001). Our paleohabitat models statistically support only one scenario of two refugia (North Conception and Vizcaíno; Table 2-S6), which geographically coincide with the previously identified (Bernardi & Talley 2000; Huang & Bernardi 2001) southern California and central Baja phyletic clades of *G. mirabilis* and *F. parvipinnis*. We used greater sampling, an additional taxon (*Q. y-cauda*), and large microsatellite datasets to further evaluate this prediction genetically. These additional genetic data further support northern and southern clades,

and STRUCTURE analyses favored two north-south groups in *G. mirabilis* and *Q. y-cauda,* and northern, central, southern groups in *F. parvipinnis*. Assuming the microsatellite data reflect slightly different temporal influences than mtDNA data (see Appendix 2-1) and our interpretations are valid, the northern and southern mtDNA clades observed in both sets of topologies may have resulted from successive Pleistocene glaciations, suggesting these refugia have been geographically stable through more than one glacial cycle.

While postglacial northward expansion from a refugium is commonly observed in Northern Hemisphere taxa (Figure 2-S1B; reviewed in Hewitt 2000), here refugium-associated allele frequencies decay bi-directionally with geographic distance (Figures 2-4B, 2-S1A). As predicted, individuals in non-refugium populations appear genetically mixed from the northern and southern refugia in STRUCTURE and Discriminant Function Analysis (DFA) results. This bi-directional expansion generated populations that were mixed from genetically distinct sources to produce broadly similar levels of genetic diversity relative to the source refugia (see Appendix 2-1 and Figure 2-S5), not a decreased, subsampling of diversity as expected in dispersal from a single source (Petit 2003). An alternative explanation of the discriminant allele patterns is an expansion from a single southern source (i.e. Vizcaíno Refugium) where alleles 'surf' on the northward expanding front and produce certain alleles at high frequencies in the northern populations most distant from the source (Excoffier & Ray 2008). However, such 'surfing' may be less likely in taxa with marine larval dispersal and discontinuous habitat. Also, a Vizcaíno-only refugium scenario is not statistically supported, highlighting the power and complementarity of this independent genetic-habitat modeling approach.

112

Some interspecific differences in the steepness and shape of the mixing curves (Figure 2-4B) and favored K in STRUCTURE analyses suggest that while habitat availability imparts a first-order control on genetic patterns, species-specific ecology and life-history traits are also influential (Bilton *et al.* 2002). Factors affecting offspring retention in estuaries may apply in particular (Bernardi & Talley 2000). For instance, *F. parvipinnis* eggs adhere to estuarine vegetation and their larvae have not been sampled in the nearshore plankton (Watson 1996). Such limited dispersal could account for the relatively low intrapopulation variance in the DFA discriminant allele scores for *F. parvipinnis* (Figure 2-4B). Differential population sizes, fecundities and body sizes may also be factors (Waples 1991), along with different abilities to persist in bar-built estuaries. Overall, however, the three taxa show less genetic differentiation than small bar-built estuary specialists such as *Eucyclogobius newberryi* (Dawson *et al.* 2001), and more differentiation than *Clevelandia ios*, which inhabits open, sandy flats in larger bays as well as estuaries (Dawson *et al.* 2002; Earl *et al.* 2010).

 In the discriminant allele regressions (Figure 2-4B) for *G. mirabilis* and *Q. y-cauda,* prevalence of southern alleles begins to decrease at Bahía San Quintín (BSQ), as expected since this is the first habitat north of the southern (Vizcaíno) refugium. However, BSQ individuals of *F. parvipinnis* are enriched in southern alleles. Since a large habitat area is predicted to have arisen early at BSQ (Figures 2-2, 2-3C), an early founder event and random drift may have increased the presence of southern alleles in this population (Allendorf 1986; Pardo *et al.* 2005). Alternatively, low salinity tolerance in this species (Griffith 1974) may have enabled it to persist upstream at BSQ through the LGM. Such upstream habitat would not be reflected in the tidal estuary models developed

113

here. However, BSQ is not as genetically differentiated in STRUCTURE results as would be expected if it were indeed a lowstand refugium.

Environmental influences   Postglacial recolonization of terrestrial species is thought to proceed through successive founder events along an expanding front, as in the case of incremental stepping-stone models or 'allele surfing' (Kimura & Weiss 1964; Excoffier & Ray 2008). Many studies have focused on changing temperature during glacial cycles as a control on this process (Waltari & Hickerson 2013), but see (Gaylord & Gaines 2000). Several factors, however, mitigate the effect of temperature along the southern California coast. The cold California Current, upwelling, and upwelling-induced low clouds and fog along the Pacific coast limit seasonal and latitudinal temperature changes relative to, for instance, the Atlantic coast (Yamamoto 2009), and limit temperature excursions in coastal estuary settings. In addition, in the northern part of our study region, sea-surface temperatures appear to have increased by only 2.7 °C between LGM and present (Lyle *et al.* 2010), which is similar to or less than temperature changes produced by modern El Niño events (Thunell *et al.* 1999). Thus, limited temperature change and the results herein indicate sea-level change and coastal topography are more important than temperature limitations in controlling tidal estuarine habitat formation and estuarine species distributions through time along topographically complex coastlines (Appendix 2-2).

Conclusions

Our understanding of how glacial-interglacial cycles influenced recent evolution of modern biota is dominated by work on temperate and terrestrial species living on glaciated coastlines, and is often associated with northern range expansion. Such range shifts likely pertain to some coastal regions and species (Edmands 2001; Marko 2004), but see (Dawson 2001; Kelly & Palumbi 2010). However, our analysis of western North American estuarine fishes reveals that sea-level change and shelf topography interacted to form estuarine refugia separated by long stretches of unoccupied coast during the last glaciation. Postglacial habitat expansion via sea-level rise onto lower-sloping shelf area was dramatic in the 1,000-km wide inter-refugial coastline. This rapid expansion is associated with genetic mixing between distinct allele sets sourced from distinct refugia, and not expansion to the north of southern sourced alleles, as in the case of *F. heteroclitus* on the tectonically passive, low grade Atlantic Coast (Adams *et al.* 2006).

These findings were possible through paleohabitat modeling using physical coastal attributes and larger DNA datasets with a new application to extract population-specific alleles. These techniques should be tested and applied to other habitat types, geographic areas, and taxa. Here, they illuminate a previously undocumented process of refugial isolation followed by recolonization. Similar processes may be important in the evolution of the many coastal species that specialize on discontinuously distributed habitat. Distribution of such habitat is likely to be often controlled by changing sea level and requires more tailored modeling than is typically undertaken. Finally, given that both climate and sea level are likely to change significantly in the coming decades, it will be important to apply physical and genetic models in combination to predict the impacts of anthropogenic effects on coastal fauna.

Appendix 2-1: Additional genetics methods

Age of genetic patterns

Comparison of our microsatellite to mtDNA sequence data indicates that the microsatellite data are informative for timescales relevant to the glacial-interglacial processes of interest. North-south mitochondrial clades of *Gillichthys mirabilis* on the Pacific coast (Figure 2-S2A) diverged 0.63 Mya (95% CI 0.24–1.08 Ma; Ellingson 2012; Ellingson *et al.* 2014). The same mtDNA markers were used on *Quietula y-cauda* and reveal similar mtDNA patterns, likely reflecting a similar age of diversification as observed in *G. mirabilis.* Microsatellite loci often mutate faster on average and reflect a range of mutation rates (Wan *et al.* 2004), and the microsatellite loci used here exhibit high degrees of polymorphism (average number of alleles per locus ranged 9.8-18.0 for individuals sampled across 1,000 km). Given the inferred higher mutation rates of microsatellites, our microsatellite data reflect a range of evolutionary processes and events younger than the 0.63 Myr mtDNA divergence age. Thus, a subset of the microsatellite data would correspond to the glacial-interglacial timescale of interest. We therefore use the Discriminant Function Analysis (DFA) to obtain a refuge-associated partition of the data to examine LGM-present processes explicitly and to complement the full microsatellite data analyzed in STRUCTURE.

Diversity metrics, mismatch distributions, F_{ST}

There are competing expectations regarding patterns of traditional diversity metrics in refuge-recolonization scenarios. Refugia are usually centers of high genetic

diversity and recolonized sites are bottlenecked and exhibit lower diversity (reviewed in Hewitt 2000). However, recolonized sites that are admixed from two genetically distinct source populations (e.g., refugia) can instead lead to high diversity measures in those populations (Petit *et al.* 2003). Consistent with this latter scenario, populations inferred here to be recolonized show similar measures of allelic richness (Nei 1973) and gene diversity as the populations inferred to be the refugial sources (Figure 2-S5). In mean allelic richness, there is a very slight trend decreasing northward in *F. parvipinnis*, with a similar pattern for mean gene diversity in *Q. y-cauda*, however the northernmost population, Morro Bay, may also have been bottlenecked (see DFA training N. Conception Refugium by proxy). In addition, ranges of these taxa are extensive to the south of the study area (Pta. Eugenia), potentially providing an intermittent source of additional alleles from the south, which is beyond the scope of this study.

Gillichthys mirabilis has sufficiently distinct northern and southern mitochondrial clades (Figure 2-S2A), and adequate populations and individuals sampled such that mismatch distributions may reflect the admixed or non-admixed nature of populations (Dawson *et al.* 2002). Broadly, the mismatch distributions reveal unimodal distributions for refuge populations, and bimodal or multimodal distributions for several intervening (inferred as recolonized) populations (Figure 2-S6). This pattern suggests that, for *G. mirabilis*, refuges are stable through time (single modes) and intervening sites experience contributions from genetically distinct sources (bimodal or multi-modal patterns). The inferred recolonized populations that show unimodal distributions (DEV, USB, MGU) are within the Southern California Bight, north of the offshore islands where eddy mixing may homogenize genetic signatures during the pelagic larval phase. This is also the

location where STRUCTURE results begin showing notable admixture (Figure 2-4A). Pairwise F_{ST} measures using microsatellite data for all three species indicate *G. mirabilis* may be more dispersive than *F. parvipinnis* (Table 2-S4). Sample limitations for *Q. y-cauda* render inferences difficult due to low statistical power.

Overall, factors such as sample size and local founder events confound traditional population genetic metrics, which is why in this study we relied primarily on STRUCTURE analyses and a novel DFA approach to evaluate genetic structure. Based on such results, DFA may be a tool for population-level inference when traditional metrics are problematic due to mixing of multiple sources, founder effects, and sample sizes.

DFA training N. Conception Refugium by proxy

Modern populations immediately north and south of the North Conception Refugium (NCR) were used as a proxy for the NCR in the DFA discriminant allele analysis. Morro Bay, immediately north of the NCR, was used for each species, as well as the first population immediately south of the NCR for each species (Devereaux, Goleta, Carpinteria populations for *G. mirabilis*, *Q. y-cauda*, and *F. parvipinnis*, respectively). Since they are immediately adjacent to the NCR (Morro Bay is ~30 km and the farthest site included to the south is ~100 km), and given the early post glacial formation of habitat in Morro Bay and the Santa Barbara Channel (Figure 2-S7), we assume they were founded from the NCR prior to any southern admixture. Using these proxy populations provided a similar number of individuals relative to the southern refuge for the discriminant analysis (N:S training sample sizes were 19:14, 12:8, 26:18 for *G. mirabilis, Q. y-cauda, F. parvipinnis,* respectively)

118

This proxy was necessary because although the NCR identified in our habitat models is predicted to support tidal estuarine habitat between 140 mbpsl until about 5 mbpsl, at present it does not have tidal habitat nor support populations of these three fish species. Conversion of this habitat likely resulted from natural infilling from wave action and with sediment supply from the easily eroded Transverse Ranges (Upson 1949; Masters 2006), and anthropogenic processes of leveeing and damming that promote conversion to a closed lagoon state (Jacobs *et al.* 2011). Historical maps indicate that in 1895 the Arroyo Grande/Pismo Creek system in the NCR was larger and more open to the ocean than today (Gannet *et al.* 1895). Flood control measures now separate Arroyo Grande and Pismo Creek, precluding tidal behavior. We therefore used the two most geographically proximate populations of each species in the genetic DFA as the N. Conception training group.

DFA assumptions

Discriminant Function Analysis (DFA) assumes that independent variables are normally distributed. While the nature (0s, 1s, 2s) of allelic count data is likely to violate this normality assumption, we use DFA to identify the alleles discriminating between the two refugia. These alleles are then used in a separate exercise to analyze mixing along the coastline (Figure 2-4B). Thus we are not using DFA to test the adequacy of different classification schemes, which makes the violation of normality less consequential.

Discriminant Function Analysis also assumes equal variance among independent variables (alleles). We found that for total observations, per-allele variance ranged in *F. parvipinnis* from 0.01 to 0.25 (mean = 0.08, median = 0.06), for example. Unequal

covariance can be important because in the predictive phase of DFA samples are will more often be assigned to the group with the greater variance. This is not a concern for us, however, because we did not use DFA to assign populations in a predictive way. Another concern when using DFA is multicollinearity, in which variables are correlated. In this study, the multicollinearity of our variables is dependent on, and limited by, basic biological processes, such a random versus nonrandom mating and low recombination rates relative to the mutation rates of the microsatellite loci studied. Linkage disequilibrium and nonrandom mating could collinearize otherwise independent alleles, but this is not readily avoidable. The assumption of random sampling is satisfied to the extent possible given that individuals are components of interbreeding populations, and in that regard are not truly independent of other individuals. There may be batch effects from seine hauls if a genetic cohort was sampled, but several locales were surveyed per estuary to avoid this confounding issue.

Sampling and marker development

Individuals were collected via seining and preserved in 100% ethanol in the field (permit numbers DGOPA 14253.101005.6950 CASCP No. 2679). DNA extractions were performed using Qiagen DNeasy Blood and Tissue Kit according to manufacturer's directions for muscle tissue. Microsatellite loci were developed using sequencing on the Roche-454 platform of one individual per species and processed with MSATCOMMANDER (Faircloth 2008) to generate primers; tetra-, tri-, and di-nucleotide repeats were favored, respectively. Genetic markers were screened using a subsample of individuals across populations and repeat number of selected homozygotes were verified by standard PCR

and Sanger sequencing methods using 1.0 μL of each microsatellite primers (10 mM) in separate reactions. Microsatellite genotyping plates were run on six to twelve individuals per estuary (where available) according to Ellingson (2012) and genotyped in GENEIOUS v5.6 (http://www.geneious.com; Kearse *et al.* 2012). Some estuaries are sample-limited (Table 2-S1). After discarding loci of substandard quality and individuals with significant missing data (not genotyped for > 2 loci), the number of loci, total number of alleles, and sample sizes are as follows: *G. mirabilis* (16, 80, 100), *Q. y-cauda* (17, 148, 44), and *F. parvipinnis* (20, 199, 79).

Worth noting, the DFA and STRUCTURE analyses are fundamentally different approaches to analyzing genetic data. We analyzed the STRUCTURE output from one run ($K = 2$) of *F. parvipinnis* (it is the best-sampled taxon in this study), and identified alleles that had an estimated per-cluster allele frequency greater than 0.7, which yielded 15 alleles. Comparing the identity of these 15 alleles to the identities of the alleles found to the significant in the DFA (N = 39) yielded a match of 47%. Of the 199 total alleles, this result indicates that these approaches are drawing on some independent components of the overall genotypic dataset, analyzing them in different statistical or probabilistic frameworks, and producing nearly the same result.

PCR protocols and tree reconstruction

Microsatellite PCR reactions used one hybrid primer combination: 2.0 μl Reverse primer (100 μM), 4.0 μl Forward M13 hybrid primer (2.5 μM), 4.0 μl M13 dye-labeled primer (2.5 μM), 90 μl H_2O for a total of 100 μl. Thermocycler protocol is: 1) 95 °C for 15 min, 2) 94 °C for 30 sec, 3) 55 °C for 90 sec, 4) 72 °C for 60 sec, 5) repeat steps 2-4

24x, 6) 94 °C for 30 sec, 7) 50 °C for 90 sec, 8) 72 °C for 60 sec, 9) repeat steps 6-8 24x, 10) 60 °C for 30 min. PCR products were diluted to 5% (2.0 μl PCR product to 38.0 μl H$_2$O) for genotyping reaction with 10.0 μl of a 1:50 LIZ:Hi-Di mix (95 °C for 5 min).

Mitochondrial Control Region (mtCR) and Cytochrome B (Cyt B) were amplified and sequenced for *G. mirabilis* and *Q. y-cauda* using A and M, AJG15 and H5 primer sets (Lee *et al.* 1995; Akihito *et al.* 2000). Primers K and N from (Lee *et al.* 1995) were used to amplify and sequence mtCR for *Fundulus parvipinnis*. Amplification and sequencing protocols are available in detail (Ellingson 2012). Trees were constructed in MrBayes v3.1.2 (Ronquist & Huelsenbeck 2003) on the CIPRES Science Gateway (Miller *et al.* 2010). Sequences were partitioned by gene and a rate partitioning scheme was applied to mtCR region in *Q. y-cauda* following (Ellingson *et al.* 2014) and we eliminated the fastest of four rate partitions due to concern over homoplasy and saturation (Figure 2-S3A). Three runs of 12 million generations were completed with 4 chains per run under default model settings and a burn-in fraction of 25% trees discarded. While unresolved in our Bayesian analysis, *F. parvipinnis* structure was recovered in a Neighbor-Joining tree reconstruction method previously (Bernardi & Talley 2000) and showed north-south geographically structure clades.

The following programs were used for file conversions: CONVERT, GENODIVE, and PGDSPIDER (Glaubitz 2004; Meirmans & Van Tienderen 2004; Lischer & Excoffier 2012). Observed mtDNA mismatch distributions and pairwise F_{ST} were calculated in ARLEQUIN v3 (Excoffier *et al.* 2005); gene diversity and allelic richness were calculated in FSTAT v1.2 (Goudet 1995). STRUCTURE v2.3 (Pritchard *et al.* 2000) was used to run K = 2–5 (3 replicates each) that were analyzed in STRUCTURE HARVESTER (Earl & vonHoldt

2011). The following graphics R packages were used: LATTICE, ADE4, PLYR, RESHAPE2, GGPLOT2 (Chessel *et al.* 2004; Wickham 2007; Sarkar 2008; Wickham 2011). All other statistics were performed in JMP® v11 (SAS Institute Inc., Cary, NC, 1989-2007).

Appendix 2-2: Additional habitat modeling methods

Detailed methods

Parameterization　　To predict estuarine habitat area, we defined three criteria necessary to form estuarine habitat. First, we used Google Earth® v5 (Google Inc., Mountain View, CA) to calculate modern bathymetric slopes amongst the 18 estuaries in this study (Table 2-S3). For five relatively large and heterogeneous estuaries, we captured a range of within-estuary slopes at the center, sides, stream entry, mouth, as applicable. We calculated a single slope from each of 13 relatively small estuaries. The 'run' used for slope calculations varied with estuary size from 200–5,000 m. Slopes ranged between 0.0% and 1.3% (mean = 0.45%, median = 0.39%). Our second criterion was a sea level requirement. Using a composite sea-level curve (Chaytor *et al.* 2008), sea-level lowstand was determined as 130–140 mbpsl. The midpoint depth value was used to date each bin (e.g., 135 mbpsl). Finally, we assume estuaries require sufficient adjacent upland area to permit watershed development. We used the smallest upland area adjacent to a modern habitat (Catalina Island, 190 km^2) as a minimum requirement.

Implementation　　Using the raster calculator tool in ArcMAP v10 (ESRI, Redlands, CA), we queried an SRTM30_PLUS (Becker *et al.* 2009) Digital Elevation Model (DEM) with WGS_1984_UTM_Zone_11N projection for areas matching the slope

123

analysis range (0.0–1.3%) and 10-meter depth range (e.g., 130–140 mbpsl). We iterated

this process for 0–140 mbpsl to yield a sequence of depth-specific layers using the

following equation (Eq. 1):

Eq. 1   *("Elevation" < x) & ("Elevation" >= y) & ("Slope" <= 1.3)*

Example   *("Elevation" < - 130) & ("Elevation" >= - 140) & ("Slope" <= 1.3)*

where x is the upper and y is the lower limit of each depth bin, respectively. For the

present (0 kya) bin we used 0 ± 5 mbpsl. We converted areas matching our query (value

= 1) to a sequence of feature layers in which simplified polygons bounded areas that met

slope requirements. To obtain per-depth area estimates for individual coastal regions we

also created a feature layer for each coastal region (Figure 2-S7). With the "Select

Features by Location" tool we selected the habitat area polygons within each coastal

region using the "Target layer(s) features are within (Clementini) the source layer"

setting. On these selected features we used the "Statistics" feature to provide the

following statistical attributes: number of polygons, minimum polygon area, maximum

polygon area, total polygon area, mean polygon area, and standard deviation of polygon

area. We added a seventh additional attribute, which normalized the summed polygon

area by the coastal feature area to account for different coastal area sizes (analogous to

habitat density within a given coastal area). These statistical attributes were calculated

per depth-bin within each coastal region: 14 depth bins, 9 coastal regions, and 7 statistical

attributes per bin-region produced 882 observations. Of note, the Mercator projection

used here could bias polygon areas by a maximum of 7% of width over the latitude range studied (larger in the northern regions and smaller in the south) relative to an equal area projection. As it is, however, the northern polygon areas are already smaller than southern polygons (i.e. Vizcaíno), and would be unlikely to alter interpretations herein.

Statistical assessment　　　　To better determine whether the three fish species studied here would likely inhabit the lowstand-associated polygon habitat, we used the modern (0 kya, 0 ± 5 mbpsl) depth bin and species occurrences from this study to determine which polygon statistical attribute(s) predict species occurrences. We performed Discriminant Function Analysis (DFA) using JMP on the seven statistical attributes of 8 coastal locations grouped by habitat presence ($N = 6$) or absence ($N = 2$). Vizcaíno was excluded from the DFA analysis after a Robust Fit Outliers analysis (using Huber and Quartile methods with the default K=4) revealed anomalous coastal area size, which biased the statistical attributes. A stepwise variable selection process (SVSP) in the DFA produced two statistically significant predictive variables: Maximum polygon area (maximum size of a single polygon) and Summed habitat area. We then entered these variables into a Generalized Linear Model (GLM) with binomial distribution (variable states were 'yes' or 'no') to determine which coastal region(s) were likely to have supported refuge populations within the 130–140 m (~20 kya) depth bin. If the GLM was significant, it was re-run using Firth's Biased Adjustment estimates and False Discovery Rate. We performed this iteratively for different refuge scenarios (Table 2-S6). Unlike typical GLM analyses, this was not used to exclude variables from the refuge scenario model, but rather test whether, given the two variables identified *a priori* via DFA to be

125

predictive, the refuge scenario given was statistically significant based on p values and AICc scores. Key refuge scenarios are listed in Table 2-S6 with significance scores. Only one refuge scenario was statistically significant (Vizcaíno + North Conception). Vizcaíno was run as a refuge model individually with each additional population not listed in Table 2-S6, none of which were significant in the GLM.

Climatic, oceanographic factors

For the tidal estuarine habitat of focus here, we modeled the major physical geomorphological parameters required for estuary formation. In traditional Ecological Niche Modeling, temperature and precipitation indices are usually the foremost predictors of paleohabitat distributions for both terrestrial and intertidal species (Syphard & Franklin 2009; Waltari & Hickerson 2013). However, temperature and precipitation are less important for estuarine habitat examined here given the relatively small change in temperature from the LGM to present, and because: 1) tidal systems generally have a range of salinities within the system due to marine and freshwater (river) inputs, and 2) spring and summer estuary temperatures are often controlled by cloud cover which is in turn controlled by upwelling. The physical shape, size, and ecology of tidal estuaries can also greatly affect temperature, but are rarely well studied in modern systems, and for which there is little information about historical systems. Detailed reconstruction would very difficult for paleoestuaries because the location where one could physically assess (via coring or seismic imaging) the paleoestuary migrates over time.

Finally, there are additional oceanographic features that we did not take into account (Wares *et al.* 2001). Specifically, Point Conception marks the northern extent of

126

eddy formation in the southern California Bight (Pt. Conception to Dana Point) (Bernstein *et al.* 1977; Seapy & Littler 1980). The resulting increased retention and mixing of water in this region may have an impact on larval dispersal through a homogenizing effect in southern California specifically (Bucklin 1991). This homogenization may help explain why the north-south cline observed in Figure 2-4A begins near the southern end of eddy mixing, and why the northern (Morro Bay–Mugu) populations of all three taxa appear to be well mixed.

Uplift

Significant coastal uplift could, in theory, affect the depth-time correlations inferred from the sea-level curve. However, uplift rates along the coast are typically less than a millimeter per year and unlikely to influence the results of this work when extrapolated over the LGM to present (20 kyrs). As a sensitivity test, we used a 0.7 mm/yr uplift rate extrapolated over 20 kyr, which still produced qualitatively and quantitatively similar results, including the existence of the Conception and Vizcaíno Refugia. Estuaries along this coast are typically on the downthrown block in locally tectonically active areas and are therefore experiencing minimal or no uplift. For example, Pts. Buchon, Loma, and Banda are on uplifting blocks with rates of 0.24–0.09 mm/yr, 0.14–0.16 mm/yr, 0.22–0.25 mm/yr, providing upper limits on uplift rates for the adjacent estuaries of Morro Bay, San Diego Bay, and Banda, respectively (Lettis & Hanson 1992; Muhs *et al.* 1992). At these rates the effects of uplift on our habitat modeling are negligible.

Exceptions to low uplift rates (i.e. 2 mm/yr) are observed locally in the Santa Barbara Channel and could affect our results by biasing the habitat origination ages in this region towards younger estimates (Niemi *et al.* 2008; Gurrola *et al.* 2014). Given higher uplift rates in this region we cannot exclude the possibility of habitat in this region at lowstand 20 kya, but we did not assess whether such potential area in this region would have similar attributes to modern estuaries. It is possible that if there were lowstand habitat in this region, that it could be viewed as an extension of the adjacent North Conception Refugium, and would not greatly alter our biological interpretations.
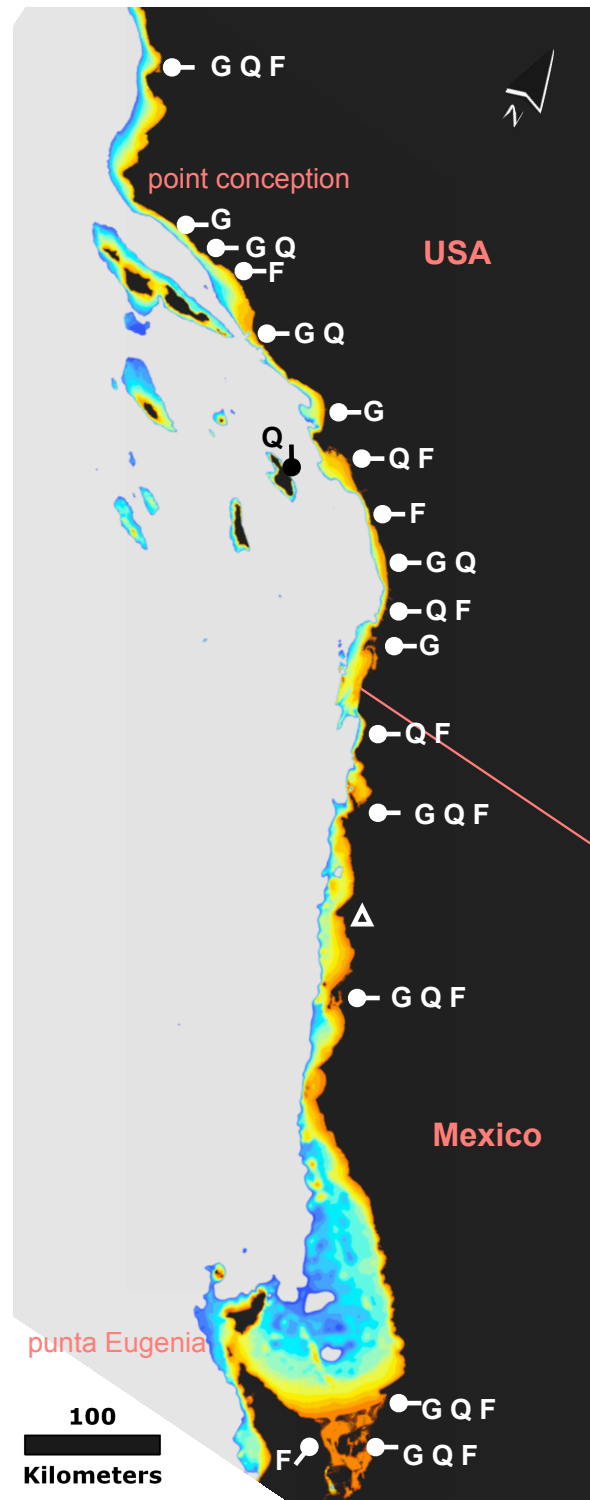
Figure 2-1. Sample collection and bathymetric map. Bathymetry is contoured at 10-meter intervals from 0 to 140 meters below present sea level (orange to dark blue, respectively). White markers note sample sites for fish species where: G- *Gillichthys mirabilis*, Q- *Quietula y-cauda*, F- *Fundulus parvipinnis*. Triangle denotes the Cabo Colonet region, which our models predict supported habitat ~10 thousand years ago (kya), but does not today. Note the distribution of offshore islands, whose sizes increased with lowered sea level.
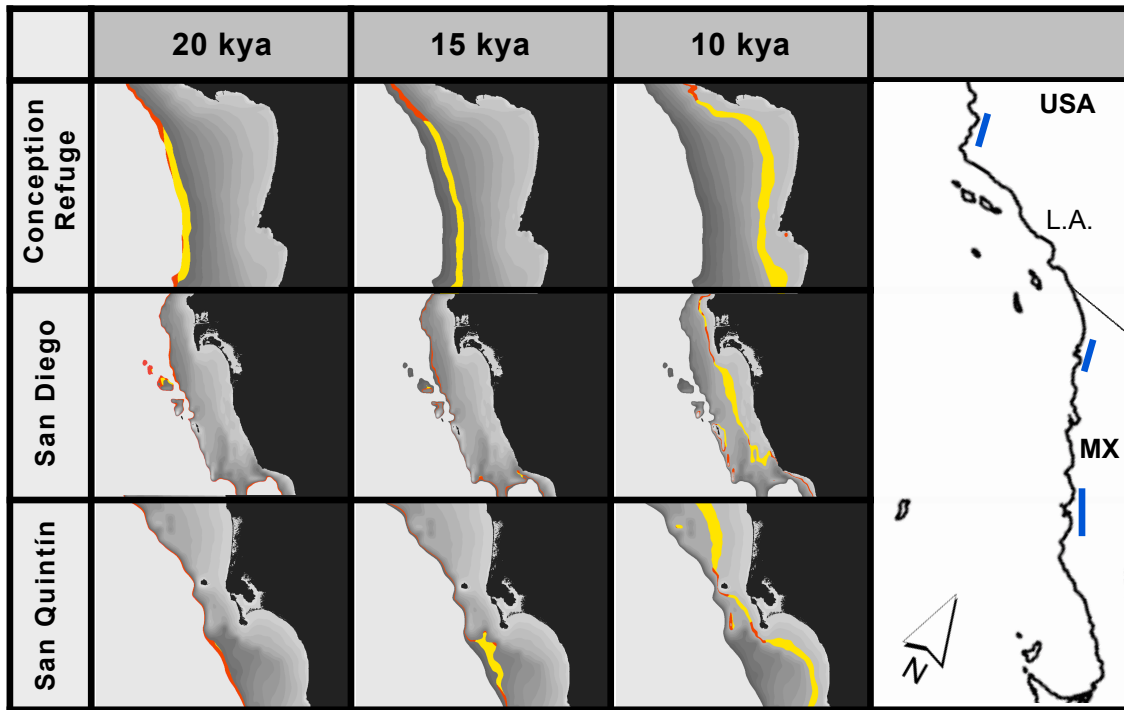
Figure 2-2. Estuarine habitat distribution through time. Time slices shown for three coastal locations (listed left) ordered by latitude and corresponding to regions indicated by blue lines on guide map (right). Area is colored as inhabitable (yellow) or too steep to form habitat (red) at ~18–20 kya (140–120 meters below present sea level), ~15 kya (110–100 meters below present sea level), ~10 kya (40–30 meters below present sea level). Bathymetry is contoured in greyscale by 10-m bins and black represents land. Modern habitats originate at different times and North Conception (top) is the only refugium amongst these three locations at lowstand (see Figure 2-S7 for the full coastline time series).
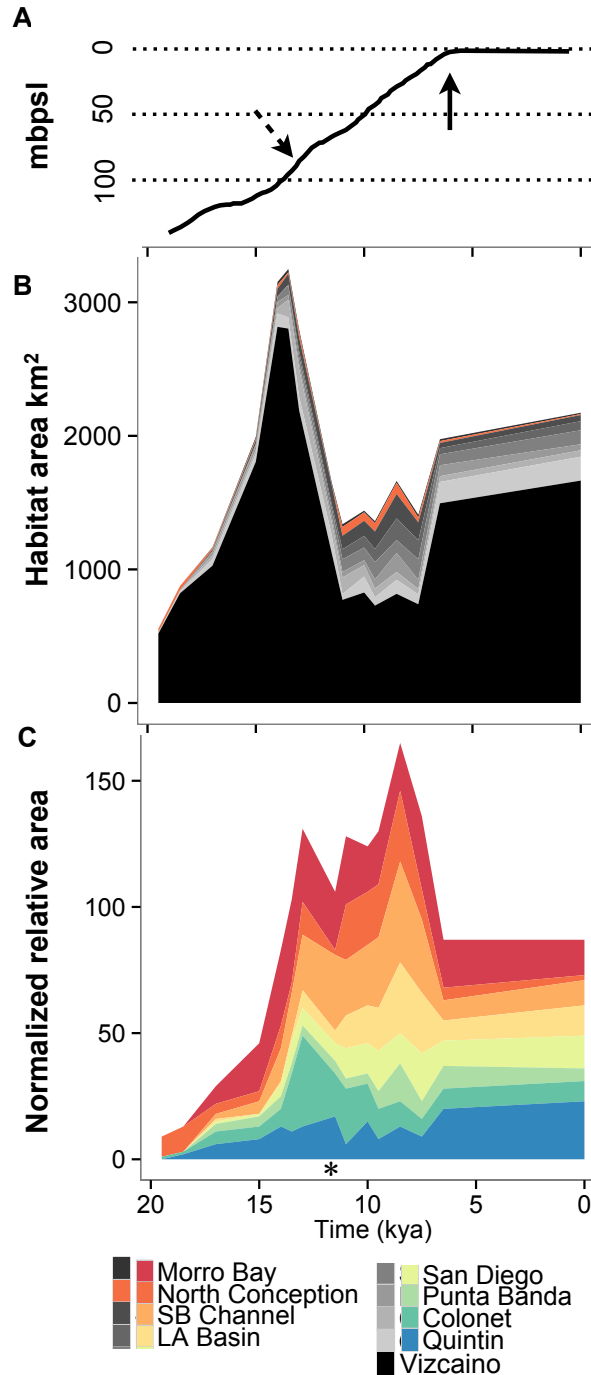
Figure 2-3. Estuarine habitat abundance through time. A) Sea-level curve adapted from (Chaytor *et al.* 2008). Dashed arrow indicates meltwater pulse 1A and solid arrow notes onset of modern stillstand. B) Total habitat area quantified through time for 9 coastal regions (see Figure 2-S8). Vizcaíno refugium is colored black and drives the overall habitat peak at ~14 kya, North Conception refugium is orange; non-refugia are colored in greyscale (see key). Locations are ordered by latitude. C) Habitat area normalized by coastal area (akin to habitat density) over time. This graph excludes Vizcaíno to show the expansion of southern Californian habitat 15–9 kya. Regions are colored by latitude in a gradient of red (north) to blue (south, see key). Asterisk denotes timing of the Younger Dryas cold period. Time on x-axis applies to panels A–C.

131
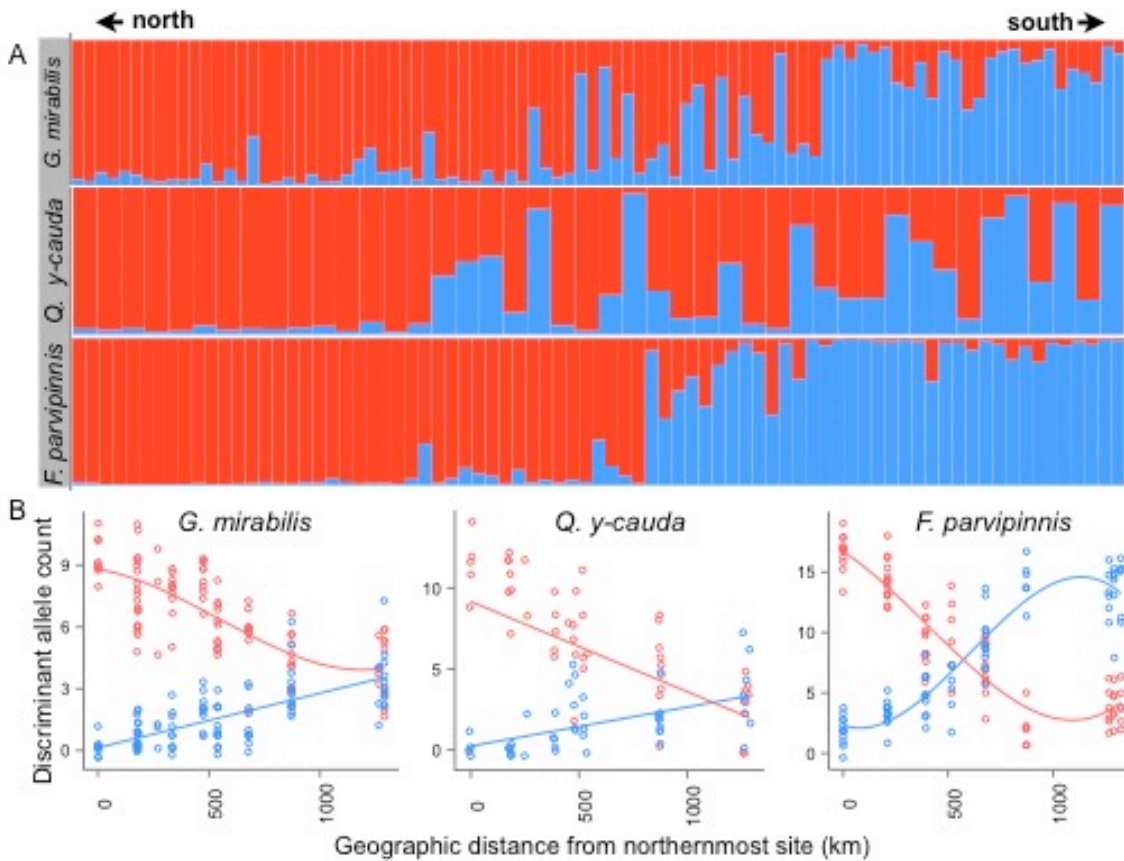
Figure 2-4. Genetic signatures of refugia and subsequent population mixing. A) Bayesian assignment tests from Structure using microsatellite data for individuals (vertical bars) ordered north (left, red) to south (right, blue). B) The numbers of northern (red) and southern (blue) discriminant allele counts are shown for all individuals against geographic coastal distance where they were collected. Favored regressions (AICc) are shown in corresponding colors (see Table 2-S5).
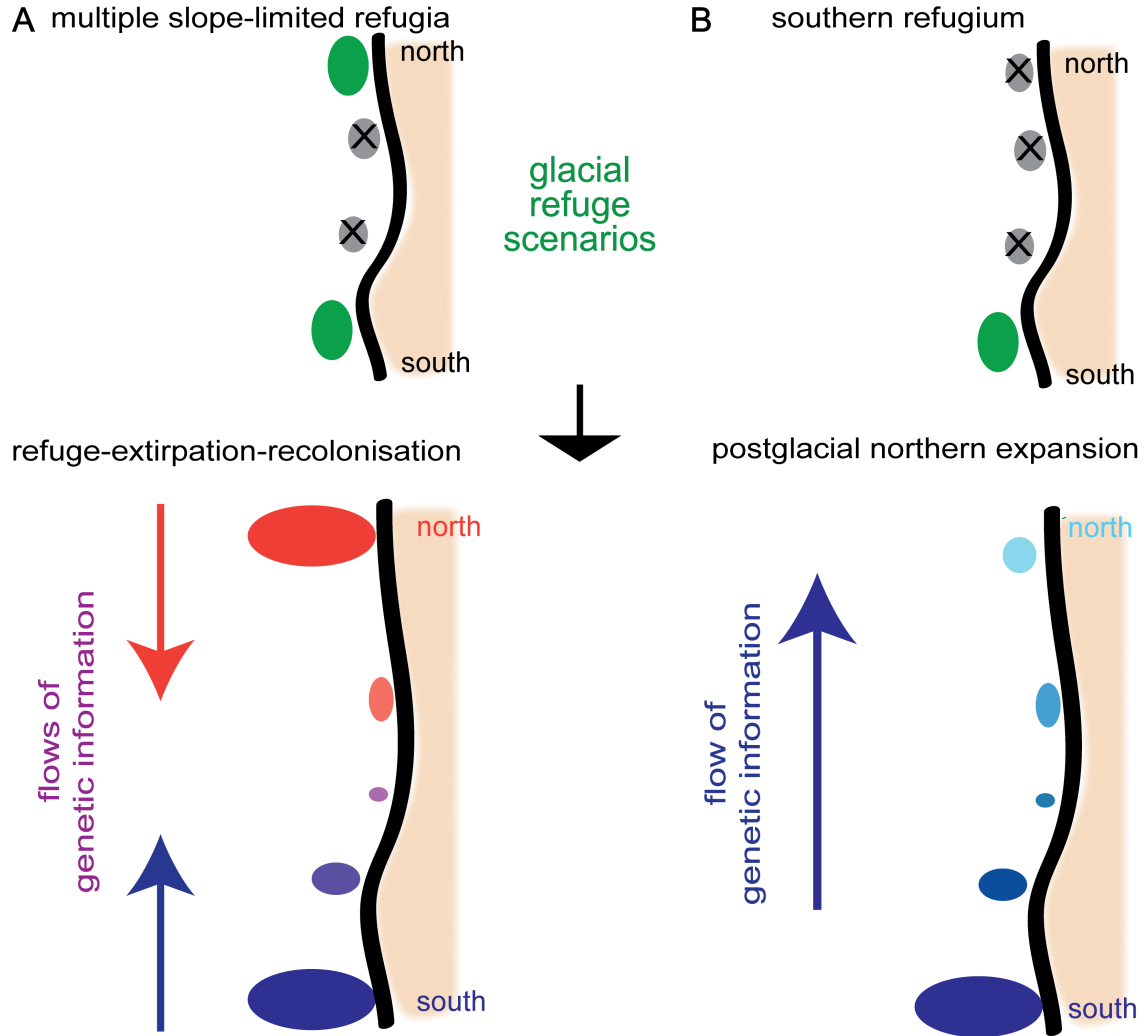
Figure 2-S1. Conceptual schematic. Presented are two refuge-recolonisation scenarios. Colors represent genetic relatedness, where more similar colors are more genetically similar. **A)** Illustration of our hypothesis where several estuarine populations reduce to two (upper), which diverge (different colors, lower panel), and admix (blending of red and blue to form purple) as they bi-directionally recolonize. **B)** This is the conventional model where individuals follow isotherms. Here, southern refuge(s) (upper) retain all the genetic diversity of the range (blue), and isolation by distance northern range expansion (lower panel) renders populations a series of genetic subsampling (blue gradient) from the south as individuals postglacially move northward.
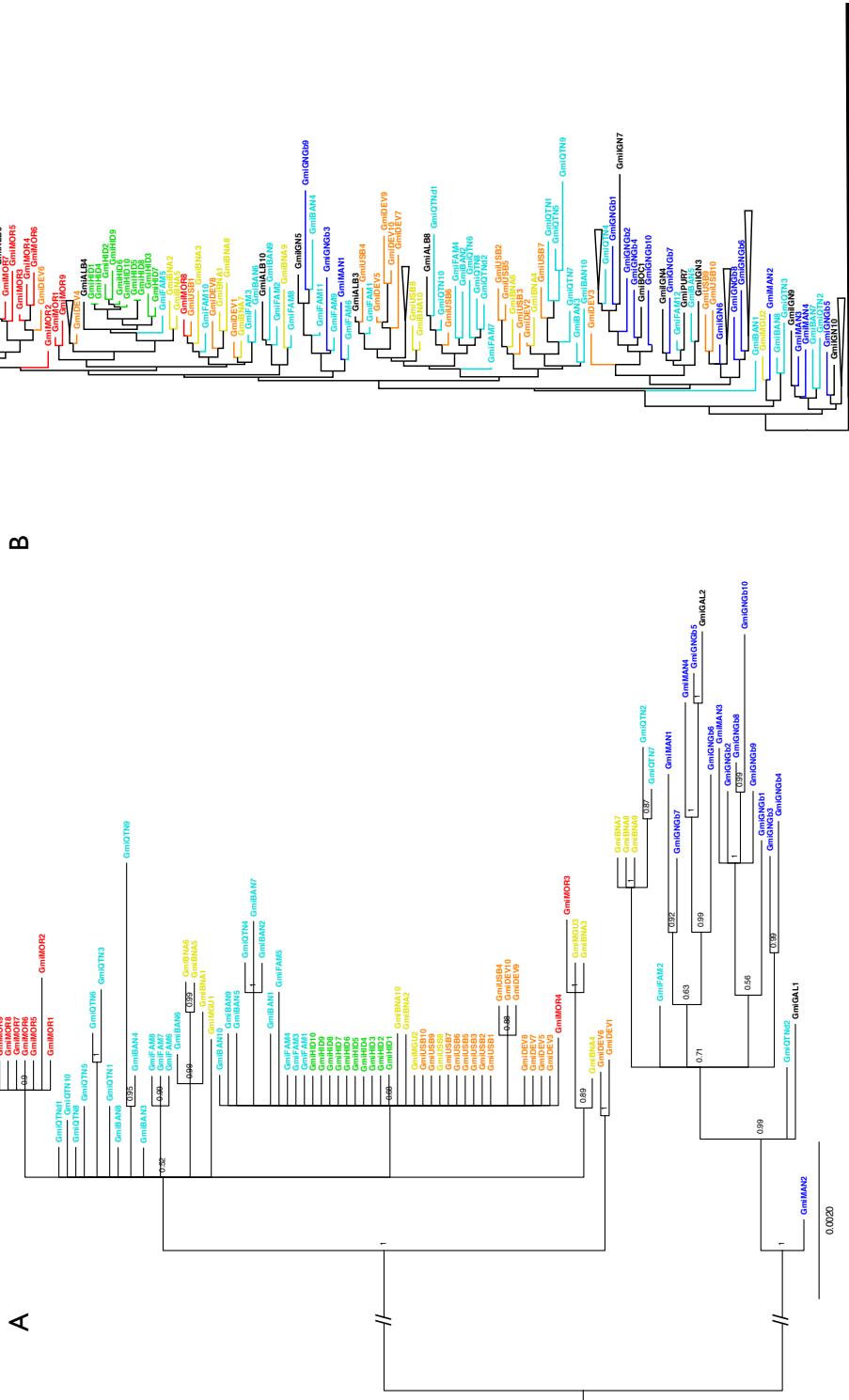
Figure 2-S2. New tree reconstructions for *Gillichthys mirabilis*. A) Construction in MRBAYES using mtDNA (mitochondrial control region and Cytochrome B, 1831 bp). Node posterior support is shown. B) Construction based on 16 microsatellite loci used in this study. Neighbor-joining tree made in POPULATIONS. Collapsed branches are samples outside the geographic region of the study. Parallel bars indicate shortened branch lengths for viewing. Individuals are color-coded by geographic region, consistent with the scale in Table 2-S1, with a red (north) to blue (south) gradient.
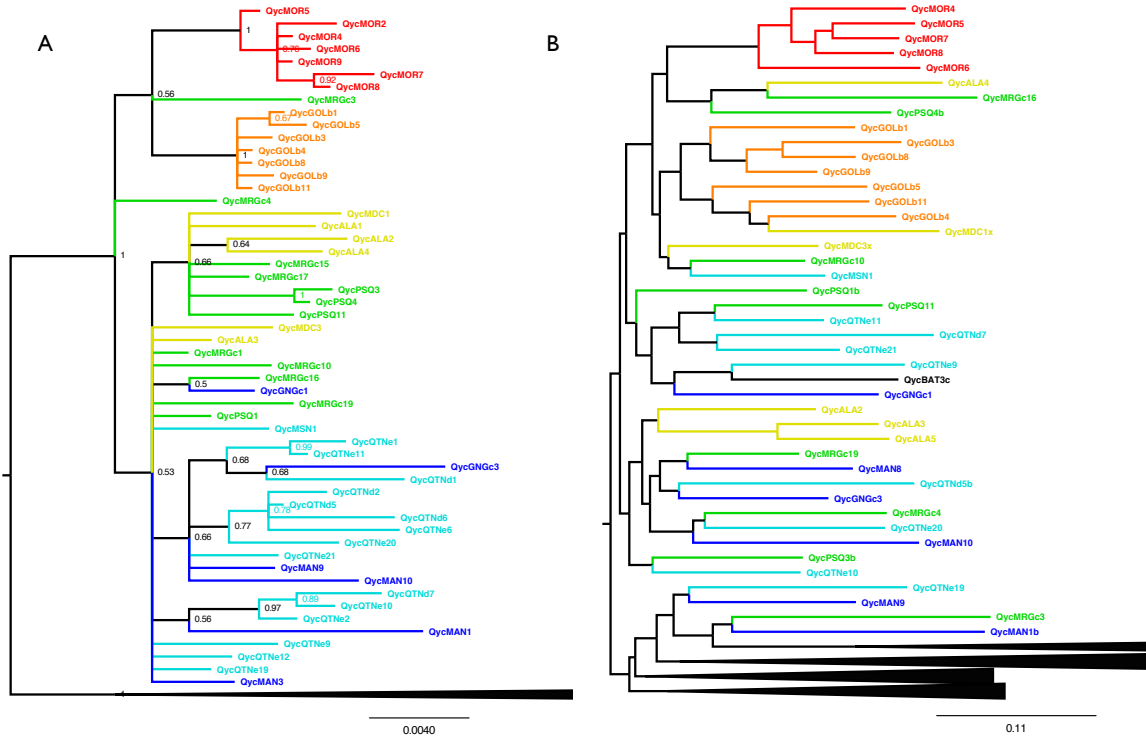
Figure 2-S3. New tree reconstructions for *Quietula y-cauda*. A) Construction in MRBAYES using mtDNA (mitochondrial control region and Cytochrome B, 1668 bp). Node posterior support is shown. B) Construction based on 17 microsatellite loci used in study. Neighbor-joining tree made in POPULATIONS. Collapsed branches are samples outside the geographic region of the study. Parallel bars indicate shortened branch lengths for viewing. Individuals are color-coded by geographic region, consistent with the scale in Table 2-S1, with a red (north) to blue (south) gradient.
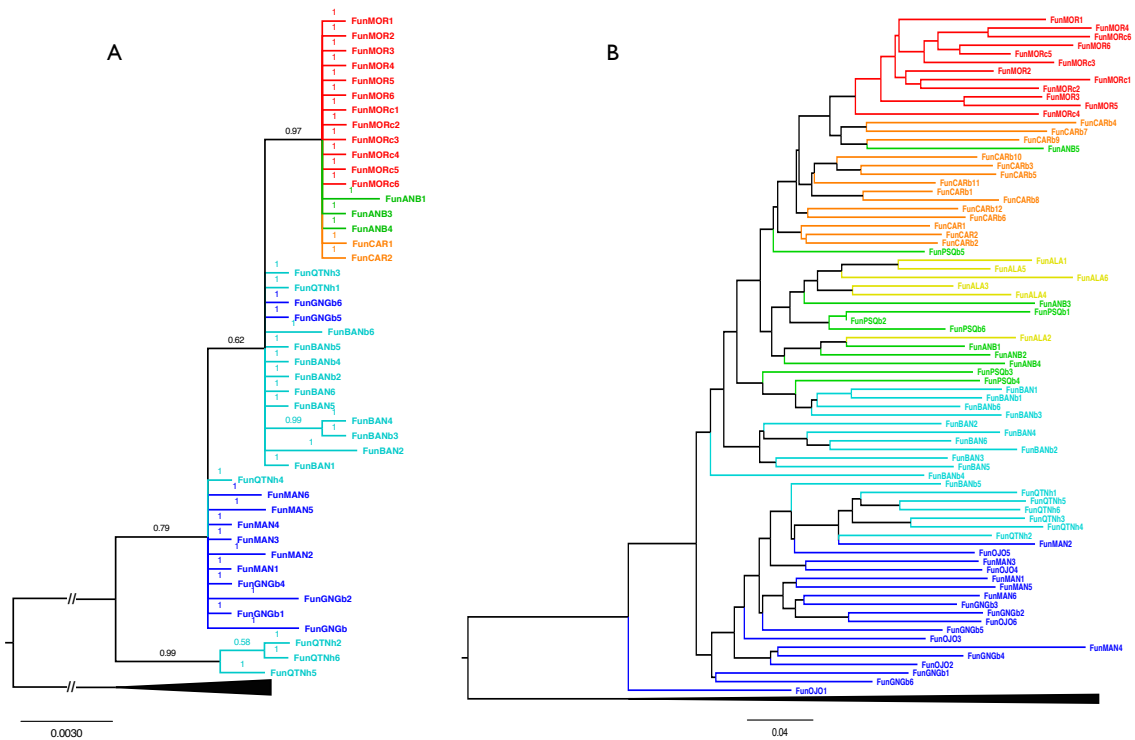
Figure 2-S4   New tree reconstructions for *Fundulus parvipinnis*. A) Construction in
MRBAYES using mtDNA (Mitochondrial Control Region, 883 bp). Branch posterior support is
shown. B) Construction based on 20 microsatellite loci used in study. Neighbor-joining tree made
in POPULATIONS. Collapsed branches are samples outside the geographic region of the study.
Parallel bars indicate shortened branch lengths for viewing. Individuals are color-coded by
geographic region, consistent with the scale in Table 2-S1, with a red (north) to blue (south)
gradient.
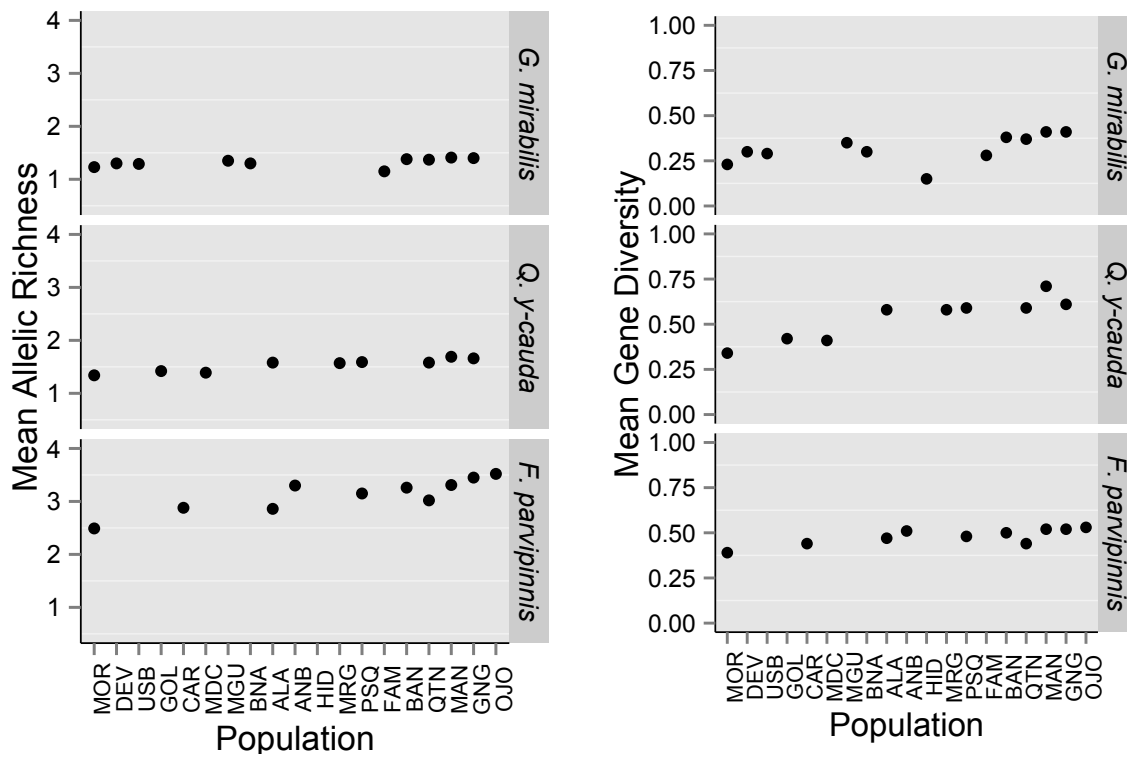
Figure 2-S5. Diversity indices. Mean allelic richness **(A)** and mean gene diversity **(B)** for species with populations oriented north to south on the x-axis. Sites thought to be admixed are not higher nor lower in diversity than refuge source populations (MOR, MAN, GNG, OJO). Note that the x-axis is not absolute geographic distance because population sites are not equidistant.
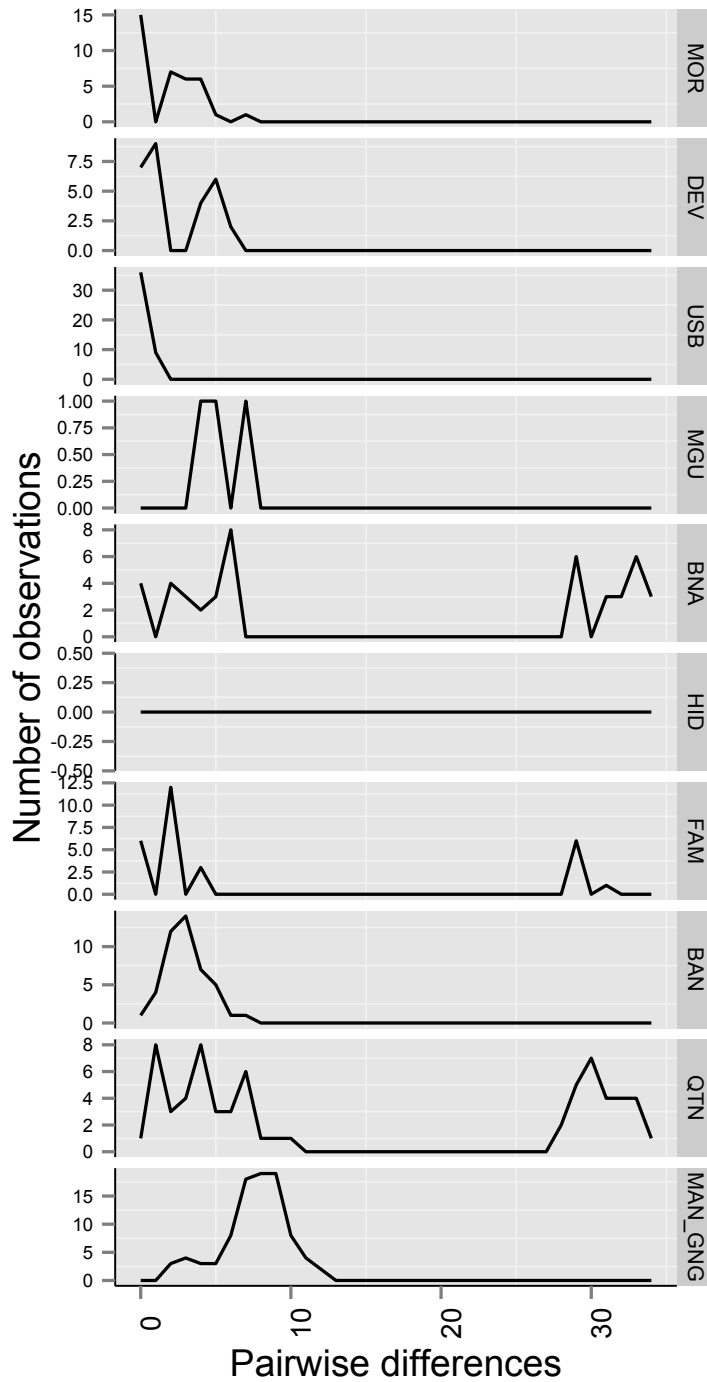
Figure 2-S6. Mismatch distribution. Pairwise differences per population for observed haplotypes in *Gillichthys mirabilis*. Sites ordered north to south. Sites expected to be admixed exhibit bimodal distributions, and unimodal distributions are observed in expected refuges (MOR, MAN_GNG). One site (HID) is monotypic and may be a founder bottleneck.
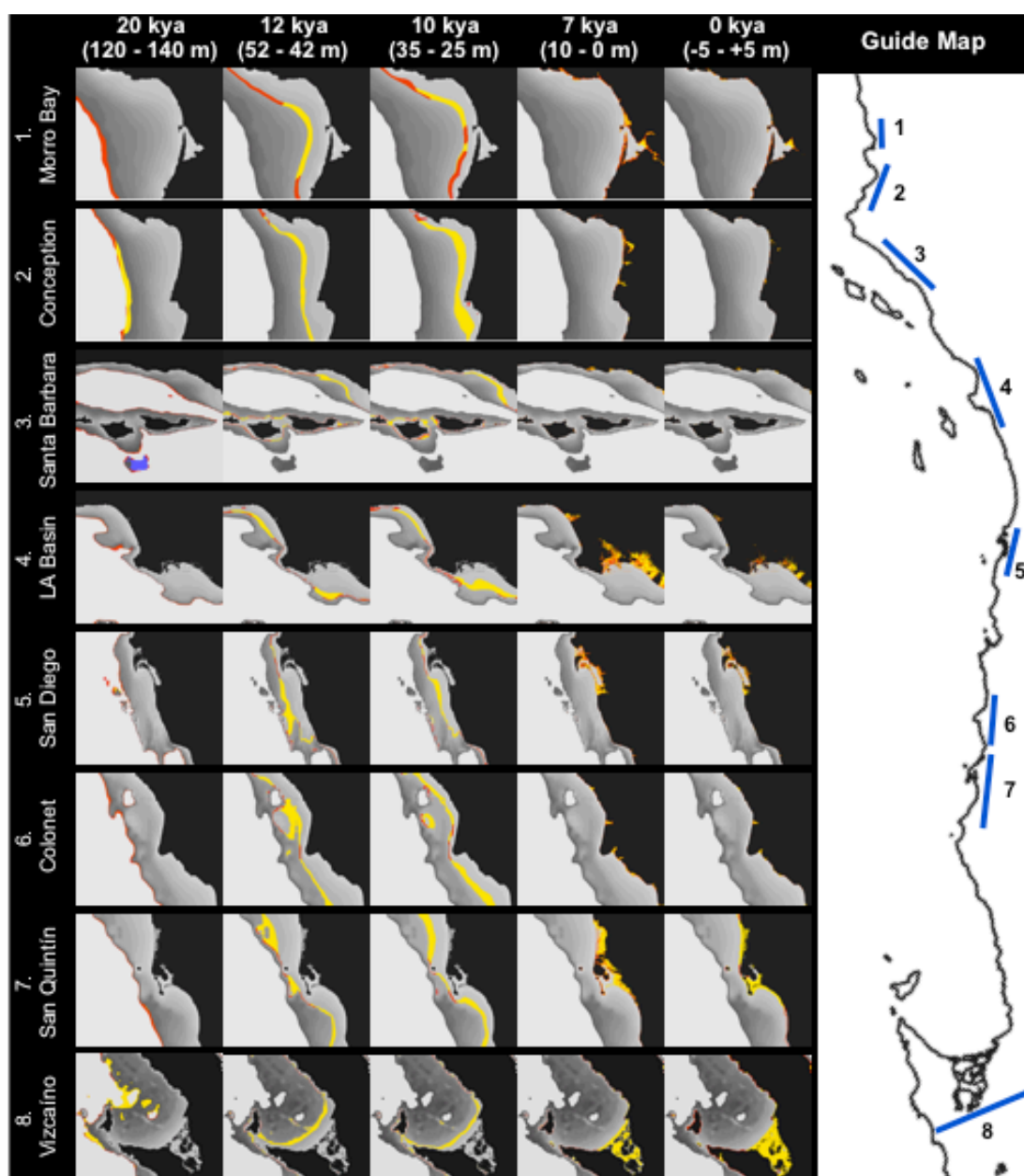
Figure 2-S7. Time-series habitat maps. Areas meeting slope requirements (yellow) or not (red) are shown for regions along the coast (rows, see guide map) for specific time points (columns). Time points and depth as meters below present sea level are listed for each column with 0 kya extending to 5 meters above present sea level (+5). Purple denotes areas that meet slope but not the minimum upland drainage area requirement to form estuarine habitat. Coastal regions are not of equal size.

Age (kya)	0	6.5	7.5	8.5	9.5	10	11	11.5	13	13.5	14	15	17	18.5	19.5
mbpsl	0 +/- 5	10 - 0	20 - 10	30 - 20	40 - 30	50 - 40	60 - 50	70 - 60	80 - 70	90 - 80	100 - 90	110 - 100	120 - 110	130 - 120	140 - 130
Morro Bay	10	14	21	14	15	13	20	17	21	24	22	14	5	0	0
Conception Refuge	7	14	36	83	62	63	66	6	38	12	28	12	13	31	25
Santa Barbara Channel	46	39	134	183	131	113	101	141	101	79	59	25	10	0	0
LA Basin	68	46	142	162	97	87	75	31	43	9	3	2	3	1	0
San Diego	105	82	154	96	131	95	95	59	54	70	38	12	6	2	3
Punta Banda	45	82	68	143	68	37	41	44	40	36	45	33	24	0	0
Colonet	48	43	41	59	66	86	124	95	204	131	41	29	27	6	7
San Quintin	179	160	74	105	62	119	44	137	104	85	100	60	50	15	2
Vizcaíno Refuge	1665	1495	739	817	729	827	772	1124	2189	2803	2816	1806	1028	821	519

Figure 2-S8. Habitat area per depth-time. Listed are habitat areas (km^2) for each time-depth bin in each coastal regions (left), which are ordered by latitude. Cells are colored by habitat abundance from low (red) to high (blue): 0–5 km^2, red; 6–14 km^2, orange; 15–29 km^2, yellow; 29–59 km^2, green; 60–150 km^2, teal; >150 km^2, blue. These values are the total summed polygon area per coastal region that meet slope requirements. Coastal regions are not of equal area. They represent areas of contiguous habitat formation might occur.

Table 2-S1. Sample locales. Sites of collections used in this study (bold) and sites only used in Figures 2-S1, 2-S2. 2-S3 (not bold) show corresponding 3-letter codes and coordinates in decimal degrees. Number of individuals per site listed; rough linear distance from the northernmost site in this study (Morro Bay) was calculated in Google Earth using the path tool and following the general orientation of the coastline. These geographic distances were used in the regression analysis in Figure 2-4. Colors correspond to color-coding in Figures 2-S1, 2-S2, 2-S3.

Site location	code	latitude°	longitude°	distance from MOR (km)	SI Fig 1 color	Number of Individuals (N)		
						F. parvipinnis	*G. mirabilis*	*Q. y-cauda*
Albany race track	ALB	37.889333	-122.311683	-	black	-	-	-
Morro Bay	MOR	35.348517	-120.8336	0	red	12	9	5
Devereaux Slough	DEV	34.41735	-119.873983	176	orange	-	10	-
U. Santa Barbara	USB	34.409383	-119.845017	179	orange	-	10	-
Goleta Slough	GOL	34.417046	-119.839374	181	orange	-	-	7
Carpenteria	CAR	34.400167	-119.538667	211	orange	14	-	-
Mandalay Canal	MDC	34.136892	-119.183952	256	yellow	-	-	2
Point Mugu	MGU	34.11391	-119.0821	269	yellow	-	3	-
Ballona Lagoon	BNA	33.962764	-118.4458	334	yellow	-	10	-
Alamitos Bay	ALA	33.745519	-118.117547	391	yellow	6	-	5
Anaheim Bay	ANB	33.736302	-118.093844	394	green	5	-	-
Catalina Island	CAT	33.430928	-118.50608	448	green	-	-	1
Hidden Lagoon	HID	33.275532	-117.451668	474	green	-	10	-
Santa Margarita	MRG	33.234	-117.410833	480	green	-	-	5
Penasquitos	PSQ	32.9325	-117.258	517	green	6	-	4
Mission Bay	MSN	32.770833	-117.232333	538	cyan	-	-	1
Famosa Slough	FAM	32.751155	-117.228381	539	cyan	-	12	-
Punta Banda	BAN	31.765157	-116.617381	678	cyan	12	10	-
San Quintín	QTN	30.418794	-116.023086	872	cyan	6	12	8
Laguna Manuela	MAN	28.247533	-114.085517	1266	blue	6	4	4
Guerrero Negro	GNG	28.021722	-114.114667	1290	blue	6	10	2
Ojo de Liebre	OJO	27.78305	-114.3129	1323	blue	6	-	-
la Bocana	BOC	26.789283	-113.675733	-	black	-	-	-
Ignacio lagoon	IGN	26.818667	-113.1815	-	black	-	-	-
el Cuarente	CUA	26.556133	-113.0028	-	black	-	-	-
Batequi	BAT	26.42715	-112.776733	-	black	-	-	-
Purisima	PUR	26.06265	-112.282083	-	black	-	-	-
el Rosario	ROS	25.698083	-112.074717	-	black	-	-	-
el Tambor	TAM	24.831932	-112.055708	-	black	-	-	-
Punta Pajaro	PPJ	24.753467	-112.043317	-	black	-	-	-
Salinas	SAL	24.582114	-111.787706	-	black	-	-	-
Gallinitas	GAL	24.557442	-111.735303	-	black	-	-	-

Table 2-S2. Microsatellite primers. Listed are primers developed for this project. *Gillichthys mirabilis* primers unlisted here are available in (Ellingson 2012). All forward primers in this study were labeled at the 5' end with the M13 complement: 5'AGGGTTTTCCCAGTCACGACGTT '3.

Species	Marker	Forward (5' - 3')	Reverse (5' - 3')
F. parvipinnis	**FMA02**	ATTTACGGCAACCACCTGC	AACCCTAGCTAACGCCTCC
F. parvipinnis	**FMA03**	TCCTGACCATCATAACAGATTTCG	CCTACCTGGCCAACAGC
F. parvipinnis	**FMA04**	GGAGGTAAACAGGGCACAG	CAGCATCCAGCAGCTTTCC
F. parvipinnis	**FMA05**	TCGAGTTGATCCAACAGATTGC	AGAGGCGGAAACATCCCTG
F. parvipinnis	**FMA07**	TCCAGTCTGAGCAAACTCC	ACGCAGGACACAGTTAGCC
F. parvipinnis	**FMA08**	GCCAACGTCAAGTCTCAAG	CTCGCCCATTGTATGCTGG
F. parvipinnis	**FMA09**	GAAGCAGGAATGGGTAGCG	AGTCAGTCCCAAACAGTCG
F. parvipinnis	**FMA10**	CACGCCTTTAACACGTCGG	CCTGGGAACGCCTTGGG
F. parvipinnis	**FMA13**	AACCCTGACCTGTATCGGC	CTGGCCTTTATCATGCTTTCC
F. parvipinnis	**FMA14**	TCATGCAAAGGTTAGTGTCGG	GAGGAGCTGGCCCAAGTAG
F. parvipinnis	**FMA15**	GCCTTGTACATAGAGCGTGG	GTGATCTTGTTGTGTACGGC
F. parvipinnis	**FMA16**	CCAGGAGAGACCATGGGAC	TTGACAGCTGGAGACAGGC
F. parvipinnis	**FMA18**	GTTCCCTGCAAGAACAGACG	CTCCAAGAGAATGTCGGGC
F. parvipinnis	**FMA19**	CGCTCCAGACAGCTAATGC	ATTCACGGTGCTACGGAGG
F. parvipinnis	**FMA21**	CCCACTCAACATACCAAGCTG	TCCATGCCAGTCATAGGCG
F. parvipinnis	**FMA23**	TCCTCCCGCTTTCATTCCG	GACTGCAGCCCAGATGTTG
F. parvipinnis	**FMA24**	CTCCAGCCACACTTTATGCG	CGGTGAATGTGCTCCAAGG
F. parvipinnis	**FMA25**	CAGAGCATCACAGAACCTCG	GTGGACTCTGATTTGCTGCC
F. parvipinnis	**FMA26**	CAGCCGCCAAATTAGAAAGC	TCCCATGCTGCAACTTGTTC
F. parvipinnis	**FMA29**	GCTACACTACCCACCTCTGG	GCATGCAGGCGCTCAACAAG
G. mirabilis	**GMA01**	GATTCCGATTCCAATGTTC	TTGCAACTTACAAGAAATTCAC
G. mirabilis	**GMA03**	TTGAAGACGTACAGCACCAC	CCAGTCAGAATGTGTTCCAC
G. mirabilis	**GMA08**	TAATGACGCAGTGTTTGATG	CTGTGTGCCTTGAAGGTG
G. mirabilis	**GMA14**	CATGAATTTAGCACCATCATC	TTCTTGTGGAGTCTCTTCAAAG
G. mirabilis	**GMA20**	GACTCTTTGTCCAGCATTTC	TGTTATTCAAGTGCCATCATC
Q. y-cauda	**QMA01**	CTGTGACTTTGGGCATTAG	AATGCCCTGGTTATCTGTC
Q. y-cauda	**QMA03**	CGACATTCACGACACAAATC	ACGAATTTGACCTGAGAGC
Q. y-cauda	**QMA04**	AATGAAACGGTGAAAGAAAC	TTCAGCTCCTTCAGTTTGAC
Q. y-cauda	**QMA05**	TTCTTTCTTGCCTTGTCC	CATGAAGGCACGAAAGAG
Q. y-cauda	**QMA06**	GACTGTTCCATGTTCCTGTG	TCAGAGCAGTTTAATCCAAAG
Q. y-cauda	**QMA07**	CTTCCTCCACTCTCTCACAG	AGCGACGTACTTCTGAAGAG
Q. y-cauda	**QMA08**	ACTGAAGCTCCAAGGACAC	TGATTGTGCTGTGACTCATG
Q. y-cauda	**QMA09**	AGTGCAGGCATACATACATG	TTTGATTTGATGTATGCACTG
Q. y-cauda	**QMA10**	GTGATTTATGCGTCCAGATG	TTCAGGGTCGTCTTTAAATC
Q. y-cauda	**QMA13**	AGGCTCAGGACTCTCATGTAC	CTTCTCCTCTACCGCTCAG
Q. y-cauda	**QMA17**	TATTTGTCATCGCCCTAATG	CAAATTAAAGCCAATTGTTG
Q. y-cauda	**QMA24**	CCCGCTCCGTCAACACTC	CAATGGTGAGCGCGTACATG
Q. y-cauda	**QMA25**	GACATGCTCCTCGTTTGACC	CACGCCCACATTTCAAGGAC
Q. y-cauda	**QMA26**	TTCGTCTGACTGTGCTGGTTG	CTCCTGCTCGGTTCATGCC
Q. y-cauda	**QMA27**	GACTGTTCCATGTTCCTGTGAG	ACCTACTTCGACTGACTGGC
Q. y-cauda	**QMA28**	ATCTGCAGTAACGTGGGCTC	AGTGTGCTCGTGACTTATGC
Q. y-cauda	**QMA30**	TTGACTGCGCTCTTACATGG	CACGGACTGTTCGACAATATTG

Table 2-S3. Slope measurements. Sites where at least two of the three species co-occur were measured five times, others were measured once. Run lengths vary based on what portion of the estuary was being measured and overall size of the system.

Site	Slope (%)	Run Length (km)
Morro Bay	0.499	500-600
Morro Bay	0.906	500-600
Morro Bay	1.111	500-600
Morro Bay	1.150	500-600
Morro Bay	0.363	500-600
Alamitos Bay	0.498	200-400
Alamitos Bay	0.256	200-400
Alamitos Bay	0.455	200-400
Alamitos Bay	0.578	200-400
Alamitos Bay	0.000	200-400
Banda	0.000	200-600
Banda	0.00	200-600
Banda	0.687	200-600
Banda	0.192	200-600
Banda	0.241	200-600
San Quintín	0.000	1000-1700
San Quintín	0.000	1000-1700
San Quintín	0.312	1000-1700
San Quintín	0.100	1000-1700
San Quintín	0.198	1000-1700
Vizcaíno	0.106	2000-5000
Vizcaíno	0.116	2000-5000
Vizcaíno	0.254	2000-5000
Vizcaíno	0.743	2000-5000
Vizcaíno	1.263	2000-5000
Devereaux Slough	0.424	250
Santa Barbara Channel	0.713	400
Carpenteria	0.952	100
Goleta Slough	1.330	75
Point Mugu	0.542	350
Catalina	0.298	350
Mandalay Canal	0.498	200
Ballona	0.862	120
Anaheim Bay	0.000	500
Los Penasquitos	0.571	175
Famosa Slough	0.437	250
Santa Margarita	0.305	985
Mission Bay	0.328	305

Table 2-S4. Fixation Index. Pairwise F_{ST} values listed on the lower half of the table and significance indicated (p-value < 0.01) on the upper half for: *G. mirabilis* **(A)**, *Q. y-cauda* **(B)**, and *F. parvipinnis* **(C)**. Note that populations may be sample-limited for this metric, particularly in *Q. y-cauda.*

A	MOR	DEV	USB	MGU	BNA	FAM	HID	BAN	QTN	MAN	GNG
MOR		-	+	-	+	+	+	+	+	+	+
DEV	0.11259		-	-	-	-	+	-	+	-	+
USB	0.1585	-0.00284		-	-	+	+	+	+	-	+
MGU	0.02382	-0.02909	-0.00054		-	-	+	-	+	-	-
BNA	0.14001	0.04147	0.04251	-0.01184		+	+	-	+	-	+
FAM	0.15165	0.04154	0.086	0.03708	0.061		+	+	+	+	+
HID	0.36703	0.28492	0.37074	0.26191	0.30592	0.23939		+	+	+	+
BAN	0.11088	0.04977	0.07244	0.02616	0.05321	0.05381	0.35553		+	-	+
QTN	0.23894	0.16832	0.14758	0.15631	0.19337	0.15255	0.42318	0.08467		-	+
MAN	0.17583	0.06185	0.07306	0.02963	0.11049	0.11616	0.42224	-0.00465	0.04351		-
GNG	0.16641	0.11276	0.13273	0.08537	0.15241	0.09274	0.2881	0.05073	0.06413	-0.00933	

B	MOR	GOL	CAT	MDC	ALA	MRG	PSQ	MSN	QTN	MAN	GNG
MOR		+	-	-	+	+	-	-	+	+	-
GOL	0.18882		-	-	-	+	-	-	+	+	-
CAT	0.35014	0.35305		-	-	-	-	-	-	-	-
MDC	0.02749	0.0252	0.22865		-	-	-	-	-	-	-
ALA	0.14909	0.06344	0.21702	0.02549		-	-	-	-	-	-
MRG	0.2212	0.12796	0.22574	0.08269	0.01366		-	-	-	-	-
PSQ	0.16498	0.08628	0.20494	0.03161	-0.00175	-0.02079	-	-	-	-	-
MSN	0.07978	0.0898	0.45455	-0.03927	0.00809	0.04493	0.02279		-	-	-
QTN	0.21292	0.13986	0.25464	0.10784	0.056	0.04772	-0.01143	0.03424		-	-
MAN	0.23235	0.21966	0.25788	0.12299	0.08238	0.09591	0.0878	0.03725	0.08041		-
GNG	0.30393	0.21731	0.32613	0.14373	0.10027	0.02961	-0.01873	-0.00267	0.00494	0.0298	

C	MOR	CAR	ALA	ANB	PSQ	BAN	QTN	MAN	GNG	OJO
MOR		+	+	+	+	+	+	+	+	+
CAR	0.12178		+	+	+	+	+	+	+	+
ALA	0.18952	0.1248		-	+	+	+	+	+	+
ANB	0.14079	0.06373	0.04448		-	+	+	+	+	+
PSQ	0.18514	0.0925	0.0784	0.03604		+	+	+	+	+
BAN	0.20903	0.1308	0.10186	0.11841	0.08601		+	+	+	+
QTN	0.36129	0.29639	0.23719	0.25691	0.26707	0.111		+	+	+
MAN	0.2809	0.19879	0.16387	0.15858	0.17707	0.1074	0.09602		-	-
GNG	0.23274	0.16499	0.1211	0.10075	0.12859	0.08157	0.1129	0.01897		-
OJO	0.26223	0.17876	0.13097	0.13189	0.13236	0.04938	0.07599	0.0082	0.0167	

Table 2-S5. AICc regression values. Comparison of corrected Akaike Information Criterion (AICc) values for linear, quadratic, and cubic regressions of northern and southern allele counts versus geographic distance. Yellow cells indicate the statistically favored regression for each allele set.

Taxon	AICc regression scores		
	linear	quadratic	cubic
G. mirabilis- North	369.045	368.924	368.88
G. mirabilis- South	297.835	299.836	301.451
Q. y-cauda- North	208.753	209.045	211.482
Q. y-cauda- South	177.798	179.985	181.337
F. parvipinnis- North	378.669	347.987	343.632
F. parvipinnis- South	354.81	354.537	335.681

Table 2-S6. Refuge habitat model values. Comparison of p-value and corrected Akaike Information Criterion (AICc) scores for different refuge scenarios (left column). Results are from Generalized Linear Models using the predictive variables identified via DFA (Maximum Polygon Area and Summed Habitat Area). Asterisks denote significant values, dagger denotes models performed with Firth's Biased Adjustment estimates, double daggers were models run with False Discovery Rate. The only significant scenario is Vizcaíno and North Conception refugia (shown in yellow). A Vizcaíno only refugium is not supported.

Refugium Model Scenario	Habitat	
	p-value	AICc
Vizcaíno + N. Conception	0.0085*	18.0000
Vizcaíno + N. Conception†‡	0.0240*	12.9156
Vizcaíno + Morro Bay	0.0813	17.2383
Vizcaíno + Morro Bay + N. Conception	0.0599	23.8280
Vizcaíno + Morro Bay + N. Conception†‡	0.1297	25.3831
Vizcaíno + Morro Bay + N. Conception + LA Basin	0.2165	20.1049
Vizcaíno + LA Basin	0.0889	15.4952
Vizcaíno + LA Basin†‡	0.2716	24.9661
Vizcaíno + Santa Barbara Channel	0.0889	15.4952
Vizcaíno + Santa Barbara Channel†‡	0.2716	24.9661
Vizcaíno only	0.0433*	10.8000
Vizcaíno only†‡	0.1147	20.0641
San Quintín + N. Conception	0.1786	16.8895
Vizcaíno + San Quintín + N. Conception	0.0633	16.7370
Vizcaíno + San Quintín + N. Conception†‡	0.1146	25.1359

References

Adams SM, Lindmeier JB, Duvernell DD (2006) Microsatellite analysis of the phylogeography, Pleistocene history and secondary contact hypotheses for the killifish, *Fundulus heteroclitus*. *Molecular Ecology*, **15**, 1109–1123.

Akihito, Iwata A, Kobayashi T *et al.* (2000) Evolutionary aspects of gobioid fishes based upon a phylogenetic analysis of mitochondrial cytochrome B genes. *Gene*, **259**, 5–15.

Allendorf FW (1986) Genetic drift and the loss of alleles versus heterozygosity. *Zoo biology*, **5**, 181–190.

Becker JJ, Sandwell DT, Smith WHF *et al.* (2009) Global Bathymetry and Elevation Data at 30 Arc Seconds Resolution: SRTM30_PLUS. *Marine Geodesy*, **32**, 355–371.

Benumof BT, Storlazzi CD, Seymour RJ, Griggs GB (2000) The relationship between incident wave energy and seacliff erosion rates: San Diego County, California. *Journal of Coastal Research*, **16**, 1162–1178.

Bernardi G, Talley D (2000) Genetic evidence for limited dispersal in the coastal California killifish, *Fundulus parvipinnis*. *Journal of Experimental Marine Biology and Ecology*, **255**, 187–199.

Bernstein RL, Breaker L, Whritner R (1977) California Current Eddy Formation: Ship, Air, and Satellite Results. *Science*, **195**, 353–359.

Bilton DT, Paula J, Bishop JDD (2002) Dispersal, Genetic Differentiation and Speciation in Estuarine Organisms. *Estuarine, Coastal and Shelf Science*, **55**, 937–952.

Bucklin A (1991) Population genetic responses of the planktonic copepod *Metridia pacifica* to a coastal eddy in the California Current. *Journal of Geophysical Research letters*, **96**, 14977–14808.

Chaytor JD, Goldfinger C, Meiner MA *et al.* (2008) Measuring vertical tectonic motion at the intersection of the Santa Cruz-Catalina Ridge and Northern Channel Islands platform, California Continental Borderland, using submerged paleoshorelines. *Geological Society of America Bulletin*, **120**, 1053–1071.

Chessel D, Dufour AB, Thioulouse J (2004) The ade4 package-I-One-table methods. *R news*, **4**, 5–10.

Dawson MN (2001) Phylogeography in coastal marine animals: a solution from California? *Journal of Biogeography*, **28**, 723–736.

Dawson MN, Louie KD, Barlow M, Jacobs DK, Swift CC (2002) Comparative phylogeography of sympatric sister species, *Clevelandia ios* and *Eucyclogobius newberryi* (Teleostei, Gobiidae), across the California Transition Zone. *Molecular Ecology*, **11**, 1065–1075.

Dawson MN, Staton JL, Jacobs DK (2001) Phylogeography of the Tidewater Goby, *Eucyclogobius Newberryi* (Teleostei, Gobiidae), in Coastal California. *Evolution*, **55**, 1167–1179.

Earl DA, vonHoldt BM (2011) STRUCTURE HARVESTER: a website and program for visualizing STRUCTURE output and implementing the Evanno method. *Conservation Genetics Resources*, **4**, 359–361.

Earl DA, Louie KD, Bardeleben C, Swift CC, Jacobs DK (2010) Rangewide microsatellite phylogeography of the endangered tidewater goby, *Eucyclogobius newberryi* (Teleostei: Gobiidae), a genetically subdivided coastal fish with limited marine dispersal. *Conservation Genetics*, **11**, 103–114.

Edmands S (2001) Phylogeography of the intertidal copepod *Tigriopus californicus*

reveals substantially reduced population differentiation at northern latitudes. *Molecular Ecology*, **10**, 1743–1750.

Ellingson R (2012) Phylogenetics and phylogeography of North Pacific bay gobies: adaptive convergence, relictual endemism, and climate-driven population structure. Univeristy of California, Los Angeles.

Ellingson RA, Swift CC, Findley LT, Jacobs DK (2014) Convergent evolution of ecomorphological adaptations in geographically isolated Bay gobies (Teleostei: Gobionellidae) of the temperate North Pacific. *Molecular Phylogenetics and Evolution*, **70**, 464–477.

Excoffier L, Ray N (2008) Surfing during population expansions promotes genetic revolutions and structuration. *Trends in Ecology & Evolution*, **23**, 347–351.

Excoffier L, Laval G, Schneider S (2005) Arlequin (version 3.0): an integrated software package for population genetics data analysis. *Evolutionary bioinformatics online*, **1**, 47–50.

Faircloth BC (2008) MSATCOMMANDER: detection of microsatellite repeat arrays and automated, locus-specific primer design. *Molecular Ecology Resources*, **8**, 92–94.

Fraser CI, Nikula R, Spencer HG, Waters JM (2009) Kelp genes reveal effects of subantarctic sea ice during the Last Glacial Maximum. *Proceedings of the National Academy of Sciences of the United States of America*, **106**, 3249–3253.

Gannet H, Goode RU, Fletcher LC (1895) California. Arroyo Grande quadrangle (15'), 1987 (1925). *U.S.C. G. Survey*, 35.00000,–120.50000; 35.25000,–120.50000; 35.25000,–120.75000; 35.00000,–120.75000; 35.00000,–120.50000.

Gaylord B, Gaines SD (2000) Temperature or Transport? Range Limits in Marine

Species Mediated Solely by Flow. *The American Naturalist*, **155**, 769–789.

Glaubitz JC (2004) CONVERT: A user-friendly program to reformat diploid genotypic data for commonly used population genetic software packages. *Molecular Ecology Notes*, **4**, 309–310.

Goudet J (1995). FSTAT (version 1.2): a computer program to calculate F-statistics. *The Journal of Heredity*, **86**, 485–486.

Graham MH, Dayton PK, Erlandson JM (2003) Ice ages and ecological transitions on temperate coasts. *Trends in Ecology & Evolution*, **18**, 33–40.

Griffith RW (1974) Environment and salinity tolerance in the genus *Fundulus*. *Copeia*, **1974**, 319.

Gurrola LD, Keller EA, Chen JH (2014) Tectonic geomorphology of marine terraces: Santa Barbara fold belt, California. *Geological Society of America Bulletin*, **126**, 219–233.

Hewitt G (2000) The genetic legacy of the Quaternary ice ages. *Nature*, **405**, 907–913.

Hewitt GM (2004) Genetic consequences of climatic oscillations in the Quaternary. *Philosophical Transactions of the Royal Society B: Biological Sciences*, **359**, 183–195.

Huang D, Bernardi G (2001) Disjunct Sea of Cortez–Pacific Ocean *Gillichthys mirabilis* populations and the evolutionary origin of their Sea of Cortez endemic relative, *Gillichthys seta*. *Marine Biology*, **138**, 421–428.

Ilves KL, Huang W, Wares JP, Hickerson MJ (2010) Colonization and/or mitochondrial selective sweeps across the North Atlantic intertidal assemblage revealed by multi-taxa approximate Bayesian computation. *Molecular Ecology*, **19**, 4505–4519.

Ingersoll RV, Rumelhart PE (1999) Three-stage evolution of the Los Angeles basin, southern California. *Geology*, **27**, 593–6.

Jacobs DK, Haney TA, Louie KD (2004) Genes, Diversity, and Geologic process on the Pacific coast. *Annual Review of Earth and Planetary Sciences*, **32**, 601–652.

Jacobs D, Stein ED, Longcore T (2011) Classification of California estuaries based on natural closure patterns: Templates for restoration and management. *Southern California Coastal Water Research Project*, **619**, 1–50.

Jakobsson M, Rosenberg NA (2007) CLUMPP: a cluster matching and permutation program for dealing with label switching and multimodality in analysis of population structure. *Bioinformatics*, **23**, 1801–1806.

Kearse M, Moir R, Wilson A *et al.* (2012) Geneious Basic: an integrated and extendable desktop software platform for the organization and analysis of sequence data. *Bioinformatics*, **28**, 1647–1649.

Kelly RP, Palumbi SR (2010) Genetic Structure Among 50 Species of the Northeastern Pacific Rocky Intertidal Community. *PLoS ONE*, **5**, e8594–13.

Kimura M, Weiss GH (1964) The Stepping Stone Model of Population Structure and the Decrease of Genetic Correlation with Distance. *Genetics*, **49**, 561–576.

Kinlan BP, Graham MH (2005) Late-Quaternary changes in the size and shape of the California Channel Islands: implications for marine subsidies to terrestrial communities. In: *Proceedings of the California Islands Symposium* (eds Garcelon DK, Schwemm CA). Arcata, CA.

Kirby JT, Dalrymple RA (1986) Modeling waves in surfzones and around islands. *Journal of Waterway*, **112**, 78–93.

Lee WJ, Conroy J, Howell WH, Kocher TD (1995) Structure and evolution of teleost mitochondrial control regions. *Journal of Molecular Evolution*, **41**, 54–66.

Lettis WR, Hanson KL (1992) Quaternary tectonic influences on coastal morphology, south-central California. *Quaternary International*, **15/16**, 135–148.

Lischer HEL, Excoffier L (2012) PGDSpider: an automated data conversion tool for connecting population genetics and genomics programs. *Bioinformatics*, **28**, 298–299.

Lyle M, Heusser L, Ravelo C *et al.* (2010) Pleistocene water cycle and eastern boundary current processes along the California continental margin. *Paleoceanography*, **25**, PA4211–19.

Marko PB (2004) "What's larvae got to do with it?" Disparate patterns of post-glacial population structure in two benthic marine gastropods with identical dispersal potential. *Molecular Ecology*, **13**, 597–611.

Masters PM (2006) Holocene sand beaches of southern California: ENSO forcing and coastal processes on millennial scales. *Palaeogeography, Palaeoclimatology, Palaeoecology*, **232**, 73–95.

Mayr E (1944) Wallace's Line in the Light of Recent Zoogeographic Studies. *The Quarterly Review of Biology*, **19**, 1–14.

Meirmans PG, Van Tienderen PH (2004) GENOTYPE and GENODIVE: two programs for the analysis of genetic diversity of asexual organisms. *Molecular Ecology Notes*, **4**, 792–794.

Miller MA, Pfeiffer W, Schwartz T (2010) Creating the CIPRES Science Gateway for inference of large phylogenetic trees. *2010 Gateway Computing Environments*

Workshop (GCE), 1–8.

Muhs DR, Rockwell TK, Kennedy GL (1992) Late Quaternary uplift rates of marine terraces on the Pacific coast of North America, southern Oregon to Baja California Sur. *Quaternary International*, **15-16**, 121–133.

Nei M (1973) Analysis of gene diversity in subdivided populations. *Proceedings of the National Academy of Sciences*, **70**, 3321–3323.

Niemi NA, Oskin M, Rockwell TK (2008) Southern California Earthquake Center Geologic Vertical Motion Database. *Geochemistry, Geophysics, Geosystems*, **9**, 1–14.

Pardo LM, MacKay I, Oostra B, van Duijn CM, Aulchenko YS (2005) The Effect of Genetic Drift in a Young Genetically Isolated Population. *Annals of Human Genetics*, **69**, 288–295.

Petit RJ (2003) Glacial Refugia: Hotspots But Not Melting Pots of Genetic Diversity. *Science*, **300**, 1563–1565.

Petit RJ, Aguinagalde I, de Beaulieu J-L *et al.* (2003) Glacial refugia: hotspots but not melting pots of genetic diversity. *Science*, **300**, 1563–1565.

Plattner C, Malservisi R, Govers R (2009) On the plate boundary forces that drive and resist Baja California motion. *Geology*, **37**, 359–362.

Pritchard JK, Stephens M, Donnelly P (2000) Inference of population structure using multilocus genotype data. *Genetics*, **155**, 945–959.

Ronquist F, Huelsenbeck JP (2003) MrBayes 3: Bayesian phylogenetic inference under mixed models. *Bioinformatics*, **19**, 1572–1574.

Sarkar D (2008) *Lattice: multivariate data visualization with R* (R Gentleman, K Hornik,

G Parmigiani, Eds,). Springer Science & Business Media.

Seapy RR, Littler MM (1980) Biogeography of rocky intertidal macroinvertebrates of the Southern California Islands. In: *The California islands* (ed Powers DM), pp. 307–323.

Sommerfield CK, Lee HJ (2004) Across-shelf sediment transport since the Last Glacial Maximum, southern California margin. *Geology*, **32**, 345–5.

Sunamura T (1976) Feedback relationship in wave erosion of laboratory rocky coast. *The Journal of Geology*, **84**, 427–437.

Swift CC, Haglund TR, Ruiz M, Fisher RN (1993) The status and distribution of the freshwater fishes of southern California. *Bulletin of the Southern California Academy of Sciences*, **92**, 101–167.

Syphard AD, Franklin J (2009) Differences in spatial predictions among species distribution modeling methods vary with species traits and environmental predictors. *Ecography*, **32**, 907–918.

Taberlet P, Fumagalli L, Wust-Saucy AG, Cosson JF (1998) Comparative phylogeography and postglacial colonization routes in Europe. *Molecular Ecology*, **7**, 453–464.

Thunell R, Tappa E, Pride C, Kincaid E (1999) Sea-surface temperature anomalies associated with the 1997–1998 El Niño recorded in the oxygen isotope composition of planktonic foraminifera. *Geology*, **27**, 843–846.

Upson JE (1949) Late Pleistocene and Recent changes of sea level along the coast of Santa Barbara County, California. *American Journal of Science*, **247**, 94–115.

Waltari E, Hickerson MJ (2013) Late Pleistocene species distribution modelling of North

Atlantic intertidal invertebrates (C McClain, Ed,). *Journal of Biogeography*, **40**, 249–260.

Wan Q-H, Wu H, Fujihara T, Fang S-G (2004) Which genetic marker for which conservation genetics issue? *ELECTROPHORESIS*, **25**, 2165–2176.

Waples RS (1991) Heterozygosity and life-history variation in bony fishes: an alternative view. *Evolution*, **45**, 1275.

Wares JP, Gaines SD, Cunningham CW (2001) A comparative study of asymmetric migration events across a marine biogeographic boundary. *Evolution*, **55**, 295–306.

Watson W (1996) *The early stages of fishes in the California current region* (HG Moser, Ed,). California Cooperative Oceanic Fisheries Investigations.

Wickham H (2007) Reshaping data with the reshape package. *Journal of Statistical Software*, **21**, 1–20.

Wickham H (2011) The split-apply-combine strategy for data analysis. *Journal of Statistical Software*, **40**, 1–29.

Yamamoto M (2009) Response of mid-latitude North Pacific surface temperatures to orbital forcing and linkage to the East Asian summer monsoon and tropical ocean - atmosphere interactions (T Oba, K Ikehara, C Turney, Eds,). *Journal of Quaternary Science*, **24**, 836–847.

CHAPTER 3

Glacially driven sea-level change generates refugia on subtropical coasts

Abstract

Estuaries are interesting study systems from an evolutionary perspective because their distributions change over space and time. We performed paleohabitat modeling and genetic analyses along 4,600 km of coastline from San Francisco, California (USA, 38 °N) to Sinaloa, Mexico (23 °N). Our models estimated estuarine habitat distribution at near-millennial resolution from the Last Glacial Maximum (LGM) 20 thousand years ago (kya), when sea level was ~130 m lower, to the present. We assessed genetic subdivision of co-distributed tidal estuarine fishes within these habitats using mitochondrial sequence data and 16–20 microsatellite loci on a total of 524 individuals of three species: *Fundulus parvipinnis*, *Quietula y-cauda*, and *Gillichthys mirabilis*. Results from genetic analyses and habitat models independently indicate that estuarine habitat was reduced to three refugia along the Pacific coast and eight refugia in the Gulf of California at lowstand. Our results also reveal that San Francisco Bay was extirpated at lowstand and subsequently recolonized from the south. We propose a working hypothesis in which tectonics and oceanographic processes control coastal shelf topography. Sea-level change operates across this topography to eliminate, isolate, and re-form estuarine habitat over time. Regions with steeper coastlines (central and southern California and the western Gulf of California) support only a few small, isolated refugia in which populations differentiate genetically at lowstand. This extirpation-recolonization model likely pertains to other species inhabiting discontinuous coastal habitat at latitudes far from the presence of glaciers, and suggests isolation in sea-level driven refugia may be an important driver of genetic differentiation.

Introduction

To understand evolution it is critical to determine mechanisms that govern population subdivision and connectivity over time (Wright 1931; Slatkin 1987; Hastings & Harrison 1994). A pattern of isolation and reconnection among populations may contribute to genetic diversity (Hewitt 2000; 2004; Briggs 2006), alter species ranges (Marko 2004; Kelly & Palumbi 2010), and facilitate speciation (Briggs 2006). We expand on recent work (Dolby *et al. in revision*) to show how glacially driven sea-level change and coastal shelf topography operate together to eliminate and re-form habitats, thereby isolating and reconnecting coastal populations over millennia. We assess these patterns on local to regional geographic scales (100s to 1,000s km).

Previous research uncovered biogeographic provinces, phylogeographic breaks, and several noteworthy patterns within the subtropical eastern Pacific and Gulf of California. Promontories along the Pacific (Californian and Baja Californian; Figure 3-1) coast are thought to principally structure populations and serve as range limits (Bernardi & Talley 2000; Dawson 2001; Dawson *et al.* 2002; Jacobs *et al.* 2004; Kelly & Palumbi 2010; Ellingson 2012). Within the Gulf of California (hereafter, Gulf), north-south oceanographic gyres (Marinone *et al.* 2008; Munguía-Vega *et al.* 2014; Soria *et al.* 2014), localized upwelling in the east and at the Midriff Islands (Roden 1964; Zeitzschel 1969; Santamaría-del-Angel *et al.* 1994) and trans-peninsular seaways (Riddle *et al.* 2000; Riginos 2005; Lindell *et al.* 2006; Leache *et al.* 2007; Munguía-Vega 2011; Dolby *et al.* 2015) have been thought to influence population connectivity. Work has also suggested that incipient speciation is occurring among disjunct Pacific and Gulf populations due to Pleistocene glacial cycles (Terry *et al.* 2000; Bernardi *et al.* 2003).

158

Many of the aforementioned factors believed to control population connectivity in this region have not been explicitly tested with independent physical data or models. Here, we address the role of sea-level change, a previously overlooked driver of population extirpation, isolation, and connectivity in the subtropical eastern Pacific and Gulf of California, as a potential driver of population subdivision. We model paleohabitat distribution through time to reconstruct the distribution of tidal estuarine habitat between 23 °N–38 °N since the Last Glacial Maximum (LGM) at near-millennial resolution. We also assess the population genetic structure of three co-distributed, low-dispersal tidal estuarine fishes inhabiting these tidal estuaries to independently infer population history and range-wide intraspecific genetic patterns. Using mitochondrial (mtDNA) and large microsatellite datasets (16–20 loci), we compare our genetic results to those of our paleohabitat models and previously cited drivers of population structure, such as currents and seaways.

The strengths of such an interdisciplinary approach are threefold. First, the habitat modeling and genetic analyses provide independent lines of evidence that can be interpreted separately, and then compared for increased power. Secondly, we use primary geological data, including a sea-level curve and knowledge of factors governing coastal geomorphology (e.g., waves, uplift, faults, barrier features). These data enable estimation of habitat at greater temporal resolution than that of many habitat models, and comparable to the fine-scale genetic patterns of some species within them (Earl *et al.* 2010; Jacobs *et al.* 2011). Finally, integration of these independent data reveals the dynamism and co-evolutionary processes of estuaries and their inhabitants.

159

Estuaries are semi-enclosed coastal bodies of water with both marine and freshwater inputs. Estuaries are of particular interest from an evolutionary perspective because they are intermittent in both space and time, and can form highly genetically isolated populations (Bertness & Gaines 1993; Earl *et al.* 2010). They are therefore ideal systems in which to study evolutionary consequences of changing population connectivity through time and thus levels of population differentiation and diversity. They also provide a unique opportunity to study the link between causal physical processes and biological evolution using simple topo-bathymetric models. Several classes of estuaries exist in the subtropical eastern Pacific and other Mediterranean climates, from closed bar-built lagoons to perpetually open, tidal systems (Jacobs *et al.* 2011). Here we focus primarily on tidal estuaries, with some regional variability dictated by our species occurrences. The co-distributed tidal estuarine fishes we used were *Quietula y-cauda* (Shadow Goby), *Gillichthys mirabilis* (Longjaw Mudsucker), and *Fundulus parvipinnis* (California Killifish), which have limited dispersal and are thereby likely to retain signatures of population history.

Materials and methods

Paleohabitat modeling

We modeled estuarine habitat through time in two phases. The first phase (Parameterization and Application) determined the physical parameters that constrain where estuaries can form using physical features (i.e. sea level, slope, upland area) characteristic of modern estuaries in which our three study species occur today. The second phase (Assessment) is a series of statistical assessments that use the size and

density characteristics of habitats in which the species presently occur, to test whether areas that meet slope requirements at lowstand were similar to modern habitat, and thus likely to provide habitat these species in particular.

Parameterization

To estimate the habitat requirements of Pacific coast estuaries (south of Punta Eugenia and north of Morro Bay), we followed the parameterization of Dolby *et al.* (*in revision*), which used a slope range of 0.0–1.3% and minimum adjacent upland area of 190 km^2, which eliminates classifying shallow offshore features as potential habitat. Due to different oceanographic patterns (Littler & Littler 1981) and geologic histories (Ingersoll & Rumelhart 1999; Helenes & Carreno 1999; Oskin & Stock 2003; Dolby *et al.* 2015) between the Pacific and Gulf, we parameterized the slope limit separately for Gulf estuaries inhabited by *G. mirabilis* and *Q. y-cauda* (*F. parvipinnis* does not occur in the Gulf). In each of 23 estuaries we calculated the slope at five haphazardly chosen locations to accommodate intra-estuarine variability (mean slope = 1.0%, median slope = 0.7%, Table 3-S3). The elevations and 'runs' were calculated in Google Earth® v5 (Google Inc., Mountain View, CA). We applied the maximum slope observed as a cutoff, and thus 0.0–3.4 % was used as the suitable slope envelope within the Gulf. This cutoff differs from the 0.0–1.3 % slope used for Pacific coast estuaries and thus subsequent habitat analyses were performed separately for the Pacific and Gulf regions. We ignored islands within the Gulf because estuarine habitat on Gulf islands is minimal at present and likely minimal and ephemeral in the past.

Application

We partitioned bathymetry into 10-meter depth bins from 0–140 mbpsl with the addition of a 'modern' depth bin (0 kya, 0 mbpsl ± 5 m). In ArcMAP v10.2 (ESRI, Redlands, CA) using the Raster Calculator tool we queried the 30-arc-second SRTM30_PLUS Shuttle Radar Topography Mission (Becker *et al.* 2009) Digital Elevation Model (DEM) for regions matching the slope criteria for each depth bin. Areas that positively matched slope and depth criteria were converted to a series of simplified polygon feature layers. We then subdivided regions of the Gulf coastline into coastal regions based on shelf topography and modern distribution of estuarine habitat (Figures 3-S2, 3-S3). We used Select Features by Location tool with 'Target layer(s) features are within (Clementini) the source layer' to summarize polygon statistics for habitat area within each coastal region. We recorded these polygon attribute statistics for each depth bin. The statistics summarized were: number of polygons, minimum polygon area, maximum polygon area, total polygon area, mean polygon area, and standard deviation of polygon area. We added a seventh attribute that normalized the summed polygon area by the coastal region area to provide a proxy for habitat density because the size of coastal regions varied. The 14 depth bins, 7 statistical attributes, and 9 Gulf coastal regions produced 882 observations within the Gulf. Our separate calculations in the Pacific expanded the coastal regions covered in Dolby *et al.* (*in revision*) by 3, yielding 294 additional observations. Finally, we correlated ages to the mid-point depth of each depth bin using a composite sea level curve (Chaytor *et al.* 2008).

Assessment

To assess whether the physical characteristics of lowstand habitat meeting the

slope requirements were statistically similar to present habitat, and thus likely to support

populations of the species studied here, we used a Discriminant Function Analysis

(habitat DFA) and series of Generalized Linear Models (GLMs). First, using the polygon

attribute (potential habitat) data we performed a search for outliers in JMP v11 (SAS,

Cary, NC) using Quantile Range Outliers with default settings (Tail Quantile = 0.1, Q =

3), and Huber Robust Fit Outliers (K = 4). No outliers were discovered using the 7

polygon attribute variables and thereby all coastal regions were included in the habitat

DFA. Next, we used the habitat DFA to determine which polygon attributes statistically

predict where our three species presently occur. We performed this training because it is

unlikely that all areas of coastline that met the slope criterion at lowstand would have

been estuaries where our three species lived. In other words we expected there to be a

minimum size or additional physical attribute that would predict species occurrences at

lowstand. We therefore performed habitat DFA on the statistical polygon attributes of

modern coastal areas divided into two groups: those that have populations of these fishes

today (N = 6, Reforma, mid-eastern Gulf, Kino, Colorado Delta, Francisquito, Zacatecas;

see Figures 3-S3, 3-4), and those that do not (N= 3: Angel de la Guarda/western Gulf,

south of Francisquito, and north of Zacatecas; see Figures 3-S3, Table 3-4). Habitat DFA

used Stepwise Variable Selection Process (SVSP), pseudoinverses, and linear common

covariance, which did not produce a statistically significant model without

misclassifications. Normalized area was the only significant variable in this model, and it

produced 3 misclassifications. Values for normalized area varied for the habitat group

(mean = 88.7, standard deviation = 51.9, standard error mean = 21.2) compared to the

non-habitat group (mean = 10, standard deviation = 16.5, standard error mean = 9.5), which may be partly due to different sample sizes (6:3, respectively). We therefore re-ran the analysis using quadratic (different covariances) with SVSP, which produced two models. Of these two models, the first had only one significant variable (normalized habitat area, p = 0.04) and one misclassification. To improve the misclassification result we added the next, non-significant variable (number of polygons) which produced p = 0.08 with zero misclassifications. We chose this last, two-variable unequal covariance model with normalized habitat area and number of polygons for further analyses. We used these two predictive variables from the habitat DFA in a series of GLMs to test which of the areas meeting lowstand slope requirements were areas similar to modern habitat. In other words, we used these variables to test the statistical support for several refugium hypotheses. GLMs used a binomial distribution and logit link function and in a given scenario each region was classified as 'yes' or 'no' for whether it was habitat at lowstand. These classifications produced either a statistically significant or non-significant model, which was evaluated with p values and AICc scores (Table 3-S4). Statistically significant models were re-run using Firth Biased Estimates and False Discovery Rates to correct for correlated variables (Table 3-S4).

For Pacific coast sites, we ran habitat DFA using the previously established predictive variables (maximum polygon area & summed area, Dolby *et al. in revision*) applied to the three additional coastal regions described here (Magdalena refugium, central CA coast, San Francisco; Table 3-S4).

Inferring population structure and history

DNA extraction and mtDNA amplification

We isolated DNA from posterior muscle tissue using the Qiagen DNeasy Blood and Tissue extraction kit (QIAGEN #69506). Polymerase Chain Reaction (PCR) amplification for mitochondrial Control Region (mtCR) used CRA and CRM primers (Lee *et al.* 1995) with the following specifications: preheat 94 °C for 120 sec, denaturing 94 °C for 30 sec, annealing 52 °C for 30 sec, extension 68 °C for 90 sec with 35 cycles and a final extension of 68 °C for 10 minutes. Amplification of Cytochrome B used AJG15 and H5 primers (Akihito *et al.* 2000) with the following thermocycler protocol: preheat 95 °C for 120 sec, denaturing 95 °C for 30 sec, touch-up annealing gradient 48.5–54 °C for 20 sec with +0.5 °C/cycle, extension of 68 °C for 90 sec with 40 cycles and a final extension time of 68 °C for 10 minutes. Reaction volumes were 25 μl for both markers: 19 μl ddH$_2$O, 2.5 μl 10x Taq buffer w/MgCl$_2$, 1.0 μl Primer 1, 1.0 μl Primer 2, 0.5 μl 10 mM dNTPs, 0.1 μl Taq DNA Polymerase, 1.0 μl template DNA per sample. If amplification was unsuccessful as assessed via 1.5% agarose gel electrophoresis run at 80 volts for 30 minutes, then 1.0 μl of water was replaced with 1.0 μl of BSA (10 mg/mL). Independent sequencing reactions for forward and reverse primers were performed and sent to DNA Analysis Facility at Yale University for Sanger sequencing. We performed quality control and processed chromatograms in Codoncode Aligner® v4 (CodonCode Corporation, Centerville, MA) or Geneious® Pro v5.6.7 (Biomatters, Aukland, New Zealand).

Microsatellite analysis

Populations not previously analyzed in Dolby *et al.* (*in revision*) were amplified

for the same microsatellite loci, following the same protocols, and genotyped at the

UCLA GenoSeq Core (for methods see Dolby *et al. in revision*). Not all individuals were

run for both mtDNA and microsatellite markers (Tables 3-S1, 3-S2). Sample sizes and

numbers of loci are as follows: *F. parvipinnis* (N = 109, 20 loci), *Q. y-cauda* (N = 177,

17 loci), *G. mirabilis* (N = 238, 16 loci). To assess population structure, microsatellite

datasets for each taxon were analyzed thrice, once as the full dataset (*K* = 2–5), once with

Pacific-only samples (*K* = 2–4), and once with Gulf-only samples (*K* = 2–4) in

STRUCTURE (Pritchard *et al.* 2000). For *G. mirabilis, K* = 1 was run post hoc to assess the

relative likelihood of a two-population versus one-population model using Δ*K*. This post

hoc test was necessary because the paleohabitat models predict one less refugium for *G.

mirabilis* than *Q. y-cauda* due to its smaller range (it does not occur in the southwestern

Gulf) and the favored *K* for *Q. y-cauda* was 3. Three replicates for each *K* were run and

parameterized with correlated frequencies and admixture models; iterations included 1

million burnin and 5 million post-burnin generations each. Results of the three iterations

were analyzed in STRUCTURE HARVESTER (Earl & vonHoldt 2011) and combined for

each *K* in CLUMPP v1.1.2 (Jakobsson & Rosenberg 2007) using the GREEDY algorithm

(M = 2 with greedy option 1) and S of 1 (using G statistic). To infer phylogenetic history

of these groups we constructed Neighbor-Joining trees with the microsatellite data in

POPULATIONS v1.2.3 (©Langella, www.bioinformatics.org/populations) following the

Nei minimum distance algorithm with 5,000 bootstrap replicates on loci (Figure 3-S4).

To assess population-level patterns of genetic diversity we calculated the

following basic diversity statistics per taxon using the full dataset where individuals were

grouped by collection site (Tables 3-S1, 3-S2): Fisher's Exact G test for genotypic

population differentiation (Table 3-S6), pairwise F_{ST} (Table 3-S7), and global Hardy-

Weinberg tests for heterozygote deficit and excess (Table 3-S8); all of these tests were

executed in GENEPOP v4.2 using 10,000 dememorization steps, 20 batches, 5,000

iterations per batch where applicable. To further assess genetic diversity of populations

we calculated average gene diversity, and mean observed and expected heterozygosities

in ARLEQUIN v3 (Excoffier *et al.* 2005). Finally, we used HIERFSTAT v0.04 (Goudet

2005) to calculate allelic richness per locus per population in R v3.2 (the R Foundation

for Statistical Computing, www.R-project.org) for each taxon, which we used to calculate

the per-population mean and median allelic richness (Table 3-S8).

Mitochondrial analyses

Mitochondrial datasets were developed for *Fundulus parvipinnis* (N = 80 plus 3

samples of *Fundulus sciadicus*—Genbank accession numbers: EU182727.1,

EU182728.1, EU182729.1; 889 bp of mitochondrial control region), *Quietula y-cauda* (N

= 195; 912 bp of Cytochrome B), and *Gillichthys mirabilis* (N = 233 plus one sample of

G. detrusus; 1827 basepairs of mitochondrial control region and Cytochrome B).

Gillichthys detrusus and *F. sciadicus* were used as outgroups to determine the order

('directionality') of branching events. We used MRBAYES v3.1.2 (Huelsenbeck &

Ronquist 2001; Ronquist & Huelsenbeck 2003) on the CIPRES Science Gateway (Miller

et al. 2010) for phylogenetic tree reconstruction to enable inference of historical

relationship among populations. Tree reconstructions were parameterized as follows: *F.*

parvipinnis (3 runs, 4 chains per run, 6 million generations, Nst = 2, rates = equal, burnin

fraction = 0.25), *Q. y-cauda* (3 runs, 4 chains per run, 10 million generations, Nst = 2, rates = equal, burnin fraction = 0.25), and *G. mirabilis* (2 runs, 4 chains per run, 10 million generations, Nst = mixed, rates = gamma, burnin fraction = 0.25). For *G. mirabilis*, basepairs were partitioned by evolutionary rate using a rate partitioning method (Ellingson *et al.* 2014). Closely related species to *F. parvipinnis* (*F. sciadicus*) and *G. mirabilis* (*G. detrusus*) were used for outgroups and rooting (Figures 3-S5, 3-S7, respectively). *Quietula y-cauda* has only one congener, which is thought to have diverged ~13 Ma (Ellingson 2012), and thus no outgroup was used in tree reconstruction and the tree is rooted on the longest internal branch (Figure 3-S6).

Results

Paleohabitat modeling

Temporal and regional habitat patterns

The maximum slope observed in estuaries inhabited by *G. mirabilis* and *Q. y-cauda* in higher in the Gulf ($\leq$ 3.4%) than Pacific ($\leq$ 1.3%). The maximum observed habitat area for any depth bin in a Pacific coastal region is 2,390 km^2 (Magdalena Refugium 100–90 mbpsl; Figure 3-S3), compared with 3,483 km^2 within the Gulf (Reforma Refugium, 0 ± 5 mbpsl; Figure 3-S3). These maximum observed areas are comparable in size, which suggests the higher slope cutoff for the Gulf does not appear to overestimate habitat abundance. Total refugial habitat area at lowstand in the Pacific was 1,006 km^2, and in the Gulf was 1,557 km^2. While these maximum areas are of a similar scale, comparing estuarine habitat abundance through time (Figure 3-2) reveals different patterns between the Pacific (Figure 3-3A) and Gulf (Figure 3-3B). Total habitat area

along the Pacific coast exhibits a heterogeneous pattern in which habitat area varies by both region and depth/time. For example, total habitat area in southern California (Morro Bay–San Diego; Figure 3-S3) peaks 12–9 kya with ~436 km^2, yet Vizcaíno is the single largest habitat on the Pacific coast and its size peaks ~15 kya (2,815 km^2; Figure 3-S3), while habitat at San Francisco peaks about 7 kya with 3,242 km^2. By contrast, habitat area in the Gulf appears to lack this heterogeneity and was simply reduced at lowstand and increases exponentially between 15 and 5 kya. Total change in estimated Gulf habitat area from 20 kya to 0 kya is 1,557 to 10,331 km^2 (Figures 3-3B, 3-S3).

Refuge assessments

   According to our series of GLMs, four separate refugium models were statistically supported ($\alpha = 0.05$) within the Gulf. The simplest of these four scenarios classified the Colorado Delta, Bahía Kino, mid-eastern Gulf, and Reforma as refugia (p = 0.01, AICc = 20.8), all of which are within the northern or eastern Gulf. Note that the mid-eastern Gulf refugium comprises three small, adjacent individual refugia. It was unclear if these would have been separate, or effectively one single refugium, and therefore we combined these three refugia into the eastern Gulf refugium (labeled ME in Figure 3-4B). In this simplest model, all other habitats were classified as non-refugial. In the most complex GLM, the addition of two western Gulf regions (Francisquito and Zacatecas) to the simplest refugium model was also statistically significant (p = 0.02, AICc = 21.9). Refugium scenarios with and without Francisquito and Zacatecas are both significant, which may be because these western refugia are much smaller than the northern/eastern refugia (mean lowstand habitat size for Francisquito and Zacatecas = 41

km^2, mean lowstand habitat for the Reforma, mid-eastern Gulf, Bahía Kino and Colorado Delta = 369 km^2).

Along the Pacific coast we expanded the area of the previous study (Dolby *et al. in revision*) by ~1,000 km of coastline northward to San Francisco, and southward to Baja California Sur (south of Punta Eugenia; Figure 3-1). Over this increased study area, the GLM using Magdalena (south of Punta Eugenia) and the previous two refugia (Vizcaíno and North Conception) was statistically significant (p = 0.04). In this model, all other regions were classified as non-refugia. The previous scenario of only two refugia (Vizcaíno and North Conception) was not supported over this expanded geographical area (p = 0.19). Our results suggest that two refugia were large (Magdalena refugium, 462 km^2 and Vizcaíno refugium, 519 km^2) and one was relatively small (North Conception refugium, 25 km^2). In summary, over the entire Pacific range of these three species, only three lowstand refugia were statistically supported in our paleohabitat models for the Pacific coast. Despite a large habitat today, San Francisco was not statistically supported as a refugium (p = 0.07). Although the San Francisco region has area that meets the slope requirements (≤ 1.3%, 62 km^2) in the 130–140 mbpsl bathymetric bin that corresponds to the LGM lowstand, the GLM test for lowstand habitat produced a non-significant result. It could be that the attributes of this area do not reflect those of modern habitat, perhaps because the area meeting slope requirements at lowstand was distributed patchily and would not support an estuary.

Inferring population structure and history

Regional diversity patterns

170

Mean pairwise F_{ST} values for populations of: *F. parvipinnis* (N = 109, 20 loci, 14 populations), *Q. y-cauda* (N = 177, 17 loci, 38 populations), *G. mirabilis* (N = 238, 16 loci, 31 populations) were 0.24, 0.21, 0.25, respectively. The Pacific and Gulf populations appear genetically isolated in both *Quietula y-cauda* and *Gillichthys mirabilis*. Pairwise fixation indices (F_{ST}) among intra-Pacific and intra-Gulf populations, compared with trans-Pacific-Gulf populations were analyzed using two-tailed unpaired t tests and revealed statistically reduced F_{ST} values ($p < 0.0001$ for *Q. y-cauda* and *G. mirabilis*; Tables 3-S7B, 3-S7C). Minimal observed admixture in STRUCTURE analyses (Figure 3-6) and reciprocally monophyletic clades within microsatellite-based Neighbor-Joining tree topologies in both species (Figure 3-S4) further support Pacific-Gulf isolation. Finally, highly significant p values from Fisher's exact G test for pairwise population differentiation (Table 3-S6) also support this finding, and have previously demonstrated reliability and power with microsatellite data (Ryman *et al.* 2006).

Mean allelic richness for populations of the three species were as follows: *F. parvipinnis* (mean = 4.8, range = 3.7–4.6), *Q. y-cauda* (mean = 2.5, range = 1.8–2.8), and *G. mirabilis* (mean = 2.4, range = 1.9–2.8). We compared mean allelic richness between Pacific (2.4, 2.5) and Gulf populations (2.5, 2.6) for *Q. y-cauda* and *G. mirabilis*, respectively, and found that generally mean allelic richness is higher for Gulf populations than Pacific populations. This finding was statistically significant in *G. mirabilis* ($p < 0.0001$) and not significant in *Q. y-cauda* ($p = 0.18$) using two-tailed unpaired t tests. *Fundulus parvipinnis* does not occur in the Gulf, so we compared F_{ST} values among populations distributed on the Pacific coast north and south south of Punta Eugenia (a previously determined biogeographic break; Bernardi and Talley 2000) and found

171

significantly reduced F_{ST} across this boundary (p < 0.001). Based on Fisher's Exact (G) test, *F. parvipinnis* appears more differentiated than *Q. y-cauda* or *G. mirabilis* (Table 3-S6), though all three species exhibit strong genetic subdivision. Despite this observed genetic differentiation, F_{ST} values for neighboring populations within all three species are not high (mean F_{ST} = 0.08, 0.04, and 0.07 for neighboring populations of *F. parvipinnis*, *Q. y-cauda*, *G. mirabilis*, respectively).

Refugial population structure

We used the ΔK metric (Evanno *et al.* 2005) to choose which number of groups was favored for each taxon in order to compare the favored number of genetic groups with the number of lowstand refugia predicted in the paleohabitat models. The ΔK provided in STRUCTURE HARVESTER results revealed that, for Pacific coast populations, *K* = 3 was favored for each taxon: *F. parvipinnis* (ΔK = 2069), *Q. y-cauda* (ΔK = 28), and *G. mirabilis* (ΔK = 20). Within the Gulf, *K* = 3 was favored for *Q. y-cauda* (ΔK = 707), and *K* = 2 was favored for *G. mirabilis* (ΔK = 357). These favored numbers of genetic groups are identical to the number of refugia expected from the paleohabitat modeling for the Pacific (Figure 3-4). The favored *K*s in the Gulf are fewer than the number of lowstand refugia predicted by the paleohabitat models. The 2 and 3 *K* favored in the Gulf suggest that the northern and eastern Gulf refugia are not isolated genetically. The expected number of refugia for *G. mirabilis* in the Gulf is one fewer than *Q. y-cauda* because the distribution of *G. mirabilis* does not extend south of Bahía Concepción to the Zacatecas refugium. This expectation is consistent with the favoring of *K* = 2 for *G. mibrabilis* and *K* = 3 groups for *Q. y-cauda*.

Discussion

To assess the role of refugia in coastal estuarine fishes on different geographical scales, we employed paleohabitat modeling and genetic analysis of three tidal estuarine fish species over the entirety of their ranges from San Francisco, CA (USA) to Sinaloa (MX), covering ~4,600 km of coastal distance. This geographical study range spans 15 degrees of latitude, from tropical to temperate (23 °N–38 °N). This coastal extent also has regions of varying shelf topography, coastal orientation, oceanography, and offshore islands (Figure 3-1; Dolby *et al. in revision*). Encompassing coastal shelf heterogeneity over such a wide area enabled us to assess: 1) conditions under which estuarine habitats were isolated during lowstand, 2) when they were able to support genetic connectivity, and 3) how this manifested spatially in genetic data.

Formation of coastlines and regional habitat patterns
Pacific coast

The Pacific and Gulf of California have different tectonic histories, which have shaped the shelf topography, width, and orientation of their coastlines. Each of these regions, however, have historical processes that are thought to have contributed to regional shelf heterogeneity. Portions of the Farallon tectonic oceanic plate subducted beneath the North American plate along California ~30–12 Ma (Humphreys 1995). Postsubduction pull-apart rifting (Ingersoll & Rumelhart 1999) and the San Benito fault (Plattner *et al.* 2009) have likely both contributed to coastal steepness from Punta Eugenia through southern California (Figure 3-1). Uplift (positive vertical movement of

173

Earth's crust) up to 2 mm/yr (Muhs *et al.* 1992; Niemi *et al.* 2008) has also probably contributed to its steepness. In contrast, Punta Eugenia and areas south (e.g., Bahía Magdalena), did not experience the same rifting or uplift, and the Tosco-Abreojos fault system south of Punta Eugenia is farther offshore than the San Benito fault (Michaud *et al.* 2007). These factors combine to produce a wider continental shelf in Vizcaíno and Magdalena than in Baja California Norte and southern California. These two broad regions are the sites of the two large lowstand refugia predicted by our paleohabitat models, and the third refugium in southern California is along a steeper margin, which might explain its relatively small size.

Gulf of California coast

The Gulf, by comparison, is a young rift margin with a steep western flank and a broader, more shallowly sloping eastern flank. This asymmetry is probably caused in part from the shifting of the rift margin from the eastern to western Gulf (Aragón-Arreola & Martín-Barajas 2007) about 3 million years ago (Ma; Stock 2000), and from greater sediment supply to the eastern coast from the rivers of mainland Mexico (Nava-Sánchez *et al.* 2001). Uplift of the western flank (the Baja peninsula) between 5.6 and 3.2 Ma (Mark *et al.* 2014) may also have contributed to steepness of the western Gulf. This heterogeneity in coastal steepness has produced variability in the distribution of modern coastal habitat within the Gulf (Brusca *et al.* 2005; Hendrickx *et al.* 2007). Similar to the Pacific coast patterns we observe, our models predict two relatively small refugia along the steep western Gulf coast, and four large refugia along the north and eastern Gulf, which may have maintained gene flow at lowstand.

Regional habitat patterns

Several broad, regional patterns emerge from interpreting our paleohabitat modeling results within this geological context. The coastline south of southern California near Vizcaíno and south of Punta Eugenia (e.g., Magdalena Bay) hosts broad shallow-sloping areas. Within the Gulf, the Colorado Delta and eastern coastline are also broad. These three shallowly sloping regions support the highest modern estuary abundance. Our paleohabitat models suggest these regions also retain the largest number and size of refugia at lowstand (Figures 3-2, 3-4). In contrast, much of the California and western Gulf coastlines are too steep today to form estuaries (Figures 3-1, 3-S1), and instead host rocky-shore and intertidal habitat (Bernardi 2000; Dawson 2001; Dawson *et al.* 2002; Hendrickx *et al.* 2014). Such regions with narrower coastal shelves generally have smaller modern habitats and have very little lowstand habitat (Figures 3-2, 3-S2, 3-S3). Our results suggest estuarine habitat in these steeper regions is either eliminated at lowstand, in which case long stretches of coast are uninhabited by estuarine species, or small refugia persist in isolation and produce individuals with unique genetic signatures as revealed in STRUCTURE analyses (Figure 3-4) and tree topologies (Figure 3-S4).

Gulf-Pacific patterns

Disjunction and speciation

We find evidence for little to no gene flow between Pacific and Gulf populations of *Quietula y-cauda* and *Gillichthys mirabilis* (Figure 3-6), inferred from significantly reduced F_{ST} values (p < 0.0001) among populations disjunct between these regions (*F.*

parvipinnis does not occur in the Gulf). Microsatellite tree topologies of both species

(Figure 3-S4) and mtDNA tree topology for *Q. y-cauda* further reveal reciprocally

monophyletic clades of Pacific-Gulf populations. Bernardi et al. (2003) previously found

similar monophyly in eight of twelve fish species studied, most of which were rocky-

shore associated. The authors therein note this may be a sign of incipient speciation, in

which the warm waters of interglacial periods prohibit migration around the Cabo Block

(Figure 3-1). Our results support this pattern, which has been observed in many other

species (Maldonado *et al.* 1995; Terry *et al.* 2000; Bernardi *et al.* 2003; Bernardi 2014).

If warm waters near the Cabo region presently limit Pacific-Gulf migration, then it

follows that gene flow has typically occurred during the cooler temperatures of glacial

periods. While this may be true, we observe a similar level of genetic differentiation

between Pacific and Gulf populations. We suggest that isolation in the lowstand refugia

described here have also contributed to the genetic differentiation of these Pacific-Gulf

populations in our species and in those previously studied. Lowstand isolation may be

particularly important in species that are absent from the southwestern Gulf, such as *G.*

mirabilis. Our habitat models and genetic data predict *G. mirabilis* was absent from the

Zacatecas refugium at lowstand because it does not occur south of Bahía Concepción and

has only two genetic groups in the Gulf (Figures 3-4, 3-S4, 3-S7). Several disjunct

species exhibit similar southwest-limited distributions that, combined with lowstand

extirpation of many habitats, would likely contribute to Pacific-Gulf isolation over

repeated glaciations. Additionally, differences in tidal range and temperature variability

(Roden 1964; Ellingson 2012), mangrove distributions (Aburto-Oropeza *et al.* 2008),

seasonal upwelling (Zeitzschel 1969), and faunal distributions between the Pacific and

Gulf may impart different selection pressures (Littler & Littler 1981). Differential

selection pressures may have been particularly acute during lowstand when population

sizes are likely reduced and populations isolated to greater degree than at present.

Pacific coast patterns

We extended paleohabitat modeling for the entirety of the Pacific coast from San

Francisco to the southern tip of the Baja Peninsula, which expanded on previous work

(Dolby *et al. in revision*). Across this broader geographic scale we find statistical support

for the addition of the Bahía Magdalena refugium in addition to the two refugia found

previously (p = 0.04, AICc = 20.7, Table 3-S4). A model with only the two previously

found refugia (North Conception and Vizcaíno) is not supported in this larger

geographical extent (p = 0.19). Therefore, we infer for populations of *F. parvipinnis*, *Q.

y-cauda*, and *G. mirabilis* located along the Pacific coast, only three refugia existed

during lowstand along ~2,100 km of coastline. Our results suggest that the Vizcaíno and

Bahía Magdalena refugia were large and the North Conception refugium was relatively

small (Figures 3-4, 3-S3). The larger refugia encompass what are many individual

estuaries today. Importantly, nearly all present-day populations of these fishes south of

Punta Eugenia (Figure 3-1) fall within the Bahía Magdalena refugium. If these habitats

south of Punta Eugenia persisted through time this would have important consequences

because they would not experience the loss of genetic diversity that results from

extirpation. Consistent with this hypothesis, we observe higher mean allelic richness in

populations south of Punta Eugenia than in populations north of Punta Eugenia. When

tested with unpaired two-tailed t tests, this difference was significant in *F. parvipinnis* (p

= 0.004) and *G. mirabilis* (p = 0.04)*,* and not significant in *Q. y-cauda* (p = 0.07). In further support for closely associated lowstand habitat among populations south of Punta Eugenia, within each species these populations appear to be genetically similar to one another; they lack population subdivision (Figures 3-4A, 3-S8), have non-significant scores for Fisher's exact (G) test for population differentiation (Table 3-S6), and exhibit low pairwise F_{ST} values (Table 3-S7). We also find reduced gene flow across Punta Eugenia in *F. parvipinnis*, which supports the subspecies designation between *F. parvipinnis parvipinnis* (north) *F. parvipinnis brevis* (Miller & Hubbs 1954).

In contrast to the habitat stability south of Punta Eugenia, our models suggest that to the north of Punt Eugenia, almost all Californian populations were extirpated at lowstand and subsequently recolonized when habitat formed during sea-level rise (Figure 3-4A). This pattern of recolonization is independently supported by results from genetic analyses. Populations thought to be recolonized show signatures of admixture between the two identified source refugia (Vizcaíno and North Conception) in STRUCTURE results (Figures 3-4A, 3-S8), allele frequencies (Dolby *et al. in revision*), and in unresolved or mixed tree topologies (Figures 3-S4, 3-S5, 3-S6, 3-S7, 3-S8).

San Francisco

Although the San Francisco Bay (SFB, Figures 3-1, 3-5) area had an estimated 62 km^2 of habitat within the slope parameter (≤ 1.3%) at lowstand (130–140 mbpsl), our GLM assessments suggest the size characteristics of this area were not similar to modern habitats. *Gillichthys mirabilis* is our only study species whose range extends as far north as SFB. The northern range limit for both *Fundulus parvipinnis* and *Quietula y-cauda* is

in southern California at Morro Bay, CA (near Point Conception; Figure 3-1). Point

Conception is a common biogeographic break between Oregonian and Californian marine

fauna (Seapy & Littler 1980; Dawson 2001), and may be partly controlled by temperature

(Hellberg *et al.* 2001). Our genetic analyses independently suggest SFB was not a refuge

during lowstand. Individuals of *G. mirabilis* from SFB are not genetically unique in

STRUCTURE results (Figure 3-4) or tree reconstructions (Figures 3-S4, 3-S7), as one

would expect if a population existed there in isolation during glaciations. Instead, *G.

mirabilis* individuals in SFB genetically resemble populations from southern California,

Baja California Norte, and even Baja California Sur (BCS, south of Punta Eugenia), a

region that is 1,300—1,800 km to the south. The strength of the northerly California

Current between 20 kya and today is unclear; a weakened current may have facilitated

northern colonization of SFB from the south, as has happened during El Niño events

(Johnson *et al.* 2009). Kellet's whelk (Zacherl *et al.* 2003) and the aeolid nudibranch

Phidiana hiltoni (Goddard *et al.* 2011) have extended their ranges northward to SFB or

just beyond in association with El Niño conditions. Additional biological support for

recent colonization of SFB comes from the California grunion. Microsatellite results for

the California grunion reveal its disjunct populations in Monterey Bay and San Francisco

Bay are not genetically distinct and are also sourced from the south (Johnson *et al.* 2009;

Byrne *et al.* 2013), which is consistent with our results for *G. mirabilis*. While grunion

spawn on sandy beach habitat, and thus may be influenced by additional ecological

factors, Johnson and authors (2009) suggested the colonization of SFB may be recent and

mediated by El Niño events. The warmer waters of SFB compared to the Pacific coast

179

(Conomos 1979) could potentially sustain more subtropically associated species following colonization.

There is a possibility of artificial (i.e. anthropogenic) colonization of *Gillichthys mirabilis* to SFB since its use as live bait for fishing began in the 1930s (Turner & Sexsmith 1967). However, *G. mirabilis* existed in SFB by the late 1800s, as it was noted in 1877 that locals ate individuals of this species (Lockington 1877; Love 2012). That, combined with the fact that *G. mirabilis* was more commonly used for fishing in regions to the south and for inland freshwater fishing (Turner & Sexsmith 1967), suggests colonization through artificial means was unlikely.

In combination, our paleohabitat modeling and genetic analyses strongly suggest that San Francisco did not support tidal estuarine habitat 20 kya. Previous work by Atwater (1979) indicates the San Francisco estuary did not reach its modern extent until between 5–10 kya, which is consistent with our models. Extralimital populations such as those found in SFB are of interest in evolution because they are often genetic sinks, whereby genetic diversity in these populations is imported from the rest of a species range. Over consecutive glacial periods SFB would likely have been extirpated repeatedly, in which case populations in SFB may be genetic sinks over evolutionary time despite possible repeat colonizations during interglacial periods. Although, if coastal sea-surface temperatures increase along the California coast in association with future climate change, and species accommodate this increase by shifting northward as often predicted (McFarlane *et al.* 2000; Roessig *et al.* 2004; Ficke *et al.* 2007), then SFB populations may cease to be disjunct in time. With this northward migration, the disjunct

SFB population of many species might no longer be a sink for southern genetic diversity as they become established as a more integral part of their range.

Gulf of California patterns

Quietula y-cauda in particular, and *Gillichthys mirabilis* to a lesser degree, appear to inhabit more steeply-graded estuaries along the western Gulf of California (Gulf) than eastern Gulf or Pacific coastlines (Table 3-S3). Our paleohabitat models suggest that potential habitat area within the Gulf was reduced by 85% at lowstand 20 kya relative to today (Figures 3-3B, 3-S3). The increase in total habitat area between 15 and 5 kya appears to be exponential and driven primarily by northern (Colorado Delta) and eastern (mainland Mexico) estuarine habitat. This pattern is reasonable given the different coastal geomorphologies of these regions, as there is a much wider shelf on which habitat could expand in the north and east, and much less in the west (Figures 3-1, 3-S1).

Our suite of GLMs assessed the statistical support for lowstand refugia in different areas within the Gulf based on modern habitat characteristics. These models produced several similar statistically significant results (Table 3-S4). The simplest significant model included Reforma, mid-eastern Gulf, Bahía Kino, and Colorado Delta as lowstand refugia (p = 0.03, AICc = 33.3; Figure 3-4). Addition of two western Gulf refugia (Francisquito and Zacatecas) to the model was also significant (p = 0.02, AICc = 21.9). This second model when run without the mid-eastern Gulf or without Zacatecas was not significant. The AICc scores from refugium models and independent genetic results indicate that Francisquito and Zacatecas were indeed refugia and produced genetically differentiated clades over time (Figures 3-4B, 3-S4, 3-S6, 3-S7). This

example highlights the complementarity of these habitat and genetic approaches when interpreted together.

Our models suggest that lowstand refugia were larger and more connected in the northern and eastern Gulf than in the western Gulf or along the Pacific coast. These findings are supported by STRUCTURE results (Figure 3-4B) and microsatellite tree topologies (Figure 3-S4) in which the northern and eastern Gulf are genetically homogeneous. By contrast, the two western Gulf refugia (Francisquito and Zacatecas) appear to be geographically and genetically isolated. Unique genetic signatures for central (Francisquito, orange region of Figure 3-4B) and southern (Zacatecas, pink region of Figure 3-4B) refugia in STRUCTURE plots (Figure 3-4B) support the concept of genetically isolated refugia. Neighbor-Joining trees (Figure 3-S4) also support these as two refugia that evolve in isolation during recurrent periods of glacial lowstand (Figures 3-S4, 3-S6, 3-S7).

Deng and Hazel (2010) suggested the way in which the physical footprint of the Gulf shrinks with lowered sea level may be an important factor when interpreting phylogeographic patterns. The converse of this general idea has been considered, in which the expansion of island footprints may have facilitated migration between mainland Mexico and the Baja peninsula via the Midriff Islands (Clark-Tapia & Molina-Freaner 2003; but see Pfeiler & Markow 2011). For coastal marine taxa, however, as the size of the Gulf's footprint decreases during lower sea level, the proximity of populations on the eastern and western coasts increases. For example, at the latitude of Isla Tiburón, trans-Gulf populations are separated by only ~70 km at lowstand relative to 100 km at present, and ~150 km versus ~180 km at the latitude of Bahía Concepción. Increased

182

proximity may facilitate trans-Gulf migration as habitat forms during sea-level rise (Figure 3-3B). Evidence for trans-Gulf migration exists in several individuals between the eastern (blue) and western (orange) groups in Figure 3-4. However, migration across the middle of the Gulf may also be aided by the upper arm of the seasonal southern gyre (Marinone 2003; Soria *et al.* 2014). The curvature of the upper Gulf and Colorado Delta would cause this region to be affected to perhaps an even larger degree with habitats becoming much more closely spaced during lowstand (Deng & Hazel 2010). An absence of population differentiation (Tables 3-S6B, S6C) and subdivision (Figure 3-4), and low pairwise F_{ST} values (Tables 3-S7B, 3-S7C) suggest genetic homogeneity across the northern Gulf, which may be a consequence of this reduced footprint at lowstand.

Theoretical framework for lowstand refugia

We propose the following working hypothesis to explain how physical processes control habitat distribution and genetic connectivity through time. Rifting, uplift, and faulting in combination with wave erosion and other oceanographic factors work to shape offshore islands, coastal orientation and regional geomorphology of tectonically active coastlines. The grade and width of the coastline that results from these processes dictate where estuarine, and likely many coastal habitats, can form. Sea-level oscillations over this heterogeneous shelf topography during glacial-interglacial periods eliminate and re-form estuarine habitat over millennia. Biological populations exhibit two primary genetic signatures as a consequence: genetically distinct clades that result from isolation in lowstand refugia, and admixed populations that are recolonized from multiple genetically distinct refugial sources. These genetic patterns are commonly observed in studies of

glacial-interglacial phylogeography (reviewed in Hewitt 2000; 2004). Yet, this working

hypothesis differs from previous studies because the combination of tectonically-driven

shelf heterogeneity and sea-level change are global phenomena that may produce this

extirpation-isolation-recolonization process in coastal species at latitudes far from the

glacial front. While this extirpation-recolonization pattern is likely relevant for species

with discontinuous habitats regardless of latitude, at tectonically passive coastlines with

broad shelves, a simpler north-south migration pattern may still be observed (Marko

2004; Adams *et al.* 2006).

Comparisons to non-estuarine taxa

Phylogeographic studies within the Gulf have focused on rocky intertidal

(Hurtado *et al.* 2007; Deng & Hazel 2010), rocky shore (Riginos & Nachman 2001;

Riginos 2005), sandy beach (de Jesús Suárez-Moo *et al.* 2013; Byrne *et al.* 2013; Hurtado

et al. 2013), reef (Lin *et al.* 2009), and pelagic species (Segura *et al.* 2006). Most of these

habitats are discontinuously distributed along the coastline (Riginos & Nachman 2001),

and the focal taxon within each of these studies exhibited population level structure

within the Gulf of California. While the specific location of lowstand refugia would differ

by habitat type, the pattern of extirpation, isolation, and recolonization as revealed here

with sea-level change may be applicable to these habitats. For example, rocky intertidal

habitat is common in the western Gulf and less abundant in the eastern Gulf, which is the

opposite pattern observed with estuarine habitat. Lowstand refugia for rocky-associated

species may therefore have been common in the western Gulf with sustained gene flow

between populations, and more isolated in the eastern Gulf. This pattern is opposite to

184

what we observe for estuaries, which we estimate were abundant in the northern and mid-eastern Gulf, and minimal in the western Gulf. Based on regional shelf topography one might indeed expect opposite habitat distribution patterns for low slope habitats (e.g., estuaries) and higher sloping habitats (e.g., rocky intertidal). Regardless of specific refugial patterns, the role of glacial refugia has not often been considered when interpreting patterns of population subdivision in such studies but may provide insight into isolation mechanisms in future work.

Mid-peninsular seaway hypothesis

Many studies have treated a longstanding and contentious hypothesis regarding the presence of a transient trans-peninsular seaway 1–2 Ma across the middle of the Baja Peninsula (reviewed in Dolby *et al.* 2015). Findings from marine studies have echoed the pattern found in terrestrial work of a north-south genetic break among populations on either side of this purported feature (Riginos & Nachman 2001; Riginos 2005; Dolby *et al.* 2015). It was recently suggested that instead of yielding a north-south genetic break in nearshore species, that a mid-peninsular seaway could have acted as a dispersal corridor for many marine and coastal taxa (Dolby *et al.* 2015). Based on the reciprocal monophyly between Pacific and Gulf populations and the results from STRUCTURE analyses, we find evidence in microsatellite or mtDNA data that suggests individuals adjacent to the purported seaway region were not in recent genetic contact. The mtDNA topology for *G. mirabilis* is the only result potentially consistent with a seaway interpretation. Colonization of the Pacific and the first branching event between northern Gulf (dark blue/purple, Figure 3-S7) and the other clades could have been facilitated by dispersal

185

through and cessation of a seaway. This mtDNA tree topology was previously recovered in *G. mirabilis* (Huang & Bernardi 2001), but could also arise from incomplete lineage sorting or selection on the mitochondrion, or through migration around the peninsula and extirpation south of Punta Eugenia on the Pacific coast. If this topology was produced by a seaway in part, then a similar pattern should be observed in other species; but to the authors' knowledge there is not evidence from previous marine literature that indicates individuals dispersed through such a seaway. The mitochondrial tree topology presented here for *Q. y-cauda* suggests the opposite—that the southwestern Gulf clade (light blue clade, Figure 3-S6) is sister to the Pacific clades and that the Pacific was colonized around the peninsula as opposed to across it.

Glacial refugia have not previously been considered in interpreting this north-south genetic discordance across the mid-peninsular region in marine taxa, perhaps due to challenges with modeling paleohabitat distributions. Our findings here suggest, however, that isolated glacial refugia may be a viable alternative explanation for the pattern of north-south discordance observed in marine species in the Gulf (Riginos & Nachman 2001; Riginos 2005; Ellingson 2012). In this scenario, during sea-level rise non-refugial populations are recolonized from genetically distinct sources (refugia), and this pattern could appear as a genetic break in that recolonized region or as individual clades in tree topologies (Figures 3-S6, 3-S7). The location, number, and characteristics of refugia would vary by habitat type. Our specific refugia predictions would not translate to rocky-shore, mangrove, or coral reef habitat per se, though the generalized pattern of refugial isolation may be widespread. The role of refugia and postglacial colonization should therefore be assessed in future studies of such habitats.

Conclusion

We expanded on recently developed paleohabitat models of estuaries and complemented these models with comparative population genetic assessments of three co-distributed fishes over ~4,600 km of coastline. We find that the proximate mechanism controlling connectivity of estuarine populations through time is changing sea level against a coastal shelf topography that varies on a regional scale. The ultimate mechanism underlying estuarine habitat distribution through time, and thus genetic population subdivision in part, is the tectonic history of the region and ongoing oceanographic processes that control the overall shelf topography itself. This working hypothesis may find relevance in many coastal and nearshore species that inhabit coastlines far from the glacial front, and be a significant driver of intraspecific diversity and cladogenesis. Beyond refugial processes, our data support previous assertions of incipient speciation among populations disjunct between the Pacific and Gulf of California. Finally, we broadly find evidence in conflict with a mid-peninsular seaway, which would likely have facilitated dispersal between the Pacific and Gulf. Instead, we suggest such north-south discordance and other marine phylogeographic patterns found previously may be a consequence of isolation in lowstand refugia and postglacial recolonization.
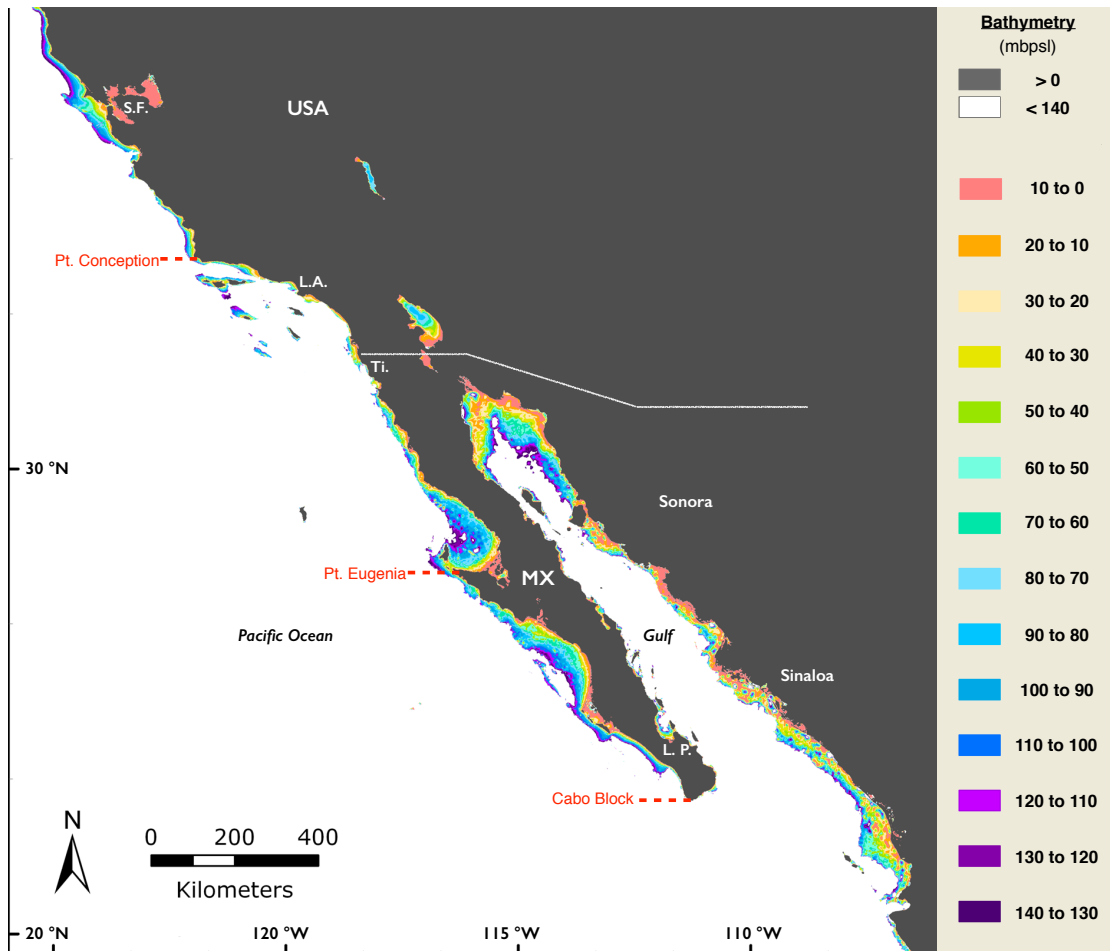
Figure 3-1 Areas meeting slope requirements for estuarine habitat are shown for each 10-m depth bin from 140 to 0 mbpsl (for colors see legend). Select localities are labeled: S.F.- San Francisco, L.A.- Los Angeles, Ti- Tijuana, L.P.- La Paz, and the Mexican states of Sonora and Sinaloa. Select biogeographic barriers are also mapped: Point Conception, Punta Eugenia, and the Cabo Block region.
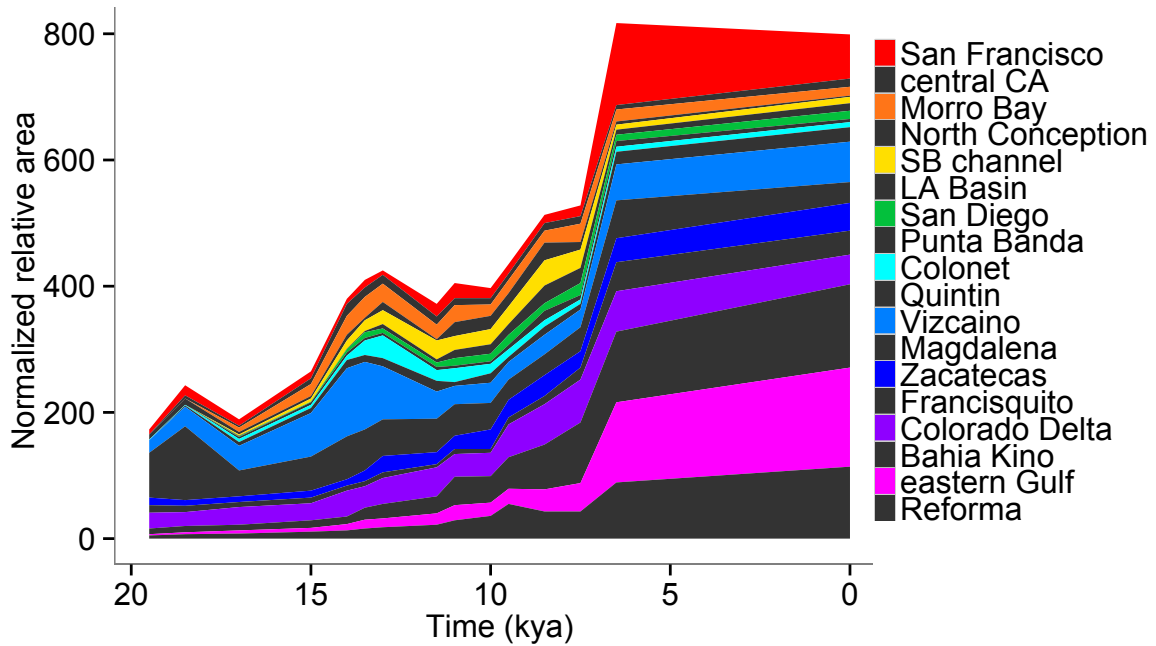
Figure 3-2   Habitat area normalized by coastal region for all populations from San Francisco, USA to Reforma, Mexico for ease of visualization and to show the relative change in habitat size across coastal regions. Sites are in coastal order and area is in km^2. Note that habitat area measured per time-point (depth bin) is independent of other measurements and therefore this graph is not displaying cumulative area through time.
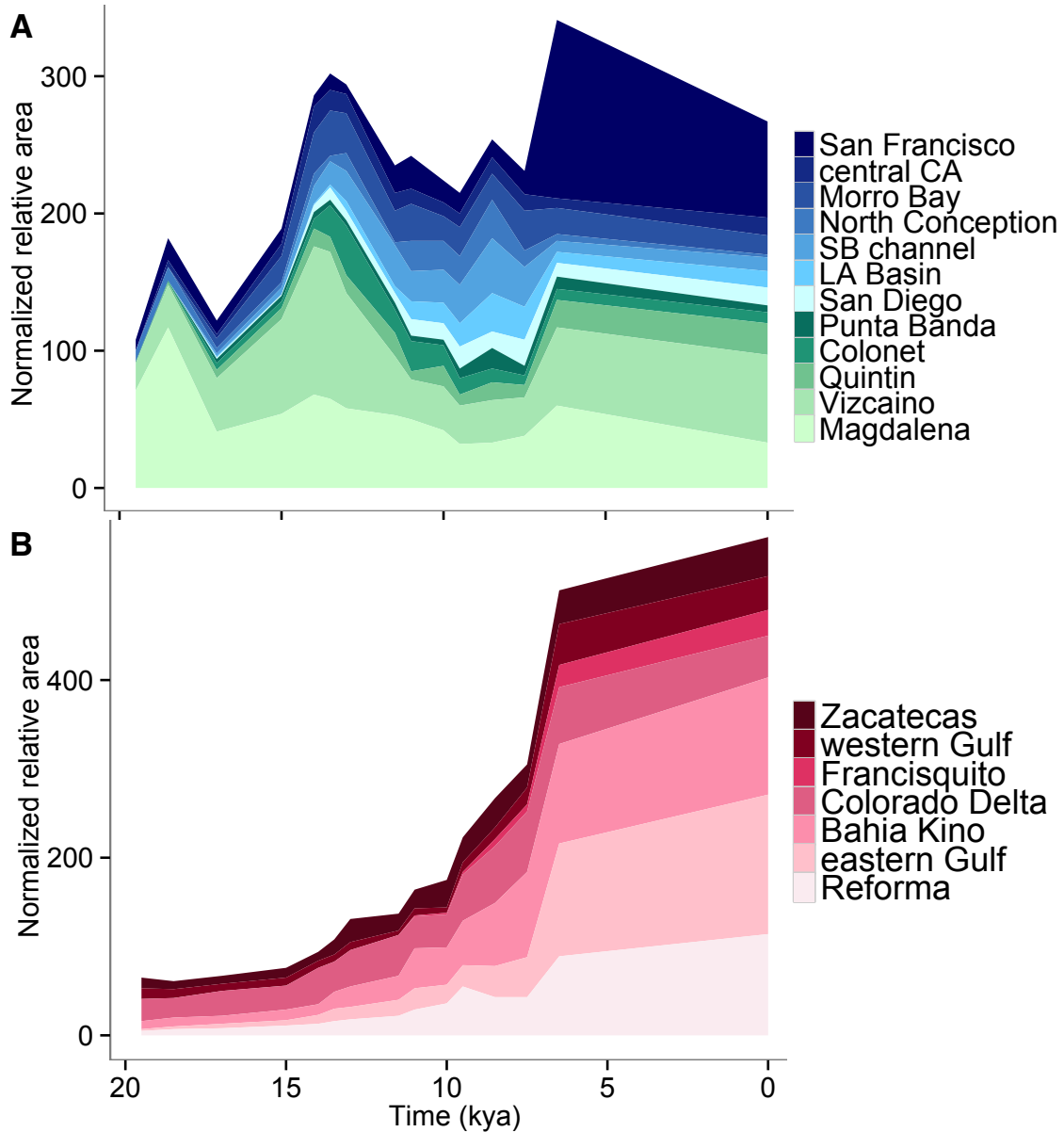
Figure 3-3 Habitat area per site, normalized by coastal region size shown here for populations divided between **A)** Pacific sites, and **B)** Gulf sites. Area was calculated for each location per-time bin and is not cumulative through time. Normalized relative area shown here divided total habitat area for a region by its coastal region size which enables visualization of all sites rather than just the largest sites that otherwise drive this curve (Vizcaíno, Magdalena, Colorado Delta). For total area values see Figure 3-S3. All sites are color-coded (see legends) and ordered by coastal location from northernmost (San Francisco, top) to bottom. Gulf sites are ordered clockwise around the Gulf of California (Zacatecas to Reforma).
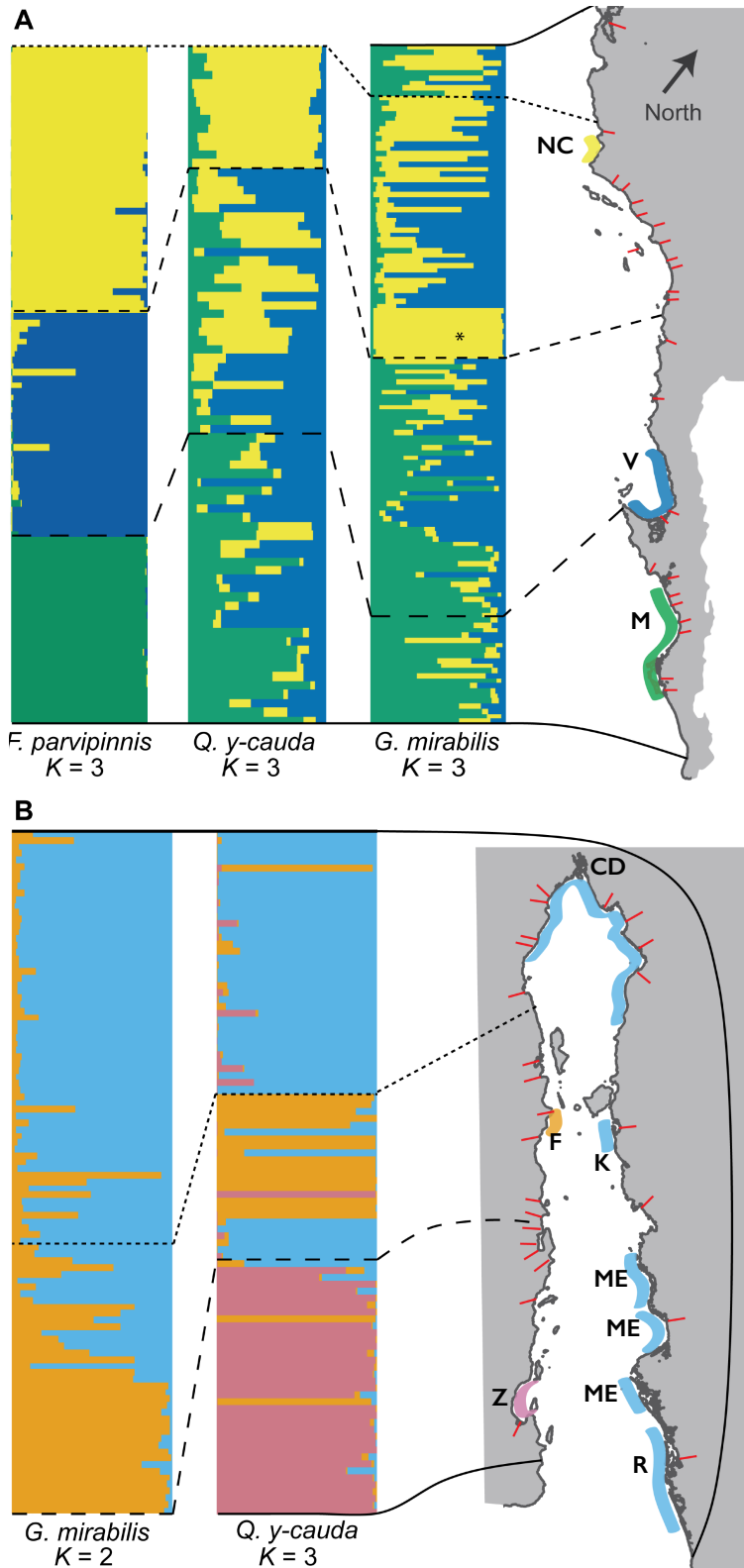
Figure 3-4 STRUCTURE results with corresponding reference maps showing refugia predicted through paleohabitat models (Figure 3-1). Red ticks mark collection locations for fish samples (details in Table 3-S1). Individuals in STRUCTURE plots are in coastal order (top to bottom); varying dashed lines denote predicted or inferred geographic barriers. Species and number of groups (K) listed beneath each plot. The ranges of *F. parvipinnis* and *Q. y-cauda* do not extend northward of the small dashed line (panel A) and *G. mirabilis* does not extend southward of the widely hashed line (panel B). **A)** Pacific samples corresponding to black-outlined coast. Asterisk denotes an inferred founder event in population HID within *G. mirabilis*. Breaks listed are: San Francisco (small dash), southern California Bight (medium dash), Punta Eugenia (large dash). **B)** Gulf samples corresponding to black-outlined coast (clockwise around the Gulf perimeter). Breaks listed are: Bahía Concepción (large dash) and San Felipe (small dash).

Refugia labeled as referenced in the text: NC- North Conception, V= Vizcaíno, M- Magdalena, Z- Zacatecas, F- Francisquito, CD- Colorado Delta, K- Bahía Kino, ME- mid-eastern Gulf, R- Reforma. Note the mid-eastern Gulf (ME) groups three refugia; according to genetic data these appear to function as a series of genetically connected refugia that, unlike Francisquito and Zacatecas, are not isolated genetically at lowstand and through time (Figures 3-S4, 3-S6, 3-S7).
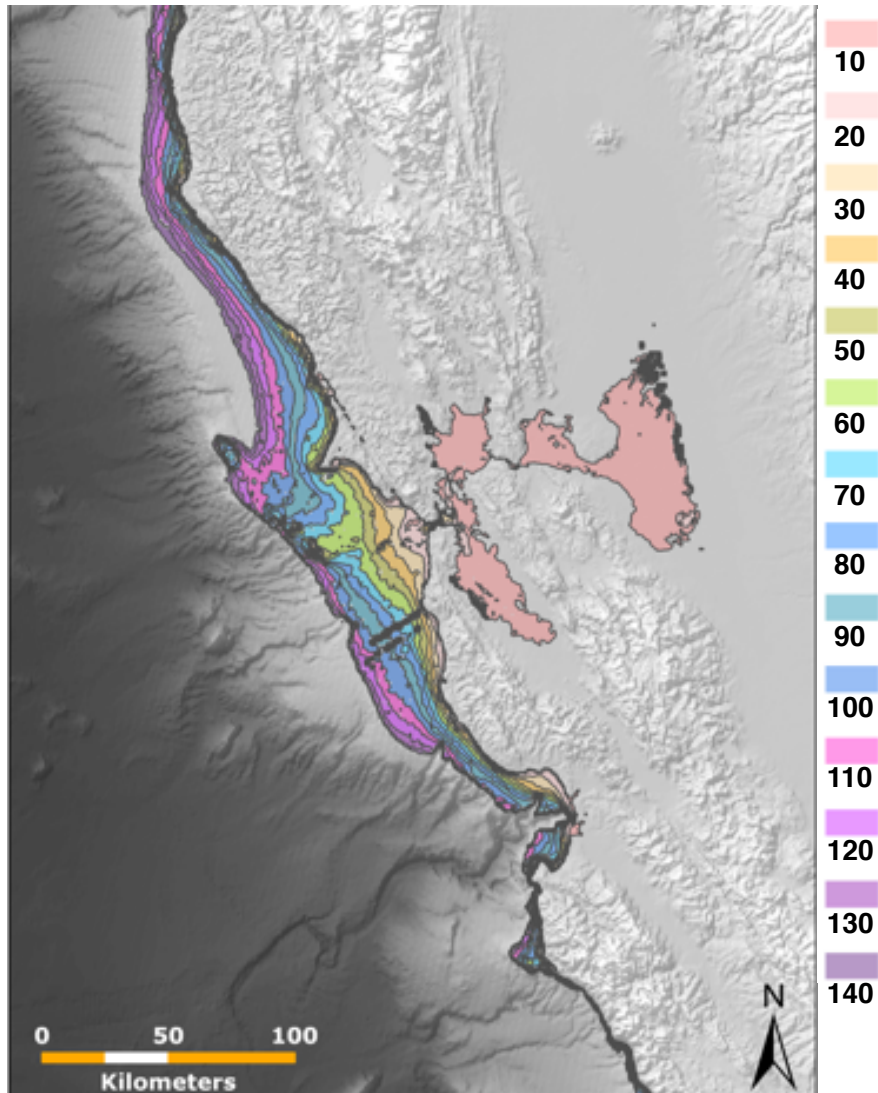
Figure 3-5   Here we depict the San Francisco Bay area with a hillshade DEM where light grey is land and dark gray is ocean. Ten-meter depth bins are contoured from 0–140 mbpsl and labeled to the right by the lower limit of each bin. The limited area available within the 120–140 mbpsl bins is likely what limits lowstand habitat. Note that much of the Sacramento and San Joaquin Delta region (coral color on right-hand side) is actually below sea level and has been dyked and modified for land use purposes.
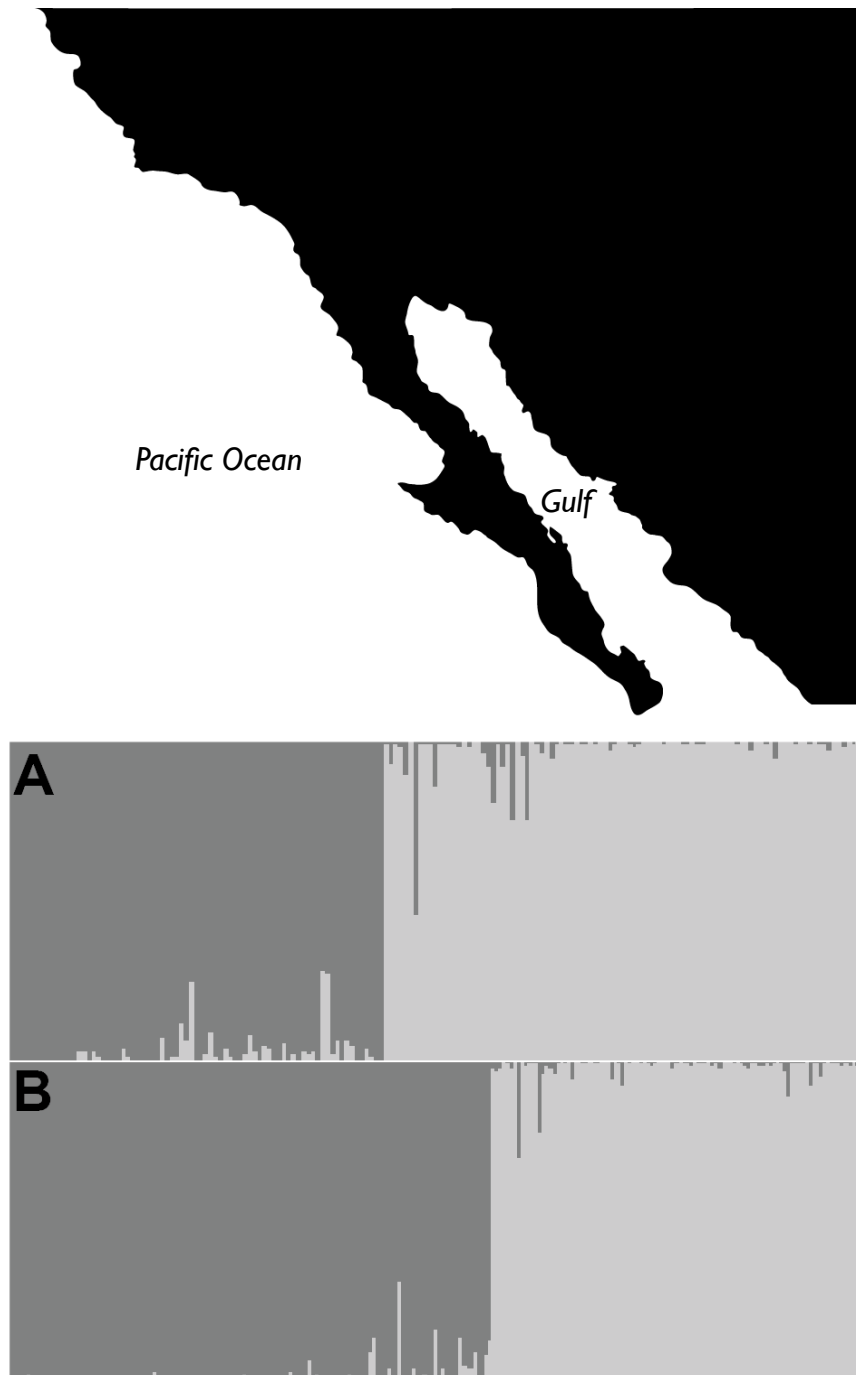
Figure 3-6 Structure results ($K = 2$) for **A)** *Q. y-cauda*, and **B)** *G. mirabilis* showing low levels of genetic mixing between Pacific (dark grey) and Gulf of California (light grey) individuals.
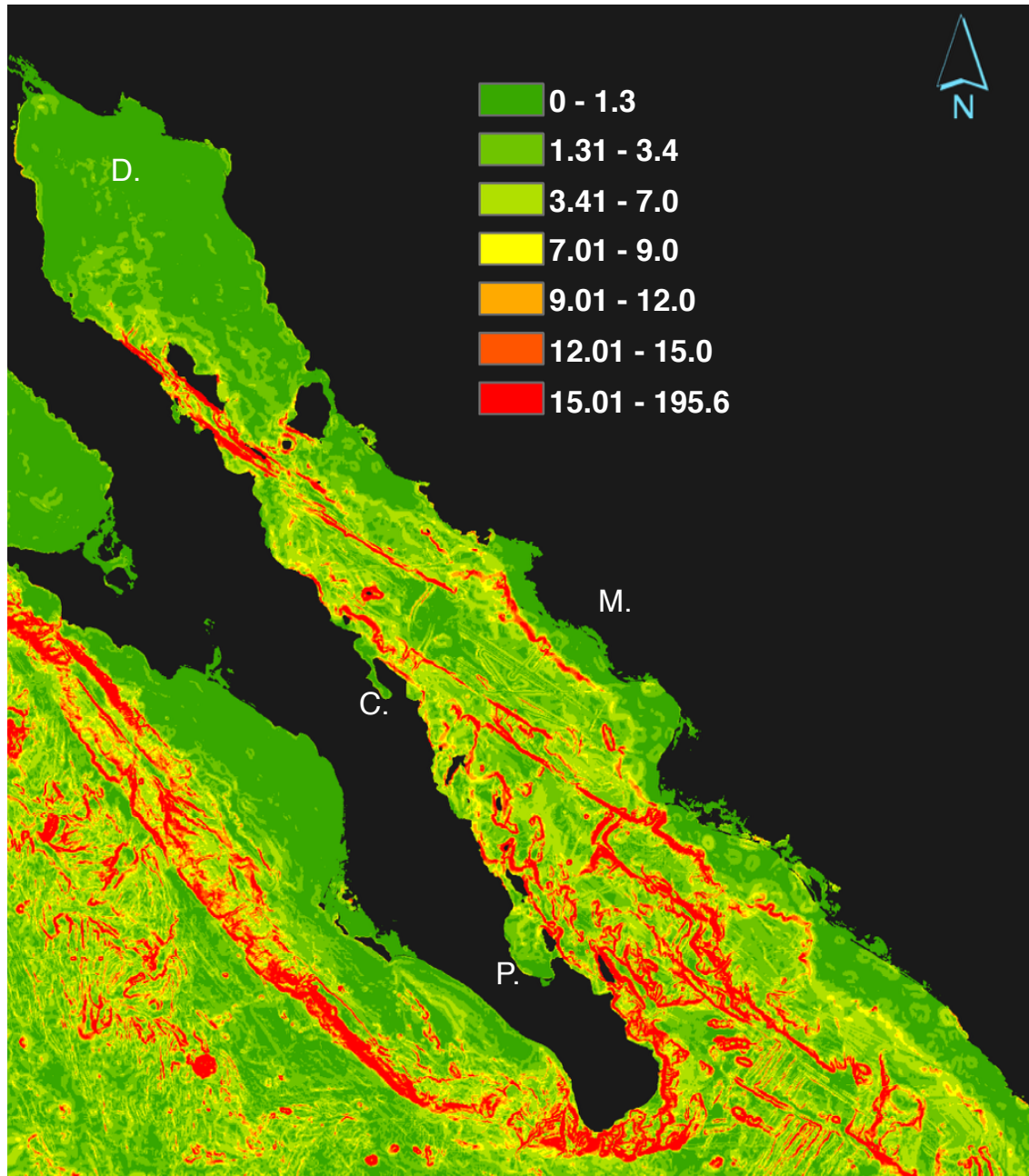
Figure 3-S1 Map presented to shows slope values based on STRM30_PLUS DEM. Slope classification scheme emphasizes values suitable for Pacific coast estuaries (0.0–1.3%, Dolby *et al. in revision*), slope values suitable for Gulf of California estuaries (0.0–3.4%, this study) and some seafloor spreading and fault zones within the Gulf of California basin (red, slope >15.0). Here the steeper slopes of the western Gulf shelf are visible except for Conception (C.) and La Paz (P.) bays. The less steep, wider coastal shelf along the Colorado Delta (D.) and mainland Mexico (M.) shelves are also shown.
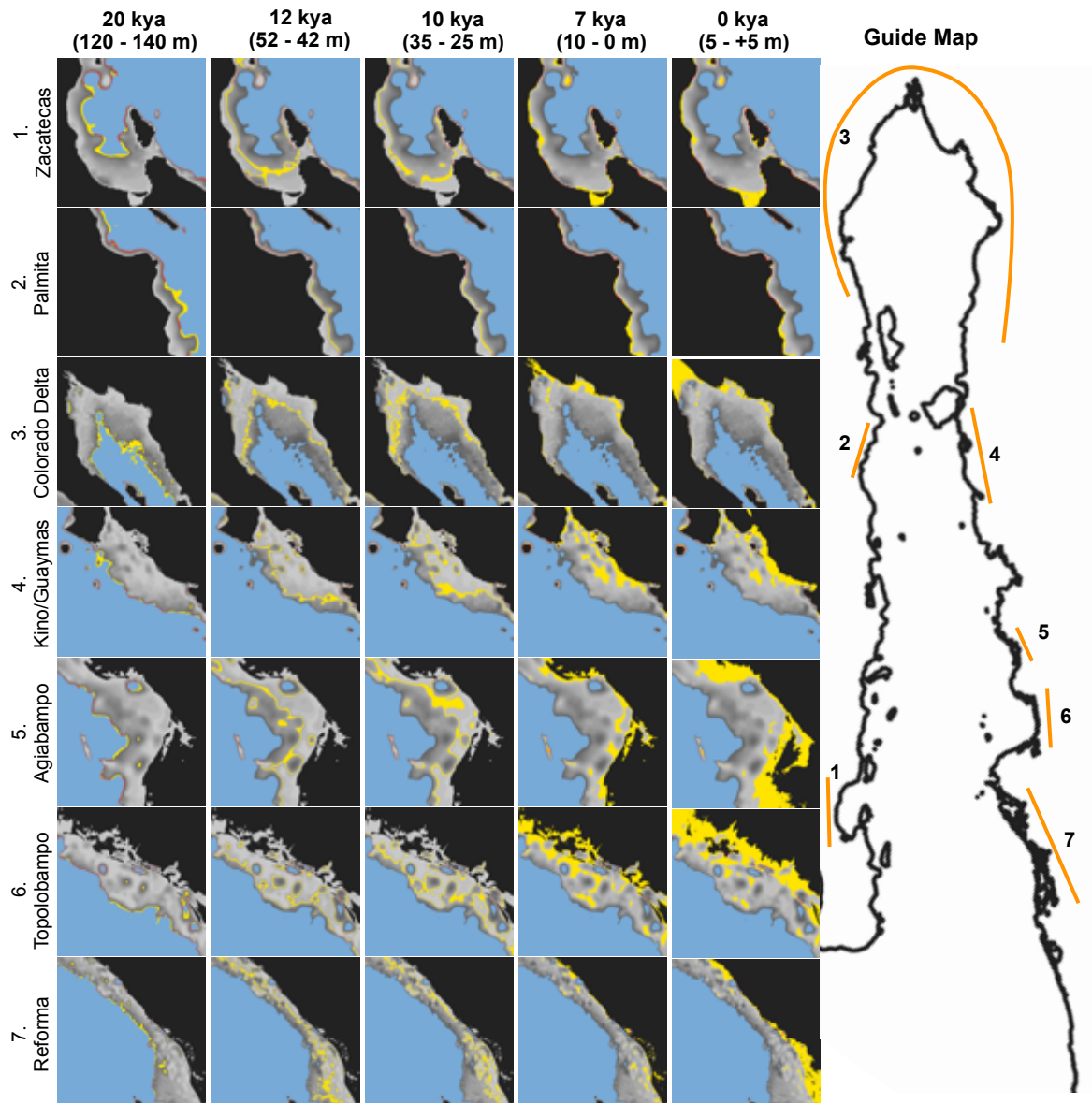
Figure 3-S2   A time series of habitat maps are shown for chosen Gulf regions. Areas meeting slope ($\leq 3.4\%$) requirements (yellow) for chosen bathymetric bins are depicted. Land is shown in black, ocean shown in blue, and bathymetry is contoured by 10-m bins and colored in greyscale. Coastal regions 1–7 (left) correspond to regions numbered on the guide map in orange (right).
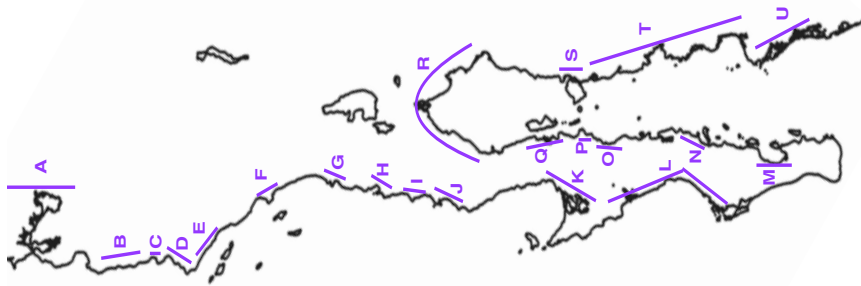
	Age (kya)	19.5	18.5	17	15	14	13.5	13	11.5	11	10	9.5	8.5	7.5	6.5	0
	mbpsl	140 - 130	130 - 120	120 - 110	110 - 100	100 - 90	90 - 80	80 - 70	70 - 60	60 - 50	50 - 40	40 - 30	30 - 20	20 - 10	10 - 0	0 +/- 5
A	San Francisco	62	131	259	267	195	308	181	505	596	400	380	333	414	3242	1761
B	central CA coast	0	3	27	76	153	125	114	107	88	85	81	102	101	61	103
C	Morro Bay	0	0	5	14	22	24	21	17	20	13	15	14	21	14	10
D	N. Conception	25	31	13	12	28	12	38	6	66	63	62	83	36	14	7
E	Santa Barbara Channel	0	0	10	25	59	79	101	141	101	113	131	183	134	39	46
F	LA Basin	0	1	3	2	3	9	43	31	75	87	97	162	142	46	68
G	San Diego	3	2	6	12	38	70	54	59	95	95	131	96	154	82	105
H	Punta Banda	0	0	24	33	45	36	40	44	41	37	68	143	68	82	45
I	Colonet	7	6	27	29	41	131	204	95	124	86	66	59	41	43	48
J	San Quintin	2	15	50	60	100	85	104	137	44	119	62	105	74	160	179
K	Vizcaino	519	821	1028	1806	2816	2803	2189	1124	772	827	729	817	739	1495	1665
L	Magdalena	462	764	1443	1923	2390	2310	2058	1858	1767	1486	1140	1158	1331	2106	1172
M	Zacatecas	53	41	42	51	47	75	117	85	94	142	128	148	118	172	199
N	N. of Zacatecas	0	0	0	0	0	0	0	0	0	0	0	0	0	1	1
O	S. of Fancisquito	0	0	0	0	0	0	0	0	0	0	0	0	0	0	0
P	Francisquito	28	23	19	21	19	18	22	11	18	14	26	30	44	107	88
Q	Angel de la Guarda	0	0	1	0	1	1	0	1	2	5	10	23	25	74	87
R	Colorado Delta	1228	1042	1339	1282	1967	1620	2001	2207	1748	1799	2511	3106	3284	3108	2255
S	Bahia Kino	57	67	61	77	83	125	157	179	303	279	335	472	643	748	886
T	mid-eastern Gulf	44	73	103	126	204	290	303	388	511	443	505	755	950	2712	3332
U	Reforma	147	204	245	348	403	487	557	669	884	1102	1672	1321	1297	2712	3483

Figure 3-S3 Values for habitat area per time (column) per coastal region (alphabetic rows corresponding to the guide map on the right) are presented. Qualitative color-coding follows: little to no habitat, to abundant habitat (0–5 km^2, red; 5–15 km^2, orange; 15–30 km^2, yellow; 30–60 km^2, green; 60–150 km^2, teal; >150 km^2, medium blue). Note that the coastal region subdivisions (A–U) are not of equal size, but rather based on coastal topography and modern habitat distribution patterns.

196
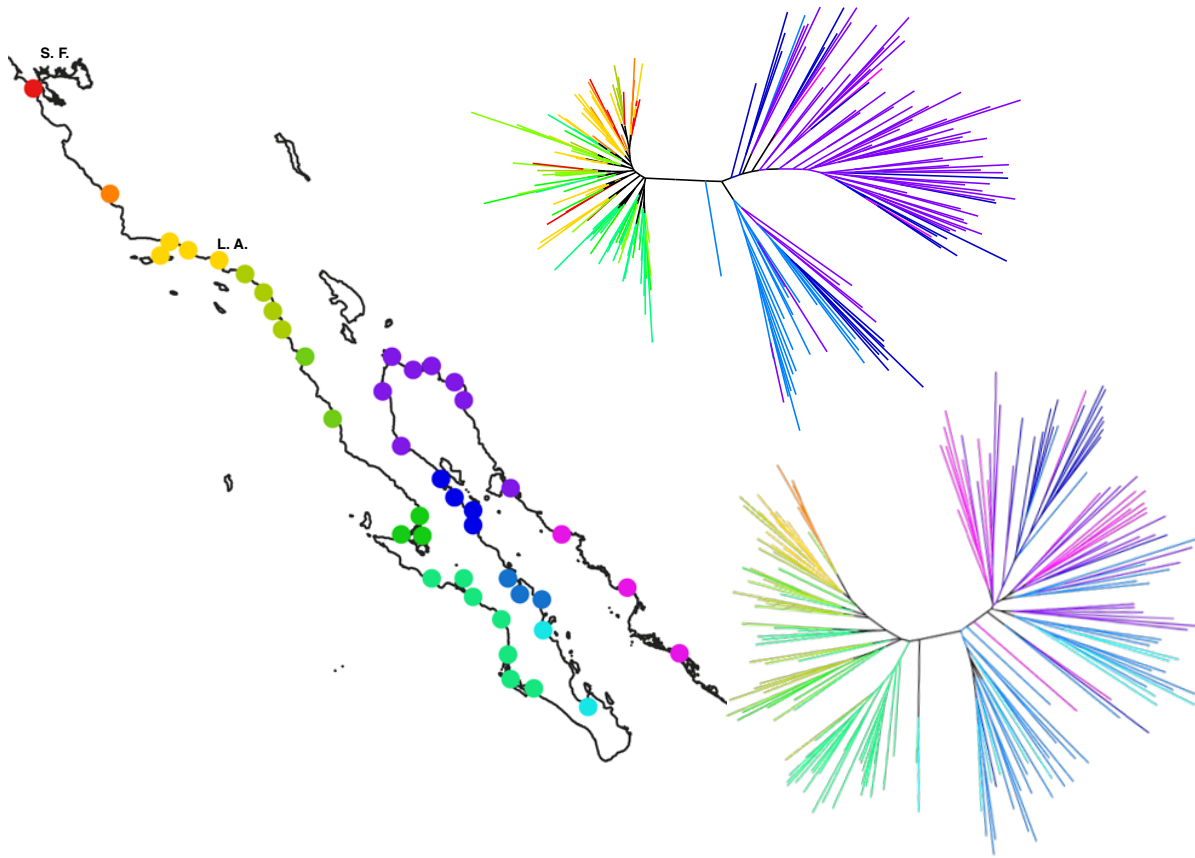
Figure 3-S4 Neighbor-Joining trees constructed with microsatellite data for *Gillichthys mirabilis* (top), and *Quietula y-cauda* (bottom) are shown where the collection locations of the taxa are colored according to the map. The Pacific and Gulf form reciprocally monophyletic clades in each species. Not all sample sites are shown on the map for visual clarity.
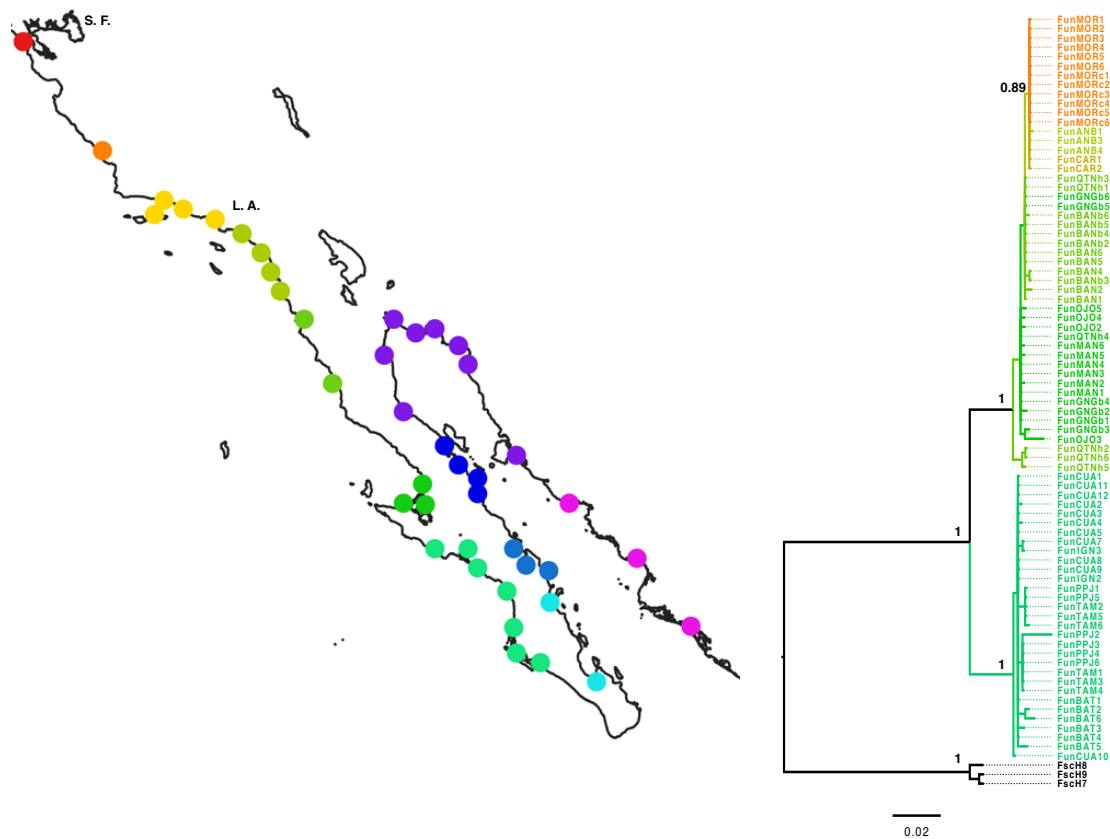
Figure 3-S5 Phylogenetic tree created in MʀBᴀʏᴇs with 889 bp of mitochondrial control region (Dloop) and 81 individuals of *Fundulus parvipinnis* plus three outgroup samples of *Fundulus sciadicus*, which is not its sister species. Three runs were parameterized and summed as follows: nchains = 4, Nst = 2, lset rates = equal, generations = 8 million, burnin fraction = 25 %.
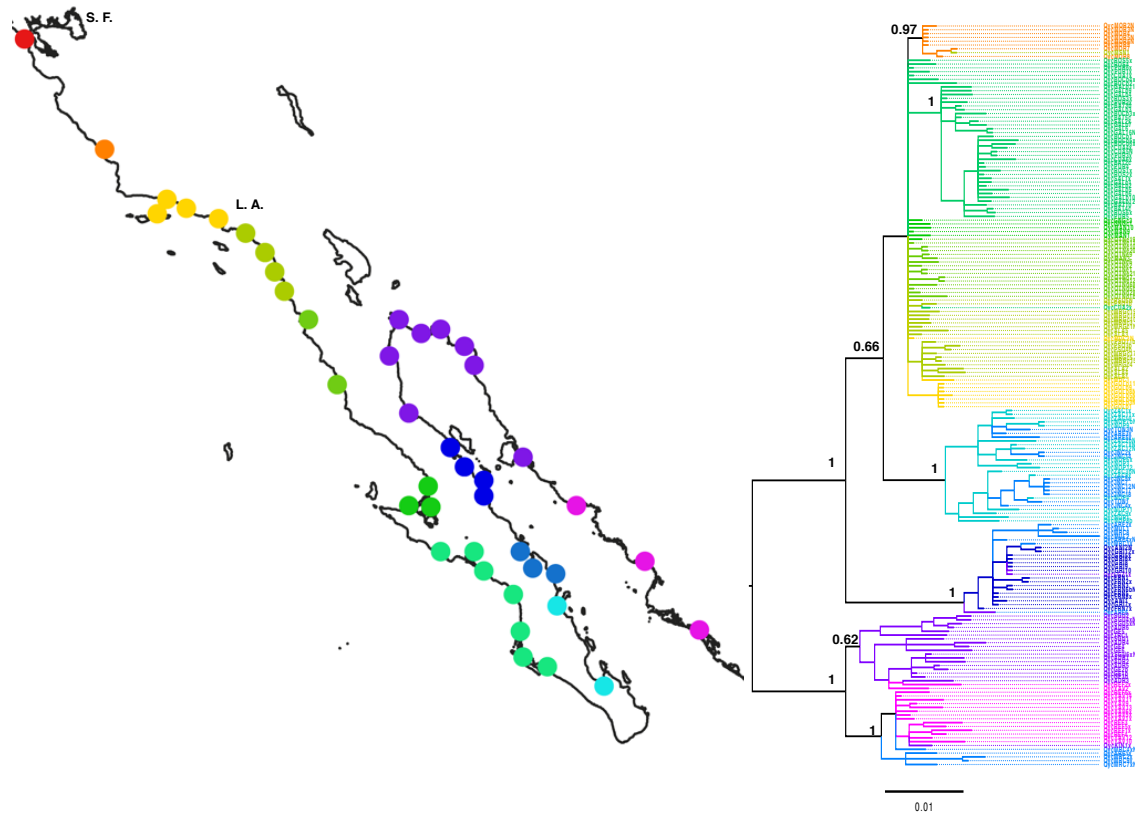
Figure 3-S6   Phylogenetic tree created in MRBAYES with 912 bp of Cytochrome B and 195 individuals of *Quietula y-cauda* with no outgroup samples. Three runs were parameterized and summed as follows: nchains = 4, Nst = 2, lset rates = equal, generations = 10 millions, burnin fraction = 25 %.
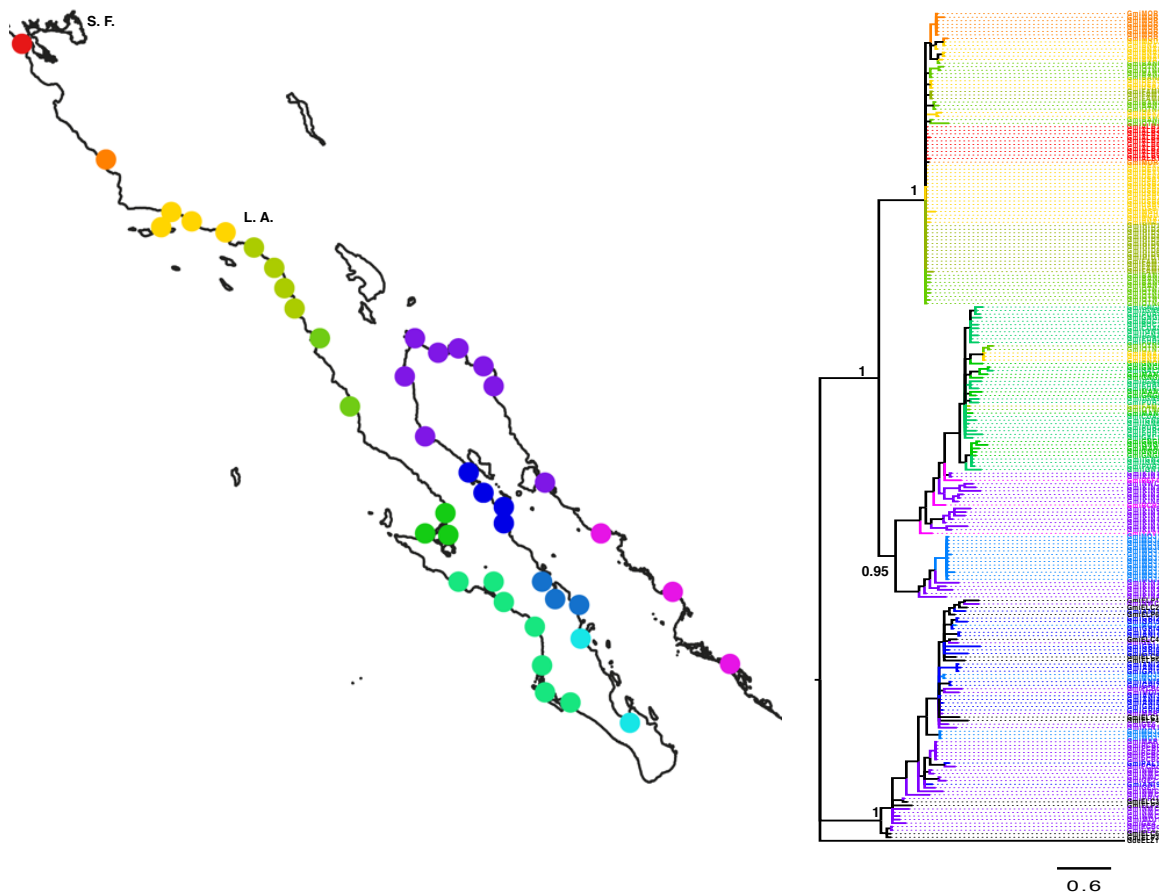
Figure 3-S7   Phylogenetic tree created in MRBAYES with 1827 bp of
mitochondrial control region (Dloop) and Cytochrome B, with 233 individuals of
Gillichthys mirabilis with one outgroup sample from its sister taxon *G. detrusus*. Two
runs were parameterized and summed as follows: nchains = 4, Nst = mixed, lset rates =
gamma, generations = 10 millions, burnin fraction = 25 %.
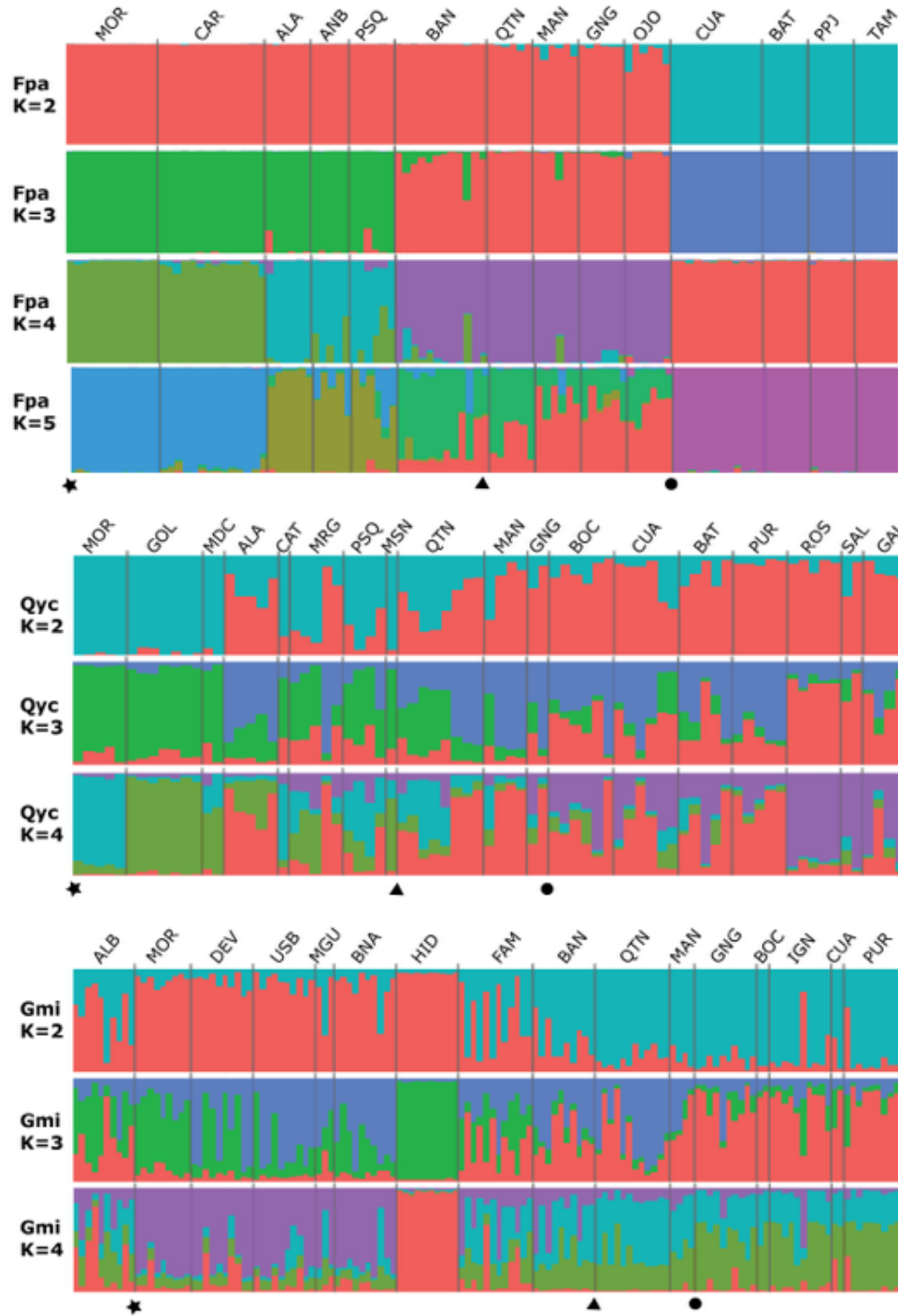
Figure 3-S8 Structure results for Pacific samples of *Quietula y-cauda* (Qyc),
Gillichthys mirabilis (Gmi), *Fundulus parvipinnis* (Fpa). Vertical bars delineate sampled
populations, which are labeled with population three-letter codes (see Table 3-S1).
Shapes denote the hypothesized or inferred geographic breaks from Figure 3-2: San
Francisco–southern California (star), southern California Bight (triangle), Punta Eugenia
(circle). Structure results are shown for *K* = 5 for *F. parvipinnis* because the results for *K*
= 4 were well resolved.
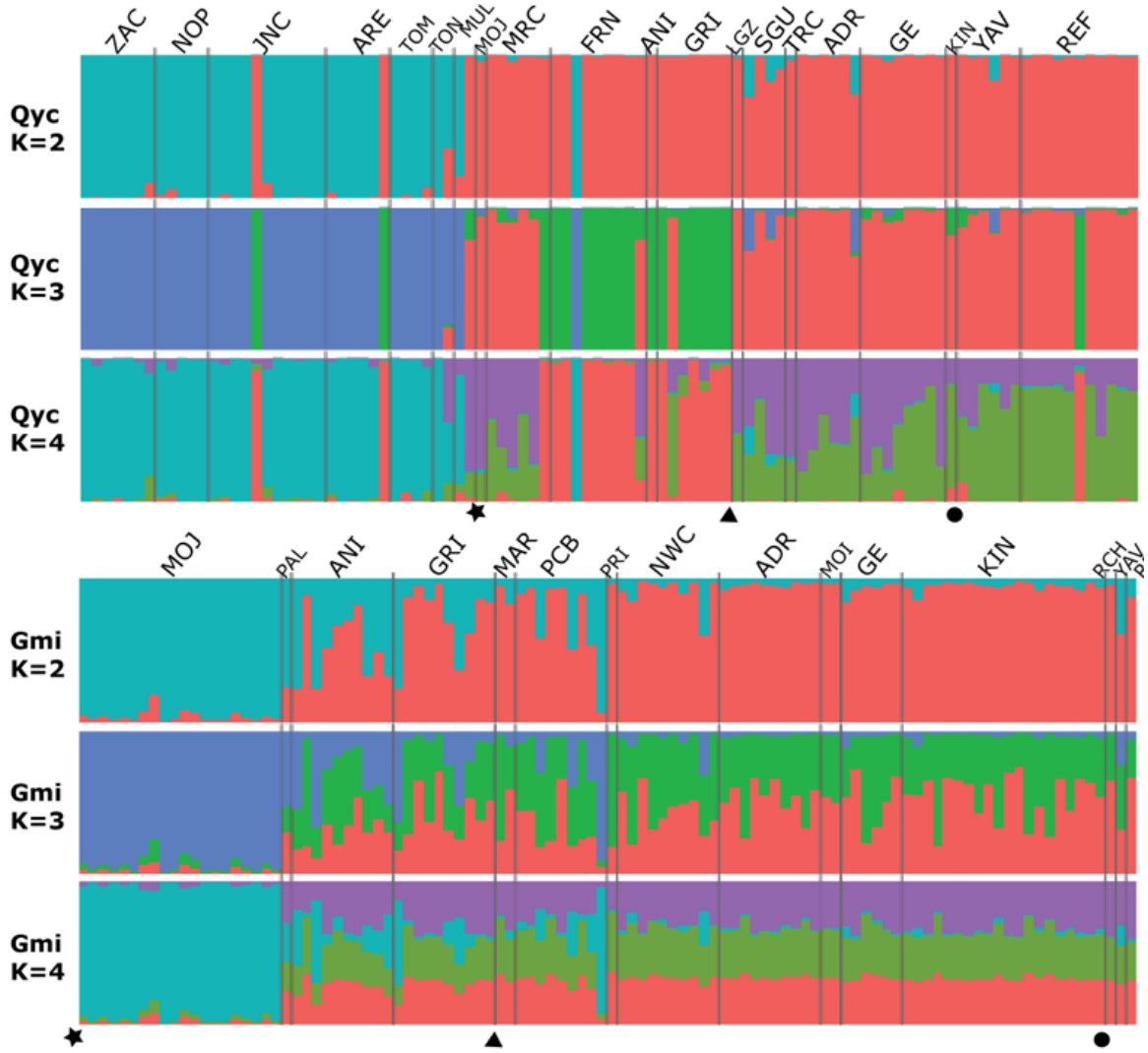
Figure 3-S9 Structure results for Gulf samples of *Quietula y-cauda* (Qyc) and *Gillichthys mirabilis* (Gmi). Vertical bars delineate sampled populations, which are labeled with population three-letter codes (see Table 3-S1). Shapes denote the hypothesized or inferred geographic breaks from Figure 3-2: southern-central refugia (star), central-Delta refugia (triangle), Delta refuge–mid-eastern Gulf (circle).
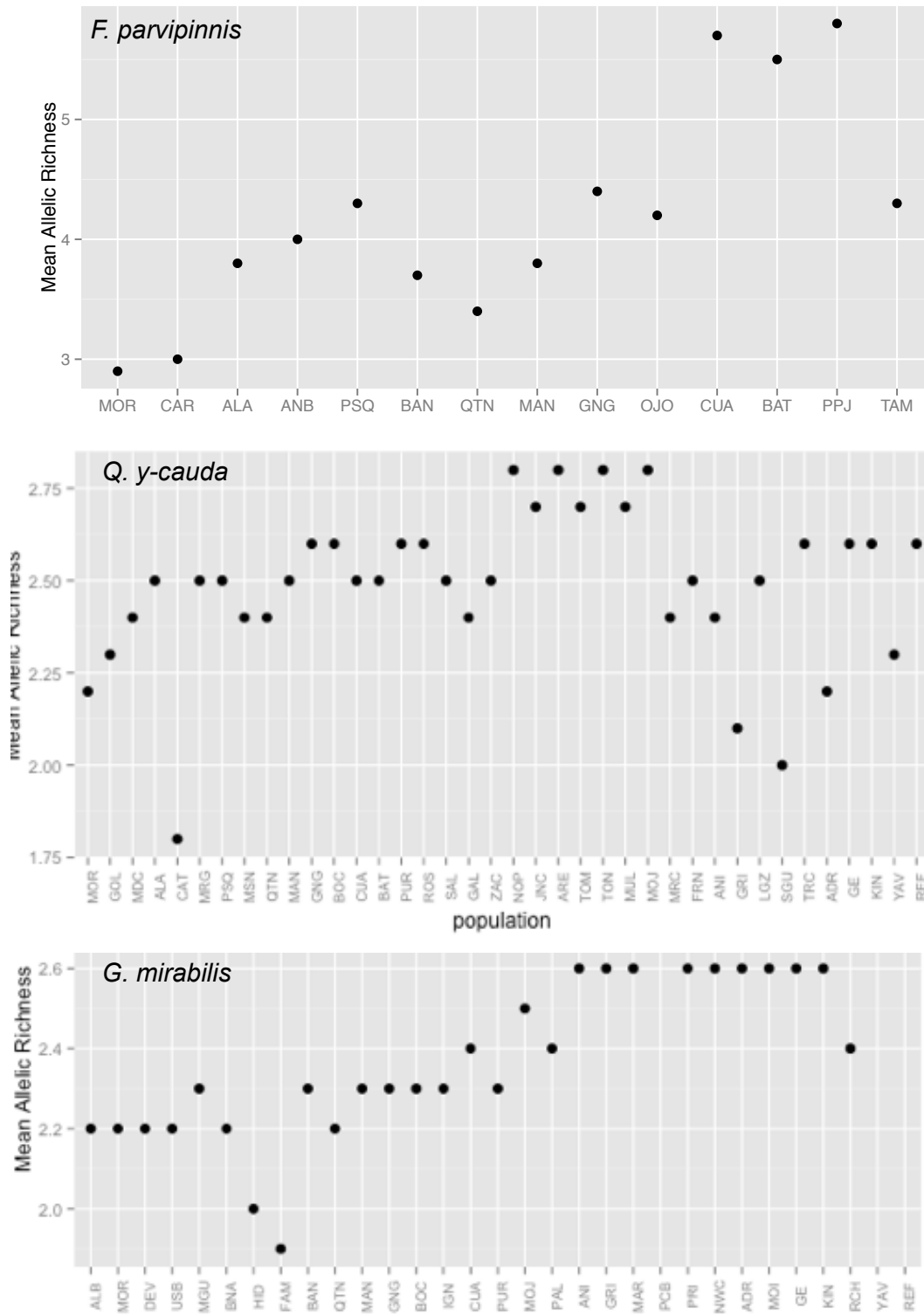
Figure 3-S10 Mean allelic richness is shown against population order from north (left) to south (right) for all three species. Mean population allelic richness values were obtained by averaging across loci at each population, using the results from HEIRFSTAT.

Table 3-S1   Listed is information for Pacific locations used in this study. Site names, 3-letter codes, GPS coordinates in decimal degrees, and sample sizes for each species are noted. Not all individuals were both genotyped for microsatellites and sequenced for mtDNA (see sample sizes).

Pacific collection sites										
Site location	code	latitude°	longitude°	color hue	Sample Size: microsatellites			Sample Size: mtDNA		
					F. parvipinnis	G. mirabilis	Q. y-cauda	F. parvipinnis	G. mirabilis	Q. y-cauda
Albany race track	ALB	37.889333	-122.311683	0	-	10	-	-	10	-
Morro Bay	MOR	35.348517	-120.833600	30	12	9	5	12	9	7
Devereaux Slough	DEV	34.417350	-119.873983	50	-	10	-	-	8	-
U. Santa Barbara	USB	34.409383	-119.845017	50	-	10	-	-	10	-
Goleta Slough	GOL	34.417046	-119.839374	50	-	-	7	-	-	7
Carpenteria	CAR	34.400167	-119.538667	50	14	-	-	2	-	-
Mandalay Canal	MDC	34.136892	-119.183952	50	-	-	2	-	-	2
Point Mugu	MGU	34.113910	-119.082100	50	-	3	-	-	3	-
Ballona Lagoon	BNA	33.962764	-118.445800	50	-	10	-	-	10	-
Alamitos Bay	ALA	33.745519	-118.117547	70	6	-	5	-	-	5
Anaheim Bay	ANB	33.736302	-118.093844	70	5	-	-	3	-	-
Catalina Island	CAT	33.430928	-118.506080	70	-	-	1	-	-	-
Hidden Lagoon	HID	33.275532	-117.451668	70	-	10	-	-	10	-
Santa Margarita	MRG	33.234000	-117.410833	70	-	-	5	-	-	9
Penasquitos	PSQ	32.932500	-117.258000	70	6	-	4	-	-	5
Mission Bay	MSN	32.770833	-117.232333	70	-	-	1	-	-	1
Famosa Slough	FAM	32.751155	-117.228381	70	-	12	-	-	8	-
Punta Banda	BAN	31.765157	-116.617381	90	12	10	-	11	10	-
San Quintín	QTN	30.418794	-116.023086	90	6	12	8	6	12	15
Laguna Manuela	MAN	28.247533	-114.085517	120	6	4	4	6	4	4
Guerrero Negro	GNG	28.021722	-114.114667	120	6	10	2	6	10	2
Ojo de Liebre	OJO	27.783050	-114.312900	120	6	-	-	4	-	2
la Bocana	BOC	26.789283	-113.675733	150	-	2	6	-	2	6
Ignacio lagoon	IGN	26.818667	-113.181500	150	-	10	-	2	10	-
el Cuarente	CUA	26.556133	-113.002800	150	12	2	6	11	2	11
Batequi	BAT	26.427150	-112.776733	150	6	-	5	6	-	5
Purisima	PUR	26.062650	-112.282083	150	-	10	5	-	10	6
el Rosario	ROS	25.698083	-112.074717	150	-	-	5	-	-	6
el Tambor	TAM	24.831932	-112.055708	150	6	-	-	6	-	-
Punta Pajaro	PPJ	24.753467	-112.043317	150	6	-	-	6	-	-
Salinas	SAL	24.582114	-111.787706	150	-	-	2	-	-	2
Gallinitas	GAL	24.557442	-111.735303	150	-	-	4	-	2	12

Table 3-S2   Listed is information for Gulf locations used in this study. Site names, 3-letter codes, GPS coordinates in decimal minutes, and sample sizes for each species are noted. Not all individuals were both genotyped for microsatellites and sequenced for mtDNA (see sample sizes). The range of *Fundulus parvipinnis* does not extend to the Gulf, and *Gillichthys mirabilis* is not found south of el Mojon.

Gulf of California collection sites								
Site location	code	latitude	longitude	color hue	Sample size: microsatellites		Sample size: mtDNA	
					G. mirabilis	*Q. y-cauda*	*G. mirabilis*	*Q. y-cauda*
Zacatecas	ZAC	24° 09.616'N	110° 25.594'W	180	-	7	-	9
Nopolo	NOP	25° 54.970'N	111° 20.978'W	180	-	5	-	9
Boca San Juanico	JNC	26° 23.638'N	111° 27.332'W	210	-	10	-	8
Arementa	ARE	26° 37.618'N	111° 48.879'W	210	-	6	-	6
Tombolo	TOM	26° 38.273'N	111° 49.902'W	210	-	4	-	-
Tondo	TON	26° 38.267'N	111° 50.159'W	210	-	2	-	2
Mulege	MUL	26° 54.219'N	111° 57.366'W	210	-	2	-	2
el Mojon	MOJ	27° 01.420'N	112° 00.624'W	210	20	1	19	-
San Marcos	MRC	27° 07.391'N	112° 03.284'W	210	-	6	-	6
la Palmita	PAL	28° 06.558'N	112° 48.678'W	240	1	-	1	-
San Francisquito	FRN	28° 25.520'N	112° 51.883'W	240	-	9	-	7
Animas	ANI	28° 47.855'N	113° 20.894'W	240	10	1	10	2
la Gringa	GRI	29° 02.375'N	113° 32.461'W	240	10	8	10	7
San Luis	LGZ	29° 48.260'N	114° 23.490'W	270	-	1	-	1
Santa Maria	MAR	30° 44.730'N	114° 42.010'W	270	2	-	2	-
Estero Percebu	PCB	30° 48.500'N	114° 42.040'W	270	9	-	8	-
Estero Primero	PRI	31° 11.540'N	114° 53.260'W	270	1	-	1	-
Estero Segundo	SGU	31° 15.355'N	114° 53.011'W	270	-	4	-	5
Estero Tercero	TRC	31° 17.354'N	114° 54.831'W	270	10	-	-	1
Bahía Adaír	ADR	31° 32.244'N	113° 58.910'W	270	-	1	-	6
NW of Cholla	NWC	31° 27.822'N	113° 37.898'W	270	10	6	10	-
Puerto Peñasco	MOI	31° 17.200'N	113° 15.170'W	270	2	-	2	-
Gated Estero	GE	30° 57.350'N	113° 05.566'W	270	6	8	6	6
Bahía Kino	KIN	28° 47.500'N	111° 54.540'W	270	20	1	20	1
el Ranchero	RCH	27° 58.206'N	110° 58.794'W	300	1	-	1	-
Yavaros	YAV	26° 40.700'N	109° 29.600'W	300	1	6	1	10
la Reforma	REF	25° 04.233'N	108° 03.533'W	300	1	12	1	6

Table 3-S3   Slope calculations are provided here for the 23 Gulf sites (5 calculations per site) used to train the slope parameter in the habitat modeling. The maximum observed slope (3.4 %, yellow) was used as a cutoff value in the models. Many slope values are greater than those observed for Pacific Coast sites (see Dolby *et al. in revision*); 13 of the 23 sites (32 calculations shown in orange or yellow) have values greater than the Pacific 1.3 % cutoff (mean slope = 1.0 %, median = 0.7 %, standard deviation = 0.9 % within the Gulf).

Site	Slope (%)	Run Length (km)	species present
Zacatecas	0.1%	2,000	
	0.1%	2,000	
	0.0%	3,100	Qyc
	0.1%	1,945	
	0.1%	1,700	
Nopolo	3.0%	100	
	3.0%	135	
	1.6%	122	Qyc
	1.6%	128	
	2.3%	215	
San Juanico	1.3%	400	
	0.4%	250	
	0.8%	260	Qyc
	1.9%	215	
	2.5%	162	
Arementa	2.3%	300	
	0.1%	4,700	
	0.1%	5,000	Qyc
	0.5%	3,000	
	0.7%	5,440	
el Mojon	1.5%	270	
	1.3%	235	Gmi
	1.8%	110	Qyc
	2.0%	100	
	2.2%	90	
San Marcos	3.3%	122	
	3.0%	66	
	0.7%	150	Qyc
	0.2%	550	
	1.1%	95	
la Palmita	2.4%	42	
	1.6%	62	
	1.5%	65	Gmi
	0.0%	12	
	1.4%	144	
San Francisquito	3.0%	100	
	1.4%	140	Qyc
	0.6%	310	
	2.7%	112	

Site	Slope (%)	Run Length (km)	species present
San Franciscuito	3.3%	90	
Animas	1.3%	240	
	0.6%	180	
	0.5%	210	Qyc Gmi
	0.4%	260	
	0.4%	280	
la Gringa	1.7%	117	
	0.7%	150	
	0.8%	120	Qyc Gmi
	1.3%	157	
	3.1%	130	
San Luis Gonzaga	1.2%	344	
	0.4%	460	
	0.5%	220	Qyc
	1.9%	160	
	2.4%	247	
Santa Maria	1.2%	250	
	0.5%	221	
	0.4%	230	Gmi
	0.4%	240	
	0.8%	130	
Estero Percebu	1.3%	75	
	1.0%	100	
	0.4%	450	Gmi
	0.3%	330	
	1.0%	100	
Estero Primero	0.7%	135	
	0.7%	450	
	0.7%	275	Gmi
	1.2%	170	
	1.2%	568	
Estero Segundo	0.3%	750	
	0.1%	1,300	
	0.5%	660	Qyc
	0.5%	740	
	1.0%	290	
Bahía Adair	1.5%	66	Qyc
	0.0%	129	

Site	Slope (%)	Run Length (km)	species present
Bahía Adair	0.0%	75	
	0.0%	165	
	0.0%	335	
NW of Cholla	2.1%	145	
	2.0%	50	
	0.9%	112	Qyc Gmi
	0.9%	116	
	0.7%	150	
Gated Estero	0.5%	219	
	0.4%	225	
	0.2%	811	Qyc Gmi
	0.3%	290	
	1.4%	143	
Puerto Peñasco	3.4%	58	
	3.0%	100	
	0.8%	1,200	Gmi
	0.5%	1,228	
	2.4%	125	
Bahía Kino	0.8%	130	
	0.4%	281	
	0.2%	490	Qyc Gmi
	0.6%	165	
	0.7%	150	
el Ranchero	1.3%	530	
	0.7%	540	
	0.3%	380	Gmi
	0.3%	331	
	0.5%	650	
Yavaros	0.6%	162	
	0.5%	381	
	0.3%	950	Qyc Gmi
	0.3%	800	
	1.2%	241	
la Reforma	0.6%	717	
	0.2%	1,200	
	0.1%	1,785	Qyc Gmi
	0.1%	1,600	
	0.8%	500	

Table 3-S4   P-values and corrected Akaike Information Criterion (AICc) scores are provided for selected Generalized Linear Model (GLM) refuge scenarios within the Pacific (top) and Gulf (bottom). Yellow rows and asterisks denote statistically significant models. Dagger denotes models run with False Discovery rate applied, and double dagger marks models performed with Firth Biased corrections to mitigate issues of low sample size and correlated variables.

Refugium Model Scenario: Gulf	Habitat	
	p-value	AICc
Reforma + eastern Gulf + Bahia Kino + Colorado Delta + Francisquito + Zacatecas*	0.010	18.0
Reforma + eastern Gulf + Bahia Kino + Colorado Delta + Francisquito + Zacatecas* † ‡	0.023	21.9
Reforma + eastern Gulf + Bahia Kino + Colorado Delta + Francisquito*	0.034	23.6
Reforma + eastern Gulf + Bahia Kino + Colorado Delta + Francisquito † ‡	0.094	25.6
Reforma + eastern Gulf + Bahia Kino + Colorado Delta + Zacatecas*	0.002	18.0
Reforma + eastern Gulf + Bahia Kino + Colorado Delta + Zacatecas* † ‡	0.008	20.8
all 9 Gulf sites	1.000	18.0
Reforma + eastern Gulf + Bahia Kino + Colorado Delta*	0.002	18.0
Reforma + eastern Gulf + Bahia Kino + Colorado Delta* † ‡	0.029	33.3
Reforma + Bahia Kino + Colorado Delta*	0.003	18.1
Reforma + Bahia Kino + Colorado Delta † ‡	0.119	35.6
Colorado Delta only*	0.043	18.0
Colorado Delta only † ‡	0.126	20.3
Reforma + Colorado Delta + Francisquito + Zacatecas*	0.004	19.2
Reforma + Colorado Delta + Francisquito + Zacatecas* † ‡	0.026	23.1
Refugium Model Scenario: Pacific	Habitat	
	p-value	AICc
Magdalena + Vizcaíno + N. Conception*	0.001	13.7
Magdalena + Vizcaíno + N. Conception* † ‡	0.038	20.7
Magdalena + Vizcaíno + N. Conception + San Francisco*	0.001	13.7
Magdalena + Vizcaíno + N. Conception + San Francisco † ‡	0.069	23.6
Vizcaíno + N. Conception*	0.042	18.2
Vizcaíno + N. Conception † ‡	0.195	21.3

Table 3-S5 Allele information for all microsatellite loci used in this study, including the total number of alleles observed per locus, the fragment size range, and the motif as predicted by MSATCOMMANDER. Loci and primer info are provided in Dolby *et al.* (*in revision*).

Locus – *F. parvipinnis*	fragment size range	# alleles	suggested motif	Locus – *G. mirabilis*	fragment size range	# alleles	suggested motif	Locus – *Q. y-cauda*	fragment size range	# alleles	suggested motif
FMA02	302-322	5	CCAT	GMA01	362-422	19	AAT	QMA01	142-223	21	CAGAGA
FMA03	227-311	22	CTAT	GMA02	406-436	10	ACT	QMA03	225-289	16	AGC
FMA04	312-328	5	TTTA	GMA03	255-285	10	AAC	QMA04	212-254	10	GTTT
FMA05	206-230	6	GGAT	GMA04	192-216	9	ACT	QMA05	199-257	17	CTTT
FMA07	220-256	10	GATT	GMA06	310-402	14	ACT	QMA06	375-489	20	CAA
FMA08	214-376	35	CCAT	GMA08	118-193	21	AAT	QMA07	107-225	32	TAG
FMA09	196-320	27	TCCA	GMA11	354-366	4	AATT	QMA08	164-264	22	TCAA
FMA10	213-265	14	CCAT	GMA13	204-228	8	AAAC	QMA09	118-202	22	TACA
FMA13	255-322	14	TGGA	GMA14	473-494	4	AAT	QMA10	100-212	26	TGGTCC
FMA14	234-246	4	CATC	GMA16	146-198	14	AACT	QMA13	210-266	12	CAA
FMA15	146-306	12	TCAA	GMA17	124-136	5	AGC	QMA17	120-228	21	CAA
FMA16	291-319	7	CCAT	GMA20	157-190	8	AAT	QMA24	144-198	23	CA
FMA18	215-235	6	TTTA	GMA23	123-147	9	ATC	QMA25	233-296	20	CAT
FMA19	396-412	2	CTT	GMA24	114-132	8	AGC	QMA26	226-262	13	AC
FMA21	191-218	10	AGT	GMA31	144-176	8	ACTC	QMA27	337-448	16	CAA
FMA23	256-262	3	GCC	GMA36	139-159	6	AAAC	QMA28	147-174	8	GAA
FMA24	237-240	2	GAG					QMA30	290-308	9	TA
FMA25	179-188	4	ATT								
FMA26	179-282	2	GAT								
FMA29	223-263	13	TAA								

Table 3-S6   Listed in this table are p-values generated by GENEPOP for Fisher's exact test (G) for population differentiation using genotypes for A) *Fundulus parvipinnis,* B) *Quietula y-cauda*, and C) *Gillichthys mirabilis*. Analyses used 10,000 dememorization steps, 20 batches, and 5,000 iterations per batch for each taxon. Coloring of cells indicate: significant ($\alpha < 0.05$, yellow), highly significant (chi square approached infinity, orange), and populations that were sample limited (no data, dark grey). Populations are listed by 3-letter codes in coastal order (see Table 3-S1 and 3-S2), where light pink are Pacific coast sites north of Punta Eugenia, dark pink are Pacific coast sites south of Punta Eugenia, and Gulf sites are teal.

P values for Fisher's exact test (G) for population differentiation — *Fundulus parvipinnis*													
A	**CAR**	**ALA**	**ANB**	**PSQ**	**BAN**	**QTN**	**MAN**	**GNG**	**OJO**	**CUA**	**BAT**	**PPJ**	**TAM**
MOR	HS	HS	HS	HS	HS	HS	HS	HS	HS	HS	HS	HS	HS
CAR		HS	0.00	0.00	HS	HS	HS	HS	HS	HS	HS	HS	HS
ALA			0.02	0.00	HS	HS	HS	0.00	HS	HS	HS	HS	HS
ANB				0.22	HS	HS	HS	0.00	HS	HS	HS	HS	HS
PSQ					0.00	HS	HS	0.00	HS	HS	HS	HS	HS
BAN						0.00	HS	HS	0.00	HS	HS	HS	HS
QTN							0.00	0.00	0.02	HS	HS	HS	HS
MAN								0.25	0.67	HS	HS	HS	HS
GNG									0.46	HS	HS	HS	HS
OJO										HS	HS	HS	HS
CUA											0.94	0.01	0.17
BAT												0.00	0.05
PPJ													0.30

P values for Fisher's exact test (G) for population differentiation — *Quietula y-cauda*

B	GOL	MDC	ALA	CAT	MRG	PSQ	MSN	QTN	MAN	GNG	BOC	CUA	BAT	PUR	ROS	SAL	GAL
MOR	0.00	0.27	0.00	0.50	0.00	0.00	0.45	0.00	0.00	0.00	0.00	0.00	0.00	0.00	0.00	0.00	0.00
GOL		0.46	0.00	0.35	0.00	0.00	0.86	0.00	0.00	0.00	0.00	0.00	0.00	0.00	0.00	0.00	0.00
MDC			0.99	0.98	0.92	0.92	0.95	0.83	0.98	0.92	0.78	0.33	0.93	0.49	0.11	0.96	0.60
ALA				0.95	0.73	0.08	0.97	0.00	0.17	0.17	0.05	0.00	0.05	0.01	0.00	0.34	0.01
CAT					0.96	0.98	NA	0.89	0.95	1.00	0.93	0.63	0.99	0.90	0.51	0.98	0.68
MRG						0.97	0.99	0.12	0.24	0.54	0.07	0.01	0.08	0.09	0.09	0.66	0.17
PSQ							0.97	0.63	0.32	0.72	0.37	0.10	0.40	0.03	0.06	0.88	0.60
MSN								0.98	0.99	0.90	0.99	0.98	0.99	0.96	0.82	0.98	0.99
QTN									0.05	0.33	0.00	0.01	0.01	0.01	0.00	0.00	0.18
MAN										0.95	0.50	0.16	0.64	0.07	0.00	0.59	0.22
GNG											0.55	0.34	0.91	0.48	0.12	0.94	0.32
BOC												0.98	1.00	0.53	0.51	1.00	0.86
CUA													0.94	0.54	0.39	0.69	0.95
BAT														1.00	0.89	1.00	0.95
PUR															0.30	0.76	0.59
ROS																1.00	0.84
SAL																	1.00
GAL																	

P values for Fisher's exact test (G) for population differentiation — *Quietula y-cauda* —continued

Qyc	ZAC	NOP	JNC	ARE	TOM	TON	MUL	MOJ	MRC	FRN	ANI	GRI	LGZ	SGU	TRC	ADR	GE	KIN	YAV	REF
MOR	0.00	0.00	HS	0.00	0.00	0.00	0.00	0.01	0.00	0.00	0.01	0.00	0.01	0.00	0.02	0.00	0.00	0.02	0.00	HS
GOL	0.00	0.00	HS	0.00	0.00	0.00	0.00	0.00	0.00	Highl	0.00	0.00	0.01	0.00	0.00	HS	0.00	0.01	0.00	HS
MDC	0.00	0.02	0.00	0.00	0.26	0.41	0.47	0.35	0.00	0.00	0.35	0.00	0.36	0.06	0.35	0.00	0.00	0.50	0.01	0.00
ALA	0.00	0.00	0.00	0.00	0.00	0.00	0.05	0.12	0.00	0.00	0.12	0.00	0.13	0.00	0.31	0.00	0.00	0.36	0.00	0.00
CAT	0.31	0.37	0.06	0.54	0.78	0.36	1.00	NA	0.18	0.05	NA	0.07	NA	0.51	NA	0.12	0.17	NA	0.45	0.06
MRG	0.00	0.00	0.00	0.00	0.00	0.00	0.03	0.06	0.00	0.00	0.14	0.00	0.09	0.00	0.09	0.00	0.00	0.15	0.00	0.00
PSQ	0.00	0.00	0.00	0.00	0.00	0.00	0.01	0.10	0.00	0.00	0.19	0.00	0.12	0.00	0.27	0.00	0.00	0.30	0.00	0.00
MSN	0.30	0.24	0.05	0.35	0.60	0.82	1.00	NA	0.31	0.11	NA	0.12	NA	0.38	NA	0.10	0.07	NA	0.38	0.08
QTN	0.00	0.00	HS	0.00	0.00	0.00	0.00	0.01	0.00	0.00	0.05	0.00	0.02	0.00	0.04	0.00	0.00	0.12	0.00	HS
MAN	0.00	0.00	0.00	0.00	0.00	0.08	0.09	0.25	0.00	0.00	0.31	0.00	0.25	0.00	0.38	0.00	0.00	0.49	0.00	0.00
GNG	0.02	0.05	0.00	0.02	0.49	0.53	0.36	0.36	0.01	0.00	0.36	0.00	0.36	0.10	0.36	0.00	0.00	0.55	0.02	0.00
BOC	0.00	0.00	0.00	0.00	0.00	0.00	0.00	0.11	0.00	0.00	0.32	0.00	0.09	0.00	0.19	0.00	0.00	0.19	0.00	HS
CUA	0.00	0.00	0.00	0.00	0.00	0.00	0.00	0.02	0.00	0.00	0.09	0.00	0.03	0.00	0.15	0.00	0.00	0.14	0.00	HS
BAT	0.00	0.00	0.00	0.00	0.02	0.00	0.02	0.04	0.00	0.00	0.17	0.00	0.06	0.00	0.16	0.00	0.00	0.16	0.00	0.00
PUR	0.00	0.00	0.00	0.00	0.00	0.00	0.01	0.03	0.00	0.00	0.14	0.00	0.05	0.00	0.14	0.00	0.00	0.22	0.00	0.00
ROS	0.00	0.00	0.00	0.00	0.00	0.00	0.01	0.06	0.00	0.00	0.08	0.00	0.06	0.00	0.18	0.00	0.00	0.13	0.00	0.00
SAL	0.05	0.15	0.00	0.09	0.60	0.95	0.85	0.58	0.02	0.00	0.58	0.00	0.36	0.17	0.33	0.00	0.00	0.58	0.05	0.00
GAL	0.00	0.00	0.00	0.00	0.00	0.00	0.01	0.11	0.00	0.00	0.08	0.00	0.08	0.00	0.36	0.00	0.00	0.19	0.00	0.00
ZAC		0.98	0.06	0.46	0.46	0.59	0.76	0.23	0.00	0.00	0.27	0.00	0.48	0.00	0.30	0.00	0.00	0.14	0.00	0.00
NOP			0.64	0.95	0.76	0.90	0.56	0.65	0.00	0.00	0.47	0.00	0.62	0.01	0.37	0.00	0.00	0.33	0.00	0.00
JNC				0.19	0.54	0.59	0.18	0.59	0.00	0.00	0.33	0.00	0.29	0.00	0.15	0.00	0.00	0.13	0.00	HS
ARE					0.75	0.99	0.62	0.38	0.00	0.00	0.38	0.00	0.22	0.00	0.29	0.00	0.00	0.28	0.00	HS
TOM						0.99	1.00	0.99	0.02	0.04	0.92	0.02	0.83	0.22	0.83	0.01	0.00	0.59	0.04	0.00
TON							0.99	0.90	0.04	0.04	0.70	0.03	0.36	0.14	0.35	0.03	0.01	0.63	0.03	0.00
MUL								1.00	0.12	0.01	1.00	0.01	NA	0.55	1.00	0.17	0.22	1.00	0.14	0.01
MOJ									0.80	0.57	NA	0.62	NA	0.79	NA	0.93	0.98	NA	0.66	0.31
MRC										0.00	0.31	0.00	0.12	0.02	0.54	0.19	0.16	0.44	0.04	0.00
FRN											0.52	0.04	0.89	0.00	0.09	0.00	0.00	0.11	0.00	HS
ANI												0.52	NA	0.78	NA	0.77	0.40	NA	0.63	0.59
GRI													0.70	0.00	0.14	0.00	0.00	0.29	0.00	0.00
LGZ														0.28	NA	0.41	0.79	NA	0.79	0.45
SGU															0.91	0.52	0.11	0.73	0.25	0.02
TRC																0.70	0.41	NA	0.47	0.21
ADR																	0.54	0.62	0.27	0.02
GE																		0.95	0.28	0.16
KIN																			0.99	0.82
YAV																				0.50

P values for Fisher's exact test (G) for population differentiation — *Gillichthys mirabilis*

C	MOR	DEV	USB	MGU	BNA	HID	FAM	BAN	QTN	MAN	GNG	BOC	IGN	CUA	PUR	MOJ	PAL	ANI	GRI	MAR	PCB	PRI	NWC	ADR	MOI	GE	KIN	RCH	YAV	REF
ALB	0.00	0.00	0.00	0.06	0.00	0.00	0.00	0.02	HS	0.02	0.00	0.26	0.00	0.01	HS	HS	0.00	HS	HS	0.00	HS	0.00	HS	HS	0.00	0.00	HS	0.02	0.01	0.00
MOR		0.01	0.00	0.03	0.00	HS	0.00	0.00	HS	0.00	0.00	0.02	0.00	0.00	HS	HS	0.00	HS	HS	0.00	HS	0.00	HS	HS	0.00	0.00	HS	0.01	0.00	0.00
DEV			0.03	0.06	0.16	0.00	0.13	0.05	0.00	0.00	0.00	0.03	HS	0.01	0.00	HS	0.01	HS	HS	0.00	HS	0.00	HS	HS	0.00	0.00	HS	0.02	0.00	0.00
USB				0.01	0.04	0.00	0.00	HS	0.00	0.00	0.00	0.00	HS	0.00	HS	HS	0.00	HS	HS	0.00	HS	0.00	HS	HS	0.00	0.00	HS	0.01	0.01	0.00
MGU					0.81	0.00	0.48	0.32	0.00	0.87	0.09	0.65	0.05	0.89	0.15	0.00	0.23	0.00	0.00	0.01	0.00	0.22	0.00	0.00	0.04	0.00	0.00	0.49	0.41	0.28
BNA						0.00	0.00	0.07	0.00	0.12	0.00	0.01	0.00	0.04	0.00	HS	0.00	HS	HS	0.00	HS	0.00	HS	HS	0.00	0.00	HS	0.02	0.01	0.00
HID							HS	HS	HS	0.00	HS	0.00	HS	0.00	HS	HS	0.00	HS	HS	0.00	HS	0.00	HS	HS	0.00	HS	HS	0.00	0.00	0.00
FAM								0.04	0.00	0.01	0.00	0.27	0.00	0.41	0.00	HS	0.00	HS	HS	0.00	HS	0.00	HS	HS	0.00	HS	HS	0.02	0.00	0.00
BAN									0.00	0.96	0.42	0.98	0.07	0.23	0.00	HS	0.01	HS	HS	0.00	HS	0.00	HS	HS	0.00	HS	HS	0.09	0.01	0.01
QTN										0.08	0.00	0.09	0.00	0.02	0.00	HS	0.00	HS	HS	0.00	HS	0.00	HS	HS	0.00	HS	HS	0.05	0.01	0.00
MAN											0.87	1.00	0.46	0.83	0.44	0.00	0.30	0.00	0.00	0.00	0.00	0.25	0.00	0.00	0.01	0.00	0.00	0.58	0.60	0.17
GNG												0.87	0.81	0.73	0.89	HS	0.01	HS	HS	0.00	HS	0.00	HS	HS	0.00	0.00	HS	0.06	0.04	0.01
BOC													1.00	1.00	1.00	0.00	0.69	0.01	0.00	0.81	0.01	0.49	0.01	0.00	0.89	0.23	0.00	0.84	0.51	0.66
IGN														1.00	0.66	HS	0.01	HS	HS	0.00	HS	0.00	HS	HS	0.00	HS	HS	0.01	0.03	0.00
CUA															0.77	0.00	0.78	0.00	0.01	0.48	0.00	0.62	0.01	0.00	0.50	0.06	0.00	0.51	0.50	0.35
PUR																HS	0.02	HS	HS	0.00	0.00	0.02	HS	0.00	0.00	0.00	HS	0.05	0.00	0.00
MOJ																	0.44	0.00	HS	0.00	0.00	0.02	HS	HS	0.00	0.00	HS	0.02	0.40	0.17
PAL																		0.94	0.99	0.88	0.99	NA	0.94	0.96	0.98	1.00	0.50	NA	NA	NA
ANI																			0.56	0.23	0.00	0.25	0.00	HS	0.03	0.00	HS	0.99	0.83	1.00
GRI																				0.48	0.09	0.45	0.00	0.00	0.33	0.21	0.00	0.99	0.98	1.00
MAR																					0.99	0.99	0.50	0.84	0.97	0.51	0.16	0.98	1.00	0.99
PCB																						0.96	0.02	0.04	0.21	0.41	0.00	0.79	0.98	0.99
PRI																							0.80	0.39	0.93	0.74	0.11	NA	NA	NA
NWC																								0.02	0.45	0.98	0.01	0.77	0.80	0.97
ADR																									0.90	0.65	0.00	0.58	0.97	0.96
MOI																										0.89	0.67	0.82	0.93	1.00
GE																											0.18	0.89	0.44	0.99
KIN																												0.75	0.42	0.96
RCH																													NA	NA
YAV																														NA

Table 3-S7 Fixation indices (F_{ST}) for pairwise population comparisons for A) *Fundulus parvipinnis,* B) *Quietula y-cauda*, and C) *Gillichthys mirabilis*. Cell coloring schemes denote: high gene flow (0.0–0.05, dark green), moderate gene flow (0.05–0.25, light green), reduced gene flow (0.25–0.5, orange), and extremely limited gene flow (> 0.5, red). Populations are listed by 3-letter codes in coastal order (see Table 3-S1 and 3-S2), where light pink are Pacific coast sites north of Punta Eugenia, dark pink are Pacific coast sites south of Punta Eugenia, and Gulf sites are teal.

Pairwise Populuation Fst— *Fundulus parvipinnis*													
A	**MOR**	**CAR**	**ALA**	**ANB**	**PSQ**	**BAN**	**QTN**	**MAN**	**GNG**	**OJO**	**CUA**	**BAT**	**PPJ**
CAR	0.12												
ALA	0.19	0.12											
ANB	0.14	0.06	0.04										
PSQ	0.19	0.10	0.08	0.03									
BAN	0.21	0.13	0.10	0.11	0.09								
QTN	0.36	0.30	0.24	0.26	0.26	0.11							
MAN	0.28	0.20	0.16	0.15	0.17	0.10	0.09						
GNG	0.24	0.17	0.13	0.10	0.13	0.08	0.12	0.02					
OJO	0.26	0.18	0.14	0.13	0.13	0.05	0.08	0.00	0.02				
CUA	0.44	0.40	0.38	0.35	0.37	0.35	0.34	0.32	0.31	0.30			
BAT	0.45	0.41	0.38	0.35	0.37	0.35	0.36	0.32	0.32	0.30	0.00		
PPJ	0.49	0.45	0.41	0.39	0.41	0.39	0.37	0.35	0.35	0.33	0.02	0.04	
TAM	0.49	0.45	0.41	0.39	0.42	0.38	0.38	0.37	0.36	0.35	0.01	0.03	0.01

Pairwise Fst values for *Quietula y-cauda*

B	MOR	GOL	MDC	ALA	CAT	MRG	PSQ	MSN	QTN	MAN	GNG	BOC	CUA	BAT	PUR	ROS	SAL	GAL	ZAC	NOP	JNC	ARE	TOM	TON	MUL	MOJ	MRC	FRN	ANI	GRI	LGZ	SGU	TRC	ADR	GE	KIN	YAV
GOL	0.28																																				
MDC	0.21	0.04																																			
ALA	0.24	0.12	0.07																																		
CAT	0.26	0.27	0.03	0.09																																	
MRG	0.25	0.10	0.02	0.02	0.10																																
PSQ	0.19	0.12	0.01	0.09	0.08	0.00																															
MSN	0.29	0.09	0.00	0.00	0.65	0.00	0.01																														
QTN	0.18	0.11	0.05	0.07	0.12	0.04	0.00	0.00																													
MAN	0.24	0.19	0.07	0.04	0.05	0.04	0.07	0.03	0.02																												
GNG	0.31	0.21	0.12	0.05	0.20	0.01	0.04	0.06	0.00	-0.03																											
BOC	0.25	0.19	0.11	0.09	0.11	0.09	0.05	0.06	0.08	0.06	0.06																										
CUA	0.25	0.20	0.12	0.13	0.18	0.11	0.06	0.05	0.08	0.10	0.07	0.00																									
BAT	0.24	0.18	0.08	0.10	0.07	0.10	0.06	0.00	0.07	0.20	0.02	0.00	0.00																								
PUR	0.35	0.23	0.16	0.12	0.16	0.12	0.12	0.07	0.10	0.06	0.14	0.06	0.01	0.08																							
ROS	0.36	0.31	0.22	0.20	0.27	0.15	0.11	0.14	0.17	0.12	0.07	0.04	0.06	0.00	0.09																						
SAL	0.33	0.31	0.21	0.17	0.04	0.08	0.01	0.04	0.12	0.15	0.11	0.00	0.06	0.00	0.09	0.00																					
GAL	0.30	0.23	0.18	0.17	0.27	0.12	0.06	0.10	0.11	0.15	0.11	0.01	0.01	0.07	0.07	0.00	0.00																				
ZAC	0.34	0.33	0.23	0.18	0.19	0.20	0.20	0.15	0.18	0.17	0.15	0.18	0.18	0.15	0.20	0.15	0.17	0.20																			
NOP	0.40	0.38	0.28	0.22	0.23	0.24	0.24	0.18	0.21	0.20	0.17	0.19	0.19	0.17	0.21	0.17	0.22	0.20	0.00																		
JNC	0.37	0.33	0.27	0.21	0.28	0.21	0.23	0.20	0.20	0.19	0.12	0.20	0.21	0.16	0.20	0.19	0.21	0.20	0.02	0.00																	
ARE	0.39	0.35	0.26	0.20	0.22	0.21	0.21	0.18	0.19	0.17	0.16	0.17	0.18	0.16	0.20	0.16	0.19	0.21	0.01	0.00	0.00																
TOM	0.37	0.35	0.22	0.18	0.16	0.20	0.18	0.11	0.18	0.15	0.12	0.15	0.13	0.14	0.20	0.15	0.16	0.20	0.01	0.00	0.00	0.00															
TON	0.52	0.45	0.37	0.26	0.24	0.30	0.24	0.23	0.24	0.21	0.21	0.22	0.22	0.20	0.28	0.21	0.27	0.27	0.02	0.00	0.00	0.00	0.00														
MUL	0.48	0.40	0.32	0.20	0.23	0.22	0.21	0.09	0.21	0.18	0.19	0.21	0.22	0.20	0.27	0.18	0.24	0.24	0.01	0.02	0.04	0.01	0.05	0.00													
MOJ	0.68	0.61	0.57	0.39	0.86	0.41	0.43	0.76	0.36	0.37	0.48	0.36	0.41	0.36	0.44	0.36	0.45	0.45	0.12	0.14	0.12	0.15	0.12	0.16	0.00												
MRC	0.46	0.43	0.36	0.29	0.34	0.32	0.33	0.33	0.30	0.30	0.29	0.29	0.28	0.29	0.32	0.29	0.33	0.33	0.13	0.12	0.12	0.17	0.15	0.21	0.10	0.00											
FRN	0.42	0.42	0.34	0.29	0.41	0.31	0.30	0.30	0.25	0.27	0.24	0.28	0.28	0.27	0.32	0.27	0.32	0.32	0.15	0.14	0.15	0.17	0.18	0.24	0.17	0.25	0.15										
ANI	0.65	0.52	0.53	0.81	0.74	0.26	0.32	0.74	0.29	0.41	0.26	0.31	0.26	0.41	0.33	0.40	0.40	0.15	0.16	0.18	0.16	0.17	0.07	0.09	0.27	0.19	0.61	0.25	0.15								
GRI	0.43	0.41	0.33	0.27	0.37	0.30	0.30	0.25	0.26	0.24	0.27	0.27	0.29	0.26	0.32	0.27	0.32	0.24	0.15	0.14	0.13	0.16	0.07	0.09	0.16	0.15	0.17	0.04	0.08	0.08							
LGZ	0.71	0.59	0.60	0.88	0.81	0.38	0.41	0.81	0.30	0.41	0.24	0.30	0.22	0.42	0.27	0.42	0.46	0.16	0.22	0.23	0.25	0.14	0.13	0.25	0.36	0.31	0.63	0.05	0.71	0.13	0.13						
SGU	0.44	0.39	0.29	0.22	0.21	0.24	0.22	0.19	0.25	0.20	0.21	0.22	0.23	0.23	0.23	0.15	0.23	0.23	0.07	0.07	0.11	0.10	0.05	0.10	0.23	0.10	0.08	0.15	0.10	0.10	0.20						
TRC	0.65	0.54	0.49	0.29	0.86	0.36	0.36	0.78	0.30	0.35	0.47	0.31	0.36	0.26	0.35	0.26	0.36	0.26	0.14	0.14	0.24	0.16	0.12	0.09	0.30	0.26	0.71	0.21	0.29	0.67	0.25	0.75					
ADR	0.41	0.38	0.31	0.24	0.26	0.27	0.26	0.20	0.27	0.26	0.22	0.23	0.27	0.24	0.26	0.21	0.26	0.21	0.10	0.11	0.11	0.15	0.07	0.14	0.05	0.01	0.05	0.00	0.10	0.12	0.25	0.04	0.11				
GE	0.40	0.36	0.28	0.22	0.23	0.25	0.24	0.20	0.25	0.24	0.21	0.22	0.26	0.22	0.24	0.18	0.24	0.21	0.10	0.11	0.11	0.13	0.07	0.15	0.05	0.01	0.05	0.13	0.08	0.12	0.06	0.04	0.11	0.00			
KIN	0.60	0.44	0.39	0.23	0.78	0.26	0.29	0.70	0.26	0.27	0.37	0.25	0.29	0.31	0.25	0.23	0.27	0.23	0.13	0.15	0.19	0.18	0.09	0.19	0.11	0.64	0.19	0.25	0.57	0.12	0.68	0.04	0.69	0.00	0.00		
YAV	0.42	0.39	0.32	0.24	0.29	0.27	0.27	0.28	0.26	0.26	0.24	0.24	0.27	0.23	0.22	0.22	0.27	0.24	0.14	0.12	0.14	0.12	0.09	0.17	0.16	0.11	0.11	0.12	0.17	0.12	0.09	0.12	0.19	0.19	0.00	0.07	
REF	0.41	0.40	0.35	0.28	0.35	0.29	0.29	0.27	0.28	0.28	0.26	0.26	0.29	0.27	0.28	0.25	0.25	0.29	0.17	0.18	0.16	0.21	0.14	0.22	0.16	0.20	0.12	0.18	0.08	0.12	0.09	0.06	0.20	0.05	0.01	0.05	0.03

Pairwise Fst values for *Gillichthys mirabilis*

C	ALB	MOR	DEV	USB	MGU	BNA	HID	FAM	BAN	QTN	MAN	GNG	BOC	IGN	CUA	PUR	MOJ	PAL	ANI	GRI	MAR	PCB	PRI	NWC	ADR	MOI	GE	KIN	RCH	YAV	REF
ALB																															
MOR	0.13																														
DEV	0.08	0.09																													
USB	0.11	0.12	0.00																												
MGU	0.06	0.12	0.05	0.06																											
BNA	0.10	0.12	0.03	0.06	0.04																										
HID	0.20	0.32	0.25	0.31	0.32	0.26																									
FAM	0.08	0.16	0.04	0.08	0.04	0.06	0.24																								
BAN	0.09	0.09	0.04	0.06	0.05	0.05	0.30	0.06																							
QTN	0.18	0.19	0.14	0.11	0.13	0.15	0.35	0.15	0.06																						
MAN	0.08	0.17	0.07	0.10	0.05	0.08	0.34	0.12	0.00	0.05																					
GNG	0.11	0.13	0.11	0.12	0.11	0.14	0.27	0.09	0.03	0.07	0.00																				
BOC	0.08	0.21	0.10	0.14	0.10	0.17	0.44	0.10	0.00	0.09	0.00	0.00																			
IGN	0.12	0.16	0.13	0.16	0.09	0.14	0.25	0.08	0.04	0.11	0.02	0.00	0.04																		
CUA	0.21	0.30	0.20	0.25	0.11	0.22	0.44	0.13	0.11	0.18	0.09	0.03	0.00	0.02																	
PUR	0.18	0.19	0.14	0.18	0.16	0.20	0.31	0.18	0.08	0.12	0.05	0.00	0.00	0.02	0.07																
MOJ	0.29	0.33	0.29	0.30	0.23	0.29	0.38	0.25	0.24	0.25	0.22	0.23	0.17	0.24	0.18	0.25															
PAL	0.54	0.67	0.56	0.59	0.52	0.58	0.76	0.57	0.48	0.49	0.44	0.43	0.38	0.45	0.52	0.48	0.11														
ANI	0.33	0.39	0.35	0.36	0.27	0.36	0.45	0.37	0.30	0.28	0.22	0.26	0.17	0.29	0.21	0.28	0.07	0.03													
GRI	0.32	0.39	0.34	0.36	0.26	0.35	0.44	0.38	0.29	0.27	0.21	0.26	0.17	0.28	0.20	0.27	0.08	0.04	0.00												
MAR	0.49	0.57	0.51	0.52	0.40	0.50	0.70	0.55	0.43	0.42	0.35	0.39	0.30	0.42	0.35	0.43	0.11	0.15	0.00	0.05											
PCB	0.32	0.38	0.34	0.35	0.24	0.33	0.44	0.35	0.28	0.28	0.20	0.26	0.17	0.28	0.19	0.28	0.05	0.05	0.03	0.01	0.00										
PRI	0.56	0.66	0.57	0.60	0.49	0.60	0.78	0.59	0.52	0.51	0.45	0.46	0.41	0.48	0.47	0.49	0.12	0.54	0.12	0.06	0.00	0.00									
NWC	0.31	0.37	0.34	0.35	0.26	0.34	0.44	0.36	0.28	0.28	0.22	0.25	0.19	0.26	0.18	0.27	0.10	0.06	0.08	0.04	0.03	0.03	0.05								
ADR	0.32	0.37	0.33	0.34	0.25	0.33	0.44	0.37	0.29	0.28	0.22	0.27	0.20	0.29	0.22	0.29	0.11	0.08	0.08	0.06	0.00	0.02	0.03	0.00							
MOI	0.46	0.54	0.46	0.48	0.37	0.48	0.67	0.52	0.41	0.41	0.35	0.38	0.31	0.42	0.37	0.42	0.16	0.16	0.13	0.07	0.08	0.07	0.06	0.05	0.00						
GE	0.32	0.40	0.34	0.35	0.24	0.34	0.49	0.38	0.28	0.28	0.22	0.26	0.18	0.30	0.22	0.30	0.09	0.04	0.04	0.02	0.02	0.00	0.05	0.00	0.00	0.01					
KIN	0.29	0.35	0.31	0.32	0.25	0.31	0.39	0.34	0.27	0.26	0.20	0.25	0.19	0.27	0.22	0.26	0.12	0.11	0.06	0.04	0.07	0.03	0.07	0.03	0.03	0.04	0.02				
RCH	0.45	0.58	0.49	0.51	0.44	0.50	0.70	0.51	0.39	0.33	0.34	0.32	0.30	0.39	0.47	0.39	0.16	0.71	0.01	0.00	0.08	0.06	0.60	0.07	0.09	0.17	0.01	0.04			
YAV	0.42	0.58	0.44	0.45	0.37	0.44	0.68	0.46	0.36	0.34	0.28	0.31	0.25	0.34	0.42	0.37	0.06	0.62	0.03	0.00	0.00	0.00	0.49	0.06	0.00	0.11	0.06	0.03	0.53		
REF	0.51	0.65	0.53	0.55	0.49	0.56	0.76	0.58	0.44	0.43	0.39	0.38	0.33	0.43	0.46	0.45	0.09	0.60	0.00	0.00	0.00	0.00	0.52	0.00	0.00	0.06	0.00	0.00	0.45	0.43	

Table 3-S8   Basic diversity indices including for A) *Fundulus parvipinnis*, B) *Quietula y-cauda*, C) *Gillicthys mibrabilis*. Scores for mean genic diversity, observed heterozygosity (H_O), expected heterozygosity (H_E), sample size (number of alleles within a population), tests for heterozygote excess and deficit, and F-statistics for within individuals (1-Qintra), between individuals (1-Qinter), and inbreeding coefficient (F_{IS}) are provided. Cells highlighted in yellow reflect a difference in H_O and H_E greater than 0.2, significance for excess heterozygotes ($p < 0.05$), or a high F_{IS} score (≥ 0.15).

A	mean genic diversity	Ho	He	sample size	Test for heterozygote deficit	Test for heterozygote excess	1-Qintra	1-Qinter	Fis
				F. parvipinnis - Pacific Sites					
MOR	0.40	0.54	0.54	24	0.39	0.61	0.41	0.39	-0.04
CAR	0.44	0.62	0.62	28	0.38	0.62	0.44	0.44	0.00
ALA	0.48	0.63	0.64	12	0.52	0.48	0.48	0.47	-0.02
ANB	0.51	0.67	0.72	10	0.07	0.93	0.47	0.51	0.08
PSQ	0.52	0.57	0.70	12	0.43	0.57	0.46	0.46	0.00
BAN	0.50	0.59	0.63	24	0.07	0.93	0.48	0.50	0.04
QTN	0.45	0.74	0.69	12	0.97	0.03	0.48	0.44	-0.09
MAN	0.51	0.54	0.61	12	0.01	0.99	0.46	0.52	0.12
GNG	0.53	0.74	0.70	12	0.88	0.12	0.56	0.52	-0.07
OJO	0.53	0.65	0.63	12	0.79	0.21	0.55	0.53	-0.04
CUA	0.62	0.60	0.69	24	0.00	1.00	0.54	0.62	0.12
BAT	0.63	0.62	0.70	12	0.01	0.99	0.56	0.64	0.12
TAM	0.56	0.51	0.66	12	0.00	1.00	0.44	0.56	0.22
PPJ	0.57	0.60	0.72	12	0.00	1.00	0.50	0.57	0.12

B	mean genic diversity	Ho	He	sample size	heterozygote deficit	heterozygote excess	1-Qintra	1-Qinter	Fis
	Q. y-cauda - Pacific Sites								
MOR	0.33	0.53	0.51	10	0.64	0.36	0.34	0.33	-0.04
GOL	0.40	0.51	0.53	14	0.31	0.68	0.39	0.41	0.05
MDC	0.39	0.67	0.74	4	0.26	0.91	0.35	0.41	0.14
ALA	0.63	0.53	0.67	10	0.02	0.97	0.54	0.63	0.15
CAT	0.12	1.00	1.00	2	NA	NA	NA	NA	NA
MRG	0.58	0.44	0.61	10	0.00	1.00	0.42	0.58	0.28
PSQ	0.59	0.55	0.67	8	0.13	0.87	0.51	0.57	0.11
MSN	0.41	1.00	1.00	2	NA	NA	NA	NA	NA
QTN	0.62	0.51	0.66	16	0.00	1.00	0.49	0.62	0.22
MAN	0.65	0.50	0.69	8	0.00	1.00	0.51	0.65	0.22
GNG	0.65	0.68	0.79	4	0.52	0.70	0.61	0.63	0.03
BOC	0.64	0.52	0.64	12	0.02	0.98	0.57	0.65	0.13
CUA	0.61	0.51	0.61	12	0.12	0.88	0.55	0.61	0.09
BAT	0.66	0.42	0.66	10	0.00	1.00	0.48	0.65	0.26
PUR	0.63	0.49	0.63	10	0.00	1.00	0.52	0.62	0.17
ROS	0.55	0.52	0.62	10	0.03	0.96	0.47	0.55	0.14
SAL	0.52	0.58	0.68	4	0.16	0.92	0.47	0.59	0.21
GAL	0.58	0.52	0.61	8	0.24	0.76	0.52	0.55	0.07
	Q. y-cauda - Gulf Sites								
ZAC	0.80	0.57	0.80	14	0.00	1.00	0.60	0.82	0.26
NOP	0.78	0.62	0.78	10	0.00	1.00	0.66	0.80	0.17
JNC	0.79	0.56	0.79	22	0.00	1.00	0.61	0.78	0.22
ARE	0.77	0.55	0.77	12	0.00	1.00	0.57	0.85	0.32
TOM	0.78	0.48	0.83	8	0.00	1.00	0.57	0.93	0.38
TON	0.70	0.50	0.74	4	0.01	1.00	0.50	0.80	0.37
MUL	0.78	0.47	0.78	4	0.01	1.00	0.57	0.93	0.38
MOJ	0.47	1.00	1.00	2	NA	NA	NA	NA	NA
MRC	0.65	0.42	0.69	12	0.00	1.00	0.48	0.68	0.30
FRN	0.60	0.41	0.60	18	0.00	1.00	0.53	0.70	0.24
ANI	0.41	1.00	1.00	2	NA	NA	NA	NA	NA
GRI	0.64	0.44	0.69	14	0.00	1.00	0.56	0.76	0.27
LGZ	0.29	1.00	1.00	2	NA	NA	NA	NA	NA
SGU	0.70	0.58	0.79	8	0.01	0.99	0.66	0.83	0.20
TRC	0.35	1.00	1.00	2	NA	NA	NA	NA	NA
ADR	0.71	0.52	0.81	12	0.00	1.00	0.55	0.77	0.29
GE	0.70	0.53	0.79	16	0.00	1.00	0.61	0.80	0.24
KIN	0.47	1.00	1.00	2	NA	NA	NA	NA	NA
YAV	0.71	0.45	0.71	12	0.00	1.00	0.59	0.78	0.24
REF	0.70	0.45	0.70	24	0.00	1.00	0.53	0.71	0.25

C	mean genic diversity	Ho	He	sample size	heterozygote deficit	heterozygote excess	1-Qintra	1-Qinter	Fis
				G. mirabilis - Pacific Sites					
ALB	0.34	0.47	0.50	20	0.69	0.31	0.33	0.32	-0.04
MOR	0.26	0.37	0.42	18	0.23	0.77	0.23	0.23	-0.00
DEV	0.32	0.41	0.46	20	0.16	0.84	0.28	0.31	0.08
USB	0.31	0.43	0.49	20	0.18	0.82	0.27	0.29	0.07
MGU	0.45	0.57	0.57	6	0.57	0.48	0.35	0.35	0.00
BNA	0.30	0.35	0.37	20	0.36	0.64	0.29	0.30	0.05
HID	0.16	0.48	0.43	20	0.97	0.03	0.18	0.15	-0.23
FAM	0.22	0.38	0.36	24	0.70	0.30	0.29	0.28	-0.05
BAN	0.38	0.44	0.43	20	0.67	0.33	0.38	0.38	-0.01
QTN	0.38	0.46	0.47	24	0.40	0.60	0.38	0.37	-0.02
MAN	0.41	0.52	0.50	8	0.61	0.39	0.42	0.41	-0.04
GNG	0.40	0.45	0.50	20	0.02	0.98	0.37	0.41	0.09
BOC	0.41	0.60	0.65	4	0.36	0.84	0.38	0.42	0.11
IGN	0.40	0.46	0.54	20	0.13	0.87	0.35	0.38	0.08
CUA	0.43	0.65	0.68	4	0.87	0.33	0.43	0.36	-0.20
PUR	0.38	0.37	0.40	20	0.50	0.50	0.35	0.36	0.03
				G. mirabilis - Gulf Sites					
MOJ	0.63	0.61	0.63	40	0.24	0.76	0.61	0.64	0.04
PAL	0.38	1.00	1.00	2	NA	NA	NA	NA	NA
ANI	0.66	0.59	0.66	20	0.04	0.96	0.59	0.66	0.12
GRI	0.68	0.59	0.68	20	0.00	1.00	0.60	0.68	0.12
MAR	0.63	0.69	0.77	4	0.15	0.96	0.56	0.66	0.14
PCB	0.73	0.61	0.73	18	0.01	0.99	0.64	0.72	0.11
PRI	0.69	1.00	1.00	2	NA	NA	NA	NA	NA
ADR	0.69	0.63	0.69	20	0.10	0.90	0.64	0.69	0.08
NWC	0.71	0.65	0.71	20	0.17	0.83	0.68	0.71	0.05
MOI	0.65	0.68	0.74	4	0.34	0.86	0.60	0.65	0.08
GE	0.71	0.60	0.71	12	0.04	0.96	0.63	0.72	0.12
KIN	0.69	0.63	0.69	40	0.00	0.99	0.65	0.68	0.05
RCH	0.44	1.00	1.00	2	NA	NA	NA	NA	NA
YAV	0.75	1.00	1.00	2	NA	NA	NA	NA	NA
REF	0.69	1.00	1.00	2	NA	NA	NA	NA	NA

References

Aburto-Oropeza O, Ezcurra E, Danemann G *et al.* (2008) Mangroves in the Gulf of California increase fishery yields. *Proceedings of the National Academy of Sciences of the United States of America*, **105**, 10456–10459.

Adams SM, Lindmeier JB, Duvernell DD (2006) Microsatellite analysis of the phylogeography, Pleistocene history and secondary contact hypotheses for the killifish, *Fundulus heteroclitus*. *Molecular Ecology*, **15**, 1109–1123.

Akihito, Iwata A, Kobayashi T *et al.* (2000) Evolutionary aspects of gobioid fishes based upon a phylogenetic analysis of mitochondrial cytochrome B genes. *Gene*, **259**, 5–15.

Aragón-Arreola M, Martín-Barajas A (2007) Westward migration of extension in the northern Gulf of California, Mexico. *Geology*, **35**, 571–4.

Atwater BF (1979) Ancient processes at the site of southern San Francisco Bay: movement of the crust and changes in sea level. In: *San Francisco Bay the urbanized estuary*, pp. 31–45. San Francisco, CA.

Becker JJ, Sandwell DT, Smith WHF *et al.* (2009) Global Bathymetry and Elevation Data at 30 Arc Seconds Resolution: SRTM30_PLUS. *Marine Geodesy*, **32**, 355–371.

Bernardi G (2000) Barriers to gene flow in *Embiotoca jacksoni*, a marine fish lacking a pelagic larval stage. *Evolution*, **54**, 226–237.

Bernardi G (2014) Baja California disjunctions and phylogeographic patterns in sympatric California blennies. *Frontiers in Ecology and Evolution*.

Bernardi G, Talley D (2000) Genetic evidence for limited dispersal in the coastal California killifish, *Fundulus parvipinnis*. *Journal of Experimental Marine Biology and Ecology*, **255**, 187–199.

Bernardi G, Findley L, Rocha-Olivares A (2003) Vicariance and dispersal across Baja California in disjunct marine fish populations. *Evolution*, **57**, 1599–1609.

Bertness MD, Gaines SD (1993) Larval dispersal and local adaptation in acorn barnacles. *Evolution*, **47**, 316.

Briggs JC (2006) Proximate sources of marine biodiversity. *Journal of Biogeography*, **33**, 1–10.

Brusca RC, Findley LT, Hastings PA (2005) Macrofaunal diversity in the Gulf of California. In: *Marine reserves help preserve genetic diversity after impacts derived from climate variability: Lessons from the pink abalone in Baja California* (eds Cartron J-LE, Ceballos G, Felger RS), pp. 179–203. Nature.

Byrne RJ, Bernardi G, Avise JC (2013) Spatiotemporal Genetic Structure in a Protected Marine Fish, the California Grunion (*Leuresthes tenuis*), and Relatedness in the Genus Leuresthes. *Journal of Heredity*, **104**, 521–531.

Chaytor JD, Goldfinger C, Meiner MA *et al.* (2008) Measuring vertical tectonic motion at the intersection of the Santa Cruz-Catalina Ridge and Northern Channel Islands platform, California Continental Borderland, using submerged paleoshorelines. *Geological Society of America Bulletin*, **120**, 1053–1071.

Clark-Tapia R, Molina-Freaner F (2003) The genetic structure of a columnar cactus with a disjunct distribution: *Stenocereus gummosus* in the Sonoran desert. *Heredity*, **90**, 443–450.

Conomos TJ (1979) Properties and circulation of San Francisco Bay waters. In: *San Francisco Bay The urbanized estuary*, pp. 47–84. American Association for the Advancement of Science, San Francisco, CA.

Dawson MN (2001) Phylogeography in coastal marine animals: a solution from

    California? *Journal of Biogeography*, **28**, 723–736.

Dawson MN, Louie KD, Barlow M, Jacobs DK, Swift CC (2002) Comparative

    phylogeography of sympatric sister species, *Clevelandia ios* and *Eucyclogobius*

    newberryi (Teleostei, Gobiidae), across the California Transition Zone. *Molecular*

    Ecology, **11**, 1065–1075.

de Jesús Suárez-Moo P, Calderon-Aguilera LE, Reyes-Bonilla H *et al.* (2013) Integrating

    genetic, phenotypic and ecological analyses to assess the variation and clarify the

    distribution of the Cortes geoduck (*Panopea globosa*). *Journal of the Marine*

    Biological Association of the United Kingdom, **93**, 809–816.

Deng QE, Hazel W (2010) Population structure and phylogeography of an acorn barnacle

    with induced defense and its gastropod predator in the Gulf of California. *Marine*

    Biology, **157**, 1989–2000.

Dolby GA, Bennett SE, Lira-Noriega A, Wilder BT, Munguía-Vega A (2015) Assessing

    the Geological and Climatic Forcing of Biodiversity and Evolution Surrounding the

    Gulf of California. *Journal of the Southwest*, **57**, 391–455.

Dolby GA, Hechinger R, Ellingson RA, Findley LT, Lorda J, Jacobs DK Palaeohabitat

    and genetic modelling reveal refugia and postglacial mixing of estuarine fishes along

    Alta and Baja California coasts *Proceedings of the Royal Society B*, in revision.

Earl DA, vonHoldt BM (2011) STRUCTURE HARVESTER: a website and program for

    visualizing STRUCTURE output and implementing the Evanno method.

    Conservation Genetics Resources, **4**, 359–361.

Earl DA, Louie KD, Bardeleben C, Swift CC, Jacobs DK (2010) Rangewide

microsatellite phylogeography of the endangered tidewater goby, *Eucyclogobius newberryi* (Teleostei: Gobiidae), a genetically subdivided coastal fish with limited marine dispersal. *Conservation Genetics*, **11**, 103–114.

Ellingson R (2012) Phylogenetics and phylogeography of North Pacific bay gobies: adaptive convergence, relictual endemism, and climate-driven population structure. Univeristy of California, Los Angeles.

Ellingson RA, Swift CC, Findley LT, Jacobs DK (2014) Convergent evolution of ecomorphological adaptations in geographically isolated Bay gobies (Teleostei: Gobionellidae) of the temperate North Pacific. *Molecular Phylogenetics and Evolution*, **70**, 464–477.

Evanno G, Regnaut S, Goudet J (2005) Detecting the number of clusters of individuals using the software structure: a simulation study. *Molecular Ecology*, **14**, 2611–2620.

Excoffier L, Laval G, Schneider S (2005) Arlequin (version 3.0): an integrated software package for population genetics data analysis. *Evolutionary bioinformatics online*, **1**, 47–50.

Ficke AD, Myrick CA, Hansen LJ (2007) Potential impacts of global climate change on freshwater fisheries. *Reviews in Fish Biology and Fisheries*, **17**, 581–613.

Goddard JHR, Gosliner TM, Pearse JS (2011) Impacts associated with the recent range shift of the aeolid nudibranch *Phidiana hiltoni* (Mollusca, Opisthobranchia) in California. *Marine Biology*, **158**, 1095–1109.

Goudet J (2005) Hierfstat, a package for R to compute and test hierarchical F-statistics. *Molecular Ecology Notes*.

Hastings A, Harrison S (1994) Metapopulation Dynamics and Genetics. *Annual Review*

of Ecology and Systematics, **25**, 167–188.

Helenes J, Carreno AL (1999) Neogene sedimentary evolution of Baja California in relation to regional tectonics. *Journal of South American Earth Sciences*, **12**, 589–605.

Helenes J, Carreño AL, Carrillo RM (2009) Middle to late Miocene chronostratigraphy and development of the northern Gulf of California. *Marine Micropaleontology*, **72**, 10–25.

Hellberg ME, Balch DP, Roy K (2001) Climate-driven range expansion and morphological evolution in a marine gastropod. *Science*, **292**, 1707–1710.

Hendrickx ME, Brusca RC, Reséndiz GR (2014) Biodiversity of Macrocrustaceans in the Gulf of California, Mexico. *Zootaxa*, **3835**, 338–348.

Hendrickx ME, Brusca RC, Cordero M, Ramírez R G (2007) Marine and brackish-water molluscan biodiversity in the Gulf of California, Mexico. *Scientia Marina*, **71**, 637–647.

Hewitt G (2000) The genetic legacy of the Quaternary ice ages. *Nature*, **405**, 907–913.

Hewitt GM (2004) Genetic consequences of climatic oscillations in the Quaternary. *Philosophical Transactions of the Royal Society B: Biological Sciences*, **359**, 183–195.

Huang D, Bernardi G (2001) Disjunct Sea of Cortez–Pacific Ocean *Gillichthys mirabilis* populations and the evolutionary origin of their Sea of Cortez endemic relative, *Gillichthys seta*. *Marine Biology*, **138**, 421–428.

Huelsenbeck JP, Ronquist F (2001) MrBayes: Bayesian inference of phylogeny. Bioinformatics. *Bioinformatics*, **17**, 754–755.

Humphreys ED (1995) Post-Laramide removal of the Farallon slab, western United
States. *Geology*, **23**, 987–990.

Hurtado LA, Frey M, Gaube P, Pfeiler E, Markow TA (2007) Geographical subdivision,
demographic history and gene flow in two sympatric species of intertidal snails,
Nerita scabricosta and *Nerita funiculata*, from the tropical eastern Pacific. *Marine
Biology*, **151**, 1863–1873.

Hurtado LA, Lee EJ, Mateos M (2013) Contrasting Phylogeography of Sandy vs. Rocky
Supralittoral Isopods in the Megadiverse and Geologically Dynamic Gulf of
California and Adjacent Areas (R Cordaux, Ed,). *PLoS ONE*, **8**, e67827.

Hurtado LA, Mateos M, Santamaria CA (2010) Phylogeography of Supralittoral Rocky
Intertidal *Ligia* Isopods in the Pacific Region from Central California to Central
Mexico (SJ Goldstien, Ed,). *PLoS ONE*, **5**, e11633–13.

Ingersoll RV, Rumelhart PE (1999) Three-stage evolution of the Los Angeles basin,
southern California. *Geology*, **27**, 593–6.

Jacobs DK, Haney TA, Louie KD (2004) Genes, Diversity, and Geologic process on the
Pacific coast. *Annual Review of Earth and Planetary Sciences*, **32**, 601–652.

Jacobs D, Stein ED, Longcore T (2011) Classification of California estuaries based on
natural closure patterns: Templates for restoration and management. *Southern
California Coastal Water Research Project*.

Jakobsson M, Rosenberg NA (2007) CLUMPP: a cluster matching and permutation
program for dealing with label switching and multimodality in analysis of population
structure. *Bioinformatics*, **23**, 1801–1806.

Johnson PB, Martin KL, Vandergon TL *et al.* (2009) Microsatellite and Mitochondrial

Genetic Comparisons between Northern and Southern Populations of California Grunion (*Leuresthes tenuis*). *Copeia*, **2009**, 465–474.

Kelly RP, Palumbi SR (2010) Genetic Structure Among 50 Species of the Northeastern Pacific Rocky Intertidal Community (SA Sandin, Ed,). *PLoS ONE*, **5**, e8594–13.

Leache AD, Crews SC, Hickerson MJ (2007) Two waves of diversification in mammals and reptiles of Baja California revealed by hierarchical Bayesian analysis. *Biology Letters*, **3**, 646–650.

Lee WJ, Conroy J, Howell WH, Kocher TD (1995) Structure and evolution of teleost mitochondrial control regions. *Journal of Molecular Evolution*, **41**, 54–66.

Lin H-C, Sánchez-Ortiz C, Hastings PA (2009) Colour variation is incongruent with mitochondrial lineages: cryptic speciation and subsequent diversification in a Gulf of California reef fish (Teleostei: Blennioidei). *Molecular Ecology*, **18**, 2476–2488.

Lindell J, Ngo A, Murphy RW (2006) Deep genealogies and the mid-peninsular seaway of Baja California. *Journal of Biogeography*, **33**, 1327–1331.

Littler MM, Littler DS (1981) Intertidal macrophyte communities from Pacific Baja California and the upper Gulf of California: relatively constant vs. environmentally fluctuating systems. *Mar Ecol Prog Ser*.

Lockington WN (1877) The Long-Jawed Goby. *The American Naturalist*, **11**, 474–478.

Love MS (2012) *Certainly More Than You Want to Know About The Fishes of The Pacific Coast—A Postmodern Experience*. Really Big Press.

Maldonado JE, Davila FO, Stewart BS, Geffen E, Wayne RK (1995) Intraspecific Genetic Differentiation in California Sea Lions (*Zalophus californianus*) From Southern California and the Gulf of California. *Marine Mammal Science*, **11**, 46–58.

Marinone SG (2003) A three-dimensional model of the mean and seasonal circulation of the Gulf of California. *Journal of Geophysical Research letters*, **108**, 3325–27.

Marinone SG, Ulloa MJ, Parés-Sierra A, Lavín MF, Cudney-Bueno R (2008) Connectivity in the northern Gulf of California from particle tracking in a three-dimensional numerical model. *Journal of Marine Systems*, **71**, 149–158.

Mark C, Gupta S, Carter A, Mark DF, Gautheron C (2014) Rift flank uplift at the Gulf of California: No requirement for asthenospheric upwelling. *Geology*, **42**, 259–262.

Marko PB (2004) "What's larvae got to do with it?" Disparate patterns of post-glacial population structure in two benthic marine gastropods with identical dispersal potential. *Molecular Ecology*, **13**, 597–611.

McFarlane GA, King JR, Beamish RJ (2000) Have there been recent changes in climate? Ask the fish. *Progress in Oceanography*, **47**, 147–169.

Michaud F, Calmus T, Royer J-Y *et al.* (2007) Right-lateral active faulting between southern Baja California and the Pacific plate: The Tosco-Abreojos fault. In: *Right-lateral active faulting between southern Baja California and the Pacific plate: breojos fault*, pp. 287–300. Geological Society of America.

Miller MA, Pfeiffer W, Schwartz T (2010) Creating the CIPRES Science Gateway for inference of large phylogenetic trees. *2010 Gateway Computing Environments Workshop (GCE)*, 1–8.

Miller RR, Hubbs CL (1954) An Erroneous Record of the California Killifish, Fundulus parvipinnis, from Cabo San Lucas, Baja California. *Copeia*, **1954**, 234–235.

Muhs DR, Rockwell TK, Kennedy GL (1992) Late Quaternary uplift rates of marine terraces on the Pacific coast of North America, southern Oregon to Baja California

Sur. *Quaternary International*, **15-16**, 121–133.

Munguía-Vega A (2011) Habitat Fragmentation in Small Vertebrates from the Sonoran Desert in Baja California. Conservation Genetics Laboratory School of Natural Resources, The University of Arizona, Tuscon, AZ.

Munguía-Vega A, Jackson A, Marinone SG *et al.* (2014) Asymmetric connectivity of spawning aggregations of a commercially important marine fish using a multidisciplinary approach. *PeerJ*, **2**, e511–33.

Nava-Sánchez EH, Gorsline DS, Molina-Cruz A (2001) The Baja California peninsula borderland: structural and sedimentological characteristics. *Sedimentary Geology*, **144**, 63–82.

Niemi NA, Oskin M, Rockwell TK (2008) Southern California Earthquake Center Geologic Vertical Motion Database. *Geochemistry, Geophysics, Geosystems*, **9**, 1–14.

Oskin M, Stock J (2003) Marine incursion synchronous with plate-boundary localization in the Gulf of California. *Geology*.

Pfeiler E, Markow TA (2011) Phylogeography of the Cactophilic *Drosophila* and Other Arthropods Associated with Cactus Necroses in the Sonoran Desert. *Insects*, **2**, 218–231.

Plattner C, Malservisi R, Govers R (2009) On the plate boundary forces that drive and resist Baja California motion. *Geology*, **37**, 359–362.

Pritchard JK, Stephens M, Donnelly P (2000) Inference of population structure using multilocus genotype data. *Genetics*, **155**, 945–959.

Riddle BR, Hafner DJ, Alexander LF, Jaeger JR (2000) Cryptic vicariance in the

historical assembly of a Baja California Peninsular Desert biota. *Proceedings of the National Academy of Sciences*, **97**, 14438–14443.

Riginos C (2005) Cryptic vicariance in Gulf of California fishes parallels vicariant patterns found in Baja California mammals and reptiles. *Evolution*, **59**, 2678–2690.

Riginos C, Nachman MW (2001) Population subdivision in marine environments: the contributions of biogeography, geographical distance and discontinuous habitat to genetic differentiation in a blennioid fish, *Axoclinus nigricaudus. Molecular Ecology*, **10**, 1439–1453.

Roden GI (1964) Oceanographic aspects of Gulf of California. In: *Marine Geology of the Gulf of California* (eds van Andel TH, Shor GG Jr), pp. 30–58.

Roessig JM, Woodley CM, Cech JJ Jr, Hansen LJ (2004) Effects of global climate change on marine and estuarine fishes and fisheries. *Reviews in Fish Biology and Fisheries*, **14**, 251–275.

Ronquist F, Huelsenbeck JP (2003) MrBayes 3: Bayesian phylogenetic inference under mixed models. *Bioinformatics*, **19**, 1572–1574.

Ryman N, Palm S, André C *et al.* (2006) Power for detecting genetic divergence: differences between statistical methods and marker loci. *Molecular Ecology*, **15**, 2031–2045.

Santamaría-del-Angel E, Alvarez-Borrego S, Müller-Karger FE (1994) Gulf of California biogeographic regions based on coastal zone color scanner imagery. *Journal of Geophysical Research letters*, **99**, 7411–14.

Seapy RR, Littler MM (1980) Biogeography of rocky intertidal macroinvertebrates of the Southern California Islands. In: *The California islands* (ed Powers DM), pp. 307–

323.

Segura I, Rocha-Olivares A, Flores-Ramírez S, Rojas-Bracho L (2006) Conservation
implications of the genetic and ecological distinction of *Tursiops truncatus* ecotypes
in the Gulf of California. *Biological Conservation*, **133**, 336–346.

Slatkin M (1987) Gene flow and the geographic structure of natural populations. *Science*,
236, 787–792.

Soria G, Torre-Cosio J, Munguía-Vega A *et al.* (2014) Dynamic connectivity patterns
from an insular marine protected area in the Gulf of California. *Journal of Marine
Systems*, **129**, 248–258.

Stock JM (2000) Relation of the Puertecitos Volcanic Province, Baja California, Mexico,
to development of the plate boundary in the Gulf of California. *Special Papers-
Geological Society of America*, 143–156.

Terry A, Bucciarelli G, Bernardi G (2000) Restricted gene flow and incipient speciation
in disjunct Pacific Ocean and Sea of Cortez populations of a reef fish species, *Girella
nigricans*. *Evolution*, **54**, 652–659.

Turner CH, Sexsmith JC (1967) *Marine baits of California*. Department of Fish and
Game.

Wright S (1931) Evolution in Mendelian Populations. *Genetics*, **16**, 97–159.

Zacherl D, Gaines SD, Lonhart SI (2003) The Limits to Biogeographical Distributions:
Insights from the Northward Range Extension of the Marine Snail, *Kelletia kelletii*
(Forbes, 1852). *Journal of Biogeography*, **30**, 913–924.

Zeitzschel B (1969) Primary productivity in the Gulf of California. *Marine Biology*, **3**,
201–207.